

**Post Grouting Drilled Shaft Tips**  
*Phase I*

**Principal Investigator: Gray Mullins**

Graduate Students: S. Dapp, E. Frederick, V. Wagner  
Department of Civil and Environmental Engineering

**December 2001**

## **DISCLAIMER**

The opinions, findings and conclusions expressed in this publication are those of the authors and not necessarily those of the State of Florida Department of Transportation.

## CONVERSION FACTORS, US CUSTOMARY TO METRIC UNITS

<i>Multiply</i>	<i>by</i>	<i>to obtain</i>
inch	25.4	mm
foot	0.3048	meter
square inches	645	square mm
cubic yard	0.765	cubic meter
pound (lb)	4.448	Newtons
kip (1000 lb)	4.448	kiloNewton (kN)
Newton	0.2248	pound
kip/ft	14.59	kN/meter
pound/in <sup>2</sup>	0.0069	MPa
kip/in <sup>2</sup>	6.895	MPa
MPa	0.145	ksi
kip-ft	1.356	kN-m
kip-in	0.113	kN-m
kN-m	.7375	kip-ft

## PREFACE

The investigation reported was funded by a contract awarded to the University of South Florida, Tampa by the Florida Department of Transportation. Mr. Peter Lai was the Project Manager. It is a pleasure to acknowledge his contribution to this study.

The full-scale tests required by this study were carried out in part at Coastal Caisson's Clearwater location. We are indebted to Mr. Bud Khouri, Mr Richard Walsh, and staff for providing this site and also for making available lifting, moving, and excavating equipment that was essential for this study.

We thank Mr. Ron Broderick, Earth Tech, Tampa for donating his time, equipment and grout materials necessary for grouting shafts at Site I and II. We are indebted to Mr. Mike Muchard and Mr. Don Robertson of Applied Foundation Testing, Green Cove Springs, FL, for supplying the Statnamic test fuel and the trucking required to transport the University of South Florida's 4MN hydraulic-catching Statnamic device. Additional thanks are extended to Profession Services Industries, Inc. for permission to reprint some of their field reports concerning the construction of the Royal Park Bridge test shafts.

Special thanks are extended to the College of Engineering's Machine Shop staff of Mr. Bob Smith, Mr. Jerry Miller, Mr. Bryan O'Steen, Mr. James Christopher, and Mr. Tom Gage for their unending support. The assistance of Mr. Van Wagner in the casting and grouting of the model-scale study is duly recognized. The contribution of graduate students (*not in any order*) Mr. Chris Lewis, Mr. Ed Garbin, Mr. Danny Winters, and Mr. Andrew Goulis is gratefully appreciated.

## EXECUTIVE SUMMARY

This report presents results from a two-year experimental study to evaluate the effects of post-grouting drilled shaft tips in sand on the bearing capacity. As the project was subsequently extended to conduct more field test, this document is entitled Phase I. Both model scale and full-scale tests were conducted on drilled shafts whose tip had been grouted using various grouting systems. These were (1) flat jack (rubber confined), (2) sleeve port (tube-a-manchette), and (3) sleeve port systems with and without a backing plate. Post-grouting was conducted at three sites with cohesionless soils: Site I, shelly sand; Site II, silty sand; and Site III, cemented coquina/sand.

In the model tests, a total of twenty four 1/10 scale shaft specimens were cast and tested in a Frustum Confining Vessel (FCV). This vessel provided the means to simulated soil pressure distributions similar to those expected in the field. Comparisons were made between shafts cast without post grouting (controls) and those grouted using a flat jack type grouting cell. Improvement was found to be somewhat proportional to grout take, but more closely proportional to the maximum sustained grouting pressure.

In the full-scale tests, a total of twelve Statnamic load tests were conducted on shafts constructed in three soil types (all were intended to be cohesionless soils). At Sites I and II, 24" diameter shafts were cast in shelly sand or silty sand, respectively. At Site III, 48" diameter shafts were cast in sandy cemented coquina. Eight of the load tests were conducted on grouted shafts and four on ungrouted controls. One shaft at Site III could not be fully mobilized in side shear or end bearing after grouting, hence, the effects were inconclusive. The findings of these tests were similar to those found in the model scale tests in that the improvement was most closely proportional to maximum sustained grouting pressure.

Based on the test results design recommendations for the use of post grouted shafts have been prepared that use a grout pressure index (max sustained grout pressure / calculated bearing capacity) and the acceptable service limit displacement as expressed in percent shaft diameter ( $\Delta / D * 100\%$ ). Construction, grout mix, and grouting guidelines have also been prepared utilizing literature values as well as those found to be successful in this study.

## TABLE OF CONTENTS

1. INTRODUCTION .....	1
1.1 Problem Statement .....	1
1.2 Objectives .....	1
1.3 Work Summary .....	2
1.4 Organization .....	3
2. BACKGROUND .....	5
2.1 Soil Type Applicability .....	6
2.1.1 Sand and Silt .....	6
2.1.2 Clay .....	7
2.1.3 Rock .....	8
2.1.4 Uplift Considerations .....	8
2.2 Grouting Mechanisms .....	9
2.2.1 Permeation Grouting .....	9
2.2.2 Compaction Grouting .....	9
2.2.3 Staged Grouting .....	10
2.3 Grout Injection Apparatus .....	11
2.3.1 Stem (Orifice) .....	11
2.3.2 Sleeve-Port (Tube-a-Manchette) .....	11
2.3.3 Flat-Jack (Pre-Load Cells) .....	12
2.4 Grout Mixes .....	13
2.4.1 Grout Mixers .....	13
2.4.2 Grout Pumps .....	13
2.4.3 Access Lines .....	15
2.4.4 Grout Mixing .....	15
2.4.5 Grout Properties .....	15
2.4.6 Grout Constituents .....	17
2.4.7 Grout Mix Design Examples .....	20
3. LABORATORY SCALE INVESTIGATION .....	39
3.1 Introduction .....	39
3.2 Model Testing .....	39
3.2.1 Scaling Parameters .....	39
3.2.2 Centrifuge Testing .....	40
3.2.3 Frustum Confining System .....	41
3.3 Frustum Confining Vessel .....	41
3.4 Equipment and Facility Development .....	42
3.4.1 Overall Site Development .....	42

3.4.2	Load Test Frame	42
3.4.3	Casing and Driving Head	42
3.4.4	Tremie Assembly	43
3.4.5	Pressure Pot	43
3.4.6	Jetting Assembly/Alluviator	43
3.5	Testing Procedures	44
3.5.1	Soil Preparation	44
3.5.2	Jetting	44
3.5.3	Specimen Casting	45
3.5.4	Grouting	46
3.5.5	Load Testing	47
3.6	Test Matrix and Results	47
3.6.1	Jetted Shafts	49
3.6.2	Control Shafts	50
3.6.3	Grouted Shafts	50
3.7	Test Results	54
3.8	Conclusions	54
4.	FULL-SCALE TEST PROGRAM	75
4.1	Introduction	75
4.2	Locations and Soil Profiles	76
4.2.1	Site I (Shelly Sand) and Site II (Silty Silica Sand)	76
4.2.2	Site III (Cemented Coquina)	77
4.3	Grouting Apparatus	78
4.3.1	Flat-Jack (Used in Sites I, II, III)	79
4.3.2	Sleeve-port (Used in Sites I and II)	80
4.3.3	Skin Grouting Sleeve-port (Used in Site II)	82
4.4	Instrumentation and Data Acquisition	83
4.4.1	Site I (Shelly Sand) and Site II (Silty Silica Sand)	84
4.4.2	Site III (Cemented Coquina)	85
4.5	Drilled Shaft Construction	85
4.5.1	Site I (Shelly Sand) and Site II (Silty Silica Sand)	88
4.5.2	Site III (Cemented Coquina)	90
4.6	Grouting and Load Testing	94
4.6.1	Site I (Shelly Sand) and Site II (Silty silica sand)	94
4.6.2	Site III (Cemented Coquina)	95
5.	GROUTING AND LOAD TESTING DATA REGRESSIONS	127
5.1	Grouting	127
5.1.1	Site I (Shelly Sand)	129
5.1.2	Site II (Silty Silica Sand)	137
5.1.3	Site III (Cemented Coquina)	142

5.2	Load Testing .....	145
5.2.1	Site I (Shelly Sand) .....	146
5.2.2	Site II (Silty Silica Sand) .....	151
5.2.3	Site III (Cemented Coquina) .....	154
6.	ANALYSIS .....	157
6.1	Grouting .....	157
6.2	Load Testing Comparisons .....	158
6.2.1	Site I (Shelly Sand) .....	164
6.2.2	Site II (Silty Silica Sand) .....	165
6.2.3	Site III (Cemented Coquina) .....	165
6.3	Conclusions .....	166
7.	DESIGN AND CONSTRUCTION GUIDELINES .....	189
7.1	Design of Post-Grouted Tip Capacity .....	189
7.2	Design Example .....	191
7.3	Construction of Tip-Grouted Shafts .....	199
7.3.1	Grout Cell Considerations .....	199
7.3.2	Grouting Guidelines .....	200
	REFERENCES .....	203
	APPENDICES .....	207
	Appendix A. Soil Exploration and Construction Records .....	208
	Appendix B. Grouting Data Reduction .....	280
	Appendix C. Full-Scale Load Test Data Reduction .....	296

## LIST OF TABLES

Table 1-1. Full Scale Test Matrix . . . . .	2
Table 2-1. Descriptions of Various Pumps . . . . .	14
Table 2-2. Minimum Pump Size Based on Aggregate Classification . . . . .	16
Table 2-3. ASTM Designations for Portland Cements . . . . .	18
Table 2-4. Grout Mix Design Examples . . . . .	22
Table 3-1. Application of Scaling Parameter N . . . . .	40
Table 3-2. Laboratory Scale Data . . . . .	48
Table 4-1. Grouting Apparatus Used . . . . .	78
Table 4-2. Instrumentation Used During Testing . . . . .	83
Table 4-3. Construction Method Summary . . . . .	86
Table 4-4. Shaft As-Builts . . . . .	87
Table 5-1. Grout Data Summary . . . . .	128
Table 6-1. Load Performance at 0.5 inch Displacement . . . . .	160
Table 6-2. Load Performance at 1.0 inch Displacement . . . . .	161
Table 6-3. Load Performance at a Displacement of 5% of Shaft Diameter . . . . .	162
Table 6-4. Load Performance at Ultimate Load . . . . .	163
Table 7-1. Linear Fit Variables of Tip Grouting Design Equations . . . . .	190
Table 7-2. Example Capacity Predictions for an UngROUTED Shaft . . . . .	193
Table 7-3. Example Calculation of Grouted Shaft Capacity . . . . .	197

## LIST OF FIGURES

Figure 2-1. Comparison of two 1.5 m diameter drilled shafts (Sliwinski, et al., 1984).	23
Figure 2-2. Load-displacement of 570 mm drilled shafts (Stocker, 1983).	24
Figure 2-3. Results from 450 mm shaft load tests (Sliwinski, et al., 1984)	25
Figure 2-4. Stress / strain curves for typical loose and dense sand (Holtz and Kovacs, 1981).	26
Figure 2-5. Tip grouting pressures used at various sites worldwide.	26
Figure 2-6. Simple sleeve-port compaction grout apparatus (after Bruce, 1986).	27
Figure 2-7. Sleeve-port system used in Taipei, Taiwan (Mullins, 1999).	27
Figure 2-8. U-shaped grouting cell positioned at bottom of excavation (after Sliwinski and Fleming, 1984).	28
Figure 2-9. Mechanical compaction grout apparatus (from Lizzi, 1981).	28
Figure 2-10. Gravel pack between two steel plates (after Bolognesi and Moretto, 1973).	29
Figure 2-11. High quality mixer	29
Figure 2-12. Less efficient mixers with helical pumps for circulation	30
Figure 2-13. Lower quality mixer	30
Figure 2-14. Helical rotor pump	31
Figure 2-16. Ram pump (Houslsby, 1990)	31
Figure 2-15. Single piston pump	32
Figure 2-17. Flow of grout through access lines	32
Figure 2-18. Access lines with aggregates	33
Figure 2-19. Tip capacity of shafts in sand (AASHTO, 1999)	34
Figure 2-20. Accelerating effect of seawater on Portland cement grouts <sup>5</sup> (Domone, 1990)	35
Figure 2-21. Particle size distribution of cements (Houslsby, 1990)	36
Figure 2-22. Effects of w/c ratio on Portland cement grouts (Domone, 1990; FHWA, 2000)	36
Figure 2-23. Increase of compressive strength with the addition of a superplasticizer	37
Figure 2-24. Effect of w/c ratio on pumpability of grout mixes	37
Figure 2-25. Water reduction capabilities of superplasticizer	38
Figure 3-1 Schematic of frustum confining vessel (After Horvath, 1996).	55
Figure 3-2 Pressure regulator.	55
Figure 3-3 Installation of roofing structure.	56
Figure 3-4 Frustum with 2-ton lifting crane.	56
Figure 3-5 Load testing frame and scaffolding.	57
Figure 3-6 Casing.	57
Figure 3-7 Tremie assembly.	58
Figure 3-8 Pressure pot.	59
Figure 3-9 Jetting device.	59

Figure 3-10 (a) Removing top two portions of frustum. (b) Sealing the pieces of the frustum. . . . .	60
Figure 3-11 Schematic of frustum pressurizing equipment. . . . .	60
Figure 3-12 Expulsion of sand from quick pressurization. . . . .	61
Figure 3-13 (a) Placing pile inside jetter. (b) Positioning pile over frustum. . . . .	61
Figure 3-14 Casing driver and template. . . . .	62
Figure 3-15 (a) Excavation. (b) Clean-out bucket. . . . .	62
Figure 3-16 (a) Tremie pipe with grouting cell (b) Hopper with mix (c) Grout return. . . . .	63
Figure 3-17 Outer casing. . . . .	64
Figure 3-18 (a) Grouting cell. (b) Geotextile and metal plate. . . . .	64
Figure 3-19 Schematic of three grouting cells used. . . . .	65
Figure 3-20 Manual grout pump. . . . .	65
Figure 3-21 Valves with return. . . . .	66
Figure 3-22 Load testing apparatus. . . . .	66
Figure 3-23 Jetted model pile. . . . .	67
Figure 3-24 CS-1 . . . . .	67
Figure 3-25 CS-2 . . . . .	68
Figure 3-26 GS-1 . . . . .	68
Figure 3-27 GS-2 with corresponding bulb. . . . .	69
Figure 3-28 GS-3 with corresponding bulb. . . . .	69
Figure 3-29 GS-4 with corresponding bulb . . . . .	69
Figure 3-30 GS-5 with corresponding bulb . . . . .	70
Figure 3-31 GS-6 with corresponding bulb . . . . .	70
Figure 3-32 GS-7 with corresponding bulb . . . . .	70
Figure 3-33 GS-8 with corresponding bulb. . . . .	71
Figure 3-34 GS-9 with corresponding bulb . . . . .	71
Figure 3-35 GS-10 with corresponding bulb . . . . .	71
Figure 3-36 GS-11 with corresponding bulb. . . . .	72
Figure 3-37 GS-12 with corresponding bulb . . . . .	72
Figure 3-38 GS-13 with corresponding bulb. . . . .	72
Figure 3-39 Load-displacement with varied FCV pressures. . . . .	73
Figure 3-40 Control Shaft versus Grouted Shafts. . . . .	73
Figure 3-41 Percent improvement versus grout take. . . . .	74
Figure 3-42 Percent improvement versus maximum sustained pressure . . . . .	74
Figure 4-1. Site I and Site II locations. . . . .	97
Figure 4-2. Site I and Site II plan views. . . . .	98
Figure 4-3. Site I layout. . . . .	99
Figure 4-4. Site II layout. . . . .	99
Figure 4-5. University of South Florida's mini-cone penetrometer (MCPT). . . . .	100
Figure 4-6. FDOT Dist.1 cone penetrometer. . . . .	100
Figure 4-7. FDOT Dist.1 SPT Rig. . . . .	100
Figure 4-8. Typical CPT sounding Site I. . . . .	101
Figure 4-9. Typical CPT sounding Site II. . . . .	101
Figure 4-10. Site III location. . . . .	102

Figure 4-11. Site III layout. . . . .	103
Figure 4-12. Site III LT-3 standard penetration test (SPT) boring. . . . .	104
Figure 4-13. Site III LT-2 standard penetration test (SPT) boring. . . . .	104
Figure 4-14. Site I and Site II flat-jack style grouting apparatus. . . . .	105
Figure 4-15. Site III flat-jack grouting apparatus. . . . .	106
Figure 4-16. Large flat-jack during fabrication (used at Site III). . . . .	107
Figure 4-17. Small flat-jack during fabrication (used at Site I and Site II). . . . .	107
Figure 4-18. Small flat-jack completed (used in Sites I and II). . . . .	108
Figure 4-19. Sleeve-port grouting apparatus. . . . .	109
Figure 4-20. Drilling grout holes in sleeve-port apparatus. . . . .	110
Figure 4-21. Grout delivery pipes for sleeve-port apparatus. . . . .	110
Figure 4-22. Site I sleeve-port apparatus tied into reinforcing cages. . . . .	111
Figure 4-23. Sleeve-port device with optional top steel plate. . . . .	111
Figure 4-24. Skin grouting sleeve-port. (Site II) . . . . .	112
Figure 4-25. Skin grouting Sleeve-ports Tied into Cage (Site II). . . . .	112
Figure 4-26. Site III tension telltale fabrication. . . . .	112
Figure 4-27. Site III tension telltale installed. . . . .	113
Figure 4-28. Sites I and II reinforcing cage fabrication. . . . .	113
Figure 4-29. Sites I and II completed reinforcing cages with grouting apparatti. . . . .	114
Figure 4-30. Site I excavation with a Texoma 700 drill rig. . . . .	114
Figure 4-31. Site II excavation with a Bauer BG-7 drill rig. . . . .	115
Figure 4-32. Auger used to excavate Sites I and II. . . . .	116
Figure 4-33. Site II reinforcing cage set into excavation with Hitachi crane. . . . .	116
Figure 4-34. Site II concreting operation. . . . .	117
Figure 4-35. Site II exhumed flat-jack (left), sleeve-port (right) tips. . . . .	118
Figure 4-36. Site II exhumed Control Shaft. . . . .	118
Figure 4-37. Site III LT-2 cage with flat-jack grouting apparatus. . . . .	119
Figure 4-38. Site III LT-2 completed cage tip. . . . .	119
Figure 4-39. Slurry plume as Delmag drill rig excavates Site III LT-2. . . . .	120
Figure 4-40. Kobelco crane lifting cage for Site III LT-3. . . . .	121
Figure 4-41. Kobelco crane lifting Site III LT-2 Cage. . . . .	122
Figure 4-42. Scuff ring protecting flat-jack edge of Site III LT-2 . . . . .	122
Figure 4-43. Concrete placement for Site III LT-2. . . . .	123
Figure 4-44. Helical-style grout pump used for Sites I and II. . . . .	123
Figure 4-45. 500 ton Statnamic device being moved at Site I. . . . .	124
Figure 4-46. Statnamic load test in progress at Site II. . . . .	125
Figure 4-47. Dual-piston (ram-style) grout pump used on Site III. . . . .	125
Figure 4-48. Grout lines flushed on Site III LT-2. . . . .	126
Figure 5-1. Site I Flat-Jack 1 tip grouting load vs. displacement. . . . .	130
Figure 5-2. Site I Flat-Jack 2 tip grouting load vs. displacement. . . . .	131
Figure 5-3. Site I Sleeve-Port 1 tip grouting load vs. displacement, cycle 1. . . . .	132
Figure 5-4. Site I Sleeve-Port 1 tip grouting load vs. displacement, cycle 2. . . . .	133
Figure 5-5. Site I Sleeve-Port 1 tip grouting load vs. displacement, cycle 3. . . . .	134
Figure 5-6. Site I Sleeve-Port 2 tip grouting load vs. displacement, cycle 1. . . . .	135

Figure 5-7. Site I Sleeve-Port 2 tip grouting load vs. displacement, cycle 2. ....	136
Figure 5-8. Site II Flat-Jack tip grouting load vs. displacement. ....	138
Figure 5-9. Site II Sleeve-Port tip grouting load vs. displacement, cycle 1. ....	139
Figure 5-10. Site II Sleeve-Port tip grouting load vs. displacement, cycle 2. ....	140
Figure 5-11. Site II Sleeve-Port tip grouting load vs. displacement, cycle 3. ....	141
Figure 5-12. Site III LT-2 tip grouting load vs. displacement. ....	143
Figure 5-13. Site III LT-3 grout volume vs. time. ....	144
Figure 5-14. Site III LT-2 grout volume vs. time. ....	144
Figure 5-15. Site I Flat-Jack 1 load vs. displacement compared to Control. ....	147
Figure 5-16. Site I Flat-Jack 2 load vs. displacement compared to Control. ....	148
Figure 5-17. Site I Sleeve-Port 1 load vs. displacement compared to Control. ....	149
Figure 5-18. Site I Sleeve-Port 2 load vs. displacement compared to Control. ....	150
Figure 5-19. Site II Flat-Jack load vs. displacement compared to Control. ....	152
Figure 5-20. Site II Sleeve-Port load vs. displacement compared to Control. ....	153
Figure 5-21. Site III LT-3 cycle 2 (grouted) load vs. displacement compared to LT-3 cycle 1 (control). ....	155
Figure 5-22. Site III LT-2 cycle 2 (grouted) load vs. displacement compared to L-2 cycle 1 (control). ....	156
Figure 6-1. Area ratio vs. active grout time for flat-jack grouting apparatus. ....	171
Figure 6-2. Area ratio vs. active grout time for sleeve-port grouting apparatus. ....	172
Figure 6-3. Shaft improvement example. ....	173
Figure 6-4. Site I Flat-Jack shaft tip load vs. top of shaft displacement. ....	174
Figure 6-5. Site I Sleeve-Port shaft tip load vs. top of shaft displacement. ....	175
Figure 6-6. Site I tip load vs. top of shaft displacement comparisons. ....	176
Figure 6-7. Site II shaft tip load vs. top of shaft displacement. ....	177
Figure 6-8. Site II tip load vs. top of shaft displacement comparisons. ....	178
Figure 6-9. Site III tip load vs. top of shaft displacement comparisons. ....	179
Figure 6-10. Tip capacity improvement vs. top of shaft displacement. ....	180
Figure 6-11. Total capacity improvement vs. top of shaft displacement. ....	181
Figure 6-12. Maximum tip capacity improvement vs. dimensionless grout volume. ...	182
Figure 6-13. Maximum total capacity improvement vs. dimensionless grout volume. ...	183
Figure 6-14. Maximum sustained grout pressure vs. dimensionless grout volume. ...	184
Figure 6-15. Maximum tip capacity improvement vs. maximum sustained grout pressure. ....	185
Figure 6-16. Grouted Tip Capacity Multipliers vs. Grout Pressure Index applied to ungrouted tip capacities at 5% diameter displacement. ....	186
Figure 6-17. Grouted Tip Capacity Multipliers vs. Grout Pressure Index applied to ungrouted tip capacities at 2 % diameter displacement. ....	187
Figure 6-18. Grouted Tip Capacity Multipliers vs. Grout Pressure Index applied to ungrouted tip capacities at 1 % diameter displacement. ....	188
Figure 7-1. Example capacity predictions for an ungrouted shaft. ....	194
Figure 7-2. Example calculation of maximum grout pressure vs. depth of embedment. ....	195

Figure 7-3. Example capacity predictions for a grouted shaft .....	198
Figure A-1. Site I and II concrete mix design (1 of 4). .....	208
Figure A-2. Site I and II concrete mix design (2 of 4). .....	209
Figure A-3. Site I and II concrete mix design (3 of 4). .....	210
Figure A-4. Site I and II concrete mix design (4 of 4). .....	211
Figure A-5. Site I SPT boring log B-1 (1 of 2). .....	212
Figure A-6. Site I SPT boring log B-1 (2 of 2). .....	213
Figure A-7. Site I SPT boring log B-2 (1 of 2). .....	214
Figure A-8. Site I SPT boring log B-2 (2 of 2). .....	215
Figure A-9. Site I CPT sounding CPT-67. ....	216
Figure A-10. Site I CPT sounding CPT-68. ....	217
Figure A-11. Site I CPT sounding Control Shaft location. ....	218
Figure A-12. Site I CPT sounding Flat-Jack 1 location. ....	219
Figure A-13. Site I CPT sounding Flat-Jack 2 location. ....	220
Figure A-14. Site I CPT sounding Sleeve-Port 1 location. ....	221
Figure A-15. Site I CPT sounding Sleeve-Port 2 location. ....	222
Figure A-16. Site I Control Shaft as-built. ....	223
Figure A-17. Site I Flat-Jack 1 as-built. ....	224
Figure A-18. Site I Flat-Jack 2 as-built. ....	225
Figure A-19. Site I Sleeve-Port 1 as-built. ....	226
Figure A-20. Site I Sleeve-Port 2 as-built. ....	227
Figure A-21. Site II SPT boring log B-3 (1 of 2). ....	228
Figure A-22. Site II SPT boring log B-3 (2 of 2). ....	229
Figure A-23. Site II SPT boring log B-4 (1 of 2). ....	230
Figure A-24. Site II SPT boring log B-4 (2 of 2). ....	231
Figure A-25. Site II CPT sounding CPT-69. ....	232
Figure A-26. Site II Control Shaft as-built. ....	233
Figure A-27. Site II Flat-Jack as-built. ....	234
Figure A-28. Site II Sleeve-Port as-built. ....	235
Figure A-29. Site III concrete mix design (1 of 2). ....	236
Figure A-30. Site III concrete mix design (2 of 2). ....	237
Figure A-31. Site III drilled shaft detail. ....	238
Figure A-32. Site III boring S-1 and S-2. ....	239
Figure A-33. Site III boring S-3 and S-4. ....	240
Figure A-34. Site III boring S1-A. ....	241
Figure A-35. Site III boring N-1. ....	242
Figure A-36. Site III boring N-2 and N-3. ....	243
Figure A-37. Site III boring N-4 and N-5. ....	244
Figure A-38. Site III boring N-5A. ....	245
Figure A-39. Site II SPT boring log LT-3 location (1 of 4). ....	246
Figure A-40. Site III SPT boring log LT-3 location (2 of 4). ....	247
Figure A-41. Site III SPT boring log LT-3 location (3 of 4). ....	248
Figure A-42. Site III SPT boring log LT-3 location (4 of 4). ....	249
Figure A-43. Site III LT-3 as-built. ....	250

Figure A-44. Site III LT-3 strain gage locations. ....	251
Figure A-45. Site III LT-3 inspection log. ....	252
Figure A-46. Site III LT-3 concrete log (1 of 3). ....	253
Figure A-47. Site III LT-3 concrete log (2 of 3). ....	254
Figure A-48. Site III LT-3 concrete log (3 of 3). ....	255
Figure A-49. Site III LT-3 concrete cylinder break strengths. ....	256
Figure A-50. Site III LT-3 construction details (1 of 5). ....	257
Figure A-51. Site III LT-3 construction details (2 of 5). ....	258
Figure A-52. Site III LT-3 construction details (3 of 5). ....	259
Figure A-53. Site III LT-3 construction details (4 of 5). ....	260
Figure A-54. Site III LT-3 construction details (5 of 5). ....	261
Figure A-55. Site II SPT boring log LT-2 location (1 of 4). ....	262
Figure A-56. Site III SPT boring log LT-2 location (2 of 4). ....	263
Figure A-57. Site III SPT boring log LT-2 location (3 of 4). ....	264
Figure A-58. Site III SPT boring log LT-2 location (4 of 4). ....	265
Figure A-59. Site III LT-2 as-built. ....	266
Figure A-60. Site III strain gage locations. ....	267
Figure A-61. Site III LT-2 strain gage locations. ....	268
Figure A-62. Site III LT-2 inspection log. ....	269
Figure A-63. Site III LT-2 concrete log (1 of 3). ....	270
Figure A-64. Site III concrete log (2 of 3). ....	271
Figure A-65. Site III LT-2 concrete log (3 of 3). ....	272
Figure A-66. Site III LT-2 concrete cylinder breaks. ....	273
Figure A-67. Site III LT-2 construction details (1 of 6). ....	274
Figure A-68. Site III LT-2 construction details (2 of 6). ....	275
Figure A-69. Site III LT-2 construction details (3 of 6). ....	276
Figure A-70. Site III LT-2 construction details (4 of 6). ....	277
Figure A-71. Site III LT-2 construction details (5 of 6). ....	278
Figure A-72. Site III LT-2 construction details (6 of 6). ....	279
Figure B-1. Site I Flat-Jack 1 grouting displacement vs. time. ....	280
Figure B-2. Site I Flat-Jack 1 grouting pressure vs. time. ....	280
Figure B-3. Site I Flat-Jack 1 grouting load vs. displacement. ....	281
Figure B-4. Site I Flat-Jack 1 grouting area ratio vs. active grout time. ....	281
Figure B-5. Site I Flat-Jack 2 grouting displacement vs. time. ....	282
Figure B-6. Site I Flat-Jack 2 grouting pressure vs. time. ....	282
Figure B-7. Site I Flat-Jack 2 grouting load vs. time. ....	283
Figure B-8. Site I Flat-Jack 2 grouting area ratio vs. active grout time. ....	283
Figure B-9. Site I Sleeve-Port 1 grouting displacement vs. time. ....	284
Figure B-10. Site I Sleeve-Port 1 grouting pressure vs. time. ....	284
Figure B-11. Site I Sleeve-Port 1 grouting load vs. time. ....	285
Figure B-12. Site I Sleeve-Port 1 grouting area ratio vs. active grout time. ....	285
Figure B-13. Site I Sleeve-Port 2 grouting displacement vs. time. ....	286
Figure B-14. Site I Sleeve-Port 2 grouting pressure vs. time. ....	286
Figure B-15. Site I Sleeve-Port 2 grouting load vs. time. ....	287

Figure B-16. Site I Sleeve-Port 2 grouting area ratio vs. active grout time. . . . .	287
Figure B-17. Site II Flat-Jack grouting displacement vs. time. . . . .	288
Figure B-18. Site II Flat-Jack grouting pressure vs. time. . . . .	288
Figure B-19. Site II Flat-Jack grouting load vs. time. . . . .	289
Figure B-20. Site II Flat-Jack grouting area ratio vs. active grout time. . . . .	289
Figure B-21. Site II Sleeve-Port grouting displacement vs. time . . . . .	290
Figure B-22. Site II Sleeve-Port grouting pressure vs. time. . . . .	290
Figure B-23. Site II Sleeve-Port grouting Load vs. time. . . . .	291
Figure B-24. Site II Sleeve-Port grouting area ratio vs. active grout time. . . . .	291
Figure B-25. Site III LT-3 grouting displacement vs. time. . . . .	292
Figure B-26. Site III LT-3 grouting pressure vs. time. . . . .	292
Figure B-27. Site III LT-3 grouting load vs. time. . . . .	293
Figure B-28. Site III LT-3 grouting area ratio vs. active grout time. . . . .	293
Figure B-29. Site III LT-2 grouting displacement vs. time. . . . .	294
Figure B-30. Site III LT-2 grouting pressure vs. time. . . . .	294
Figure B-31. Site III LT-2 grouting load vs. time. . . . .	295
Figure B-32. Site III LT-2 grouting area ratio vs. active grout time. . . . .	295
Figure C-1. Site I Control shaft load vs. displacement. . . . .	296
Figure C-2. Site I Flat-Jack 1 load vs. displacement. . . . .	297
Figure C-3. Site I Flat-Jack 2 load vs. displacement. . . . .	298
Figure C-4. Site I Sleeve-Port 1 load vs. displacement. . . . .	299
Figure C-5. Site I Sleeve-Port 2 load vs. displacement. . . . .	300
Figure C-6. Site II Control shaft load vs. displacement. . . . .	301
Figure C-7. Site II Control shaft load vs. deflection (large deflection scale). . . . .	302
Figure C-8. Site II Flat-Jack load vs. deflection. . . . .	303
Figure C-9. Site II Sleeve-Port load vs. deflection. . . . .	304
Figure C-10. Site III LT-3 cycle 1 load vs. displacement (control). . . . .	305
Figure C-11. Site III LT-3 cycle 2 (grouted). . . . .	306
Figure C-12. Site III LT-2 cycle 1 (control). . . . .	307
Figure C-13. Site III LT-2 cycle 2 (grouted). . . . .	308

# 1. INTRODUCTION

## 1.1 Problem Statement

The use of drilled shafts as structural support has recently increased due to heightened lateral strength requirements for bridge foundations and the ability of drilled shafts to resist such loads. The term drilled shaft is also known worldwide as cast-in-situ piles, bored piles, rotary bored cast-in-situ piles, or simply shafts. They are particularly advantageous where enormous lateral loads from extreme event limit states govern bridge foundation design (i.e. vessel impact loads). Additional applications include highmast lighting, cantilevered signs, and most recently, cellular phone and communication towers. With respect to bridge construction design procedures, both axial and lateral load scenarios have been additionally impacted where increased unsupported pile lengths are mandated by scour depth predictions based on 100 year storm events. This dramatically changes driven pile construction where piles often can not be driven deep enough without over stressing the piles or without pre-drilling dense surficial layers. In contrast, drilled shaft construction is relatively unaffected by scour depth requirements and the tremendous lateral stiffness has won the appeal of many designers. However, drilled shaft design and construction is plagued with quality control issues (i.e. shaft bottom cleanliness or open excavation time) not experienced by pile driving.

Typically, designers must significantly reduce end bearing capacity or even discount it altogether to account for soft toe conditions when constructing drilled shafts in cohesionless soils (sands). Even in ideal conditions, end bearing is typically not mobilized in this soil type before service load displacement criteria are exceeded. The bulk of the capacity is therefore derived from side friction which can be developed with relatively small displacements. Consequently, the end bearing strength component in these cohesionless soils, which may be on the order of up to twenty times the side friction component, is unavailable to the shafts useful capacity (AASHTO, 1997).

## 1.2 Objectives

As the end bearing component of drilled shafts is highly under utilized, the overall goal of this study was to quantify the improvement that could be developed by pressure grouting the tip of the shaft. Therein, an effort to determine the usable contribution of the tip for design would be evaluated.

The research program at U.S.F. consisted of both full-scale (Dapp 2001), and a model-scale study (4 in. diameter) carried out within a frustum confining vessel (Frederick 2001) to concurrently evaluate some of the parameters affecting post-grouting performance. From these tests, guidelines for design and construction of tip-grouted drilled shafts were developed.

The full-scale testing was divided into three different sites where drilled shafts were constructed. All three of these sites were located in Florida: Sites I and II in Coastal Caisson Corporations equipment yard (5 shafts total tipped in shelly sand, and 3 shafts total tipped in silty sand, respectively), and Site III at the new Royal Park bridge (hwy 704) in West Palm Beach (2 shafts total tipped in cemented coquina).

### 1.3 Work Summary

The work plan was based on the tasks outlined in the original request for proposals (RFP) and addressed each of the objectives of the proposed study. This work plan included the compilation of information, lab-scale testing, site investigation and selection, instrumentation and installation of drilled shafts, post-grouting, full-scale load testing, and the subsequent development of design and construction guidelines.

The full-scale test matrix is shown in Table 1-1 that details each of the ten shafts tested and the significance of each.

Table 1-1. Full Scale Test Matrix

Site, and Soil Type	Grouting Apparatus Utilized				None (Control)	Total Shafts Load Tested
	Sleeve-Port (Tube-a-Manchette)		Flat-Jack (Pre-Load Cell)			
	With Plate Above Sleeve-Port	No Plate Above Sleeve-Port	Lock In Grout Pressure	Release Grout Pressure		
Site I Shelly Sand	1	1	1	1	1	5
Site II Silty Sand	1	0	1	0	1	3
Site III Cemented Coquina	0	0	2	0	2	4

## **1.4 Organization**

The background into the use of drilled shafts, grouting, and post-grouting drilled shafts is summarized in Chapter 2. Cited references, primarily from Chapter 2, are listed in the Reference section.

The model-scale study was conducted at the Frustum Testing Facility located on the University of South Florida campus. A complete description of the experimental program developed is presented in Chapter 3. Appendix A contains the plots generated from the lab-scale testing.

A description of the full-scale test program and details of the full-scale testing are described in Chapter 4. Results of the full-scale test program are presented in the following chapter, Chapter 5. Analysis of the Chapter 5 results is included in Chapter 6 with the conclusions and recommendations summarized in Chapter 7. Pertinent construction records and the soil investigations for all three Sites are contained in Appendix B. Reduction of the data obtained during the grouting of all shafts is contained in Appendix C, while the load test data reduction is contained in Appendix D.

This page is intentionally blank.

## 2. BACKGROUND

In the early 1960's, efforts began to obtain more usable tip capacity of drilled shafts using pressure grouting below the shaft tip. In 1975, Gouvenot and Gabiax presented results of a test program where post-grouting large diameter shafts led to increased ultimate load capacities up to three times in sands and clays. As a result, post-grouting techniques have become a routine construction process in many parts of the world (Bruce, 1986). The post-grouting process entails: (1) installation of grout pipes during conventional cage preparation that extend to the bottom of the shaft reinforcement cage, and (2) after the concrete in the shaft has cured, injection of high pressure grout beneath the tip of the shaft which both densifies the in-situ soil and compresses any debris left by the drilling process. By essentially preloading the soil beneath the tip, end bearing capacities can be realized within the service displacement limits.

Although the performance of a drilled shaft is bounded by the maximum contribution of end bearing and skin friction components, these values are not fully realized due to flaws introduced by full scale construction techniques. Three mechanisms, or combinations thereof, are responsible for the excessively large shaft displacements required to develop bearing capacity in sands and clays:

- (1) Strain incompatibilities typically exist between the end bearing and side friction components in relation to service displacement criteria. The ultimate side frictional component develops with relatively small shaft displacements compared to the displacements required to mobilize ultimate end bearing. Development of the side friction component can be 50% of ultimate at displacements of approximately 0.2% of the shaft diameter (D) (AASHTO, 1997), and fully developed in the range of 0.5 to 1.0 % D (Bruce, 1986). In contrast, mobilization of the end bearing component can be 50% mobilized at 2.0% D (AASHTO, 1997), and fully mobilized in the range of 10 to 15% D (Bruce, 1986). The end bearing component therefore requires 10 to 30 times more shaft displacement in order to mobilize the same percentage of its ultimate value than the side shear component. This means that the side friction is strained well beyond its ultimate strength and into a residual state by the time the end bearing capacity is realized. In addition, the service load deflection criterion is often exceeded long before any significant amount of end bearing can be developed.
- (2) The shaft toe zone is often disturbed by normal construction procedures in cohesionless soils. This disturbance can occur by soil stress relaxation due to excavation of the overburden, inflow of groundwater due to insufficient hydrostatic head or rapid removal of the excavation tool during the construction process. This soil disturbance of the shaft toe zone is often difficult or nearly impossible to eliminate. Displacements necessary to overcome this disturbance and mobilize end bearing are usually in excess of allowable service limits. In instances of less

competent cohesionless soils, such as loose sands, this problem is further compounded.

- (3) Construction methods and processes may leave soft debris/deposits at the bottom of the excavation. Primary contributing factors are: overall shaft bottom cleanliness, a non-uniform distribution of toe debris causing an initially reduced shaft area bearing on the soil, excessive sand content in the drilling fluid, prolonged time for cage and concrete placement, and deposits of drilling fluid itself at the bottom. Toe inclusions resulting from typical construction methods may cause excessive displacements to mobilize end bearing, not evident in an otherwise clean excavation.

Depending on soil type and drilling method, any or all of the above mechanisms may occur at a given excavation. However, each scenario can be mitigated by a procedure, relatively unused in the United States, where post-grouting is performed beneath the shaft tips. This grouting concept accommodates the trend toward large diameter drilled shafts due to lateral load considerations, while allowing for the end bearing component to contribute to the useful capacity of the shaft.

## **2.1 Soil Type Applicability**

End bearing strata may be grouped into three broad categories in relation to the process of post-grouting shaft tips. These categories are cohesionless soils (sands to silts), cohesive soils (clays), and soft or fractured rock formations. Although all soils can be improved to some degree by grouting techniques, the applicability and effectiveness of grouting, primarily compaction grouting, will be many times more effective in cohesionless soils than other soil types (Baker and Broadrick, 1997). Historically, nearly all of the studies and construction projects involving grouting of the shaft tips to increase end bearing have been in cohesionless soils.

### **2.1.1 Sand and Silt**

The first effective large scale grouting of shaft tips was performed in sandy soils in 1961 at the Maracaibo Bridge (Sliwinski, 1984). Since then, many studies and construction projects have proven the extreme benefits of post-grouting the shaft tips in cohesionless soils (Piccione in Cairo, 1984; Sliwinski and Fleming, 1984; Logie in Jakarta, 1984; Stocker in Jeddah-Mecca Expressway, 1983; and Bauer in Brooklyn, NY, 1988). In general, results have shown that the post-grouting of shaft tips in cohesionless soil significantly increases the end bearing capacities. Figures 2-1, 2-2 and 2-3 show the effectiveness of post-grouted shafts.

Loose to medium dense sands hold the highest potential for increase in useable shaft end bearing. This is due to this soil profile being the most susceptible to the three mechanisms contributing to lack of shaft end bearing as outlined in the previous section.

Two different grouting methods, permeation grouting and compaction grouting, are applicable to these soils. The permeation grouting can easily create a very large grout bulb, and compaction grouting can dramatically improve the soil stiffness. Both processes can be done with the use of ordinary cementitious grout.

Dense sands can be both permeation and compaction grouted with cementitious grout in the same manner as loose sands. However, a micro-fine cement may become necessary for permeation grouting, and may not yield significant improvement over compaction grouting alone. The grout volume used in dense sands would be significantly less. Bruce (1986) reviewed many cases to state that there is a direct relationship between ultimate load increase and volume of cement grout injected for all sands; when grouting dense sands the grout volume simply corresponded to the void volume of the gravel pack (discussed later, Figure 2-10).

Sandy silts can be densified by means of applying effective stresses during compaction grouting with ordinary cementitious grouts, although it is less effective than compaction grouting of clean sands. Permeation grouting in silty soil, however, would involve the use of chemical grouts, such as a silica gel, and is beyond the scope of this research.

Although disturbance to the shaft toe area during construction is of little practical importance in soft rocks and clays (Sliwinski and Philpot, 1980), Sliwinski and Fleming (1984) concluded that in sands the end bearing contribution to the total load capacity is extremely sensitive to construction induced soil disturbances. Therein, full scale load testing was used to verify the effectiveness of pressure grouting for mitigating these conditions.

### **2.1.2 Clay**

Post-grouting in clay produces only a minimal gain in end bearing governed by the amount of consolidation that can occur within the set time of the grout. The high pressures introduced by this method may only result in hydro-fracture of the soil matrix. Careful consideration would be needed so that the allowable end bearing contribution, even after grouting, would not exceed the creep limit of the clay at the grout bulb/soil interface. The most effective way of grouting in clay material would be to jet-grout, or deep-soil-mix under the shaft tip. While these are certainly viable options for remediating deep foundations in this soil type, it is not the focus of this research.

### **2.1.3 Rock**

Grouting of fractured and soft rock formations, with low strength grouts, to fill voids, fractures, seams, and solution channels are sometimes conducted to alleviate drilling problems associated with karst topography. However, this is usually accomplished prior to drilling, and is not the grouting technique that is discussed herein. These formations

typically are incapable of consolidation or densification by effective stresses induced by compaction grouting. Further, permeation grouting of the macro inclusions may effectively be accomplished by the concrete head during normal construction, as is evidenced by high concrete over-runs in such cavernous strata.

Although grouting can effectively mitigate soft toe conditions caused by excessive construction debris/deposits at an excavation bottom for all soils, current quality control procedures for drilled shaft production already effectively address shaft bottom cleanliness for clay and rock during normal construction. Thus, only a marginal benefit would be realized in these conditions through the use of post-grouting. An exception may be where shaft bottom cleanliness is problematic due to extreme depths and time requirements such as the My Thuan Bridge Project, Vietnam (Dapp, 1998), where shafts were 328 ft (100 m) deep and took approximately 72 hours to construct, or for cases where the capacity of shafts already constructed fall short of adequate (Logie, 1984).

#### **2.1.4 Uplift Considerations**

In general, upward movement of shafts during compaction grouting should be limited such that the frictional strength of the shaft is not developed beyond its ultimate value and into a lesser residual value. This is most critical in dense sand where there is a pronounced loss of frictional resistance with large strains (Figure 2-4). Historically, uplift criteria have been limited to ranges from 2 mm (Stoker, 1983) to 20 mm (Bolognesi and Moretto 1973). Presently, in Taipei, a 3mm uplift criterion is in effect (Mullins, 1999). It is unclear, however, if these criteria were placed only on top-of-shaft movement or if the tip movement associated with elastic compression was also given a maximum permissible movement. Long shafts such as those in Taipei, 262 ft. (80 m), can exhibit relatively large displacements at the tip without being detected at the top (and vice versa).

Essentially, the maximum amount of end bearing improvement is dependent on how much downward resistance the side friction component of the shaft can provide. As such, post-grouting can also be applied to the sides of the shaft to improve unit side friction values. This aids in providing downward restraint during the tip-grouting process (resisting uplift). This is of particular importance for shorter shafts, and as a consequence skin grouting has been employed to aide in providing reaction (e.g., Bauer system of shaft grouting). Additional criteria, of maximum grout volume (per stage) and minimum grout pressure, are established based on reasonable cavity expansion and the anticipated tip performance, respectively. Figure 2-5 shows grout pressures that have been used on various sites throughout the world in relation to the shaft tip depth.

## **2.2 Grouting Mechanisms**

Standard grouting techniques can be divided into two basic categories: permeation grouting and compaction grouting. Staged grouting procedures are often designed which

have a combination of these two, first permeation and then compaction. There are also state-of-the-art techniques available for cohesive soils, such as jet grouting or deep soil mixing, which alter the soil type and structure without inducing significant effective stresses.

### **2.2.1 Permeation Grouting**

Permeation grouting uses a fluid grout which is highly mobile within the soil formation, and therefore travels through the void spaces without providing any significant compaction or densification of the surrounding soils. In this manner a very large zone of improved soil below the shaft tip is developed. Careful adjustment of the water-to-cement ratio is used to control the mobility of the grout. The type of grout mix design is also crucial to achieve this mobility. For example Littlejohn (1983), at the Jeddah - Corniche Centre, first tried remediating substandard shafts with the use of a cement grout in a dense sand profile interbedded with hard sandy silt. However, grout takes were very low, and the remediation technique failed. Subsequently, a low viscosity resorcinol formaldehyde grout was successfully used.

### **2.2.2 Compaction Grouting**

In contrast to permeation grouting, compaction grouting utilizes a thick, viscous, homogeneous, typically cementitious mass designed to remain together within the soil matrix. Generally there is a distinct interface between the soil and grout material. Thus, the in-situ soil is consolidated and densified by cavity expansion of the grout bulb (Baker and Broderick, 1997). Grout mix designs for compaction grouting will be discussed in Section 2.4.

Compaction grouting develops its own "filter cake" at the soil/grout interface which differs from the Bauer system of grouting where a mechanical grouting system uses steel plates and an impermeable cover or a liner embedded between the plates (discussed later). In either case, the mechanism of soil improvement is the same; the grout applies an effective stress to the soil, thus densifying it. A notable difference is that the simple compaction grouting (i.e., with a filter cake) or a flexible membrane imparts a uniform stress condition at the shaft tip, whereas the mechanical compaction system of two steel plates with the grout pressure introduced between the two imparts a uniform strain condition. A potential benefit of compaction grouting the shaft tip is that this procedure could provide a means of proof testing shaft tip capacity during the compaction grouting procedure.

### **2.2.3 Staged Grouting**

The tip improvement has been shown to be generally correlated to grout take, and as this test program will show more appropriately to the maximum sustained grout pressure produced at the tip. Grout take is not always proportional to the pressure exerted, as the grout may find escape paths through weak, stratified, lensed, or highly permeable deposits.

As any escaping grout transports further from the shaft tip location, its contribution to the tip improvement diminishes rapidly, and cannot contribute to the beneficial locked in soil stress. If the soil stratum is likely to experience this, stage grouting is the effective alternative.

With staged grouting, the initial stage of grout injection is allowed to set and accumulate some strength before the subsequent stage of grout injection is performed. In this manner, the escape paths that the grout may find during an initial grouting stage are filled with set grout as the next grouting stage is injected. The procedure can be repeated many times until the soil beneath the tip can finally contain the grout pressure, and thus the soil mobilization, that is required of it. The limiting factor for tip improvement then becomes the amount of side shear available for the grout pressure to react against.

The sleeve-port design lends itself well to staged grouting, whereas the flat-jacks do not. Specific details of grout injection apparatus will be discussed in Section 2.3 to follow. The sleeve-ports incorporate a U shaped tube (U-tube) with the grout ports being covered by a rubber sleeve at the bottom of this U-tube. The rubber sleeve acts as a check valve that allows grout to escape, but not to return back into the line. This U-tube can thus be gently flushed with water once the grout pressure is released at the end of a grouting stage.

Flat-Jacks have a confined grout mass contained within an impermeable membrane/plate system, and the grout lines cannot be flushed without also removing the majority of the placed grout at the tips as well. Thus, flat-jack design does not lend itself to staged grouting. However, with the grout mass confined as such, it may not have the opportunity to transport through any potential escape paths, and may be an alternate consideration to staged grouting for these problematic soils.

The grout lines of the flat-jack (as well as a stem grouting tube) could be carefully flushed with an inner water tube inserted to full depth, as will be shown in Section 4.5.2. However, insufficient contact area (the cross-sectional area of the grout tubes only) would not allow the grout pressure to develop sufficient force against the set grout from the previous stage to break it free of the shaft tip and continue the soil compaction at the tip. Notable exceptions are the flat-jack designs utilized by (Lizzi, 1981) or (Bolognesi, 1973).

### **2.3 Grout Injection Apparatus**

Grouting techniques vary in the mechanism by which the grout is dispensed beneath the shaft tip. Variations include using:

- stem, sleeve-port, or flat-jack distribution system
- a gravel pack beneath the tip to aide in distribution of grout
- fixed or floating distribution system relative to the reinforcing cage
- permeation grouting, compaction grouting, or a staged combination.

Two basic distribution systems are mainly used: (1) *simple compaction grouting* in which the sleeve-port system employs a network of exposed grout tips, and (2) the *mechanical grouting system* in which the Bauer-type system of one or two steel plates with an impermeable membrane is used. Although both systems can be used in a wide variety of soils, the membrane-type mechanisms minimize hydro-fracture grout losses more common with sleeve-ports used in weakly layered soils.

### **2.3.1 Stem (Orifice)**

The simplest form of grout distribution is a pipe (or other pressure conduit such as a cored hole through an existing shaft) terminating at the desired grouting location. This system does not realize the many advantages of the sleeve-port and flat-jack systems that will be discussed in the following sections. As a result, this type of grouting apparatus is utilized as a remediation technique only, and is not a very efficient option given the opportunity to incorporate a distribution apparatus into the reinforcing cage prior to concrete placement. It has however been successful in remediating substandard shafts with inadequate capacity by its ability to be installed through a core hole to the shaft tip.

### **2.3.2 Sleeve-Port (Tube-a-Manchette)**

The sleeve-port, also known as a tube-a-manchette, has several variations, but is primarily a simple pipe network across the bottom of the shaft pre-drilled along its length on the bottom face and connected to grout tubes to the top of the shaft. The pipes are wrapped in a rubber membrane at the location of the holes to prevent the blockage of grout passage during normal shaft construction where the tubes become completely encased in concrete. A problem with fixed sleeve-port systems is that the concrete encapsulation of the sleeve-ports must be burst almost immediately after the concrete has set (24 to 48 hours), while its strength is still low. A simple sleeve-port system fixed to the cage and resting on the bottom of the excavation was used in the shafts supporting a major cable stay bridge in Thailand in 1985, as shown in Figure 2-6. A similar configuration has recently been used for the foundations supporting the cable-stay bridge over the Mekong River in Vietnam (Dapp, 1998). Presently, at the Taipei Financial Center project in Taiwan, an adaptation is being employed that closely contours the pipe network to the shaft bottom (Figure 2-7). The shape resembles the reverse circulation cutting tool and minimizes the concrete cover between the grout pipes and the shaft bottom.

Complications can arise if the excavation depth is lower than the sleeve-port elevation. In such instances, the grout pressure is unable to break the encapsulation and modify the soil. Such was the case when the first 90 m (295 ft.) deep excavation in Vietnam was inadvertently over-excavated by approximately 0.5 m (1.6 ft.) by way of extensive clean out procedures. This caused the sleeve-port to be embedded in the extra 0.5 m (1.6 ft.) of concrete. To avoid this problem, floating sleeve-ports were used for subsequent shafts which used slip joints allowing the distribution system to adjust to the actual bottom of

excavation elevation. Other systems have used flexible grout hoses to overcome this problem. It is thus recommended that suspending the sleeve-port, by either method, should be considered necessary for proper steel placement of extremely long shafts where cage length and excavation depths may not be consistent, or for instances where top of steel set is critical.

Sliwinski and Fleming (1984) described first placing a gravel plug in the excavation, then the sleeve-port with a steel plate above (both suspended from the cage). This configuration is shown in Figure 2-8. The steel plate has the benefits of isolating the sleeve-port and gravel plug from the concrete so that the post-grouting process can take place after the concrete has gained design strength, the sleeve-port is protected from the tremie during concreting operations, and the steel plate gravel interface provides a consistent bearing surface for the compaction grouting pressure to act against (important for proof testing aspects). The gravel is beneficial for both permeation and compaction grouting by exposing more soil interfaces to the grout, as well as providing aggregate to knit the soil bulb together directly below the shaft tip.

### **2.3.3 Flat-Jack (Pre-Load Cells)**

Lizzi (1981) discussed a mechanism consisting of two steel plates separated by mechanical spacers (to allow grout pressure to initially act upon the full face of the plates). This technique is similar to the Bauer system of tip grouting used on the Jeddah- Mecca Expressway (Bruce, 1983) and the Brooklyn Queen's Expressway (1988). The difference is that Lizzi had the plates covered with an impermeable liner to ensure that separation of grout injection ports and concrete was maintained (see Figure 2-9). The impermeable liner ensured that no permeation into the surrounding soil occurred. Consideration can also be given as to whether a gravel pack should be included between the two plates, as was discussed in the early work by Bolognesi and Moretto in Paranah River (1973), shown in Figure 2-10. The benefit of the gravel pack again is as stated above; however, this configuration must be suspended from, and lowered into the excavation with the cage which may become cumbersome in a high production-oriented setting.

## **2.4 Grout Mixes**

Applications of grouting in civil engineering projects are as widespread and diverse as the grout mixes used to service them. Understandably, the selection of an improper grout mix could be devastating to the success of a project. In the ensuing sub sections, an overview of mechanisms, methodologies, and physical parameters of grout mixes will be presented with emphasis on post-grouting drilled shaft tips.

### **2.4.1 Grout Mixers**

In the planning of full scale grouting procedures considerations should be given to the selection of the grout mixer type. A. C. Houlsby (1990) uses three classifications to describe grout mixers based on their ability to create a high quality semi-colloidal grout. Semi-colloidal describes a suspension of finer particles (in this case, cement, fine aggregates, and/or related additives) that resist settling or segregation. Grout mixers are simply classified as: high-quality, less efficient, and lower quality grout mixers. Applications using high pressures or small diameter access lines should use high quality mixers capable of creating a semi-colloidal mix. Applications with larger access lines and lower pressures can use lower quality mixers. A high quality or high-shear mixer, as shown in Figure 2-11, approaches a colloidal mix but in actuality produces a mechanically suspended mix. These mixers use high rotational velocities above 1500 rpm and require shorter mixing times. This style of grout mixers should be used when additives such as bentonite, metakaolin, or fly ash are required. These additives require high mixing speeds to create a homogeneous mix that will not segregate or leach during the fluid or hardened states of the grout.

The less efficient mixers have lower rotational speeds between 700 - 1000 rpms, and require more time for the grout to make multiple passes through the mixer to form a homogenous mix, Figure 2-12. These mixers are typically incapable of handling sands and will require more time in mixing of fine additives found in high quality grouts.

Lower quality mixers typically rely on a revolving paddle blade (Figure 2-13). These mixers have extremely long mixing times due to the low shear and mixing energy. A lower quality mixer will be insufficient to produce a high quality grout unless a secondary mixer is used to pre-mix the individual constituents, at which time, the lower quality mixer is used to combine the pre-mixed constituents. The quality of the mixer directly relates to the quality of the grout. Therefore, the quality of the mixer is dependent on the job and grout requirements.

### **2.4.2 Grout Pumps**

The volume and quality of grout as well as the pressure specified by job requirements determine the type of pump that should be used. Table 2-1 (Baker, 1982; Houlsby, 1990; Wagner, 2000c) shows the pressure ranges that can be expected from various pump types.

Table 2-1. Descriptions of Various Pumps

<b>Pump Classification</b>	<b>Max. Pressure</b>	<b>Constituents</b>	<b>Applications</b>
Helical (Single Stage)	150 psi	Neat Cement Slurries, No Sand	Ground Anchors, Soil Fracturing
Helical (Multiple Stages)	300 psi		
Double Diaphragm	800 psi		Low Volume, Non Robust
Ram	840 psi		
Piston (Single Stage)	1500 psi	Sand Grouts, Any	Compaction and Jet Grouting
Piston (2 or 3 Stage)	4-5000 psi		

There are two methods in which pumps work, either continual pumping or cyclic pumping. The continual pumps, such as helical rotor or centrifugal, provide continual pressures during the pumping of the grout (Figure 2-14). These pumps have a maximum pressure of 150 psi (Baker, 1982 and Houlsby, 1990) and when stacked (in series) can achieve pressures of 300 psi (Houlsby, 1990).

Cyclic pumps, such as piston, ram, diaphragm, and hand pumps, produce pulsing pressures throughout the grouting process (Figures 2-15 and 2-16). Piston pumps can typically handle higher pressures, up to 5000 psi (Wagner, 2000c), during the grouting process. With the use of 4-6 pistons, continual flow can be closely achieved.

Depending on the pump that is used, the grout needs to flow through the pump without causing blockages in the pump or damage to the blades, pistons, diaphragms, or rams. Therein the use of some aggregates may not be applicable. The grout mix design also needs to take into account any changes in the inner diameter of the pump or changes in the direction of travel. As such, unnecessary reductions in grout access lines cross-sections should be avoided. These changes can cause the grout to build up by water segregation from the paste and block the flow through the pump.

### **2.4.3 Access Lines**

The selection of access lines is integral with the grout design and its application. The distance from the pump to the site of grouting as well as the internal configuration of access lines can be instrumental in the success of a grouting program (Figure 2-17).

If there are access lines already in place then the grout mix will have to be designed with this variable fixed (i.e., smaller access lines may exclude the use of sand aggregates). If the aggregate, in the grout mix, is large in comparison to the cross sectional area of the access lines the friction and shear stresses in the grout mix will create a block in the line and impede grout flow (Figure 2-18) (Day, 1995). Minimum access line diameters should be specified as will be discussed in Section 2.4.5, Table 2-2.

### **2.4.4 Grout Mixing**

The general grout mixing method prescribes that addition of constituents begin with the finest particle size constituents and progress to the coarser particle sizes. The addition of the constituents for grout should start with the addition of the water followed by the additives, the cement, and finishing with the addition of the sand and a final mixing time (Dunnicliff, 1988). Some of the additives require large amounts of water and a long time to completely hydrate. When using these additives, a feasible solution is to use pre-hydrated additives instead of adding the dry additives to the water and forcing the mixer to hydrate the additive rapidly. Non-uniform clumps of bentonite and cement will be formed when the additive bentonite is mixed at high rotational speeds for a short time and not allowed to hydrate fully. This causes poor pumpability and lower compressive strengths. Other considerations are the addition of the fine and coarse aggregate (if applicable) and the addition of the admixtures to the mix. Unlike concrete mixes, grout mixes require the addition of fine and coarse aggregates after the cement has been added to the mix.

At the time of the grouting, a thinner paste is mixed and used as a primer for the mixer and re-circulation systems. Depending on the mixer, the pump, or the grouting process, the thinner mix will be followed by the addition of additional cement and/or sand after the paste has been thickened in an attempt to prevent blockages by a sudden introduction of larger particles or a more dense mix into the systems.

### **2.4.5 Grout Properties**

The fresh and hardened property requirements of grouts will vary from one project to the next and understanding these properties and how they can describe a grout mix is needed to determine the applicability of a grout for a specified grouting process. The fresh properties of a grout mix are the flow, the pumpability, viscosity, and the colloidal nature of the grout. Typical flow values for grouts are generated from a flow table, a slump cone test, or a marsh cone. However, a flow value does not accurately relate back to the ability of a grout to be pumped (Baker, 1997), especially at higher pressures. For example, cement

grout with a w/c ratio of 0.2, by weight, but dosed with a high dosage of a high range water reducer will produce a high slump mix. Yet if this mix is pumped, the mix will be too dense and blockages can occur especially given any changes in cross-sectional area.

Pumpability refers to the ability of a grout to be pumped. There have been many mechanisms or devices that have tried to quantify this value but with the varying job requirements, pumps and grouting access lines, a grout that is pumpable for one system might not work well with another. A grout should be classified as a pumpable using the following criteria: pump type, pressures expected, access line dimensions, and time of pumping a single mix. Therefore, a sand-cement grout that is easily pumped through a 3-inch inner diameter access line would be impossible to pump through a 0.5-inch grout line. Recommendations for the suggested size of access line and pump based on maximum aggregate size are presented in Table 2-2 (Mullins, 2000; Wagner, 2000a; Wagner, 2000c).

Table 2-2. Minimum Pump Size Based on Aggregate Classification

<b>Aggregate Size</b>	<b>Minimum Pump Size (outlet nozzle dia.)</b>
67 rock and larger	Greater of 2*Max Agg. Or 3*Nom. Agg
57 rock to 5 rock	4 inch Minimum Pump
89 rock to 6 rock	3 inch Minimum Pump
Fine Aggregate	2 inch Minimum Pump
Cement and Additive Grouts	12 mm Minimum Pump

Viscosity is the ability of a fluid or semi-fluid to develop and maintain an amount of shearing stress dependent on the amount of flow and then to offer continued resistance to flow. It is important for grouts to have a marginal amount of viscosity but not so much as to greatly impede the pumping process.

A very valuable fresh property, at high pressures, is the ability of a grout to remain at a near colloidal state. Grouts that are semi-colloidal or near colloidal are grouts that are mechanically suspended through the mixing process. By creating a near colloidal grout mix, it is possible to pump grouts at high pressure with more drastic changes in the pump and access line geometry while ensuring the grouting process can be fully developed.

Some of the hardened properties of grouts that need to be ensured are the compressive strength, the leaching or segregation, the creep, and bleeding (a quasi-hardened property). The compressive strength requirement of a grout will vary from one project to the next. It is typically specified based on the stresses anticipated by the structure; but can

be based on the permeability, chemical inertness, or durability. In general, when installing instrumentation such as inclinometer casings or magnetic extensometers for soil measurements, the grout strengths should not exceed the soil strengths (Dunnicliff, 1988). The grout needs to be flexible in order for the instrumentation to take accurate soil data. With grouted soils the required strength should exceed the compressive strengths of the soils. In drilled shaft construction, the typical strengths of the concrete mix are far stronger than that of the soil. The magnitude of strength requirements in shaft tip grouting should start with the AASHTO LRFD for bridge design using the Reese and Wright or Reese and O'Neill methods which specify the maximum tip resistance to be 40 and 45 TSF, respectively, Figure 2-19 (AASHTO, 1998). This correlates to a maximum compressive strength of 555 psi and 625 psi respectively. Grouted shafts may exhibit tip capacities many times higher than un-grouted shafts. The grout strength should reflect this higher anticipated capacity.

The leaching of the grout constituents occurs when a grout mix is poorly mixed or designed. With a poorly mixed grout the cement is not allowed to create a matrix in which the additives or aggregate will remain and therefore washes out of the grout in the hardened state (Houlsby, 1990). When segregation occurs, the area that was grouted can be left in a condition worse than the initial condition. In compaction grouting processes, the grout compacts the soil in the target area and then cures to occupy that space. In addition, segregation can also occur in sand grouts in access lines with high water contents when there is a pause in the pumping allowing the sand to settle to the bottom of the lines (Wagner, 2000a). Segregation can also occur with compliant (elastic) lines when the pumping pressure is not constant causing expansion and contraction of the lines. However, when grouting sands, high w/c ratios (0.4-0.6) can be used (providing the mix is stable) knowing that the water will squeeze into the soil leaving a lower w/c ratio grout bulb.

With increased w/c ratios there will be increased amounts of creep and bleed water. These two variables can be detrimental to the intended purpose of the grout. If there is a large amount of creep in a grout over time the effects of the compaction may be lessened due to the relaxation of the soil. This is similar to relaxation of post tension cables as a result of creep. Bentonite is a fine additive that can be used to minimize bleed water that can accumulate in high w/c ratio grouts (Ramachandran, 1995).

#### **2.4.6 Grout Constituents**

The materials (constituents) that are used in grout mixes are water, cement, aggregates, and admixtures/additives. The water used can have drastic effects on the performance of the grout. For simplicity, water can be divided into three categories; de-ionized, tap, and salt water. De-ionized water is commonly used in laboratory experiments where the highest quality assurance is needed. De-ionized water will have no chemicals or particles that will adversely interact with the hydration process. Tap water is the most common form of water that is used in mixing of grouts and concretes. Tap water contains some chlorides that will act as an extremely mild accelerator. The amount of the chloride

is so low that the effect is negligible as its concentration is far below the corrosion threshold concentration. Salt water is typically not used. The high chloride content acts as an accelerator, decreasing the set time, and potentially decreasing the ultimate strength of the grout mix (Figure 2-20) (Domone, 1990).

Over time, many different types of cement have been manufactured (Day, 1995; Ramanchandran, 1995; Rixom, 1999). The most common type of cement is Portland cement. Portland cement is broken down into five different types of cement, Table 2.3. Of the five types of Portland cement there are two types that are manufactured in any great quantities due to the advances in admixtures as well as the cost associated with manufacturing multiple types of cements.

Table 2-3. ASTM Designations for Portland Cements

ASTM Type	ASTM Designation	Composition				fine-ness cm <sup>2</sup> /g	Compressive Strength % of Type I cement		
		C <sub>3</sub> S	C <sub>2</sub> S	C <sub>3</sub> A	C <sub>4</sub> AF		1 Day	2 Day	28 Day
I	General Purpose	50	24	11	8	1800	100	100	100
II	Moderate Sulfate Resistant moderate heat of hydration	42	33	5	13	1800	75	85	90
III	High early strength	60	13	9	8	2600	190	120	110
IV	Low Heat	26	50	5	12	1900	55	55	75
V	Sulfate resisting	40	40	4	9	1900	65	75	85

Type I and Type II are very closely related in their physical and chemical properties. There is likely to be more difference in Type I from one manufacturer to the next than from Type I to Type II. This is now referred to as Type I/II. Type I/II and Type III are the two types that are most common.

Type I/II is a general construction type of cement used for most job requirements and Type III is a cement with a greater fineness leading to a higher early strength development. There are other types of cements that can be used including: micro-fine or fine cement

(Figure 2-21). Fine cements are Portland cements that are air-scaled to produce an even finer cement. Micro-fine cement combines a fine cement with blast furnace slag to create even finer cements (Houlsby, 1990). The finer the cement, the higher the flow of the paste. Unfortunately, fine cements require high water ratios and generate low compressive strengths (Rixom, 1999). In the design of a grout mix a decision should be made as to use either a Type I/II cement with admixtures or a finer cement with a higher w/c ratio. Post grouting processes typically use Type I/II.

Admixtures are constantly being developed and with more advances in admixtures, there are greater possibilities in the design of grouts. There are many admixtures available for concrete, grout and mortar mix designs. These are broken into two general categories: mineral and chemical admixtures. The term additive in grout design refers to either fines (e.g., bentonite, metakaolin, or fly-ash) or chemical admixtures that are added in larger than normal quantities. Additives will affect the flow, pumpability, viscosity, colloidal nature, compressive strength, and lessen the bleed water and may affect the set times, initial shrinkage, and the creep of a grout.

Mineral admixtures include pozzolans such as fly-ash, blast furnace slag and metakaolin and will generally have beneficial effects on the grout, however at times the benefits are not enough to warrant the added costs involved. Mineral admixtures will increase the total amount of fine material in a grout mix, which will add to the flow, pumpability, and lessen the bleed water (Figure 2-22) (Wagner, 2000c). With the reactivity of the pozzolans there will also be an increase in the ultimate compressive strength (Ramachandran, 1995). Other fine filler additives, bentonite and other clays, will increase the pumpability and the colloidal nature of the grout mix, with a decrease in the ultimate compressive strength of the grout because of the nature of the swelling and shrinking of the bentonite (Dunnicliff, 1988).

Chemical admixtures are more diverse than mineral admixtures. Chemical admixtures include: water reducers, retarders, accelerators, air en-trainers, de-air en-trainers, latexes, finishing agents, shrinkage reduction agents, corrosion inhibitors and many other chemicals that can be used to change the properties of a grout or concrete mix. For mixes that will be pumped, water reducers, retarders, and air en-trainers are mostly used. With the high pressures and temperatures that can be seen in pumping of concrete and grouts, the use of an accelerator is cautioned due the possibility of an even greater rate of acceleration leading to quicker set times than expected.

Water reducers can be used to increase the slump or flow of a mix at a constant w/c ratio, by creating an either neutral or positive ion system between the cement and water interface. This interaction will limit the ability of the cement and water to flocculate, increasing the paste's ability to flow. Grout mixes using water reducing admixtures can have higher strengths with a greater slump allowing for ease of placement and possibly better pumpability (Figure 2-23 and 2-24) (Rixom, 1999). Water reducers come in three levels of performance. They are classified by their ability to reduce the amount of water required.

Low range and mid range water reducers are the most common and achieve upwards of 15% water reduction. High range water reducers, or super plasticizers, act in the same way as do low or mid range water reducers but afford upwards of 30% water reduction (Figure 2-25) (Rixom, 1999). In dealing with admixtures it is important to know the manufacturer's specifications and recommended dosage rates for the admixtures being used. Some of the results of over dosing can be an increase in the bleed water, rapid loss of slump, extremely dense mixes, segregation of aggregates from the paste, and increase set times.

Retarders act by coating the cement grains and delaying the hydration process. Most retarders also have a water reducing component added to the admixture solution. Retarders may be useful for grouting systems that take a long time to complete or if high temperatures are expected. Retarders will allow the matrix of the hydration products to form in a more advantageous manner thus tending to yield a higher ultimate compressive strength. Over dosages of retarders can lead to incredibly long set times leading to an increase in cost and time.

Air entrainers are used to help concretes or grouts resist cracking from freeze-thaw cycles in colder climates. The use of an air entrainer will also provide additional flow to a mix. A high amount of entrained air can lead to the possibility of lower pumpability being created because the entrained air will create compressibility and cause blockages in lines and the pumps. The use of any mix design needs to be tested to ensure that all of the properties required for the grouting process will be met. This may require the in-situ pumping procedures to be tested as well as conventional strength and flow tests.

In grouting only fine aggregates (sands) are used on a regular basis. The variability of fine aggregates is hard to control. Fine aggregates come from a local supplier and can be either crushed or natural sands. Crushed aggregates are poorly graded and have angular shapes. Natural sands are well graded and have smooth edges. When pumping grout containing crushed aggregates it is necessary to increase the amount of fines in the mix in order to maintain the pumpability of the grout. Using a natural sand will have an increase in the fines and the smoother edges will create a higher pumpability (Wagner, 2000c).

#### **2.4.7 Grout Mix Design Examples**

The different applications of grouting will require that there are different mixes meeting the limitations of the grout mixer, pump, access lines, and can meet the specifications of the pressures that will be experienced, the strengths required and the pumping rates that will be used. The grout mixer, pump and access lines will limit the maximum particle size, the amount of fines and water that will be used in the grout mix. The higher the pressure that will be seen will dictate the need for more fines in a grout mix. The strength requirements will determine the cement content of the grout mix. Slower pumping rates are needed to minimize soil fracturing and heaving; therein requiring that a grout stay suspended at multiple flow rates. The following grout mix details should be considered:

- (1) In that most post grouted shaft projects use access lines 1" in diameter or smaller (Table 2-2), the use of sand mixes are immediately excluded from the user's options leaving only neat cement slurries.
- (2) The grout will be in direct contact with the tip of the shaft and therefore must be able to withstand the compressive stresses developed by the ultimate end bearing load.
- (3) The mixer type needs to be high quality or less efficient (greater than 700 rpm) so that the slurry is semi-colloidal which provides a stable grout mix during pumping.
- (4) Unless unusual circumstances exist, post-grouting shaft tips require small volumes of grout and therefore any pump that can produce sufficient grout pressure is acceptable (discussed in Chapter 7). However, some mechanism must exist that can track the grout take and pumping rate.
- (5) The water cement ratio should provide sufficient strength and pumpability parameters. These can be estimated using Figures 2-22 and 2-24, shown previously. Figure 2-22 correlated the grout strength to w/c ratios, while Figure 2-24 provided guidelines for pumpability expectations, both figures shown previously. FHWA (2000) suggests w/c values of 0.45 to 0.5 for sleeve port (sleeve-port) grouting systems. Higher values can be used in sleeve port systems (0.4 - 0.6) in sand in that some water will be expelled to the soil surrounding (Wagner, 2000c). When using flat jacks or rubber confining systems, no water can be expelled; hence, lower values should be used (typically no higher than 0.5). Figure 2-25 limits w/c ratios to a lower bound of 0.325, which from the experience of the researchers will require some form of a water reducing agent.
- (6) Pumping rates can affect the ability of the soil to resist hydro-fracturing. As such, the flow rate should be adjusted so that the developed pressure will increase steadily. If the rate of pressure increase drops, the pumping rate needs to be slowed or stopped to allow the soil to dissipate the increase in pore pressure. When using sleeve port systems, grouting can be terminated, access lines flushed with clear water, and grouting can resume when the grout has begun to set (or resume next day). A second option, for both rubber confined and sleeve port systems, is to slow pumping and decrease the w/c ratio creating a thicker, more viscous grout. If a rubber confined system fails to build pressure, a breach in the confining rubber is the probable cause; second day grouting is not a plausible option.

Grouts have been designed using many different methods. On jobs where large volumes of grout are not needed, grouts are designed using bags and volumes. For larger jobs the ACI Volumetric method is used. Table 2-4 gives several example design mixes used for various applications.

Table 2-4. Grout Mix Design Examples

<b>Cement</b>	<b>Water</b>	<b>Sand (lbs.)</b>	<b>Fly Ash (lbs.)</b>	<b>Field Notes / Comments</b>
500 lbs.	48.2 gal	2365	500	Mini-shaft compaction grout mix (Wagner, 2000c)
250 lbs.	48.2 gal	2252	750	Compaction grout mix (Wagner, 2000c)
250-500 lbs.	20 - 50 gal	1800-2200 lbs.	200 - 700 lbs.	Compaction grouting (optional 1%-2% admixture) (Mullins, 2000)
1 bag	7.5 gal	0	0	Site I and II grout mix (1:1 by volume) see Ch. 4, yields 1.5 ft <sup>3</sup>
1 bag	5 gal	0	0	Anchor Grouting, 4-6 ksi 2-3 in days (Baker, 1997)
.15 lbs.	1 lb.	.06 lbs. Bentonite		Probe extensometers in soft clays, 300 - 500 psi in 28 days (Dunnicliff, 1988)
.08 lbs.	1 lb.	.11 lbs. Bentonite		400 psi in 28 days (Dunnicliff, 1988)
2682 lbs.	97 gal	0	0	Post Grout Small Scale, 5-6 ksi in 3 days. 15 oz./cwt HRWR
1095 lbs.	153 gal	110 lbs. Bentonite		Post Grout Small Scale, 500 psi in 3 days, 1000 psi in 28 days, 4 oz./cwt HRWR

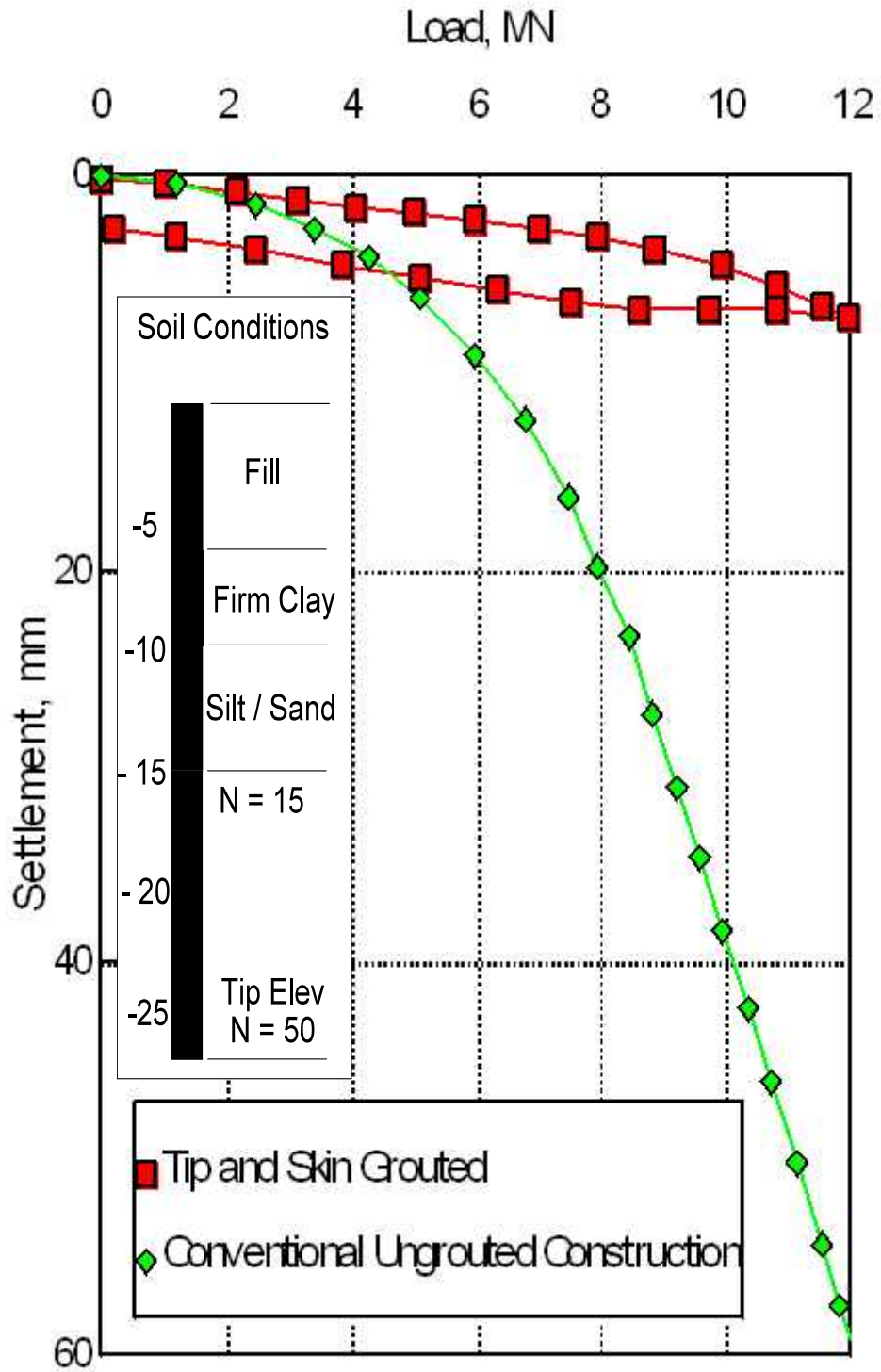


Figure 2-1 Comparison of two 1.5m diameter drilled shafts (Sliwinski, et al., 1984).

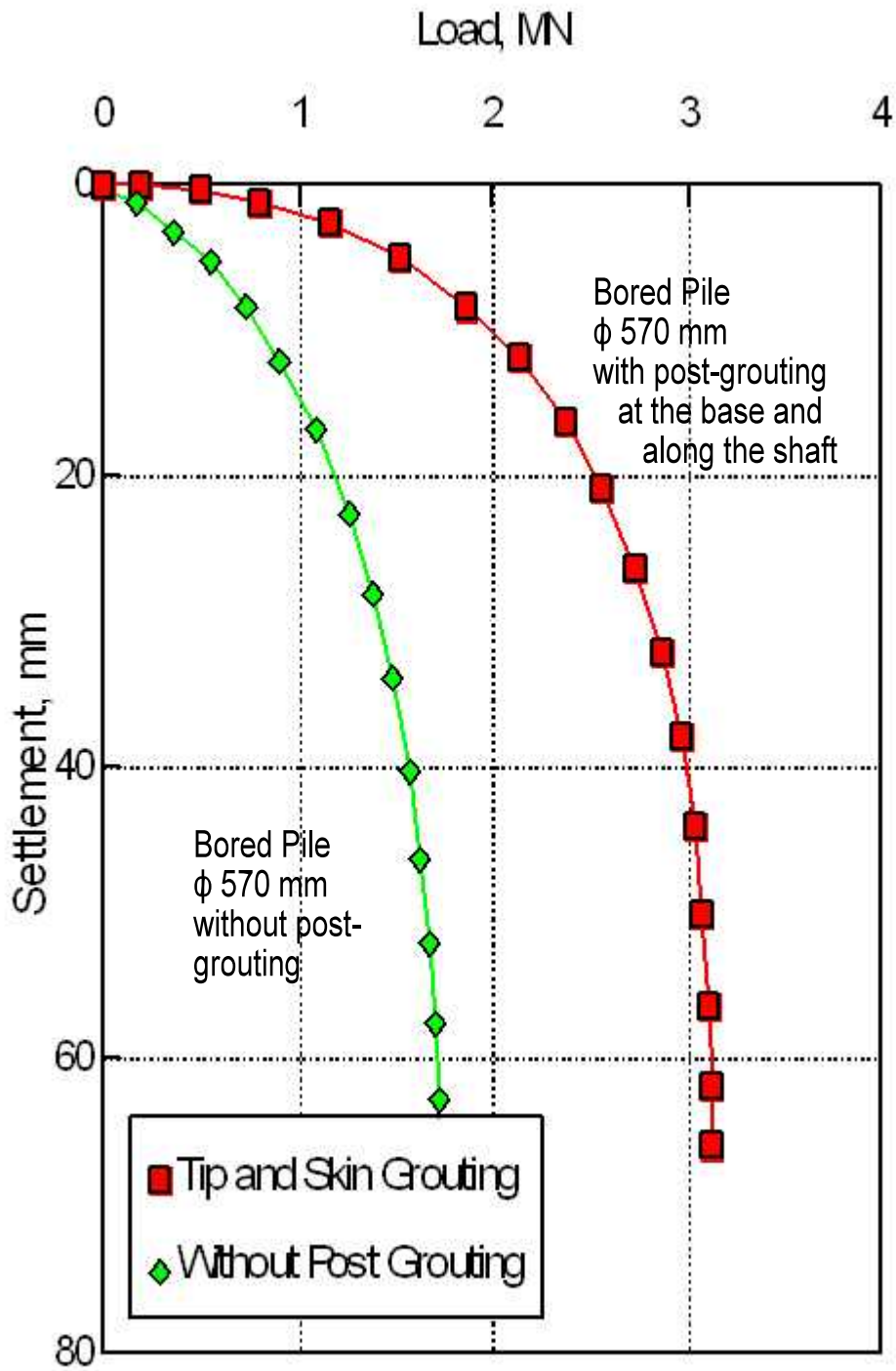


Figure 2-2 Load-displacement of 570 mm drilled shafts (Stocker, 1983).

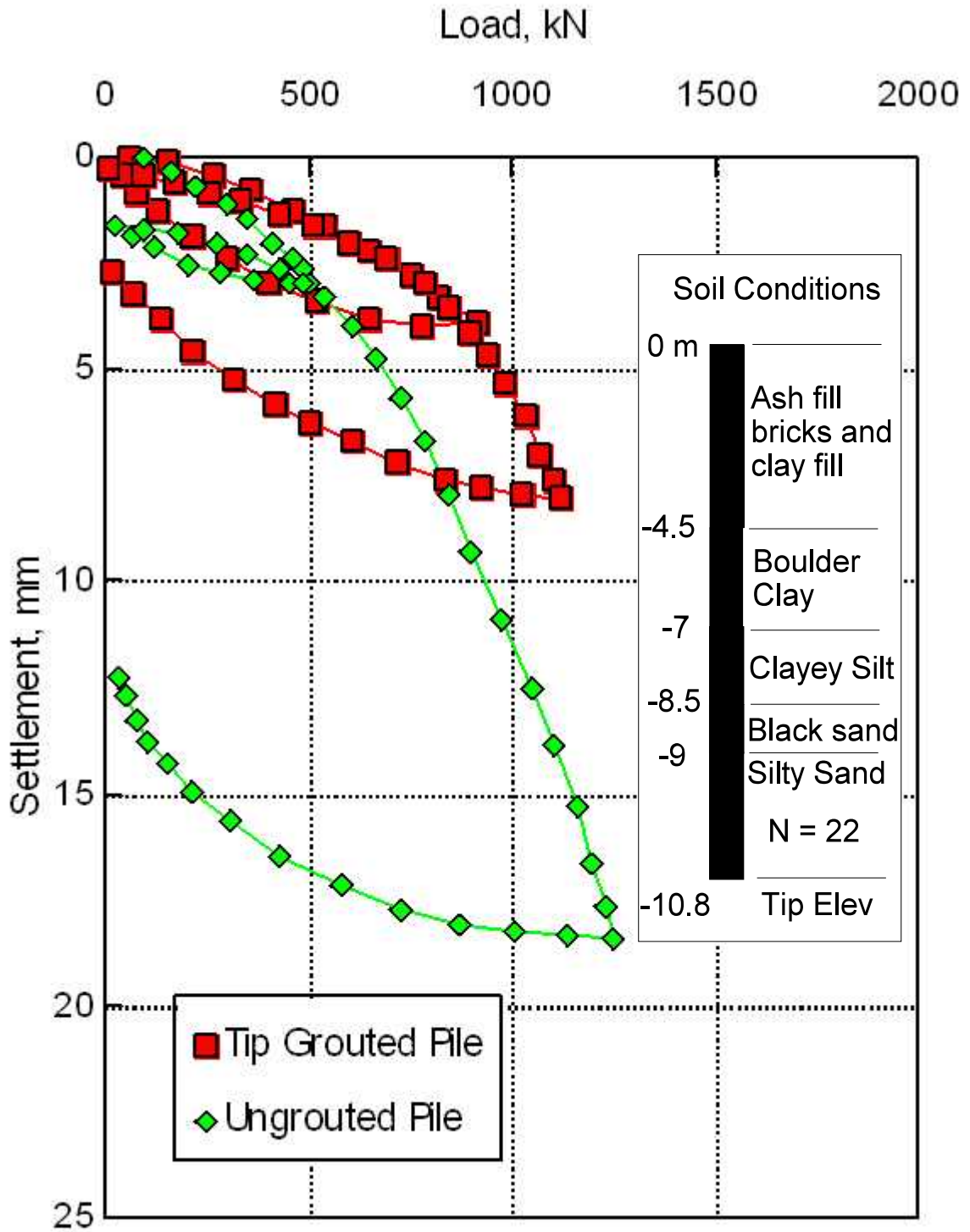


Figure 2-3 Results from 450 mm shaft load tests (Sliwinski, et al., 1984).

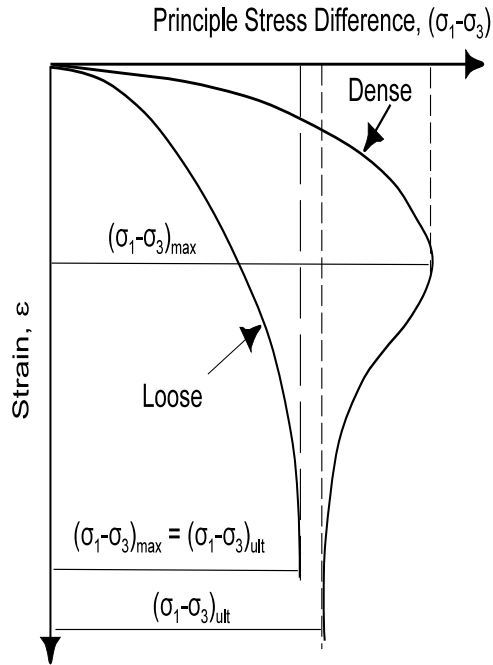


Figure 2-4 Stress / strain curves for typical loose and dense sands (Holtz and Kovacs, 1981).

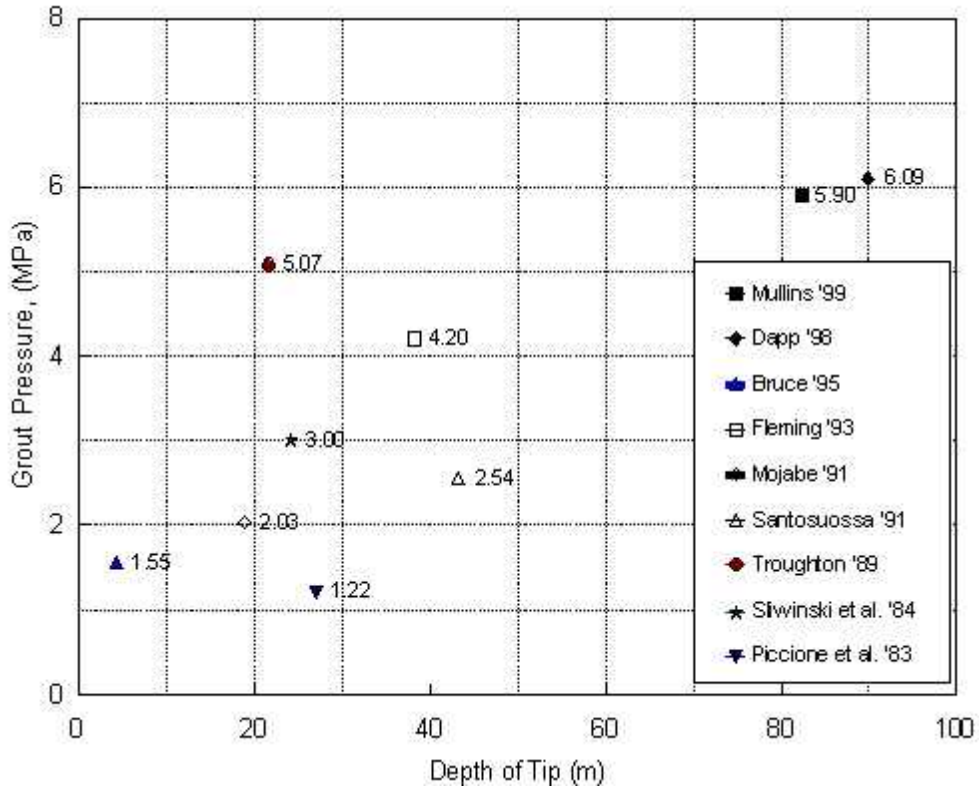


Figure 2-5. Tip grouting pressures used at various sites worldwide.

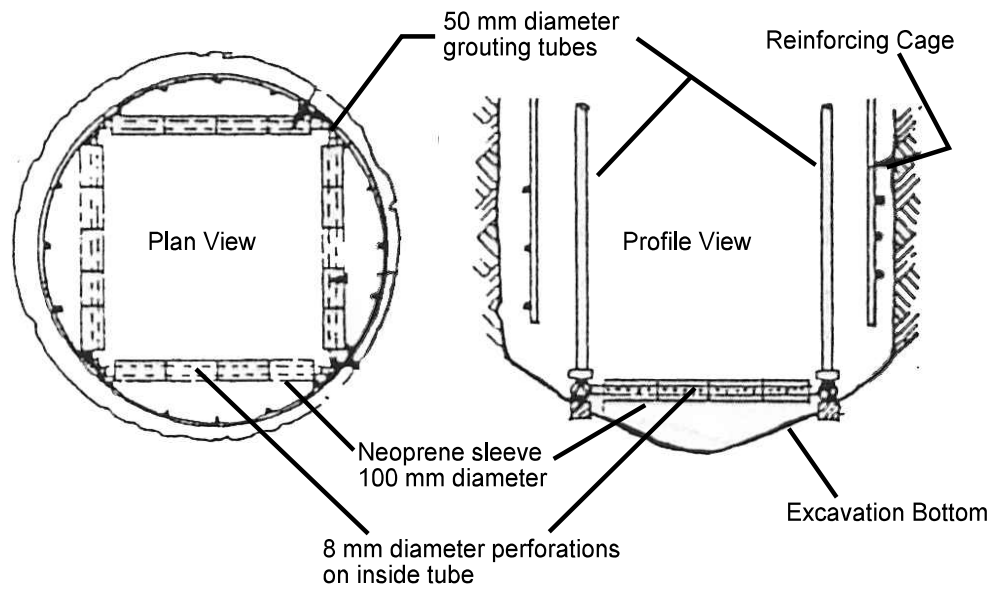


Figure 2-6 Simple sleeve-port compaction grout apparatus (after Bruce, 1986).

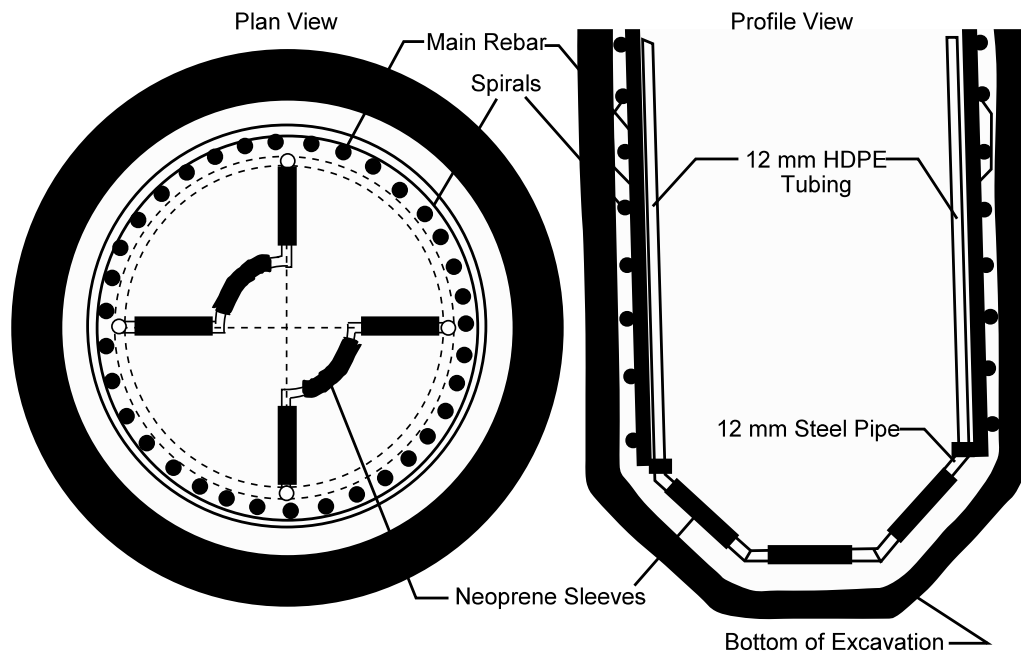


Figure 2-7 Sleeve-port system used in Taipei, Taiwan (Mullins, 1999).

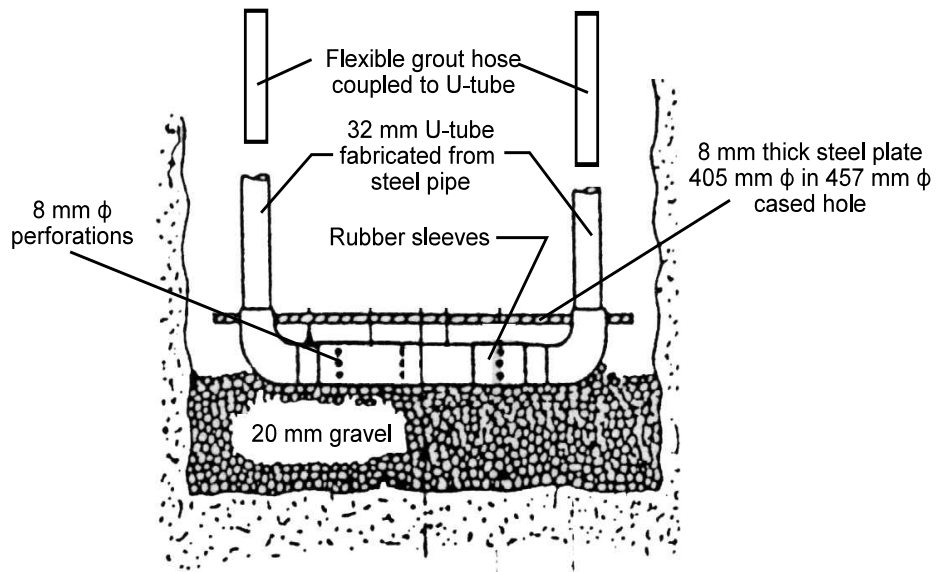


Figure 2-8 U-shaped grouting cell positioned at bottom of excavation (after Sliwinski and Fleming, 1984).

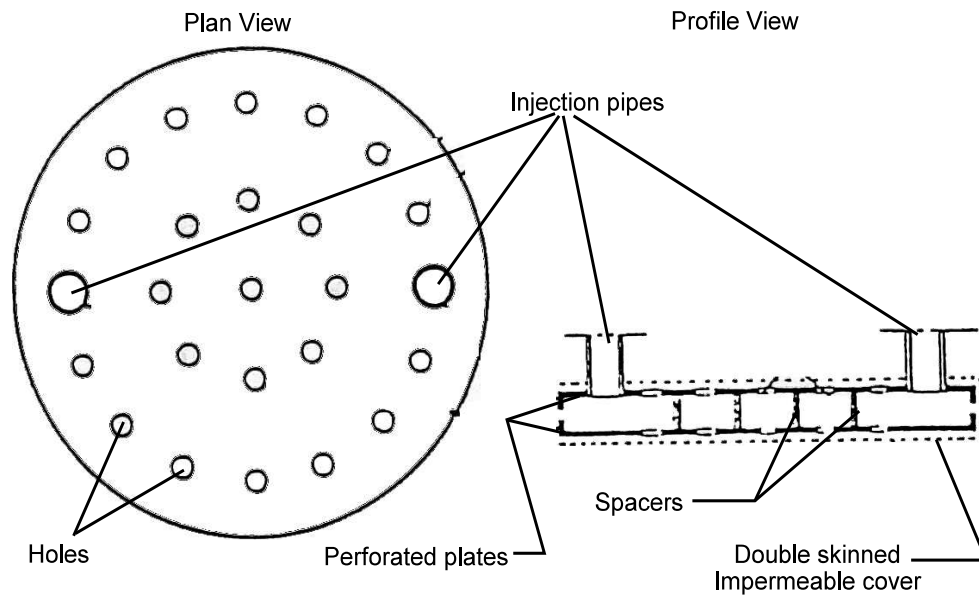


Figure 2-9. Mechanical compaction grout apparatus (from Lizzi, 1981).

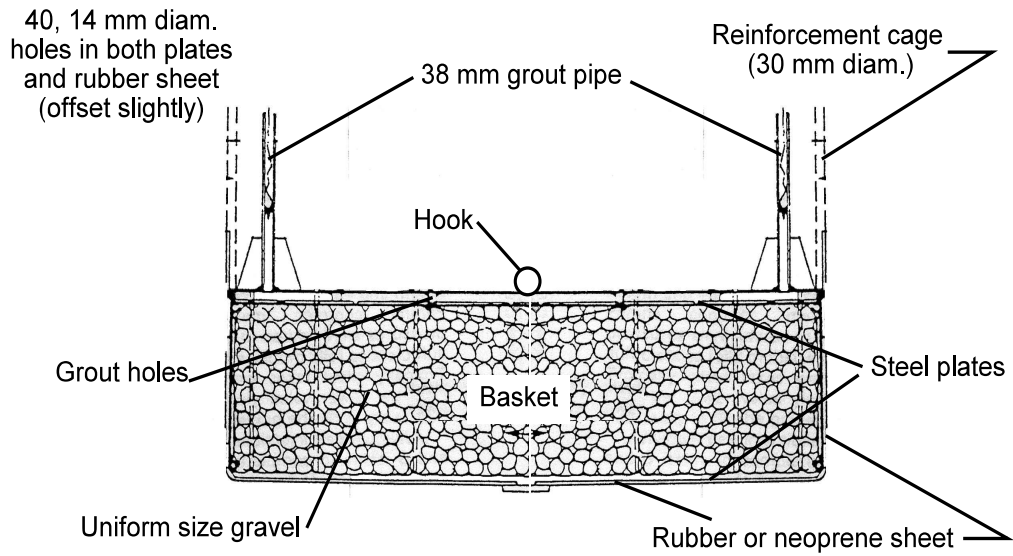


Figure 2-10 Gravel pack between two steel plates (after Bolognesi and Moretto, 1973).

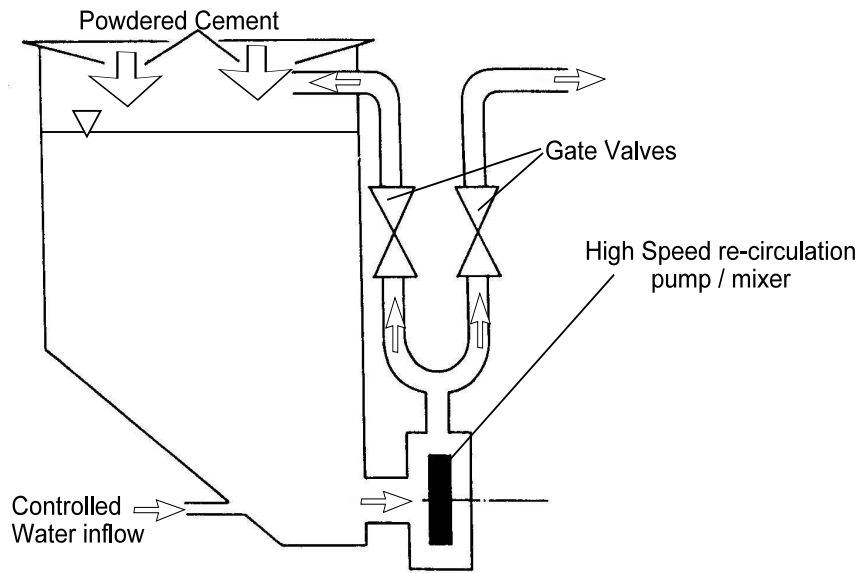


Figure 2-11. High quality mixer.

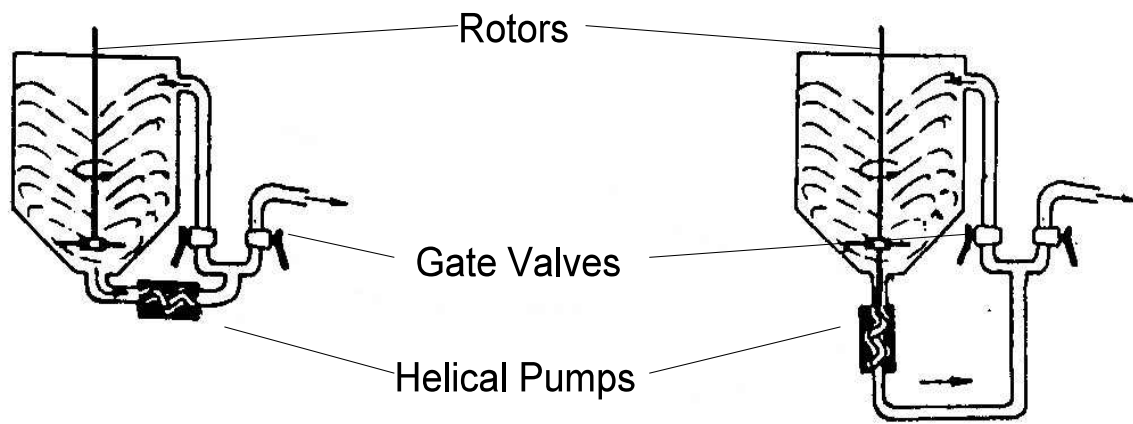


Figure 2-12. Less efficient mixers with helical pumps for circulation.

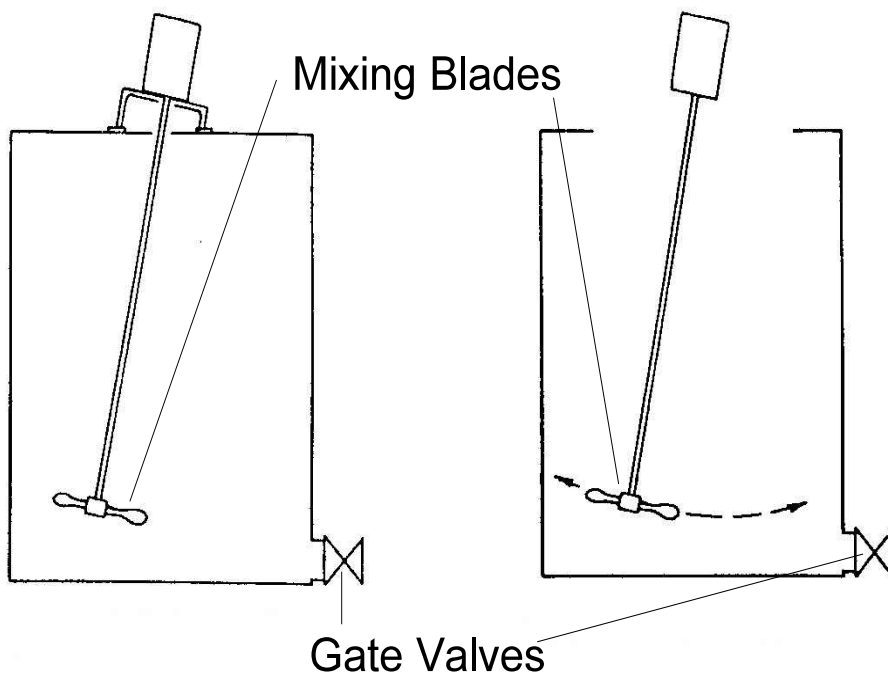


Figure 2-13. Lower quality mixer.

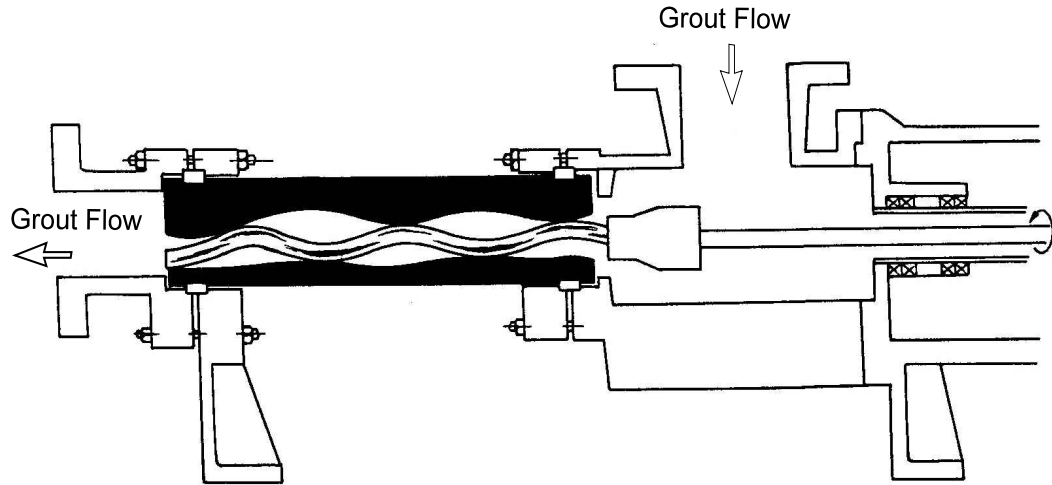


Figure 2-14. Helical rotor pump.

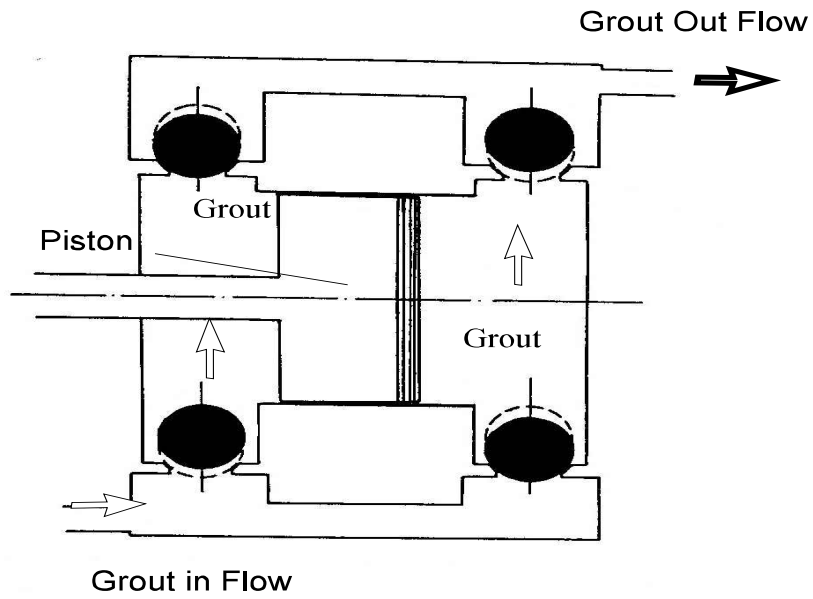


Figure 2-15. Single piston pump.

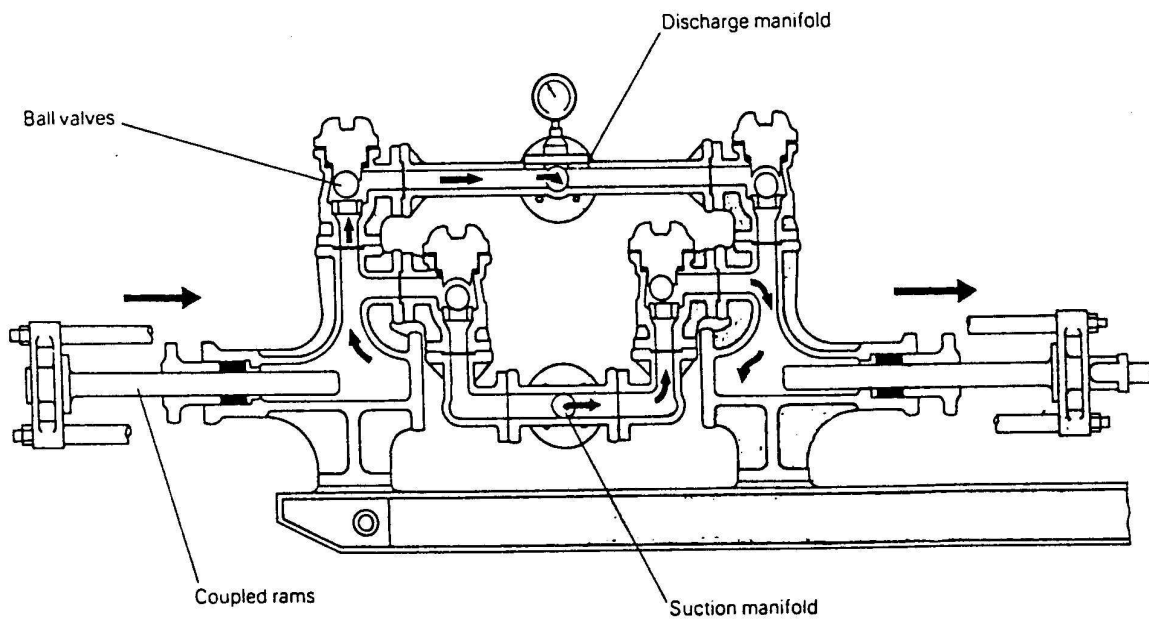


Figure 2-16. Ram pump (Houslbsy, 1990).

Different Types of Access Lines

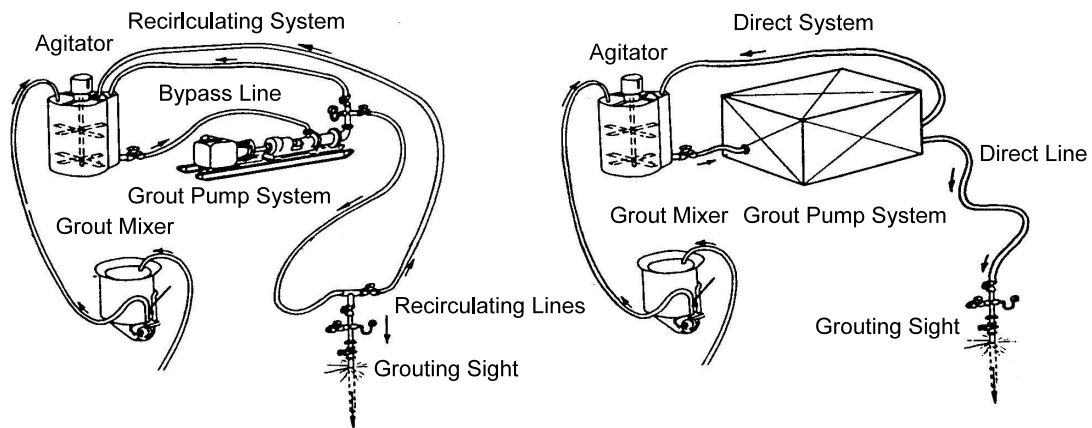


Figure 2-17. Flow of grout through access lines.

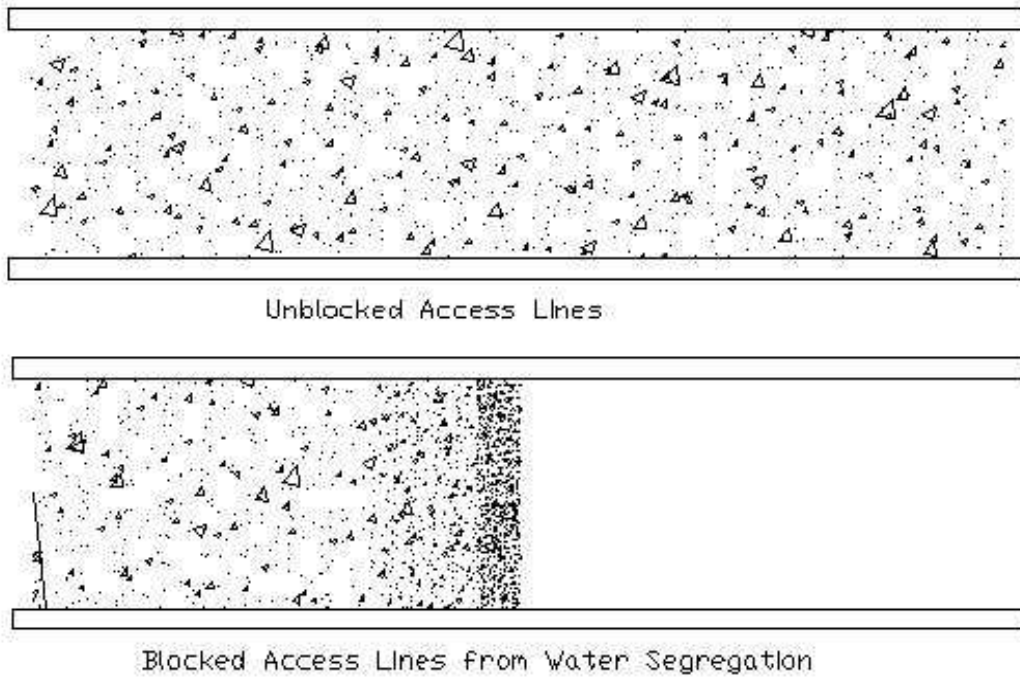


Figure 2-18. Access lines with aggregates.

REFERENCE	DESCRIPTION
Touma and Reese (1974)	Loose - $q_p$ (TSF) = 0.0 Medium Dense - $q_p$ (TSF) = $\frac{16}{k}$ Very Dense - $q_p$ (TSF) = $\frac{40}{k}$ <ul style="list-style-type: none"> <li>• <math>k = 1</math> for <math>D_p &lt; 1.67</math> FT</li> <li>• <math>k = 0.6 D_p</math> for <math>D_p \geq 1.67</math> FT</li> <li>• Applicable only if <math>D_p &gt; 10D</math></li> </ul>
Meyerhof (1976)	$q_p(\text{TSF}) = \frac{2N_{\text{corr}}D_b}{15D_p} < \frac{4}{3} N_{\text{corr}} \text{ for sand}$ $< N_{\text{corr}} \text{ for nonplastic silts}$
Reese and Wright (1977)	$q_p$ (TSF) = $\frac{2}{3} N$ for $N \leq 60$ $q_p$ (TSF) = 40.0 for $N > 60$
Reese and O'Neill (1988)	$q_p$ (TSF) = 0.6N for $N \leq 75$ $q_p$ (TSF) = 45.0 for $N > 75$

Figure 2-19. Tip capacity of shafts in sand (AASHTO, 1999).

rate of heat evolution (watts/kg)

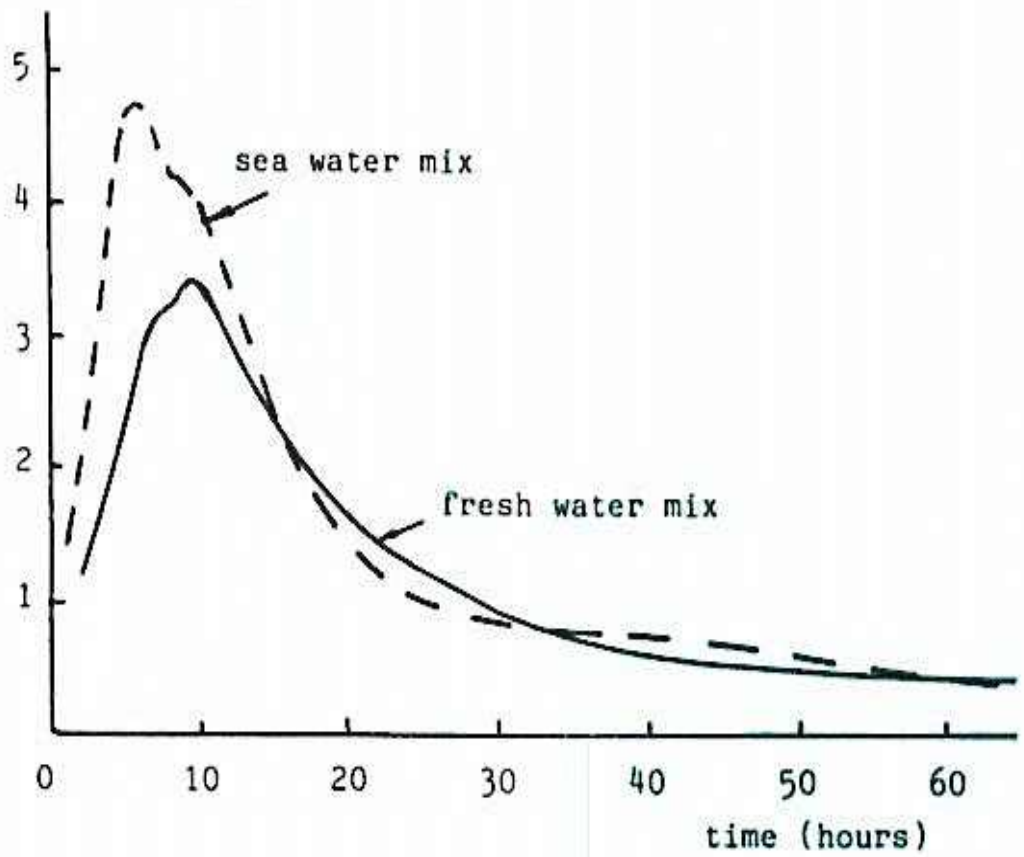


Figure 2-20. Accelerating effect of seawater on Portland cement grouts (Domone, 1990)

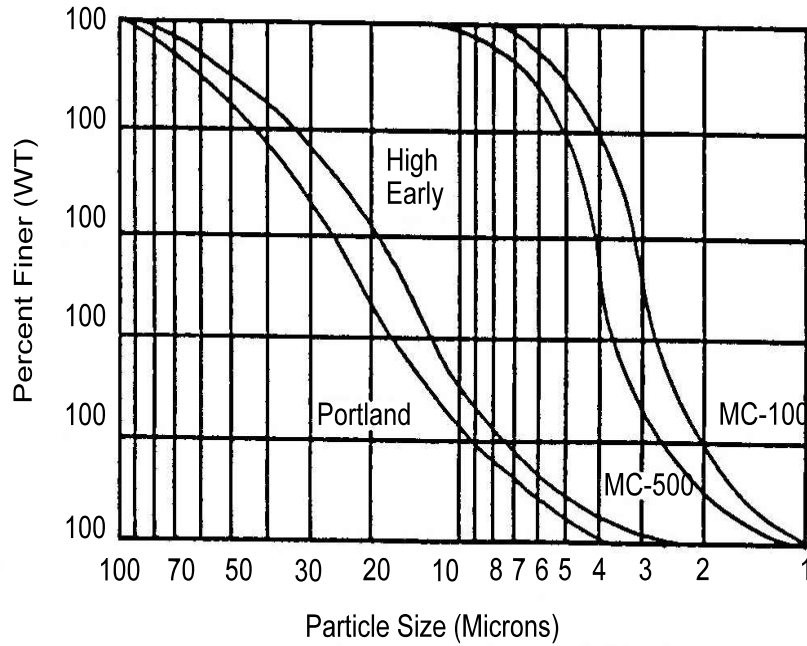


Figure 2-21. Particle size distribution of cements (Houlsby, 1990).

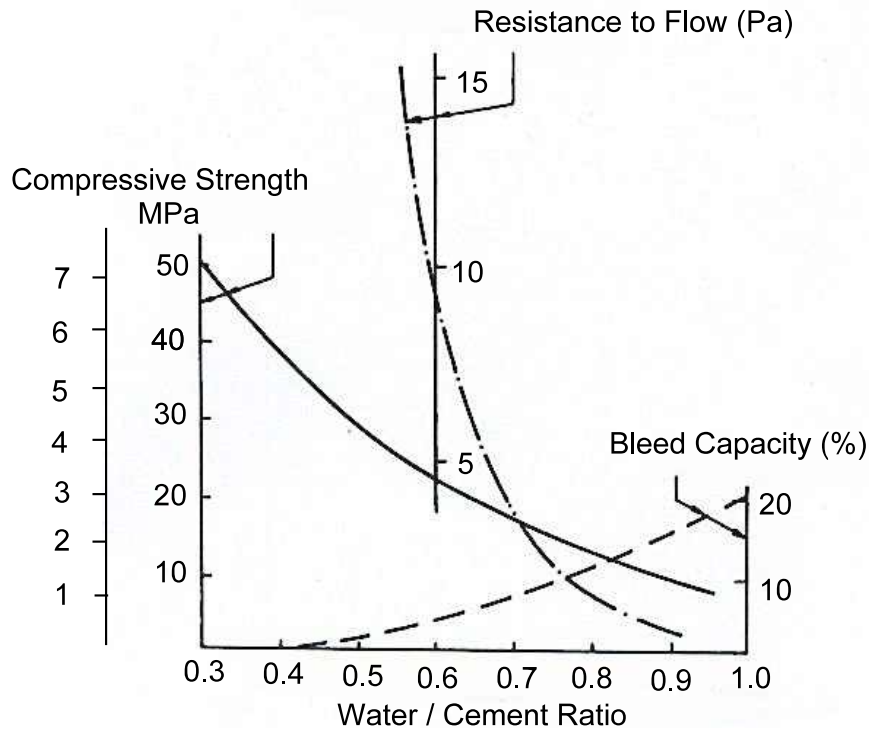


Figure 2-22. Effects of w/c ratio on Portland cement grouts (Domone, 1990; FHWA, 2000).

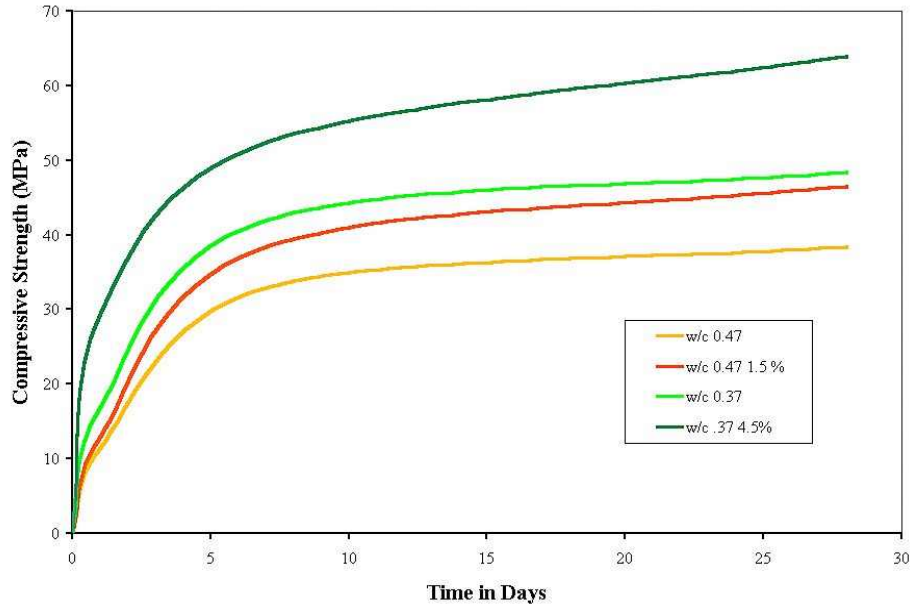


Figure 2-23. Increase of compressive strength with the addition of a superplasticizer.

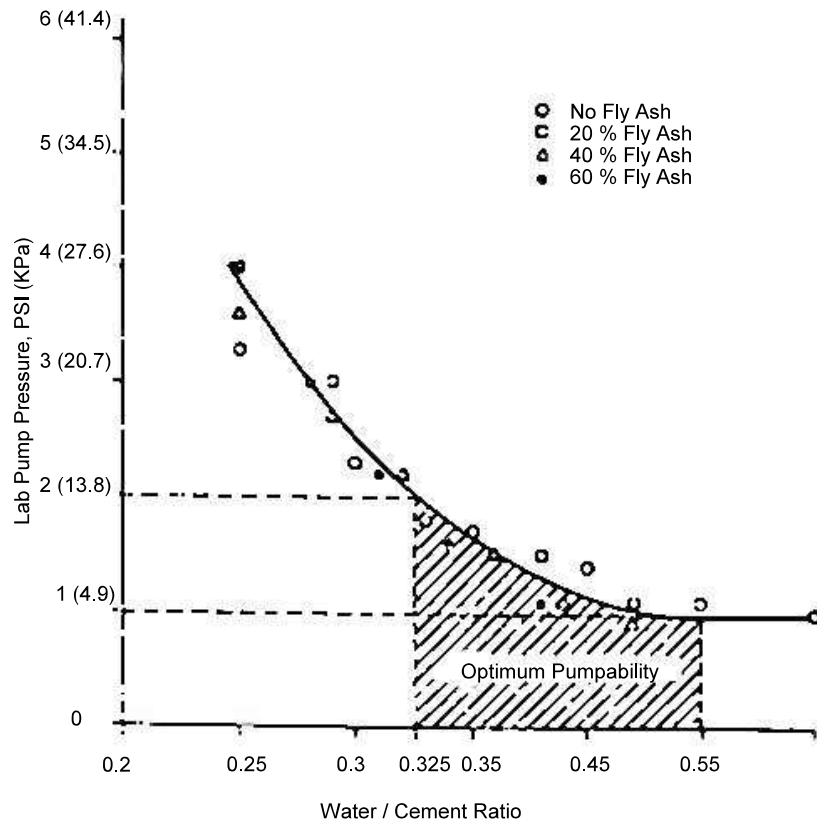


Figure 2-24. Effect of w/c ratio on pumpability of grout mixes.

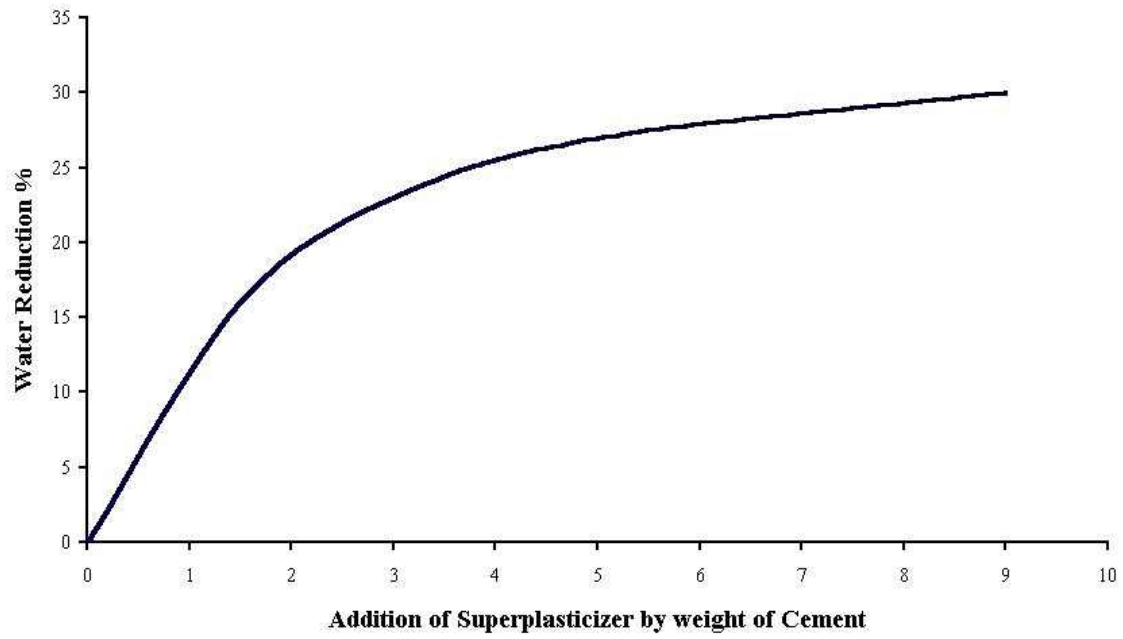


Figure 2-25. Water reduction capabilities of superplasticizer.

### 3. LABORATORY SCALE INVESTIGATION

#### 3.1 Introduction

The objective of the testing program performed at the University of South Florida was to determine the effects of lab-scale pressure grouting on drilled shaft tips. Therein, the primary concern was to show the formation of the grout bulb and isolate parameters affecting its performance, including constructability. To complete this task a series of model bored piles were cast using similar construction equipment and procedures found in the field. This chapter describes aspects of the lab-scale testing program and includes (i) a review of model testing, (ii) the testing cell selected for the study, (iii) test site development and equipment fabricated for casting specimens, (iv) procedures for casting, grouting, and load testing, and (v) a discussion of the results.

#### 3.2 Model Testing

Laboratory scale testing is a valuable tool for studying the load-displacement characteristics of pile-soil systems. In this respect, laboratory tests such as the triaxial test and the direct shear test are performed and used extensively for design of earthen structures. Likewise, scaled modeling of deep foundation systems is a low cost alternative to the full scale testing regimes being implemented today and offer a manner to exhaust the parameters governing pile-soil interaction and behavior. These parameters can be isolated, varied and investigated under laboratory conditions by testing a series of essentially identical specimens. Such a task would be difficult if not impossible to perform on full size prototypes in the field.

##### 3.2.1 Scaling Parameters

When relating the properties investigated in the laboratory to that of the prototype in the field, the theory of similarity must be followed. One must remember physical modeling of pile-soil systems is affected by the reduction in dimensions and parameters of the pile and soil being tested. The basic principle behind scaled testing consists of creating similar stress conditions as found in the field, using a suitable laboratory device, and applying those conditions to a model whose dimensions are smaller than those of the prototype (Azizi, 2000). Requirements of the similarity theorem include: (1) geometric similarity to the prototype, (2) kinematical similarity, and (3) dynamic similarity. This theory establishes the criteria that governs the relationship between the model and the prototype. When the similarity in stress conditions between model and prototype has been established the following relationship of dimensions can be generated:

$$P_p = N * P_m$$

where  $P_p$  and  $P_m$  represent dimensions of the prototype and the model respectively. The  $N$  factor of the above equation represents the scaling parameter used to reduce the properties

of the prototype to that of the model. This factor is applied to all of the dimensions and parameters governing the pile soil system under investigation. Table 3.1 demonstrates the use of the scaling factor on the parameters being investigated in this study.

Table 3-1 Application of Scaling Parameter N

Name	Symbol	Dimension of N	Model	Prototype
Length	L	N	L	N*L
Diameter	D	N	D	N*D
Force	F	N <sup>2</sup>	F	N <sup>2</sup> *F
Displacement		N		
Cross Sectional Area	A	N <sup>2</sup>	A	N <sup>2</sup> *A

### 3.2.2 Centrifuge Testing

One of the devices used to reproduce stress gradients similar in nature to those in the field is the centrifuge. The basic principle behind the centrifuge is to use centrifugal acceleration to create increased  $gh$  soil stresses thus creating stresses which are similar to those due to the acceleration of gravity in the field. Thereby, the prototype  $gh$  stress is equivalent to the model  $g(h/N)$  stress where the length of the model pile (L) is N times shorter than the prototype pile (NL). This is accomplished by placing the soil sample and the model pile into a basket located at the end of a centrifuge boom. The basket is then subjected to an inertial acceleration field. Under such loading conditions, the behavior of the model should be a representation of what occurs in the field (Azizi, 2000).

Although laboratory scale testing of deep foundations is relatively inexpensive, the use of the centrifuge device is costly (Sedran, 1999). Other limitations include the actual dimensions of the model pile used in such a device. The test specimens are extremely small in size and when the proper scaling factors are applied to the pile, the soil particle size is as if the prototype were embedded in boulder sized grains. Special consideration must be given when relating the grain size of the soil to the size of the model without changing the soils classification.

### **3.2.3 Frustum Confining System**

The frustum confining vessel is a unique laboratory device that creates the stress gradients similar to those found in the field by applying a pressure to the soil at the base of the conically-shaped apparatus. The stress gradients created are approximately linear in nature. This is very important when extrapolating data acquired in the lab to the field prototype. The frustum confining vessel allows test piles to be cast directly into the device. The following section describes the frustum in more detail.

### **3.3 Frustum Confining Vessel**

The limitations of many laboratory testing devices have prompted investigations into creating a more suitable laboratory system (Sedran, 1999). The Birmingham Foundation Corporation in conjunction with McMaster University developed such a device called the Frustum Confining Vessel (FCV). The driving idea behind the FCV is that it creates stress gradients with depth, similar in nature to those found in the field. These stress gradients are created by the shape of the FCV and the pressure applied to the base of the system. The frustum is open to the atmosphere at the top of the apparatus, creating zero stress conditions. The stress gradients increase in a nearly linear fashion to the bottom of the device where the stress is related to the applied pressure. These are important criteria when considering the extrapolation of model characteristics to full-scale behavior.

A unique characteristic of the frustum is that by varying the amount of pressure applied to the base of the device one can increase or decrease the stress gradients found in the soil. A simple schematic of this principle can be found in Figure 3-1. The pressure at the base of the frustum is applied by means of a rubber bladder that separates the soil from a hydraulic oil layer/chamber. The University of South Florida's frustum uses an air-over-oil supply system to control the pressure at the base (Figure 3-2). Again, by isolating the governing parameters the load-displacement behavior of pile-soil systems can be investigated and compared to prototypes that are constructed in the field. Complete details on the development of the FCV can be found elsewhere (Horvath, 1996).

The University of South Florida received the only frustum confining vessel in the United States in the Spring of 1999. The system owned by the University of South Florida is approximately 4.5 feet in height. The large size of this apparatus makes it a suitable environment for larger scaled piles as compared to those created for the centrifuge. The ability to cast relatively large model piles helps eliminate scaling error while allowing reasonably-sized tubing, plumbing fittings, and shaft construction tools to be used in this tip grouting project.

### **3.4 Equipment and Facility Development**

The following sections describe the development of the site and the creation of the construction equipment used to cast and test the model specimens.

#### **3.4.1 Overall Site Development**

The Department of Civil and Environmental Engineering at the University of South Florida supported this project by dedicating space to develop the testing facility housing the frustum confining vessel. A temporary shelter was constructed to protect the frustum until a more permanent structure could be constructed (Figure 3-3). Once the new roof was in place a 2-ton lifting system was installed to allow for easy movement of heavy equipment including the individual pieces of the frustum (Figure 3-4). The location of the facility provides easy access for delivery of testing materials and the transportation of such materials while on the premises. The Frustum Test Facility is now a permanent addition to the University of South Florida for future endeavors.

#### **3.4.2 Load Test Frame**

The load testing frame is comprised of steel channel sections and angle members. The base of the load frame was constructed by welding two, 8 foot C10 X 25 sections with two, 3 foot pieces of the same section at the ends. The 4 legs consisted of L6 X 4 X 5/16 angle sections and were bolted into place. The legs stand approximately 9 feet tall. A series of holes were pre-drilled at the tops of the legs to provide a range of positions for the reaction beam. The reaction beam, made from a W14 X 90 section is lowered into place by using the overhead lifting system and then bolted into place. With the series of bolt holes drilled into the legs of the load test frame there is sufficient height clearance to allow the frustum to sit on the base and position the load testing equipment (Figure 3-5).

#### **3.4.3 Casing and Driving Head**

A casing was made from a 48 inch tall steel pipe with an inner diameter of 4.25 inches. This casing is driven into the soil in the frustum by using a casing driver system. The casing drive head is approximately 25 inches tall. The casing and driving head are fastened together using socket-head bolts that fit into holes that were drilled and tapped in at the base of the driving head. Subsequent larger holes were drilled into the casing to allow the heads of the screws to recess into the casing similar to a shelby tube thrust head. A template was constructed that is placed on top of the frustum to guide the casing during driving. This template provides adjustment to assure verticality (Figure 3-6).

#### **3.4.4 Tremie Assembly**

The tremie assembly is comprised of a steel pipe with a 2 inch inner diameter. This pipe is coupled to a large steel hopper equipped with a ball valve to allow the concrete flow to be closed and opened as necessary. A “quick-connect” system was added to connect the two pieces easily (Figure 3-7). The assembly works by permitting the shaft mix to fall into the excavation under its own weight and places the concrete in the excavation from bottom up displacing water or drilling fluid as it fills. The shaft mix was also designed especially for flowability through the small diameter tremie.

This assembly is the second creation after a failed attempt to place the concrete under pressure. The main concern was the flowability of the mix in small diameter tubing. It was thought that by placing the mix into a large vessel under pressure it would be forced through the piping into the excavated hole. There were problems associated with segregation of cement particles and consequent clogging from the aggregate. It was then determined to devise another method of placing the shaft mix.

#### **3.4.5 Pressure Pot**

The pressure pot assembly is used to fill the frustum bladder with oil to provide the load necessary to create the stress gradients found within the soil. This pressure pot (Figure 3-8) is a 2.5 gallon painters pressure pot. An air compressor with a regulator assembly provides the air pressure used to pressurize the pot and thus the hydraulic oil to the frustum bladder. The pressure pot is equipped with a quick pressure release valve for safety and also a ball valve so that the pressure in the bladder can be locked in for extended periods of time without the compressed air attached.

#### **3.4.6 Jetting Assembly/Alluviator**

The jetting assembly is made of 4 steel tubes 60 inches tall with an outer diameter of 0.5 inches (Figure 3-9). The tubes were capped off at the end and drilled in the center with a 1/16 drill bit. Three other holes were drilled on the side 0.5 inches apart starting 0.5 inches from the bottom. The four tubes were then welded to the outside of two steel rings each having an inner diameter of 4.75 inches. The tubes were welded at an approximately 23 degree offset so that the jets could create a vortex located in the center of the device. A conventional garden hose along with copper elbows were used to make the water delivery system to each of the four tubes. When the hose is connected to the water supply, the jetting apparatus can be used to alluviate the sand inside the frustum or even to jet the model piles into place. The procedure for jetting model piles will be discussed later.

## **3.5 Testing Procedures**

In the progression of frustum type drilled shaft testing, several specialized steps are necessary and are discussed in the following sections.

### **3.5.1 Soil Preparation**

Reproducing the stress gradients for each of the tests warranted a standard soil preparation procedure. Following this procedure helps maintain similar conditions for each of the specimens being cast. The top two portions of the frustum were removed and sand was poured into the bottom portion. To ensure no loss of water between the pieces of the frustum a bead of silicone was placed around the lip of each of the pieces of the frustum to create a water impenetrable seal (Figure 3-10). The two top pieces were replaced and the frustum was filled completely with sand. A uniform density of sand was achieved for each testing regime by inundating the soil system with water and alluviating the soil using the jetting device (Figure 3-11). Introducing the jetting device through the opening at the top of the frustum and moving it up and down inside the soil media liquefies and suspends the soil. More sand is added until the frustum is completely filled with alluviated soil. The soil particles fall under their own weight creating a similar soil matrix and density every time. Soil is added until the saturated sand is flush with the opening of the top portion of the frustum.

When the frustum is full of saturated sand the pressurizing procedure begins. An air compressor connected in series with a pressure regulator and the pressure pot forces oil into the bladder of the frustum situated beneath the soil at the base (Figure 3-11). The regulator controls the amount of air pressure that pushes the hydraulic oil which subsequently stresses the soil at the base of the frustum. The conical shape of the frustum attenuates these stresses via arching until at the top where they are zero. Soil liquefaction and consequent expulsion of sand from the frustum can result from pressurizing to the target pressure too quickly. Water will be expunged during this process (Figure 3-12). Hence it should be done at a slow enough rate so that the sand is not disturbed. It was found that the frustum must be pressurized in 5 psi increments and allowed to come to equilibrium before proceeding. Equilibrium is determined with an internal pressure transducer in the hydraulic bladder chamber. This procedure is repeated until desired pressure is achieved.

### **3.5.2 Jetting**

With the use of the jetting device, a pile may be placed into the soil by water jetting. The jetting assembly is placed over the pile and fastened so that the pile and jetting system may be lifted in tandem by the over-head crane (Figure 3-13a). The pile and jetting system is positioned over the opening in the frustum and checked for verticality (Figure 3-13b). The water is then turned on and the system lowered slowly into the soil media. The soil liquefies allowing the system to advance to the desired depth. At this point the water is turned off and

the soil is allowed to settle. The pile itself is fastened to the crane so that while the jetting apparatus is removed the pile is not raised or lowered; staying in position at the desired depth. The jetting apparatus is removed slowly and the soil particles are permitted to come to rest providing the necessary force to keep the pile at the desired depth. At this point in the jetting sequence of the project, the frustum would be stressed to the target gradient and then the model pile either be grouted or load tested.

### **3.5.3 Specimen Casting**

All specimens were cast when the frustum soil was stressed to help create the conditions associated with shaft construction. The specimens were roughly 4.5 inches in diameter and 33 inches in length. Thirty inches of the shaft were embedded in the soil while the remaining 3 inches protruded from the opening in the top to facilitate load testing. The procedure to cast the model piles is similar to that of the cased construction of bored piles in the field. A casing with a 4.0 inch inner diameter is driven into the soil using a casing driver to an embedded depth of 30 inches. The casing is guided by a template to ensure that the casing is centered and that the model pile is cast completely vertical (Figure 3-14). Once the casing is driven the soil is excavated using a hand auger (Figure 3-15a). The final 3 inches of the excavation was performed by using a miniature clean-out bucket (Figure 3-15b). The clean out bucket required 8 to 9 turns to completely fill and is closed by reversing the direction of rotation for a full turn.

A sand/cement mix used for casting the model pile consists of 1100 pounds of cement to 2285 pounds of sand to 53 gallons of water for a 1 cubic yard batch. The mix is then tremied into the excavated hole using a small hopper connected to a tremie pipe that runs the length of the excavation (Figure 3-16a). In Figure 3-16b the hopper is connected to the tremie pipe and the valve is opened. The grouting apparatus serves as a temporary plug for the tremie to prevent segregation of concrete components from the drilling fluid or water in the excavation. Once return is noticed, the hopper is closed and the tremie is removed (Figure 3-16c). A short outer casing is placed over the driven casing and embedded a depth of 3 inches (Figure 3-17). This outer casing is 4.5 inches in diameter and 6 inches in height. The purpose of the outer casing is to allow 3 inches of the model pile to be exposed at the opening of the frustum. The pile is allowed two days to cure before testing as dictated by sufficient compressive strengths.

One of the major obstacles encountered in casting the pile specimen is the flowability of the shaft mix. In that this is a reduced scale investigation, the tools involved are likewise smaller than those encountered in field construction. The tremie pipe has an inner diameter of approximately 2.0 inches which posed a problem with the mix not flowing freely into the excavation. Hence, a 275 ounce dose of a high range water reducing agent (ADVA 100) was added to the 1 cubic yard mix allowing the cement to flow under its own weight.

### 3.5.4 Grouting

The grouting process was achieved by delivering the grout through a small grouting apparatus (Figure 3-18a) placed at the bottom of the shaft. This apparatus is comprised of a thin sheet metal plate with two holes to connect a delivery tube and a return tube that run to the top of the shaft. A rubber bladder is placed at the bottom to contain the grout. A geotextile placed between the rubber bladder and the metal plate (Figure 3-18b) provides sufficient space for the grout to travel. The small size of the openings in the grouting apparatus created difficulties in grout pumpability. Proper mix parameters were researched and the results with the solution to the pumping problem are discussed in section 2.4.

Three separate types of grouting cells were designed and used in grouting (Figure 3-19). The first failed to deliver the grout to the bottom of the shaft. It was comprised of a single grouting tube, 0.5 inch cpvc, running down the center of the shaft. The second grouting cell consisted of two, 0.5 inch cpvc, tubes; one for grout delivery and the second for the grout return. This apparatus was unreliable in delivering grout to the bottom of the shaft. The third and final grouting cell is similar to the second cell, however, a small piece of geotextile was placed between the metal plate and the rubber bladder to allow a path for the grout to travel throughout the bottom of the shaft.

The lines were flushed with water to release any obstruction in the direction of grout flow and to allow better grout mobility. This was observed to be a crucial step in the grouting process. A manual piston style pump was used to deliver the grout to the bottom of the shaft (Figure 3-20). The pump was 18 inches long and 2.9 inches in diameter. When completely full it delivered a total of 118 cubic inches of grout. The grout volume pumped into the system was determined by counting the number of turns on the pump. The pump advances one tenth of an inch for every turn. The amount of grout take is determined after grout return is confirmed from the return tube on the apparatus.

Two separate series of grouting tests were performed. The first series was comprised of model piles that were grouted with the grouting pressure “locked-in”. To lock the pressure in valves were placed at the tops of the delivery and return tubes (Figure 3-21). When the grouting process was finished the valves were simply closed and remained closed while the grout cured. The second series of tests was comprised of model piles that were grouted and the pressures were not locked in. Upon completion of the grouting process, the valves located at the tops of the delivery and return tubes were simply removed and the grout was allowed to cure with the pressure released.

The initial grout mix consisted of a simple combination of water and cement. Many problems were encountered because of the small openings used in the grouting apparatus. Grout pumpability became a serious obstacle. Research lead to a grout mix which included 5% by weight of bentonite. The bentonite prevented the segregation of the cement and water which reduced the clogging experienced in the initial specimens. While the addition of the

bentonite to the grout mix resulted in lower compressive strengths, these were still sufficient for the post-grout application.

A testing scheme was created and used by the data collection equipment to monitor the grouting process. The testing criteria was governed by upward displacement of the shaft. The criteria ranged from 0.05 inches to 0.20 inches of upward movement. After return of grout was noticed the volume of grout was recorded so that a correlation between displacement and grout take could be determined. A pressure transducer was used to record the grout pressure required to uplift the shaft the preset distance. This pressure was then converted into a load and plotted on a corresponding load displacement graph (See appendix A).

### **3.5.5 Load Testing**

The grout was given 48 hours to cure before load testing of the model pile began. The grouting tubes were removed with a saw and minor surface smoothing was necessary to ensure that a horizontal plane was available for the load test equipment. A large reaction beam was bolted into the loading frame to provide the required resistance for the jack during loading. The ASTM Standard Designation D 1143-98 was used to follow the load testing of the model piles (ASTM, 1998). The testing regime followed that of a constant rate of loading.

The load testing apparatus, depicted in Figure 3-22 consisted of two electronic displacement gages (LVDT's) at opposite sides (180° apart) to monitor the displacement of the shaft. A load cell positioned at the top of the pile measured the amount of the load applied over which a hydraulic jack was situated to press on the overhead reaction frame. An average of the two displacement readings along with the measured load were used to plot the load-displacement curves (See appendix A).

### **3.6 Test Matrix and Results**

The following section briefly describes each one of the individual tests performed in this laboratory investigation. Three series of tests are described: (1) Jetted Shafts (JS), (2) Control Shafts (CS), and (3) Grouted Shafts (GS). The jetted shaft tests were conducted using the same shaft originally cast using the cased construction method. This shaft was fully instrumented with numerous strain gage levels. It was intended for re-use to quantify the effects of grouting and help show grout bulb formation. It also served to streamline the FCV procedures (Figure 3-23). The jetted pile has the same diameter as later piles cast one-at-a-time, however, the length of the shaft is 44 inches long.

Table 3-2 Laboratory Scale Data

	Ult. Grout Press. (psi.)	Grout Disp. at Ult. (in.)	Ult. Load (lbs.)	Disp. at Ult. Load (in.)	Load at 0.05" Disp.	Load at 0.1" Disp.	Grout Take (in <sup>3</sup> )	Remarks
JS-1	N/A	N/A	2600	0.190	1930	2250	N/A	FCP = 10 psi
JS-2	N/A	N/A	4590	0.122	3830	4450	N/A	FCP = 20 psi
JS-3	N/A	N/A	6350	0.165	5450	6320	N/A	FCP = 30 psi
JS-4	N/A	N/A	6370	0.105	4770	6370	N/A	FCP = 30 psi
JS-5	N/A	N/A	9290	0.177	6310	8430	N/A	FCP = 40 psi
JS-6	N/A	N/A	4980	0.153	3760	4500	N/A	FCP = 30 psi
JS-7	N/A	N/A	3350	0.156	2490	3050	N/A	FCP = 20 psi
JS-8	N/A	N/A	5540	0.160	3900	4960	N/A	FCP = 40 psi
CS-1	N/A	N/A	4540	0.396	2540	3300	N/A	FCP = 30 psi
CS-2	N/A	N/A	1500	0.275	550	820	N/A	FCP = 10 psi
CS-3	N/A	N/A	2300	0.360	825	1400	N/A	FCP = 30 psi
CS-4	N/A	N/A	2750	0.650	325	650	N/A	FCP = 30 psi
GS-1	-	-	4810	0.160	4000	4720	-	Grouting clog
GS-2	17.91	0.034	2200	0.550	800	1200	19.81	90% Improv.
GS-3	57.72	0.007	5000	0.275	1250	2800	20.00	290% Improv.
GS-4	-	-	4000	0.245	1400	2600	-	Grouting clog
GS-5	45.78	0.030	3200	0.295	1300	2000	21.13	180% Improv.
GS-6	63.69	0.084	4000	0.270	1300	2300	27.73	238% Improv.
GS-7	123.41	0.100	6800	0.490	2200	3800	77.24	437% Improv.
GS-8	38.22	0.155	2600	0.555	800	1050	39.61	71% Improv.
GS-9	135.35	0.145	7700	0.360	3000	4500	86.48	559% Improv.
GS-10	21.89	0.104	2800	0.480	600	1000	15.84	46% Improv.
GS-11	43.79	0.145	3200	0.490	800	1300	26.41	99% Improv.
GS-12	155.25	0.103	6500	0.490	2000	3100	48.85	372% Improv.
GS-13	57.32	0.152	4200	0.530	1000	1650	59.42	152% Improv.

### 3.6.1 Jetted Shafts

- JS-1 The shaft was jetted into the frustum on May 4, 2000. The frustum confining pressure was set at 10 psi. The shaft was load tested on the same day. The ultimate load recorded was 2600 pounds at a displacement of 0.190 inches. This shaft was not grouted.
- JS-2 The shaft was jetted into the frustum on May 4, 2000. The frustum confining pressure was set at 20 psi. The shaft was load tested on the same day. The ultimate load recorded was 4590 pounds at a displacement of 0.122 inches. This shaft was not grouted.
- JS-3 The shaft was jetted into the frustum on May 9, 2000. The frustum confining pressure was set at 30 psi. The shaft was load tested the same day. The ultimate load recorded was 6350 pounds at a displacement of 0.165 inches. This shaft was not grouted.
- JS-4 The shaft was jetted into the frustum on May 9, 2000. The frustum confining pressure was set at 30 psi. The shaft was load tested the same day. The ultimate load recorded was 6370 pounds at a displacement of 0.105 inches. This shaft was not grouted.
- JS-5 The shaft was jetted into the frustum on May 9, 2000. The frustum confining pressure was set at 40 psi. The shaft was load tested the same day. The ultimate load recorded was 9290 pounds at a displacement of 0.177 inches. This shaft was not grouted.
- JS-6 The shaft was jetted into the frustum on May 9, 2000. The frustum confining pressure was set at 30 psi. The shaft was load tested on the same day. The ultimate load recorded was 4980 pounds at a displacement of 0.153 inches. This shaft was not grouted.
- JS-7 This shaft was jetted into the frustum on May 25, 2000. The frustum confining pressure was set at 20 psi. The shaft was load tested on the same day. The ultimate load recorded was 3350 pounds at a displacement of 0.156 inches. This shaft was not grouted.
- JS-8 This shaft was jetted into the frustum on June 21, 2000. The frustum confining pressure was set at 40 psi. The shaft was load tested on June 22, 2000. The ultimate load recorded was 5540 pounds at a displacement of 0.160 inches. This shaft was grouted the results of which will be discussed in GS-1.

### **3.6.2 Control Shafts**

These shafts were cast without any grouting devices and were used to form a basis of comparison for subsequent grouted shafts.

- CS-1 Control shaft 1 was originally cast Monday December 20, 1999. This shaft is the shaft used in all of the jetted shaft series. Control shaft 1 was load tested on January 4, 2000. The ultimate load recorded was 4540 pounds at a displacement of 0.396 inches. Control shaft 1 was cast at a frustum confining pressure of 30 psi.
- CS-2 Control Shaft 2 was cast on Friday October 6, 2000. The frustum confining pressure was set at 10 psi. The specimen was load tested on Friday October 13, 2000 and the ultimate load was observed to be 1500 pounds at a displacement of 0.275 inches. When casting this shaft there was no protective layer impeding the shaft mix from flowing between the outer casing and the top piece of the frustum. Consequently, the overflow bonded with the pile and the frustum creating the spike noticed at the beginning of the load displacement curve. Subsequent shafts were cast with a plastic sheet preventing cement from entering between the top of the frustum and the pile (Figure 3-24).
- CS-3 Control Shaft 3 was cast on Friday October 13, 2000. The frustum confining pressure was set at 30 psi. The specimen was load tested on Friday October 20, 2000 and the ultimate load was observed to be 2300 pounds at a displacement of 0.360 inches. This shaft was used as the standard to which the load tests of following shafts were compared to show possible improvement (Figure 3-25).
- CS-4 Control shaft 4 was cast on Friday March 30, 2001. The frustum confining pressure was set at 30 psi. The specimen was load tested on Sunday April 1, 2001 and the ultimate load was observed to be 2700 pounds at a displacement of 0.620 inches.

### **3.6.3 Grouted Shafts**

- GS-1 This shaft corresponds to JS-8. The shaft was grouted using the single delivery tube grouting cell as discussed earlier. The system clogged. When load tested the ultimate load recorded was 4810 pounds at a displacement of 0.106 inches. No improvement was noticed (Figure 3-26).
- GS-2 Grouted Shaft 2 was cast on Friday October 20, 2000. The frustum confining pressure was set at 30 psi. The specimen was grouted on Monday October 23, 2000. During the grouting process no return was noticed. Due to a clog in the grouting apparatus below the position of the pressure transducer. The grout lines were reversed and the plug was worked loose. This is evidenced by the spike in

the grouting curve (see Figure A-3). Subsequent grouting tests were flushed with clear water prior to grouting. Although a grout take of 19.81 in<sup>3</sup> was experienced, the specimen showed no improvement when load tested. The pile was load tested on Friday October 27, 2000 and an ultimate load of 2200 pounds at a displacement of 0.550 inches was observed (Figure 3-27).

- GS-3 Grouted Shaft 3 was cast on Friday October 27, 2000. The frustum confining pressure was set at 30 psi. The specimen was grouted on Monday November 6, 2000. During the grouting process no return was noticed. A grout take of 20 in<sup>3</sup> was recorded. The specimen was load tested on Friday November 10, 2000 and an ultimate load of 5000 pounds at a displacement of 0.275 inches was observed. After review of the data it was noticed that there was a slight eccentricity in the loading of the shaft resulting in a higher ultimate load than the control shaft 2 (Figure 3-28).
- GS-4 Grouted Shaft 4 was cast on Friday November 10, 2000. The frustum confining pressure was set at 30 psi. The specimen was grouted on Monday November 13, 2000. Again no grout return was noticed during the grouting process. No grout volume was recorded due to a clog in the grouting system. This prompted review into the grout chemistry and the pumpability issues encountered throughout the project due to the small scaled equipment being used; these problems were never encountered on any of the full-scale shafts. The specimen was load tested Friday November 17, 2000 and an ultimate load of 4000 pounds at a displacement of 0.245 inches was noticed. There was a slight eccentricity during the loading of the specimen leading to the increase of ultimate capacity as compared with control shaft 2 (Figure 3-29).
- GS-5 Grouted Shaft 5 was cast on Friday November 17, 2000. The frustum confining pressure was set at 30 psi. The grouting lines were flushed with water and the specimen was grouted on Monday November 20, 2000 using the special bentonite/cement mix. Grouting pressures were locked in. A slight upward displacement of 0.03 inches was observed with a grout take of 21.13 in<sup>3</sup>. The specimen was load tested on Friday November 24, 2000 and an ultimate load of 3200 pounds at a displacement of 0.295 inches. The results exhibited a slight improvement over control shaft 2 (Figure 3-30).
- GS-6 Grouted Shaft 6 was cast on Monday December 4, 2000. The frustum confining pressure was set at 30 psi. The grouting lines were flushed with water and the specimen was grouted on Tuesday December 5, 2000 using the special bentonite/cement mix. Grouting pressures were locked in. An upward displacement of 0.084 inches and a grouting pressure of 63.69 psi were observed. A grout take of 27.73 in<sup>3</sup> was recorded. The specimen was load tested on Monday December 11, 2000 and an ultimate load of 4000 pounds at 0.270 inches of

displacement was observed. When compared with the results of CS-2, GS-5 exhibited marked improvement. The grouting load of 800 pounds created by displacing the shaft upwards by 0.084 inches was roughly the same amount of improvement experienced in GS-5 over CS-2 at that same displacement (Figure 3-31).

GS-7 Grouted Shaft 7 was cast on Thursday December 14, 2000. The frustum confining pressure was set at 30 psi. The grouting lines were flushed with water and the specimen was grouted on Friday December 15, 2000 using the special bentonite/cement mix. Grouting pressures were locked in. An upward displacement of 0.1 inches and a grouting pressure of 123.41 psi were observed. A grout take of 77.24 in<sup>3</sup> was recorded. The specimen was load tested Monday December 18, 2000 and an ultimate load of 6800 pounds at 0.490 inches of displacement was observed. When compared with the results of CS-2, GS-6 exhibited substantial improvement. The grouting load of 1550 pounds created by displacing the shaft

upwards by 0.1 inches was less than the improvement in capacity experienced in GS-6 over CS-2 at the same displacement (Figure 3-32).

GS-8 Grouted Shaft 8 was cast on Monday December 18, 2000. The frustum confining pressure was set at 30 psi. The grouting lines were flushed with water and the specimen was grouted Tuesday December 19, 2000 using the special bentonite/cement mix. Grouting pressures were locked in. An upward displacement of 0.155 inches and a grouting pressure of 38.22 psi were observed. A grout take of 39.61 in<sup>3</sup> was recorded. The specimen was load tested on Thursday December 21, 2000 and an ultimate load of 2600 pounds at 0.555 inches of displacement was observed. When compared with the results of CS-2, GS-7 exhibited no improvement (Figure 3-33). As noticed in most exhumed shafts the bulb was broken during excavation.

GS-9 Grouted Shaft 9 was cast on Monday January 8, 2001. The frustum confining pressure was set at 30 psi. The grouting lines were flushed with water and the specimen was grouted on Friday January 12, 2001 using the special bentonite/cement mix. Grouting pressures were locked in. An upward displacement of 0.145 inches and a grouting pressure of 135.35 psi were observed. A grout take of 86.48 in<sup>3</sup> was recorded. The specimen was load tested on Monday January 15, 2001 and an ultimate load of 7700 pounds at 0.360 inches of displacement was observed. When compared with the results of CS-2, GS-8 exhibited great improvement. The grouting load of 1700 pounds created by the upward displacement of 0.145 was less than the improvement of the load test of GS-8 over the control CS-2 at the same displacement (Figure 3-34).

- GS-10 Grouted Shaft 10 was cast on Monday January 22, 2001. The frustum confining pressure was set at 30 psi. The grouting lines were flushed with water and the specimen was grouted on Monday January 29, 2001 using the special bentonite/cement mix. Grouting pressures were not locked in. An upward displacement of 0.104 inches and a grouting pressure of 21.89 psi were observed. A grout take of 15.85 in<sup>3</sup> was recorded. The specimen was load tested on Thursday February 1, 2001 and an ultimate load of 2800 pounds at 0.480 inches of displacement was observed. When compared with the results of CS-2, GS-10 showed little improvement (Figure 3-35).
- GS-11 Grouted Shaft 11 was cast on Tuesday February 6, 2001. The frustum confining pressure was set at 30 psi. The grouting lines were flushed with water and the specimen was grouted on Thursday February 8, 2001 using the special bentonite/cement mix. Grouting pressures were not locked in. An upward displacement of 0.145 inches and a grouting pressure of 43.79 psi were observed. A grout take of 26.41 in<sup>3</sup> was recorded. The specimen was load tested on Saturday February 10, 2001 and an ultimate load of 3200 pounds at 0.490 inches of displacement was observed. When compared with the results of CS-2, GS-11 showed little improvement (Figure 3-36).
- GS-12 Grouted Shaft 12 was cast on Wednesday February 14, 2001. The frustum confining pressure was set at 30 psi. The grouting lines were flushed with water and the specimen was grouted on Friday February 16, 2001 using the special bentonite/cement mix. Grouting pressures were not locked in. An upward displacement of 0.103 inches and a grouting pressure of 155.25 psi were observed. A grout take of 48.85 in<sup>3</sup> was recorded. The specimen was load tested on Tuesday February 20, 2001 and an ultimate load of 6500 pounds at 0.490 inches of displacement was observed. When compared with the results of CS-2, GS-11 exhibited improvement. The grouting load of 1950 pounds created by the upward displacement of 0.103 was less than the improvement of the load test of GS-11 over CS-2 at the same displacement (Figure 3-37).
- GS-13 Grouted Shaft 13 was cast on Monday March 5, 2001. The frustum confining pressure was set at 30 psi. The grouting lines were flushed with water and the specimen was grouted on Wednesday March 7, 2001 using the special bentonite/cement mix. Grouting pressures were not locked in. An upward displacement of 0.152 inches and a grouting pressure of 57.32 psi were observed. A grout volume take of 59.42 in<sup>3</sup> was recorded. The specimen was load tested on Friday March 9, 2001 and an ultimate load of 4200 pounds at 0.530 inches of displacement was observed. When compared with the results of CS-2, GS-13 exhibited little to no improvement (Figure 3-38).

### **3.7 Test Results**

The following graphs depict the various results from the different testing series. For a complete representation of the load displacement curves consult Appendix A. Figure 3-39 shows the effect of frustum pressure on the load-displacement behavior. Figure 3-40 is a composite graph of the grouted shafts as well as one of the control (ungouted) shafts.

To better quantify the level of improvement shown by grouting the shaft tips, Figures 3-41 and 42 graphically illustrate the percent improvement versus the grout take and maximum sustained grouting pressure, respectively.

### **3.8 Conclusions**

The objective of this testing program was to determine the effects of pressure grouting drilled shaft tips. Improvement in shaft capacity can be obtained when the toe is injected with grout at pressures exceeding the end bearing capacity. Therein, the improvement is derived from increasing the capacity and stiffness of the tip component. The governing principle behind pressure grouting drilled shaft tips requires sufficient skin friction on which the pressurized tip can react. When the same pile is then load tested the amount of load created by the injected grout can be used in the design capacity of the pile. This model scale test program showed that the amount of improvement is dependent on the grout take as well as the maximum sustained grout pressure. This is fully discussed in Chapter 7.

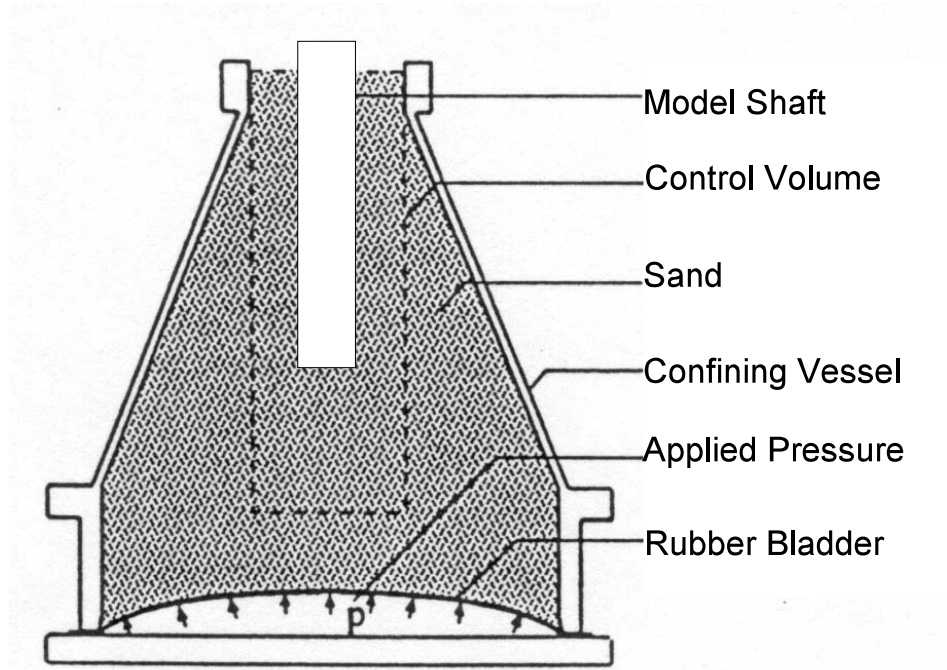


Figure 3-1 Schematic of frustum confining vessel (After Horvath, 1996).



Figure 3-2 Pressure regulator.



Figure 3-3 Installation of roofing structure.



Figure 3-4 Frustum with 2-ton lifting crane.



Figure 3-5 Load testing frame and scaffolding.



Figure 3-6 Casing.



Figure 3-7 Tremie assembly.



Figure 3-8 Pressure pot.



Figure 3-9 Jetting device.



(a)



(b)

Figure 3-10 (a) Removing top two portions of frustum. (b) Sealing the pieces of the frustum.

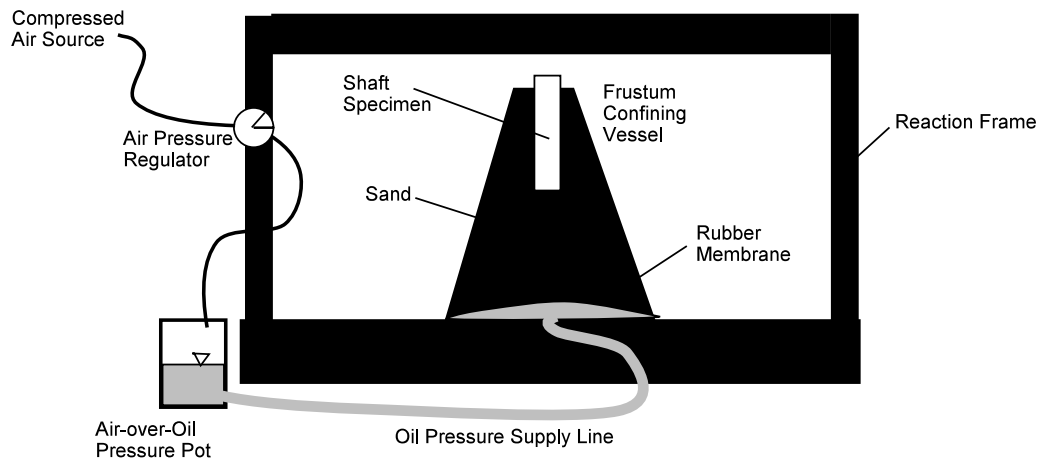


Figure 3-11 Schematic of frustum pressurizing equipment.



Figure 3-12 Expulsion of sand from quick pressurization.



(a)



(b)

Figure 3-13 (a) Placing pile inside jetter. (b) Positioning pile over frustum.



Figure 3-14 Casing driver and template.



(a)



(b)

Figure 3-15 (a) Excavation. (b) Clean-out bucket.



(A)



(B)



(C)

Figure 3-16 (a) Tremie pipe with grouting cell (b) Hopper with mix (c) Grout return.



Figure 3-17 Outer casing.



(a)



(b)

Figure 3-18 (a) Grouting cell. (b) Geotextile and metal plate.

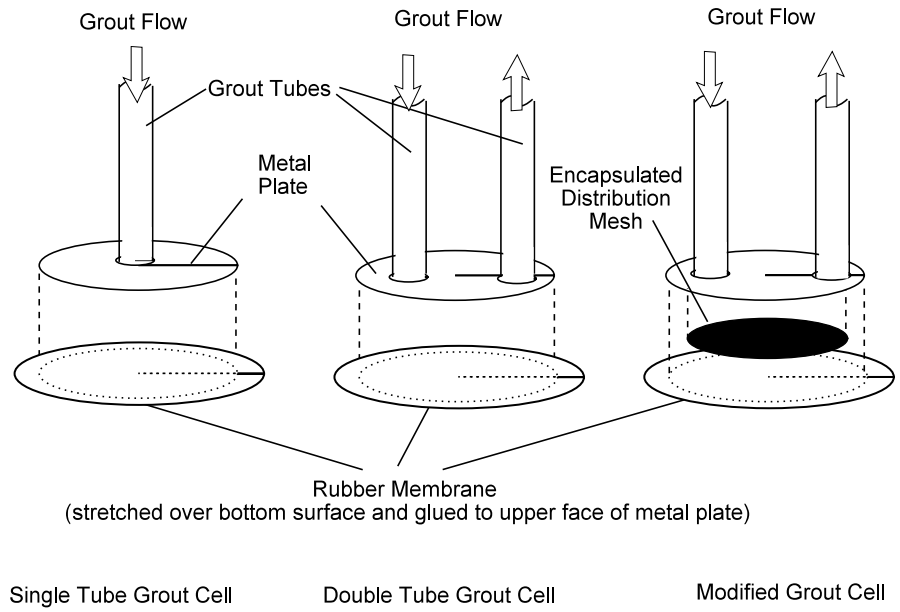


Figure 3-19 Schematic of three grouting cells used.



(a)



(b)

Figure 3-20 Manual grout pump.

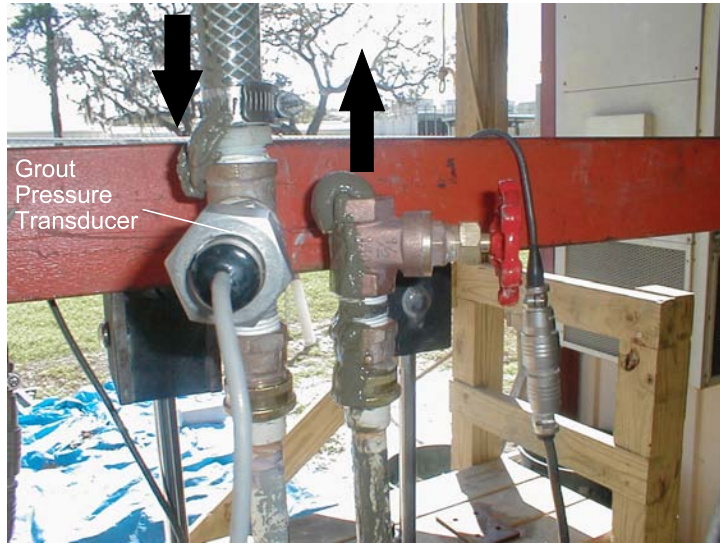


Figure 3-21 Valves with return.



Figure 3-22 Load testing apparatus.



Figure 3-23 Jetted model pile.



Shaft Concrete  
Overtopping

Figure 3-24 CS-1



Figure 3-25 CS-2



Figure 3-26 GS-1



Figure 3-27 GS-2 with corresponding bulb.



Figure 3-28 GS-3 with corresponding bulb.



Figure 3-29 GS-4 with corresponding bulb



Figure 3-30 GS-5 with corresponding bulb



Figure 3-31 GS-6 with corresponding bulb



Figure 3-32 GS-7 with corresponding bulb



Figure 3-33 GS-8 with corresponding bulb.



Figure 3-34 GS-9 with corresponding bulb



Figure 3-35 GS-10 with corresponding bulb



Figure 3-36 GS-11 with corresponding bulb.



Figure 3-37 GS-12 with corresponding bulb



Figure 3-38 GS-13 with corresponding bulb.

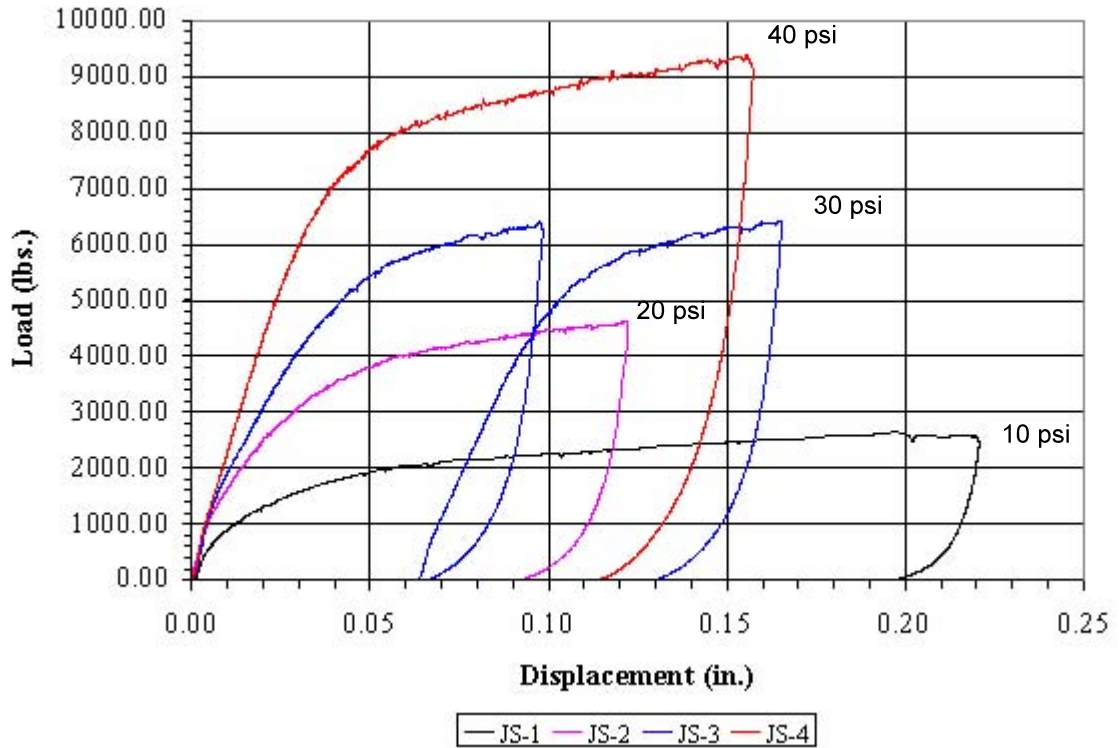


Figure 3-39 Load-displacement with varied FCV pressures.

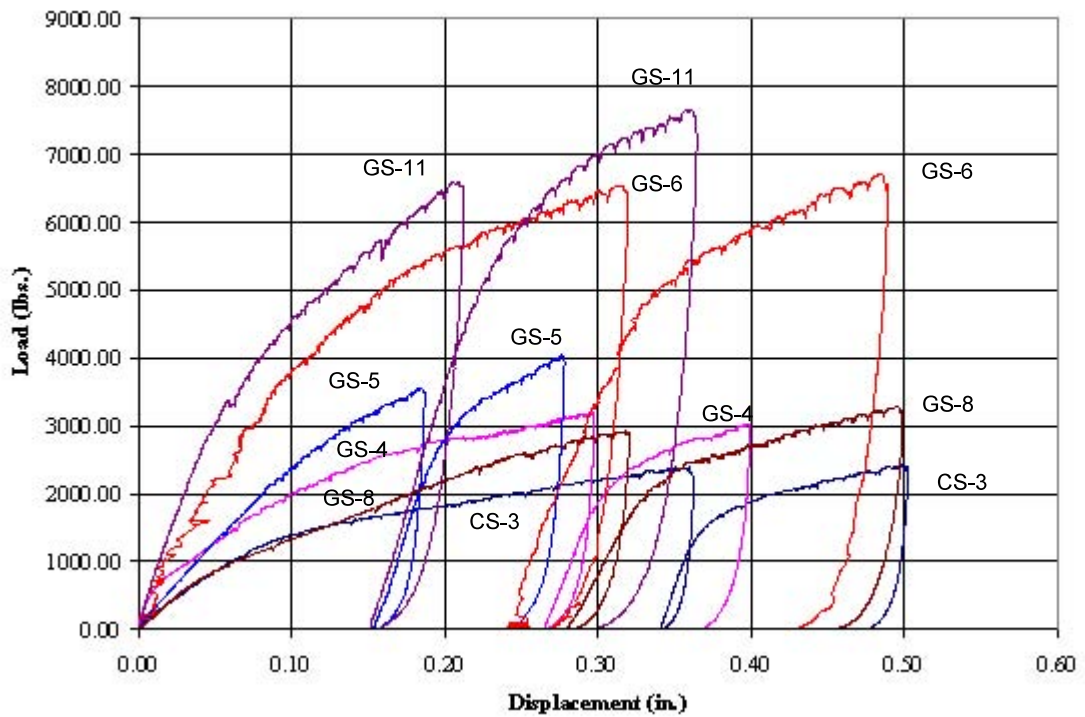


Figure 3-40 Control shaft versus grouted shafts.

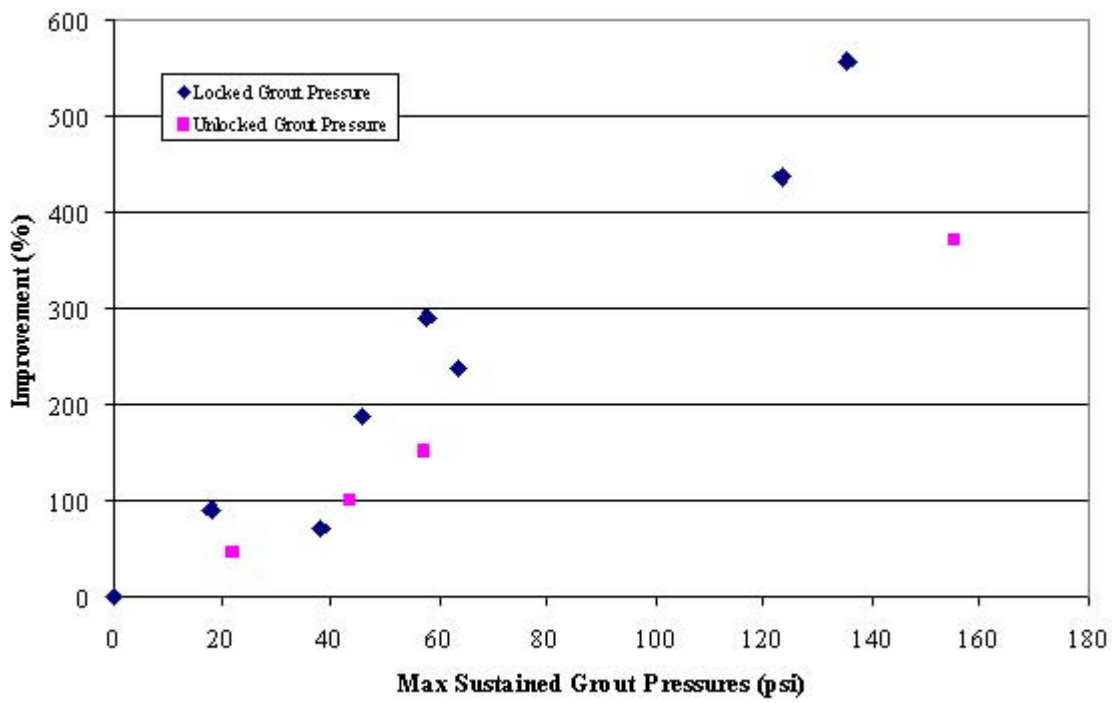
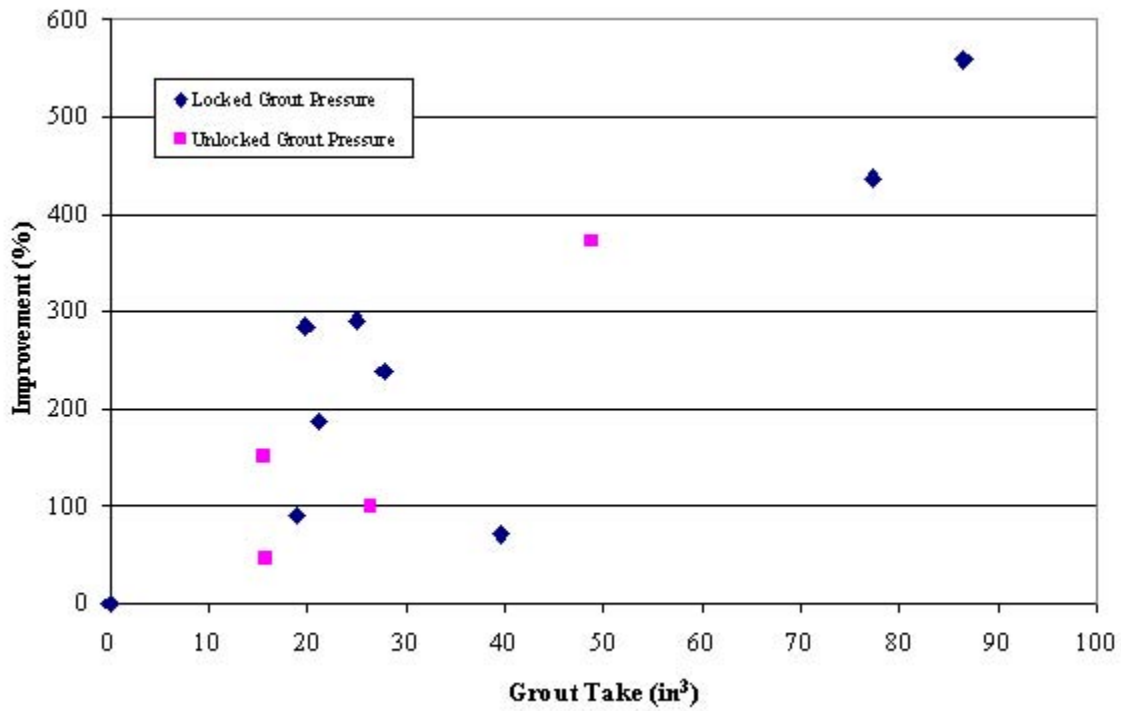


Figure 3-42 Percent improvement versus maximum sustained pressure

## 4. FULL-SCALE TEST PROGRAM

### 4.1 Introduction

The full-scale research program was divided into three Sites of drilled shafts, often referred to simply as shafts. All three of these sites were located in Florida, Sites I and II in Clearwater, and Site III in West Palm Beach. Each site investigated the load capacity effects of tip grouting the shaft tip in a different type of sand, and with different grouting apparatus types within each Site:

1. Site I (Shelly Sand): Utilized flat-jack and sleeve-port type grouting apparatus, as well as one control shaft with no grouting.
2. Site II (Silty Silica Sand): Utilized flat-jack and sleeve-port type grouting apparatus, as well as one control shaft with no grouting.
3. Site III (Cemented Coquina Sand): Utilized flat-jack style grouting apparatus (although one behaved as a sleeve-port style) with each shaft first load tested a first cycle prior to grouting to provide the control values, and then load tested a second cycle subsequent to tip grouting to study the effects.

A total of 8 shafts were constructed and tested in Sites I and II located in the Coastal Caisson Corporation's equipment yard in Clearwater, Florida. These shafts were each 2.0 ft (0.61 m) in diameter and were all approximately 15 ft (4.57 m) long. Five shafts, including one control shaft, were tested in Site I (shelly sand); while 3 shafts, including one control shaft, were tested in Site II (silty silica sand). The shafts, excluding the control shafts, were grouted using an auger style grout pump. All of the shafts were then load tested using a 500 ton (4 MN) Statnamic device with a hydraulic catch mechanism. The results from the grouted shafts have been compared to those of their respective control shafts to assess the load capacity improvement obtained from the tip grouting process.

Two tip grouted shafts were constructed and tested in Site III located at the Royal Park Bridge site in West Palm Beach, Florida. These two shafts were designated as LT-3 and LT-2, and were constructed in said order to facilitate the contractors schedule. LT-1 was the first test shaft actually constructed and tested on this site. However, LT-1 was not grouted and it was tipped in a different stratum type (limestone), and thus will not be addressed here. Test shafts LT-3 and LT-2 were 4.0 ft (1.22 m) in diameter, and 114.2 ft (34.80 m) and 87.4 ft (26.63 m) long, respectively. LT-2 was shortened due to results from LT-3 showing that its capacity had exceeded the load limit of the load testing device.

Test shafts LT-3 and LT-2 were first load tested, then tip grouted using a double piston pump, and retested. All load testing at this site utilized a 3,000 ton (30 MN) Statnamic device with a gravel catch mechanism. The load test performed after the tip

grouting process (referred herein as Cycle 2) established the amount of capacity improvement gained over the original load test (referred herein as Cycle 1) performed prior to the tip grouting process. Although this investigation method at Site III eliminated a control shaft (due to expense), it necessitated certain assumptions that were made in the analysis that will make the estimates of increased load capacity conservative.

## **4.2 Locations and Soil Profiles**

All three Sites were located in Florida; Sites I and II in Clearwater, and Site III in West Palm Beach. Sites I and II were research shafts only, and were not a part of any dedicated construction project. Site III was investigated in a production setting, and was part of a bridge construction load test program. The soils tested in Sites I and II were a shelly sand and a silty silica sand, respectively, and were both loose to medium density. These soils were chosen, based upon an exploratory investigation program, to represent the type of soil most likely to be improved with tip grouting. However, the sand particles at these two sites span the diverse range that can be expected in cohesionless soils: The shelly sand of Site I is very angular and flat, while the silty silica sand is very smooth and round. Results have shown that the difference in soil type affected the ultimate capacity displacement. Shafts tipped in the shelly sand of Site I reached ultimate capacity displacement quicker than those tipped in the silty silica sand of Site II. However, the tip improvements have shown to be very insensitive to differences in soil type.

### **4.2.1 Site I (Shelly Sand) and Site II (Silty Silica Sand)**

Sites I and II were located in the Coastal Caisson Corporation's equipment yard in Clearwater, Florida. Site I was located at the far south end of the property, while Site II was located at the northeast corner of the property. Figure 4-1 is a map showing the property location. Figure 4-2 is a plan view of the property showing the locations of Site I and Site II, and the locations of the exploratory CPT soundings and SPT borings. A dimensioned layout of Site I and Site II are provided as Figures 4-3 and 4-4, respectively, and shows the shaft positions, CPT soundings, and SPT borings within each site.

An initial exploratory investigation was first performed on this site using a mini-cone penetrometer owned and operated by the University of South Florida. The locations tested were at the perimeter of the equipment yard available for shaft installation and testing. The soundings generally showed a shelly sand profile near the south end of the yard, changing to a silty silica sand profile at the north end of the yard. However, the mini-cone device utilized was limited at the time to a 15 ft depth sounding, this is shown in Figure 4-5.

A second exploratory investigation was then performed using a full-size cone penetrometer owned and operated by the FDOT District 1, shown in Figure 4-6. These soundings were made to an average depth of 39 ft (11.7 m). These soundings were made at the four most likely locations for shaft construction and testing. These exploration soundings

performed by the FDOT District 1 were thus labeled according to their sounding logs as CPT 67 through CPT 70, as was shown previously in Figure 4-2.

It was decided that Site I would be installed at the south end of the the yard, bearing in the shelly sand profile. Pursuant to this decision was the FDOT's request for information about grouting applications in an upcoming bridge site bearing in a shelly coquina sand, which would later become Site III of this research work. The potential shaft locations were then laid out at Site I, and a CPT sounding was then made at every location by the FDOT District 1 full-size cone penetrometer. Of these 7 locations that were originally laid out for production, only 5 were utilized, as debris was discovered in two of the locations during construction. Additionally, SPT borings were made by the FDOT District 1, and mini-cone penetrometer soundings were made by USF at interstitial positions between shafts within Site I and Site II subsequent to the grouting and load testing program. The FDOT District 1 test boring rig is shown in Figure 4-7.

Representative soil profiles are shown below for Site I and Site II in Figures 4-8 and 4-9, respectively. These profiles are shown in terms of SPT blow counts and soil type descriptions, and are an average of the CPT soundings and SPT borings performed at the respective Sites. The complete set of individual CPT soundings and SPT borings are contained within Appendix B for Sites I through III.

#### **4.2.2 Site III (Cemented Coquina)**

Site III was located at the Royal Park Bridge site in West Palm Beach, Florida. This bridge crosses the intra-coastal waterway, and connects Highway 704 to Royal Palm Way, Figure 4-10 is a map showing the site location. Figure 4-11 shows the projects foundation layout, from Sheet No. D-11 of State Project No. 93280-3524, and has been annotated to show the location of LT-3 and LT-2. The soil investigation was performed by Professional Service Industries, Inc. (PSI). Figures 4-12 and 4-13 show the SPT borings at the test shaft locations for LT-3 and LT-2, respectively. The overall bridge project was planned to proceed in the following steps:

- 1) A temporary bridge was built just south of the existing bridge. This was necessary as the newly constructed bridge was to maintain the same alignment as the old bridge.
- 2) The test shafts were constructed through large openings cut away from the old existing bridge deck, and load tested (overall project relation to this research). The location was moved from north of the bridge location to the existing bridge by the FDOT at the contractors request such that the old existing bridge would be utilized as access for the construction equipment and support for the Statnamic load testing equipment.

- 3) The old bridge will be demolished, subsequent to the load testing program.
- 4) The new bridge will be constructed along the same alignment as the demolished old bridge. When completed the new bridge will thus maintain the same line of sight down Royal Palm Way.
- 5) The temporary bridge will be demolished.

### 4.3 Grouting Apparatus

All grouting apparatus for all Sites were manufactured at the U.S.F. Structural lab, and the U.S.F. Civil Engineering machine shop facilities. The materials utilized, along with their sources, and detailed drawings will be presented in the following section. A summary of the different types of grouting apparatus utilized for all three Sites is contained below in Table 4-1.

Table 4-1. Grouting Apparatus Used

		Site I	Site II *	Site III
Control Shaft (no Grouting)		1	1	2**
Flat - Jack	Hold Grout Pressure	1		2
	Release Grout Pressure	1	1	
Sleeve-port	With Steel Plate Above	1	1	
	No Plate	1		
Total Shafts		5	3	4

\* The two tip grouted shafts of Site II (only), were also skin grouted.

\*\* Control Shafts were retested after grouting.

The grouting apparatus utilized for the four grouted shafts in Site I was a combination of two flat-jacks and two sleeve-port systems. The two flat-jacks were identical in construction; however, one was allowed to release grout pressure immediately after grouting, and the other had the grout pressure locked in with the use of a ball valve on the grout supply lines during the grout cure. The two sleeve-port systems were identical in construction with the exception that one of them had a steel plate directly above it, while the other did not.

The grouting apparatuses for the two grouted shafts in Site II were identical to those used in Site I. The one flat-jack apparatus utilized locked-in grout pressure during its cure. The one sleeve-port apparatus utilized was the type that had a steel plate directly above it. These two tip grouted shafts in Site II were also skin grouted, while the control shaft was not. The skin grouting apparatus utilized will also be subsequently discussed in this section, although no useable correlation for skin grouting was obtained due to complications with the control shafts side friction values as discussed in Section 4.5.1.

The grouting apparatuses for the two test shafts in Site III were both flat-jack type. However, due to load testing and grouting complications, as will be detailed in Section 4.5.2, test shaft LT-3 experienced no communication of grout pressure across the tip of the shaft. Therefore, LT-3 behaved more like a sleeve-port in nature during the grouting process.

#### **4.3.1 Flat-Jack (Used in Sites I, II, III)**

The flat-jacks utilized in all the Sites were essentially of the same design. The only differences in the flat -jacks used at Sites I and II, and those used at Site III, were their diameter and the number of reinforcing bars used to attach the apparatus to the shaft reinforcing cage. Drawings of these flat-jack apparatus installed at Sites I and II, and Site III are shown below as Figures 4-14 and 4-15, respectively. Their construction will be discussed in the following chronological order:

1. Steel ring fabrication.
2. Steel plate fabrication
3. Natural gum rubber membrane installation

A scuff ring was incorporated into the design of these flat-jacks. From the literature search it can be concluded that this is a new addition to the flat-jack devices that have been and are continuing to be used worldwide. The scuff ring was added to protect the rubber membrane where it wraps around the edge of the plate. There was expressed concern between the investigation team, the FDOT, and industry consultants at the beginning of the project that the edge should be protected to keep the rubber from being torn at the edge in the event that the cage was improperly picked and/or set into the excavation. This design alternative proved to be a great value as will be discussed in Section 4.5.2.

The scuff ring had tabs attached to the top which allowed for the ring to be bolted to the steel plate, therefore providing a better seal between the rubber membrane and the top plate rather than just relying on the rubber cement contact adhesive alone.

The steel plates were made of  $\frac{1}{4}$ " thick steel plate for all of the flat-jacks. The small apparatus (Sites I and II) had a 21 inch diameter, and the large apparatus (Site III) had a 36 inch diameter. The steel plates first had the bolt holes drilled and tapped into them that would allow for the ring to be attached. The ring for each apparatus was used for its

respective plate as a template to drill the bolt holes such that a perfect match in alignment was obtained. There were 6 bolt holes in the small apparatus (Sites I and II), and there were 18 bolt holes in the large apparatus (Site III).

Three 1 inch diameter equally spaced grout holes were then drilled through the plate. These grout holes were placed at mid-center between scuff ring tabs. Three female couplers (1 inch pipe) were welded to the top of the steel plate. Each coupler was welded over its respective grout hole such that it formed a sealed pressure connection to it.

The 3 foot long reinforcing bar tie attachments were then welded to the top of the plates, which would be later inserted into the reinforcing cage to allow the grouting apparatus to be secured in place using tie-wire. The small apparatus had three # 4 rebar tie attachments, while the large apparatus had six # 4 rebar tie attachments. Note that this is a fixed method of suspending the grouting apparatus as opposed to a floating system.

All the flat-jacks had an impermeable membrane below the steel plate. The membrane was made from  $\frac{1}{32}$  inch thick natural gum rubber. The gum rubber was cut in the shape of a circle that would exceed the radius of its respective steel plate by approximately 4 inches, and was centered under the steel plate. This excess rubber (approximately 4 inches around the circumference) was then wrapped up around the edge of the plate, and secured to the top of the plate using a rubber cement contact adhesive. Figure 4-16 shows a large flat-jack (Site III) at this point during its construction. The rubber was then carefully cut away from where it covered the bolt holes on the top of the plate only. The tabs on the ring were then bolted down to the plate. Figure 4-17 shows a small flat-jack (Site I or II) at this point during its construction. This compressed the section of the rubber membrane that had been wrapped and glued to the top of the plate between the tabs on the ring and the plate. Figure 4-18 is a completed small flat-jack.

#### **4.3.2 Sleeve-port (Used in Sites I and II)**

The sleeve-port apparatus utilized in Sites I and II were of the same design with the option of having a steel plate above the apparatus or not. Drawings of these sleeve-port apparatus are shown below as Figure 4-19. Sleeve-ports are identical in function to the grouting apparatus used for tie-back anchors, and differ in the respect that the sleeve-port system has a U-tube delivery, rather than a single tube, to allow for the line to be easily flushed free of grout with low water pressure, and subsequently stage grouted. The construction of the sleeve-port system was considerably easier than the construction of the flat-jacks, and will be discussed in the following chronological order:

1. Drilling grout holes in grout delivery pipe section.
2. Covering grout delivery pipe with rubber tube
3. Securing into cage and optional plate.

The grout delivery pipe was simply a 10 inch section of  $\frac{3}{4}$ " galvanized steel pipe. The pipe had 7 pairs of diametrically opposed  $\frac{1}{4}$ " grout delivery holes drilled through both pipe walls at any location along the pipe. These through holes alternated in circumferential position by  $90^\circ$ , and were equally spaced along the length of the pipe. This number of holes is extremely redundant, as one hole theoretically should work. The grout will only emerge from the grout pipe at either end, or both, of the rubber tube covering the grout delivery pipe regardless of the number of holes drilled through the pipe. However, the numerous holes may have an advantage in that it may facilitate a greater grout flow for a given grouting pressure, and will allow grout to flow out of alternate holes if the first to open should clog. Figure 4-20 shows construction of these grout delivery pipes. The rubber tube was then pulled over the grout delivery pipe, with the use of soapy water as a lubricant. This was made from  $\frac{1}{4}$ " thick natural gum rubber tube with an initial inside diameter of approximately  $\frac{15}{16}$  inch. Grout delivery pipes completed with the rubber tube in place are shown as Figure 4-21. Sleeve-port systems, with and without plate, are tied into the reinforcing cage as shown in Figure 4-22.

The elastic stretch in the rubber tube was needed to seal the grout delivery system during shaft construction, and acts as a one way valve to allow for staged grouting. Inserting a compressed air nozzle between the pipe and the rubber tube while it is being pulled over the pipe will make this process considerably easier, as was discovered during the manufacture of the skin grouting apparatus to subsequently be discussed in this section. Often in industry, electrical tape will be wrapped around the edges of the rubber tube to ensure that the pipe is not infiltrated by concrete/cement during shaft construction.

Galvanized steel  $90^\circ$  elbows were then screwed onto each end of the pipe, and aligned such that the ends of both elbows could be directed towards the top of the shaft. The sleeve-port apparatus can then simply be attached to the grout pipes that are tie-wrapped into the shafts steel reinforcing cage.

When the option of a steel plate above the sleeve-port apparatus was utilized, it was still constructed and secured to the shaft reinforcing cage as described previously. However, a steel plate was also manufactured and tied into the shaft's reinforcing cage. These steel plates were  $\frac{1}{4}$ " thick and had a diameter of 21", and had three # 4 reinforcing bar tie attachments (each 3 ft long) welded to the top of the plate. Each plate had four  $1\frac{1}{2}$ " diameter holes drilled through. The male fitting from the grout pipe would then simply fit through the hole in the plate and screw into the female  $90^\circ$  elbow ends of the sleeve-port. The system was constructed in this way such that the plate assembly could be tied into the cage via its reinforcing bar tie attachments, and thus its weight (or any forces experienced during placement) would not be supported by the pressure fittings to the sleeve-port. Figure 4-23 shows this arrangement.

### 4.3.3 Skin Grouting Sleeve-port (Used in Site II)

The skin grouting apparatus is a simpler form of the sleeve-port used, as only a single pipe is used with a capped end, whereas the tip grouting sleeve-port is a U-tube configuration. Only the Site II shafts, with the exception of the control shaft, were skin grouted. Each of these two skin grouted shafts had six individual grout pipes arranged in three pairs equally spaced around the perimeter of the cage. Each grout pipe of this pair had two sets of grout holes, and terminated at a pressure cap at different elevations within the shaft. The skin grouting pipes were made of  $3/4$ " inch schedule 80 PVC, and were capped at the bottom end. Each individual pipe had two sleeve-ports in it. Each sleeve-port consisted of 16 individual grout holes in the grout pipe with an 8 inch length of  $1/4$ " thick natural gum rubber to cover the set of grout holes. This is the same gum rubber tubing that was utilized on the tip grouting sleeve-ports. Each set of sleeve-ports within the same grout pipe was spaced approximately 2 ft apart (center to center). The grout holes were  $1/4$ " diameter were constructed by drilling through both pipe walls at 8 locations. These through holes alternated in circumferential position by  $90^\circ$ , and were equally spaced along the section of the pipe that was to be covered by the gum rubber tubing. The two sleeve-ports were centered at approximately 34" and 58" from the shaft tip for the three lower grout pipes, and 85" and 108" from the shaft tip for the three upper grout pipes. For relatively long shafts with many grout injection levels, it may become advantageous to use packers within single grout pipes to isolate the grout pressure and flow during skin grouting at these various levels. A single grout pipe of the skin grouting system is shown in Figure 4-24.

The multiple holes within each set of grout delivery holes is redundant, as was discussed in Section 4.3.2 for the tip grouting sleeve-port, as grout would only escape through one, or possibly both ends of any rubber sleeve. The two sets of grout holes in each grout pipe provides further redundancy to the overall distribution of grout around the shaft. Both sets of grout holes are connected to the same grout source, thus it will result in grout escaping through either of the sets of grout holes, or potentially both.

The top of the skin grouting pipe was secured inside the cage; however the pipe is run outside the cage and secured to the hoop reinforcement where the sleeve-port levels are desired. This arrangement of the skin grouting sleeve-port system tied into a reinforcing cage for Site II is shown below in Figure 4-25. The outer edge of the sleeve-port stands off the cage by approximately 1.75 in., leaving a minimum concrete coverage of 1.25 in. as the reinforcing cage had only 3 in. minimum concrete coverage. If this system were employed in a shaft with greater concrete coverage on the steel, it may be advisable to use stand-offs on the skin grouting sleeve-ports to reduce the concrete cover and permit easy "bursting" with water pressure, as will be discussed in Section 4.6.1.

#### 4.4 Instrumentation and Data Acquisition

The components that form any data acquisition system can be divided into two broad classifications: The instrumentation, and the data acquisition and storage device(s). The instrumentation is the collection of transducers that respond in some measurable and calibrated way to changes in some physical phenomenon. The data acquisition and storage device(s) supply the instrumentation with any required input or references, supply any needed completion circuitry, and monitor and record the instrumentation output.

A regulated voltage source is the most common control input that the data acquisition device supplies to the transducers (as was the case with all the instrumentation for this project); however, many types of transducers demand a constant current source. The data acquisition device also supplied completion circuitry, as needed for the individual requirements of the various transducers, as will be discussed in the section to follow. The data acquisition device monitored and digitally recorded the transducer output and time indexed discrete points throughout the test.

Two separate data acquisition systems were utilized simultaneously during the test, and both uploaded their respective data to a common lap-top computer. A variety of transducers were utilized, in both the grouting and load testing operations. Table 4-2 shows this system arrangement, and the transducers that were monitored during grouting and load testing operations.

Table 4-2. Instrumentation Used During Testing

Location	Test Type	
	Grouting	Load Testing
Data Acquisition System	Laptop, Megadac	Laptop, FPDS, Megadac
Top of Shaft	LVDT, grout press. transducer	Loadcell, Accelerometer, Laser
Along Shaft Length	Strain gages	Strain gages
Shaft Toe	Strain gages, Tell tales	Strain gages, Accelerometer

The load impulse from a Statnamic load test has an approximate duration of only 120 milliseconds, with 40 milliseconds both before and after the event also being recorded. At the required sampling rate of 5000 readings per second, 1000 discrete measurements from each transducer are recorded during this small amount of time. It is easy to see that this requires a very sophisticated and robust data acquisition system. The two systems used

during the test were a MEGADAC manufactured by Optim Electronics, and the Foundation Pile Diagnostic System (FPDS) made by The Netherlands Organization (TNO).

The total load imparted to the top of shaft by the Statnamic device is directly measured by a load cell built into the Statnamic piston mounted to the top of shaft. Accelerometers are also built into this piston, and when double integrated over time yields the top of shaft displacement during load testing. Top of shaft displacement for Site III was also measured using a precision laser displacement transducer. Site III shafts also had an accelerometer embedded within the concrete at the shaft tip to yield the shaft tip displacements as these relatively long shafts experience significant elastic shortening during loading.

Top of shaft displacement during grouting operations was directly measured utilizing linear voltage differential transformers (LVDT's), while bottom of shaft displacements were made with linear cable potentiometers attached to the Tension Tell-tales. Note that the potentiometers were positioned directly over and secured to the cable of the telltale before the cable was wrapped over a pulley and weights were suspended to provide tension in the cable. In this way, the tension telltales measure the tip displacement directly with no adverse effects that would be caused by any eccentricities in the pulley. Grout pressure was monitored by a pressure gage tapped into the grout supply line with a pressure T-fitting. A rubber membrane and grease pocket within the fitting protected the instrument from the grout.

Strain gages in groups of three were embedded at predetermined levels within the shaft to monitor the strain during the load testing and the grouting. These strain measurements yield the force at these levels using a composite shaft modulus determined by either concrete strengths (concrete cylinder breaks), or by "modulus gages" that are simple strain gages embedded within the shaft at an elevation above any soil strata.

#### **4.4.1 Site I (Shelly Sand) and Site II (Silty Silica Sand)**

These test shafts has two levels of strain gages; the bottom level was approximately 1.5 feet up from the shaft tip, and the top level was approximately 10.5 feet up from the tip of the shaft. Each shaft was approximately 15 feet long total, with a 14.5 ft. embedment length.

The Tension Tell-tales consisted of a casing, capped at the bottom end, and a steel braided cable strung through the center of the casing. The steel braided cable was secured to the bottom end of the casing through the end cap, clamped, and sealed with the PVC glue. Ample length was left outside the end cap and looped to provide a reaction for tension that would be put upon it during their use in grouting. The casing was made from  $\frac{1}{2}$ " inch

schedule 40 PVC pipe. Significant elastic shaft shortening was not expected during grouting at these sites, nor did it occur. However, trial of this transducer system here gained the experience to use them more confidently when Site III test shafts were grouted.

#### **4.4.2 Site III (Cemented Coquina)**

These two test shafts had six levels of strain gages each; the bottom level was approximately 1.5 feet up from the shaft tip, and the top level was placed above any soil strata to be utilized as modulus gages. Locations of all strain gage levels for LT-3 and LT-2 are presented in the section to follow.

The Tension Tell-tales consisted of a casing, capped at the bottom end, and a steel braided cable strung through the center of the casing. The casing was made of 2" schedule 40 PVC pipe, and the cable was  $\frac{1}{32}$ " nominal diameter. The cable was secured to the bottom end of the casing by running through a small hole in the end cap, wrapping it twice around a 1.5 foot length of #4 reinforcement bar, reinserted back through a second small hole drilled through the end cap, and then clamped to the original length of cable. The two small holes in each end cap, with the cable threaded through, were then sealed with 100% silicone caulking. Figure 4-26 below shows construction of the telltale end cap system, while Figure 4-27 shows the bottom of the tension telltale installed into the reinforcing cage.

#### **4.5 Drilled Shaft Construction**

Sites I and II were constructed using identical techniques and tools, and were identical in size. Site III, however, utilized different techniques/tools, and were much larger in size. Sites I and II were excavated using a synthetic slurry, while Site II was excavated using an attapulgate slurry. Table 4-3 contains a summary of the shafts construction method, while Table 4-4 contains a summary of the shaft as-builts. A detailed account of construction for Site I and Site II is given, followed by details of Site III construction. The shaft construction discussed in the following order:

1. Cage construction
2. Excavation
3. Cage placement
4. Concrete placement

Table 4-3. Construction Method Summary

Shaft Designation	Site I					Site II			Site III	
	Control	Flat-Jack	Flat-Jack	Sleeve-part-1	Sleeve-part-2	Control	Flat-Jack	Sleeve-	Flat-Jack	Flat-Jack
Soil Type	Shelly Sand					Silty Silica Sand			Cemented Coquina	
Slurry Type	Polymer								Attapulgite	
Tip Diameter	2.0 ft. (0.61 m)								4.0ft.(1.22m)	
Aspect Ratio*	7.25								24.02	15.33

\* "Aspect Ratio" defined as: (length of shaft below grade) / (nominal diameter of shaft)

Table 4-4. Shaft As-BUILTS

Shaft Designation		Site I					Site II			Site III	
		Control	Flat-Jack 1	Flat-Jack 2	Sleeve-Port 1	Sleeve-Port 2	Control	Flat-Jack	Sleeve-port	Flat-Jack	LT-3 Flat-Jack
Inner Casing	Top	1.0	1.8	1.0	1.0	1.0	1.0	1.0	1.0	19.5	14.5
	Bottom	-1.0	-0.2	-1.0	-1.0	-1.0	-1.0	-1.0	-1.0	-16.2	-52.2
Outer Casing	Top	None								19.5	14.5
	Bottom	None								-16.2	-30.5
Steel Cage	Top	0.5	1.3	0.5	0.8	0.6	0.5	0.6	0.6	18.5	13.5
	Bottom	-14.3	-13.8	-14.2	-13.7	-14.1	-14.1	-14.1	-14.1	-107.4	-72.6
Grade		0								-11.5	-11.5
Water (GWT)		-9								-3.4	-3.4
Shaft Tip		-14.3	-14.5	-14.4	-14.3	-14.4	-14.3	-14.5	-14.5	-107.6	-72.8
Strain Gage		-3.5 -12.8	-2.7 -12.3	-3.5 -12.7	-3.2 -12.2	-3.4 -12.6	-3.5 -12.6	-3.4 -12.6	-3.4 -12.6	-3.4 -33.9 -50.3 -66.7 -83.1 -106.1	1.6 -21.7 -33.5 -45.3 -57.1 -71.2

LT-2

Note: all units are in “ft.”

#### 4.5.1 Site I (Shelly Sand) and Site II (Silty silica sand)

The reinforcing cages used at Sites I and II were all constructed on site by USF personnel. The reinforcing steel was first tied completely, the grout pipes and grouting apparatus were then attached, and finally the strain gages with sister bars were then secured to the longitudinal reinforcing bars. The vertical reinforcement consisted of six # 8 reinforcement bars equally spaced about the perimeter. The hoop reinforcement consisted of # 5 reinforcement bars, equally spaced every 1.5 ft, and had a lap of 25 in. All reinforcing bars used were Grade 60. The finished cages were 14.5 ft in length, and had an outside diameter at the hoops of 18 inches. Figure 4-28 shows cages during construction on-site. Figure 4-29 shows completed cage and grouting apparatus for Sites I and II.

The grout pipes were made from 1 inch high density polyethylene (HDPE) tubing (CTS SDR-9). The 1 inch male pipe thread fitting secured at either end of the grout pipe was made of brass (C84-44 1" CTS Compression MIPT Adapter) and had thin stainless steel inserts (#52 Stainless Insert) to keep the tubing from being crushed by the pipe fitting. These materials are very common and readily available. This male fitting then made a pressure connection to either type of grouting apparatus used. This system has a pressure rating of 150-200 psi (1000-1400 kPa), and was more than adequate for the grouting pressures experienced on this site. It was envisioned, as it did prove itself, that this system of continuous rolled pipe may be convenient to install, so long as the pressure requirements can be met.

The shafts of Site II, with the exception of the control shaft, were also skin grouted. These reinforcement cages for these two shafts incorporated skin grouting apparatus as well. The skin grouting apparatus consisted of six individual grout pipes (three pairs that were equally spaced around the perimeter of the cage), and two sleeve-ports per grout pipe. The two sleeve-ports were centered at approximately 34 inches and 58 in. from the shaft tip for the three lower grout pipes, and 85 in and 108 in. from the shaft tip for the three upper grout pipes.

Both Site I and II shafts with constructed using synthetic slurry. The water supply for construction at Site I was from a pond, and the water supply for construction of Site II was from a metered fire hydrant. The excavations were conditioned in order to normalize the PH level before any synthetic slurry was added.

A truck mounted Texoma 700 drill rig was utilized to excavate the shafts of Site I, while a track mounted BG-7 drill rig was used to excavate Site II. These are shown in Figures 4-30 and 4-31 respectively.

These rigs were chosen simply based upon availability of small sized drill rigs in the equipment yard at the time of construction. With only 24 inch nominal diameter shafts it was important not to oversize the drill rig, or more precisely the kelley bar size. Too large of a

kelley bar would displace an excessive amount of drill slurry each time it was re-inserted into the excavation, thus tending to create instability in the borehole walls.

Both Site I and II utilized the same drill auger in construction. Figure 4-32 shows a picture of this auger that was used. The auger had two flights with bullet teeth continuously along both edges. The outside diameter (tooth to tooth) was 24 in. A clean-out bucket was not used during construction as it would not produce a significant improvement in tip condition, nor would the use of standard down-hole or air-lift pumps. Due to the excavation's relatively shallow depth (14.5 feet), there would be insignificant sediment build up in the slurry. Additionally, such a short column height coupled with the use of synthetic slurry ensured that any sediment would settle out very quickly. Even under ideal conditions it is essentially impossible to thoroughly "clean out" any shaft excavation at the tip, as is customary with rock socketed tips, as any action taken simply tends to further upset the excavation. A benefit of tip grouting is that this condition is mitigated, and is a point that this study will confirm.

A Hitachi 60 ton track mounted hydraulic crane was used to pick the cages and set them for Site I and II. This same crane was also utilized for concreting operations, as will be subsequently discussed. The low aspect ratio of the cages, along with stiff hoops and a relatively long crane boom of approximately 80 ft, made the picking of these cages very simple, and were easily maintained in a straight fashion during the entire process. Figure 4-33 shows a cage being picked in this fashion.

As the cages were being set, a slight tolerance problem was encountered with the Flat-Jack apparatus and the sleeve-port with plate apparatus. The shafts had been excavated using a 24 inch diameter auger; while the flat-jack had a maximum diameter of 21.5 inches at the scuff ring, and the Sleeve-port with plates had a maximum diameter of 21.0 inches at the plate. Although the cages were able to be set satisfactorily for the research purposes, this proved to be too tight a tolerance for production. The setting of these cages was very unforgiving as to alignment and plumbness with the excavation.

Site I Flat-Jack 1 (locked-in pressure) was set nearly 1 foot too high due to this tolerance problem. This may have been due to some amount of scraping of soil away from the borehole walls, thus leaving a small amount of loose deposit at the tip which the apparatus rested upon. Additionally, the tip may not have been perfectly flat (rounded up at the edges), thus not allowing the cage to lower further than the elevation where the outside edge of the device contacted the upward curving edges. The result was that Site I Flat-Jack 1 had soft debris and/or voids at the tip of the shaft. Careful observations of the grouting of this shaft confirmed that 1.8 ft.<sup>3</sup> of grout was needed to fill the void under the flat-jack plate before any grout pressure above that required to pump the grout through the lines could be detected. This represents a volume that would be equivalent to a 21.5 in. diameter column (diameter of flat-jack) by 8.6 in. high. As a direct result, an unanticipated variable was tested between the two flat-Jacks of Site I; the effect of varying amounts of soft debris and/or voids

below the flat-jack grouting apparatus. Results show that this condition was mitigated by the tip grouting procedure, this grout volume of 1.8 ft.<sup>3</sup> is not included in subsequent grouting and load testing analysis.

The concreting of Site I and Site II shafts proceeded without incident. A 1/4" thick, 24" diameter surface casing was set in place at the top of each excavation. The casing was set such that its top edge was approximately 3 inches above the top of the reinforcing cage. The height of the casing above grade then depended on what elevation the cage was set. A tremie of 10 inch inside diameter was used with a top-mounted hopper. A traveling tremie plug (styrofoam peanuts) was used. The concrete was then "tailgated" directly into the hopper from the concrete trucks. Figure 4-34 shows the concreting operation. Note that in all cases, the tremie never broke seal with the concrete, and the shafts were all significantly overpoured such that good concrete was obtained at the top of the shaft.

The Site II test shafts were exhumed with the use of an extendable back-hoe and the Hitachi crane with water being jetted around the shaft to loosen the soil. Figure 4-35 shows the grouted shaft tips (much of the grout bulbs could not be retrieved), and Figure 4-36 shows the Control shaft. Unfortunately the bulges along the control shaft made a direct comparison to skin grouting improvements impossible.

#### **4.5.2 Site III (Cemented Coquina)**

Site III test shafts were located at the new Royal Park bridge (Highway 704) across the intra-coastal waterway in West Palm Beach, Florida. The Geotechnical consultant for this project, and the on-site inspection, was Professional Service Industries, Inc. (PSI), who recognized a potential benefit of tip grouting at this site. PCL was the general contractor for the test shaft and demolition phase of the project. Coastal Caisson Corp. was the deep foundation specialty contractor, responsible for construction and grouting of the test shafts, and Applied Foundation Testing (AFT) was the foundation load testing specialist. The University of South Florida (USF) fulfilled the Florida Department of Transportation's (FDOT) obligation to provide the following products and services to the project:

1. Provide the grouting apparatus and oversee its installation
2. Oversee the drilled shaft production
3. Overseeing the grouting operations and providing all instrumentation and data acquisition for grouting operations
4. Data reduction of grouting operations
5. Detailed reporting of load testing and grouting operations as they pertain to tip improvement.

The reinforcing cages for the test shafts LT-3 and LT-2 in Site III were all constructed on site by PCL. The reinforcing steel was tied completely, and cable clamps were secured

to vertical bar splices to prevent slippage. The flat-jack, grout pipes, and Tension Tell-tales were then installed in each cage under the direction of USF personnel. The strain gages with sister bars were then installed by Applied Foundation Testing technicians.

The vertical reinforcement consisted of sixteen SI #32 bars equally spaced about the perimeter. The hoop reinforcement consisted of SI #16 bars equally spaced every 0.3 m, and had a lap of 0.560 m. All reinforcing bar was ASTM A615M Grade 420. The finished cages were 38.45 m and 26.33 m in length for LT-3 and LT-2, respectively, and had an outside diameter at the hoops of 0.920 m providing for the minimum of 0.150 m of concrete cover.

The flat-jack apparatus was tied into the cage under the direction of USF personnel. The six 3 feet long #4 reinforcing bar connectors welded to the top of the flat-jack were inserted into the bottom end of the cage with the #4 bar inside the cage hoop reinforcement, and in the interstitial positions between the vertical reinforcement. The flat-jack was inserted into the cage until the top of the flat-jack contacted the first (lower-most) vertical cage reinforcement. The flat-jack was then squared up in all directions relative to the length of reinforcing cage. Then the #4 reinforcing bar connectors were securely fastened at every point that they crossed a hoop reinforcement with tie wire. Figure 4-37 shows a flat-jack tied into the cage for LT-2, and is ready to be picked.

The grout pipes were made from 1 inch schedule 80 PVC, with a total of three lengths of this grout pipe running down the length of each cage. The PVC grout pipes were connected to the flat jack with the use of 4 feet of 1 inch diameter high density polyethylene tubing (HDPE), rather than directly connected to the flat-jack itself. This is the same HDPE tubing (CTS SDR-9), brass 1 inch pipe thread connectors (CTS SDR-9), and stainless steel inserts (#52 Stainless Insert) that were utilized in Sites I and II. The benefits of the increased “flexibility” of this type of connection, as proved true in the field production, were two-fold. First, the increased “flexibility” of the grout pipe to the flat jack would not attract stresses by being too rigid and ensure that they would not be damaged during the cage lifting operation. Secondly, The flexibility would be much more tolerant of mis-alignments of the PVC grout pipe to the grout ports on the top of the flat jack, and in general add to the ease of installation. Note that the grout pipes were run full-length into the cage, the brass connectors were secured to the grout pipe, and then the HDPE tubes were inserted into the receiver of the brass connector and secured. In this manner, the HDPE tube and brass connector act as a “union” in the pipe system. Figure 4-38 shows the completed cage tip for LT-3.

The HDPE tubing had a working pressure rating of 200 psi (factor of 4 against bursting). This was well below the 400 psi requirement in the specifications, as was provided by the schedule 80 PVC rated at a working pressure of 630 psi. Additionally, the concrete coverage over this system minimizes the importance of access line pressure ratings. The primary concern was the ability of the schedule 80 PVC pipe connection at the top of these pipes to handle the working grout pressures. For this concern, special female slip

fittings were utilized where the threaded female end of the coupler was composed of a factory steel threaded insert. The coupler was secured to the schedule 80 PVC pipe with the use of PVC primer and heavy-duty PVC glue, and allowed to sit for 24 hours before grouting. One instance of fitting failure occurred when LT-2 was first pressurized. Inspection by USF personnel revealed that it had not been properly sanded. The pipe was then sanded, re-applied with the PVC glue, and grouting commenced approximately 15 minutes later without further incident, emphasizing the importance of sanding preparation and not glue set time.

Three Tension Tell-tales were tied on the inside of the reinforcing cage of both LT-2 and LT-3. They were secured to the hoop reinforcement and were equally spaced about the perimeter. These were made of 2 in. Schedule 40 PVC pipe with braided stainless steel cable of  $\frac{1}{32}$ " nominal diameter, as described previously.

Both test shafts LT-3 and LT-2 were constructed using permanent casing and had outer surface casing as well. Attapulgitte slurry was utilized to maintain borehole stability. The slurry viscosity, density, and PH were maintained within the ranges specified according to standard FDOT drilled shaft construction standards.

A track mounted Delmag drill rig on a Lehbar 890 carrier was utilized to excavate the shafts of Site III. Both test shafts of Site III utilized the same drilling tools in construction which consisted of a digging bucket with recirculation feature for the upper soil layers, a rock auger for the heavily cemented coquina layers, and a clean out bucket for the tip integrity. The surface casing was installed with a vibro-hammer. Originally, the permanent casing of LT-2 was set to approximately the same elevation as the outer casing. An incident did occur when the excavation proceeded below this permanent casing elevation, a slurry plume was observed to emanate in the vicinity just south of the test shaft location. Figure 4-39 shows the slurry plume as the Delmag drill rig continues to excavate LT-2. As a result the permanent casing was driven 23 feet deeper to the elevations shown on the as-built.

A Kobelco track mounted hydraulic crane was used to pick the cages and set them for LT-3, and the whip line of the Delmag drill rig was also used in picking LT-2 in an effort to help reduce the bending of the cage that was experienced with LT-3. This same crane was also utilized for concreting operations, as will be subsequently discussed.

The picking of the cage for LT-3 was accomplished utilizing two pick points; one about 20 ft. down from the cage top, and the other about  $\frac{1}{3}$  the cage length down from the top. The choice of the top pick point location was undoubtedly due to an insufficient boom length to suspend the entire cage. Figure 4-40 shows the cage for LT-3 being lifted. The cage for LT-3 was not maintained in a nearly straight fashion, as is more desirable for

instrumentation and grouting system integrity maintenance. The cage was placed into the excavation, secured, and then the pick point moved to the top of cage. Fortunately, the cage did not scuff the borehole wall excessively, and the cage was set to the proper elevation.

The picking of the cage for LT-2 was accomplished utilizing four pick points; one at the cage top, one at the cage bottom, and the remaining two were equally spaced along the length of the cage. The top pick point was suspended from the Kobelco crane's main block, the two pick points along the cage were suspended by the crane's whip line via the use of a traveling block, and the bottom pick point was suspended using the drill rig's whip line. This method is common for picking cages with an Osterberg load test cell(s). The cage for LT-2 was maintained in a nearly straight fashion during the entire process, as is shown in Figure 4-41. However, the bottom end containing the grouting apparatus was inadvertently allowed to drag across the concrete bridge deck, as is shown in Figure 4-42. Fortunately, the scuff ring on the apparatus protected the edge from being ruptured.

A sectional tremie of 12 in. (305 mm) inside diameter was used with a hopper for the concrete placement of both shafts in Site III. A concrete pump was used to deliver the concrete to the hopper for LT-3, as the service crane blocked access on the existing bridge deck to the shaft excavation. For LT-2, however, the concrete trucks tailgated the concrete into the hopper as the full access to the excavation was available during this concrete placement. A bottom plate was used on the tremie to prevent segregation during initial placement for both test shafts.

The sectional tremie plugged at the lower-most joint at the initial introduction of concrete into the excavation during concrete placement for both test shafts. As a result a small amount of concrete was introduced into excavations as the tremie plugged. The tremie was cleared in both cases, the concrete placement resumed by inserting the tremie, with tremie plate, back into the excavation until it had made contact with the top plate of the grouting apparatus. The tremie was then raised approximately 4 inches, and concrete was allowed to flow. A weighted tape prior to this revealed minimal amounts of concrete and/or sediment on top of the placed grouting apparatus; however the cage was not retrieved as this action would most likely rip the grouting apparatus off. The rest of the concreting operations proceeded in a typical fashion, and the shafts were all significantly over-poured such that good concrete was obtained at top of shaft.

The 1 in. schedule 80 grout pipes each had a short 4 in. schedule 40 PVC pipe section (approximately 1 foot long) surrounding it and capped on top to create a pocket inside the top of shaft for the grout pipes, as they needed to be below the top of shaft for load testing. A similar arrangement was made with the 2 inch schedule 40 PVC Tell-tale pipes. This is shown in Figure 4-43 below for LT-2 as it is being poured.

## **4.6 Grouting and Load Testing**

The grouting on Site I and Site II was performed by Earth Tech, Inc. under the direction of USF personnel using an auger-style grout pump. The grouting at Site III was performed by Coastal Caisson Corp. under the direction of USF using a dual-piston grout pump. The load testing at Site I was done with a 500 ton (4 MN) Statnamic device owned by USF, while the load testing at Site III was done with a 3,500 ton (30 MN) Statnamic device owned and operated by Applied Foundation Testing, Inc.

### **4.6.1 Site I (Shelly Sand) and Site II (Silty silica sand)**

Prior to any grouting work, the sleeve-port apparatus on these sites (both tip grouting and skin grouting) were “burst” open using water pressure. This was done the day following concrete placement, as is common practice, such that the concrete had set up, yet had not gained significant strength. The intent of this action is to open up a path for subsequent grouting, which may be performed at a later date when the shaft has reached acceptable strength, while minimizing the volumetric flow during this process to reduce the soil disturbance. The auger-style grout pump was first used; however, experience proved that a small pressure washer was ideally suited to this task for the aforementioned reason.

The tip grouting sleeve-ports were easily burst by the auger-style grout pump with most bursting at only 80 to 100 psi. This is undoubtedly due to minimal concrete coverage over these sleeve-ports, as the weight of the cage was bearing down on them during concrete placement. However, only approximately half of the skin grouting sleeve-ports burst with the limited 200 psi water pressure. The minimum concrete coverage on the cage was 3 inches, and the skin grouting sleeve-ports were placed immediately outside the cage yielding a minimal concrete coverage of approximately 1.75 in. over them. The skin grouting sleeve-ports that burst easily under the 200 psi water pressure probably had concrete coverage close to this value. The other skin grouting sleeve-ports were burst with water pressure in the range of 900 to 1500 psi using a small pressure washer. This device proved to be ideal for this task as pressure would build to the levels needed, but very small volumetric flow occurred once they did burst.

The grouting at these sites was then accomplished using an auger style grout pump, as shown in Figure 4-44. The pump was adequate for these sites as shaft uplift or grout volume proved to be the limitation at all test shafts. In all cases the shaft concrete was allowed to gain strength for approximately 20 days before grouting operations commenced. The grout mix utilized was a water-cement slurry (Type I and II cement) with a water to cement ratio of 0.5. The grouting lines of both sleeve-port and flat-jack apparatus were gently flushed with grout before the extra lines were capped and grout pressure was applied.

The load testing was carried out by USF with the heavy lifting operations accomplished with the use of the Hitachi crane owned and operated by Coastal Caisson

Corp., as shown in Figure 4-45. Three load cycles were performed on each test shaft, with the exception of four load cycles on Site I control shaft, with the use of a 500 ton Statnamic device. The hydraulic catch mechanism made reloading of the shaft proceed rapidly, as all three load cycles would typically occur within a 30 minute time span. In all cases the test shafts were displaced many times more than ultimate capacity displacement, such that the load vs. displacement curves would be fully developed. Figure 4-46 shows a test in progress at Site II.

#### **4.6.2 Site III (Cemented Coquina)**

The grouting specifications at this job site required that the grouting contractor, Coastal Caisson Corp., provide a pump capable of sustaining grout pressures up to 500 psi. A dual-piston grout pump manufactured by their parent company, Bauer Spezialtiefbau in Schrobenhausen Germany, was supplied for this purpose. Figure 4-47 shows this device. Sustained grout pressures of 500 and 450 psi were obtained in LT-3 and LT-2, respectively. After being initially mixed in a paddle-type mixing vat, the grout was then sent to a high speed colloidal mixing tank before being drawn up into the piston and pressurized. A feature that makes this device particularly suited to grout was that the dual pistons will re-circulate their grout back and forth to each other in the event that grout take is not (or very slowly) occurring while grout pressure is to be maintained.

The grouting of both test shafts at this site occurred between the first and second load test cycles on each shaft. In this manner the un-grouted load vs. displacement response was directly measured during the first load cycle. However, the grouted shaft response, as measured during the second load cycle, was undoubtedly affected by the first load cycle. These affects made the estimation of the tip improvement through tip grouting conservative, as a significantly greater improvement would have been attributed to the tip grouting had the shaft not initially been load tested.

The most obvious explanation of this is that if the soil at the shaft tip had not been initially compressed due to the first load cycle, the grout bulb formed at the tip may have had the opportunity for a greater radial expansion, and thus provide a larger bearing zone at the shaft tip. More particular to this site, was the drop off of side shear during the first load cycle to a lower residual value. This side shear not only affected the total capacity directly in the second load cycle, but it also lowered the available side shear reaction against the tip grouting pressure. Lower grout pressure are thus attained, as will be shown to be directly related to the tip improvement, before shaft uplift criteria is met. This is a good illustration of why the uplift criteria must be carefully set for grouting operations such that a dramatic loss of side shear does not result.

When LT-3 was grouted, there was no communication between the three grout hoses, even though grout take occurred in all three. Further, a pressure spike occurred in these lines just prior to grout take commencing. The most likely explanation for this is that the rubber

membrane over the flat-jack plate had been ruptured at the three grout hole locations during the first load test cycle. This test shaft behaved similar to a sleeve-port grouting apparatus; an observation that was confirmed by the strain gage data. Bending moments were observed in the shaft as each of the three independent grouting orifices (or “stems”) were pressurized, and the pressure appeared to be acting on an area less than the actual shaft tip area (area ratio  $< 1$ ) in each case. Both of these phenomena are consistent with the sleeve-port behavior, as will be discussed in the analysis section.

The three grout lines of LT-2 were inspected prior to grouting. Accumulated drill slurry was found within these lines, and was flushed out prior to the grouting operation. This was accomplished by slowly inserting a ½ in. polyethylene tube, supplied with water by a 2 in. centrifugal pump, into the grout pipes until they had reached the flat-jack level. This is shown in Figure 4-48. Once the slurry deposits had been cleared from the lines, they were flushed with grout and pressurized.



Figure 4-1. Site I and Site II locations.

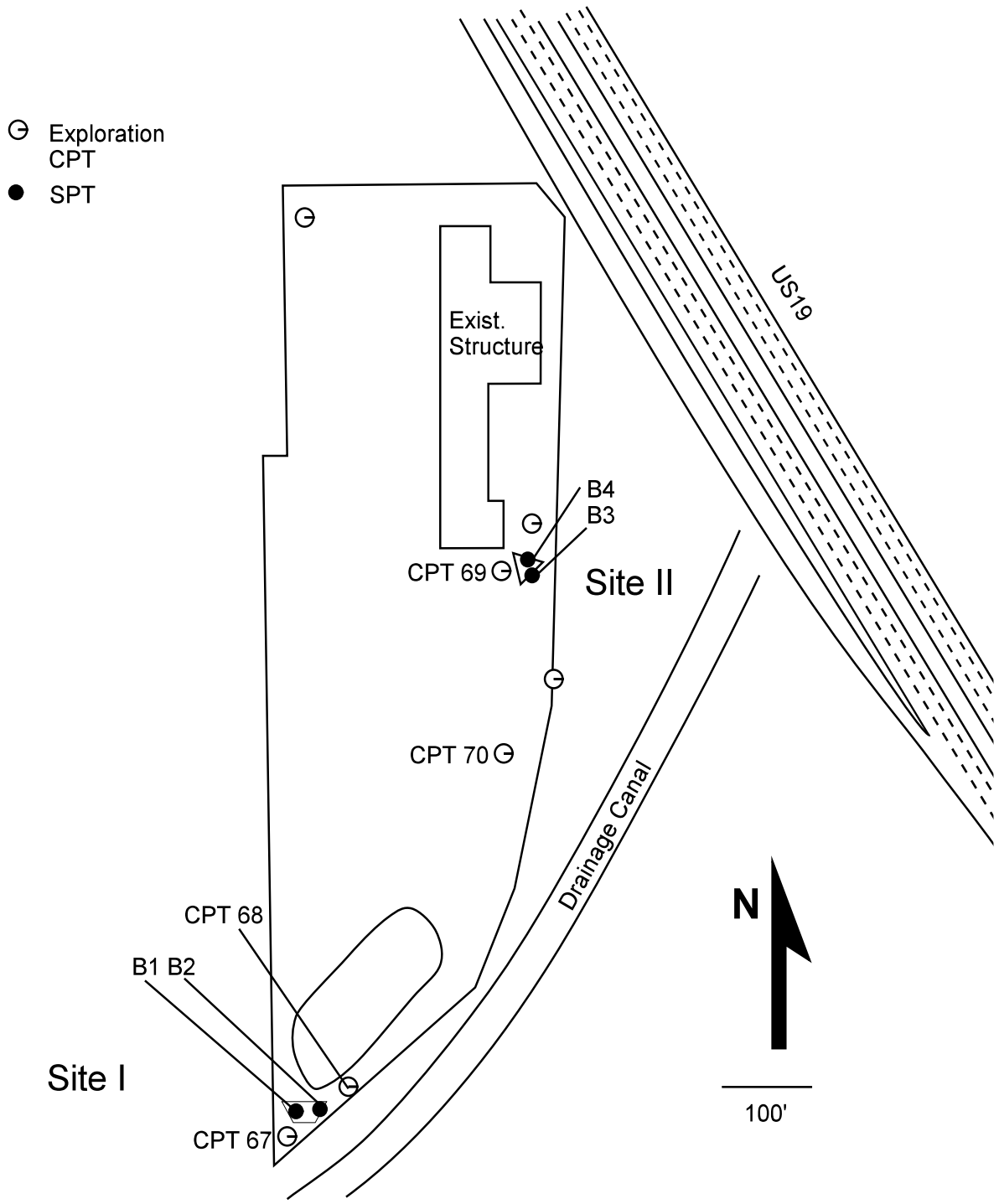


Figure 4-2. Site I and Site II plan views.

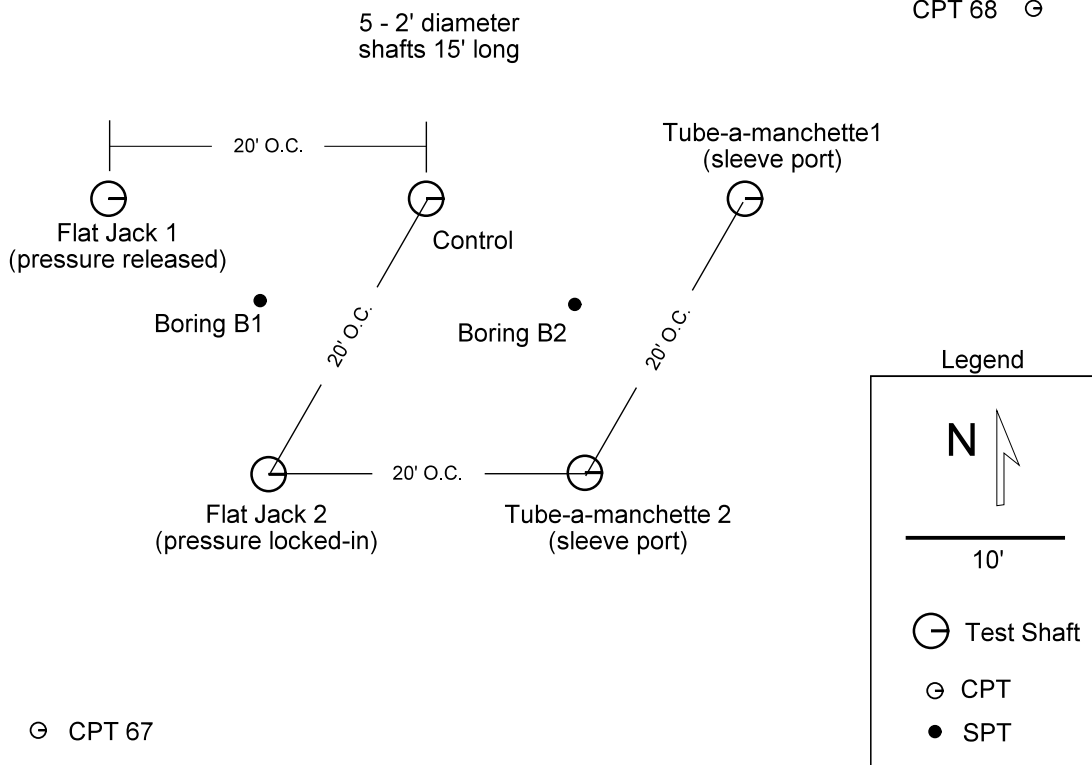


Figure 4-3. Site I layout.

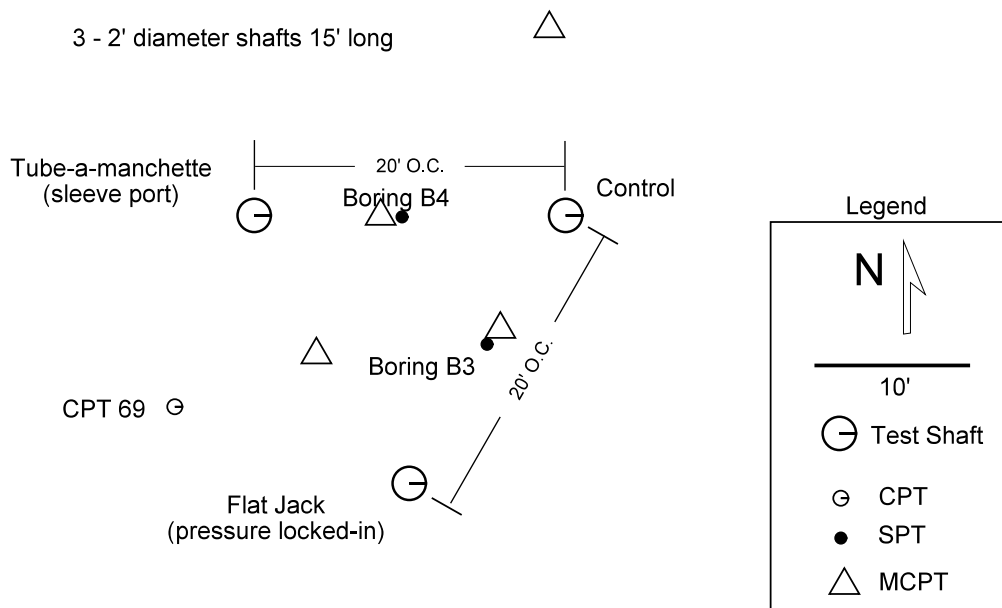


Figure 4-4. Site II layout.



Figure 4-5. University of South Florida's mini-cone penetrometer (MCPT).



Figure 4-6. FDOT Dist.1 cone penetrometer.



Figure 4-7. FDOT Dist.1 SPT Rig.

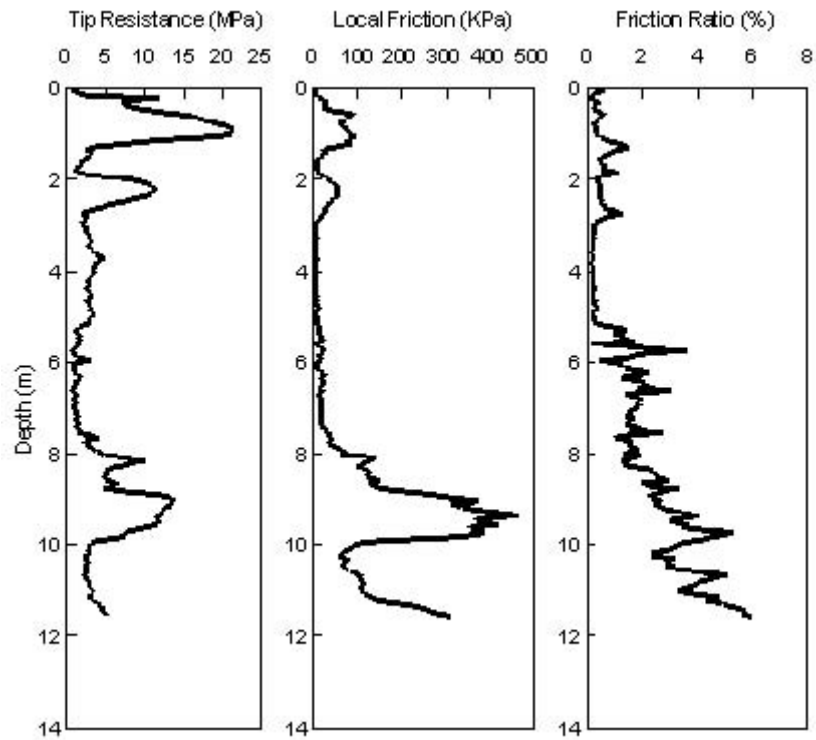


Figure 4-8. Typical CPT sounding Site I.

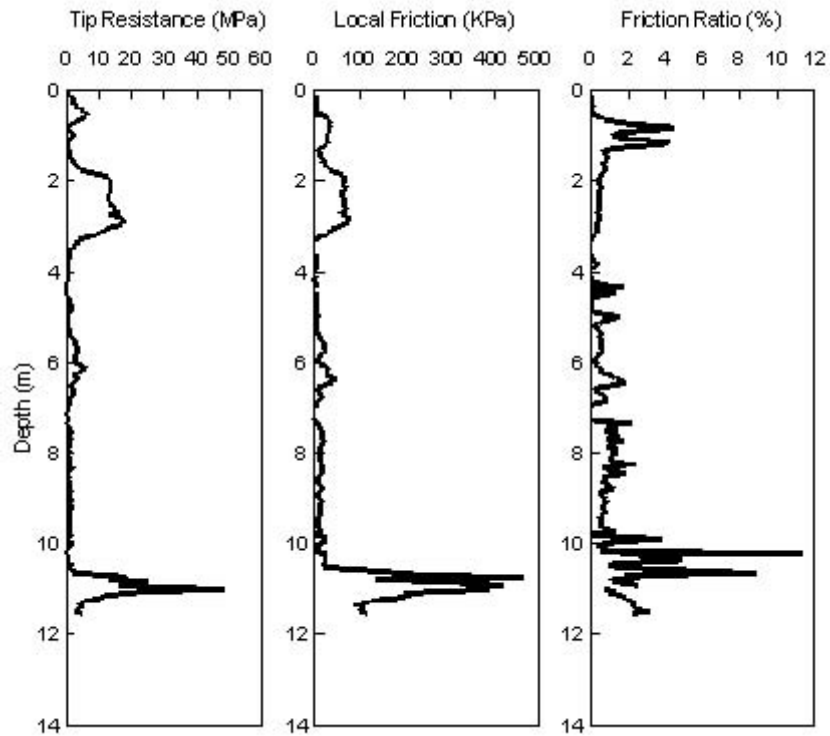


Figure 4-9. Typical CPT sounding Site II.

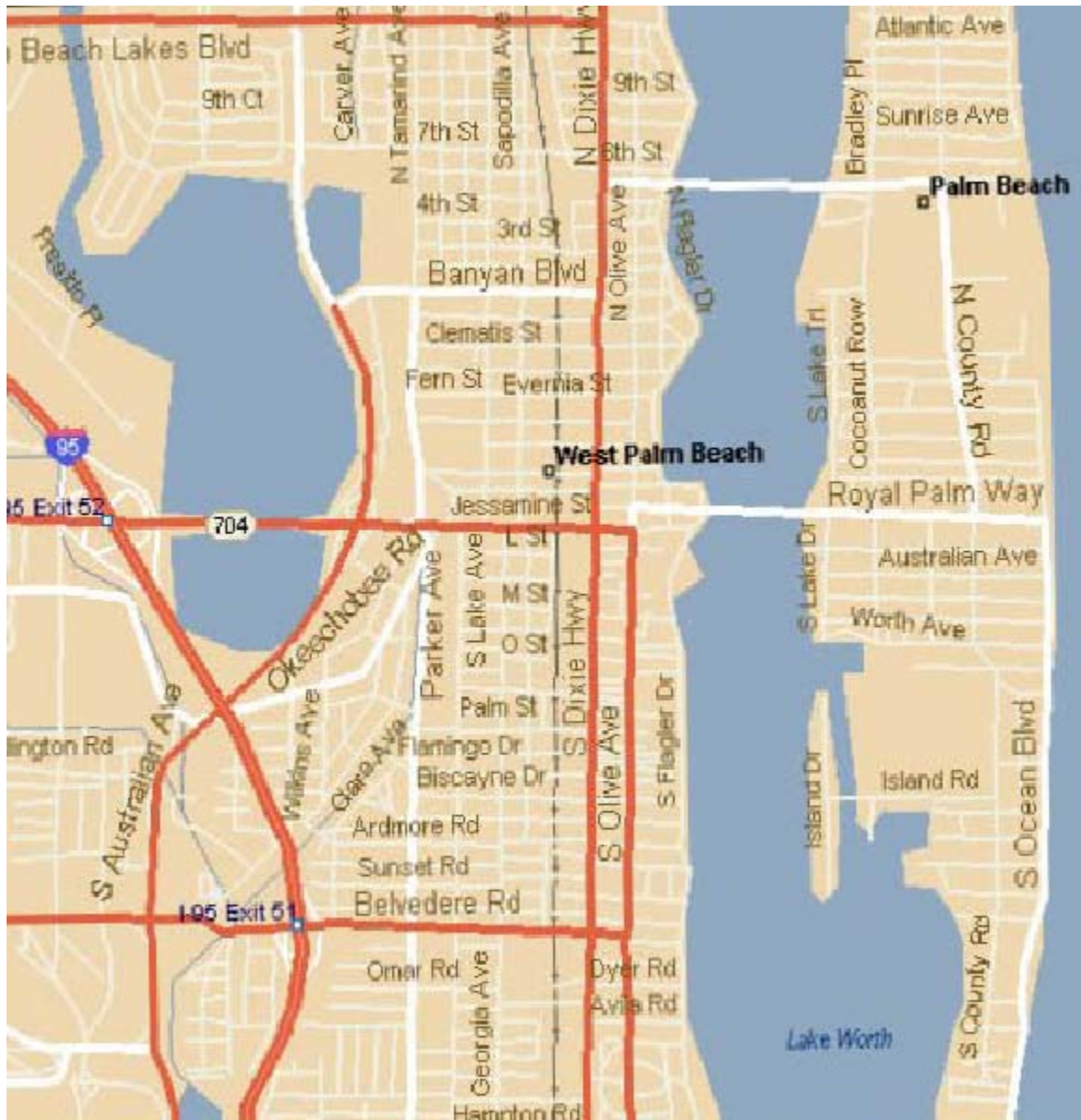


Figure 4-10. Site III location.

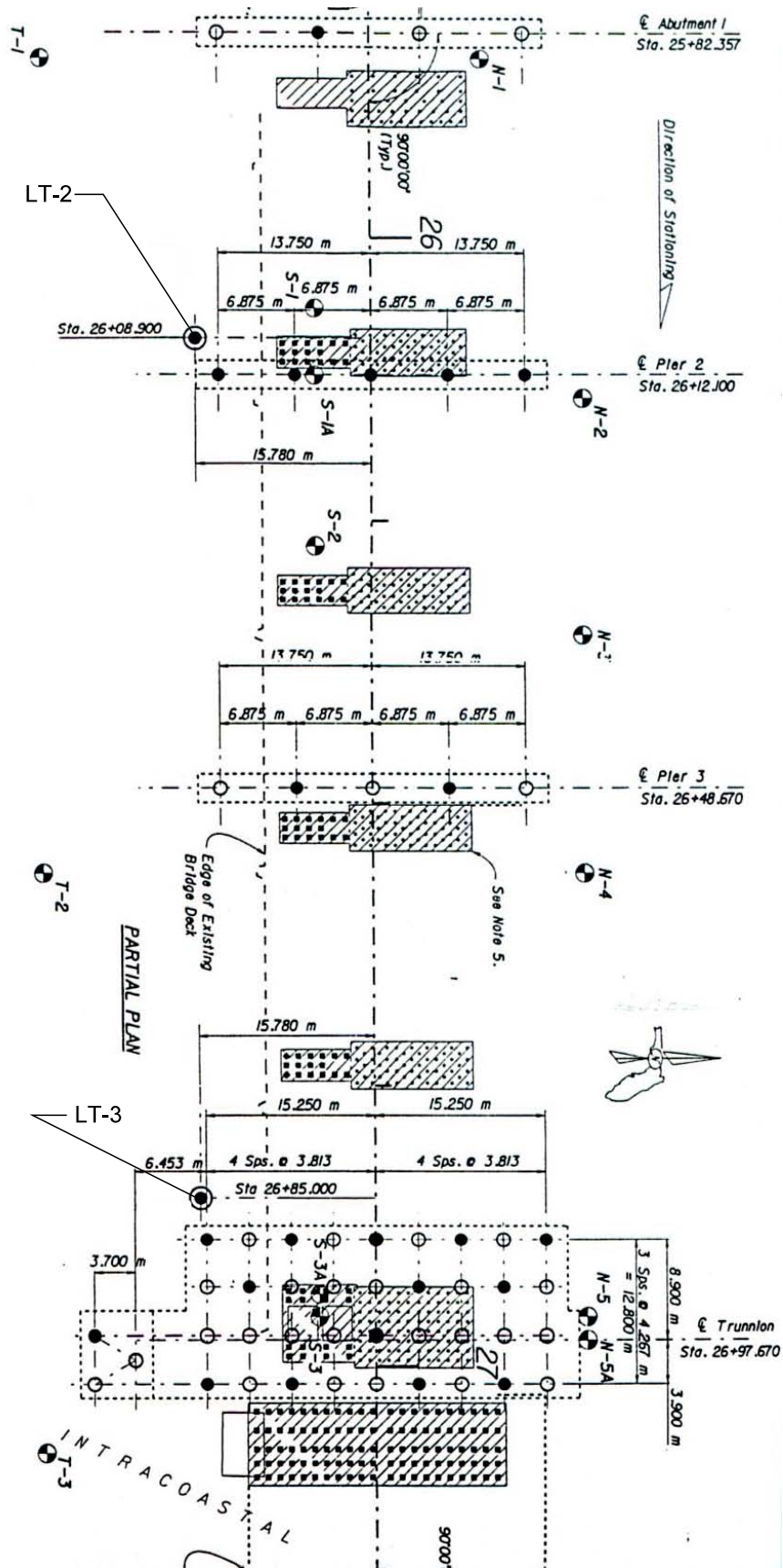


Figure 4-11. Site III layout.

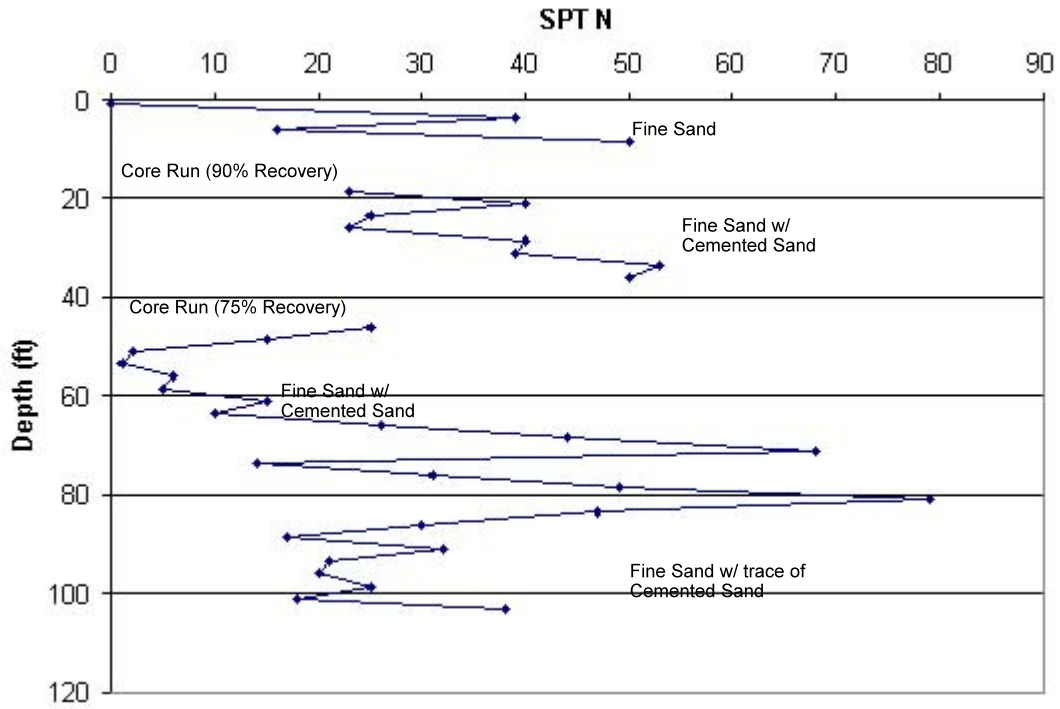


Figure 4-12. Site III LT-3 standard penetration test (SPT) boring.

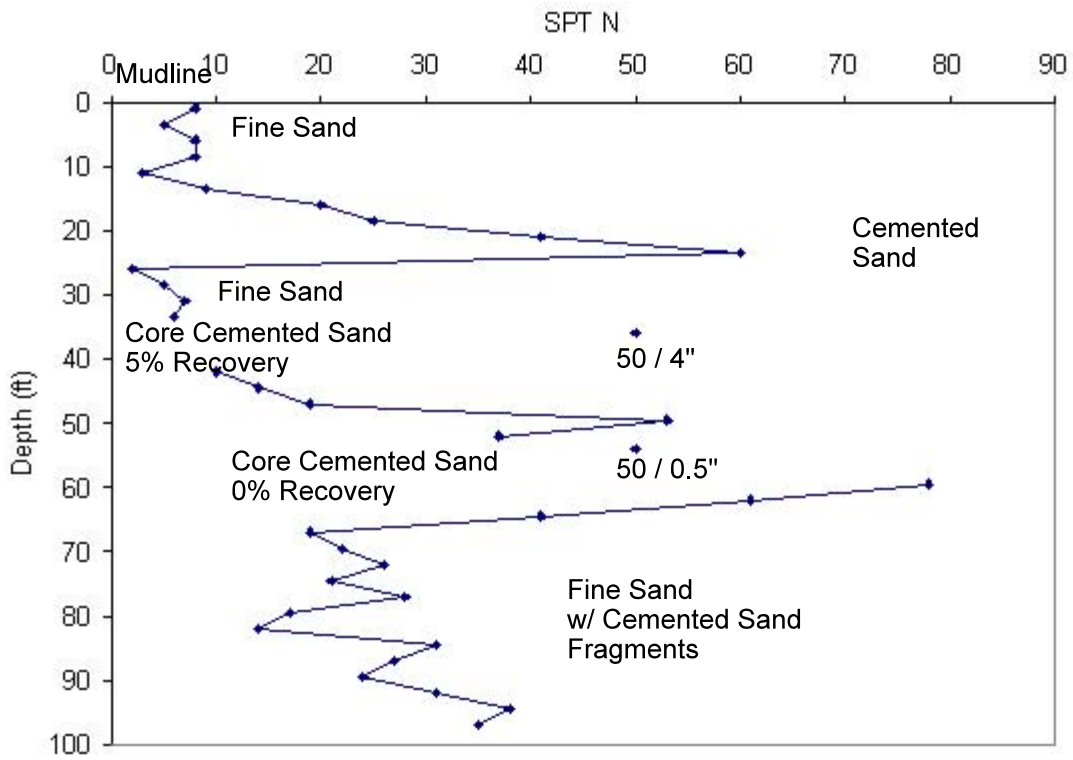


Figure 4-12. Site III LT-2 standard penetration test (SPT) boring.

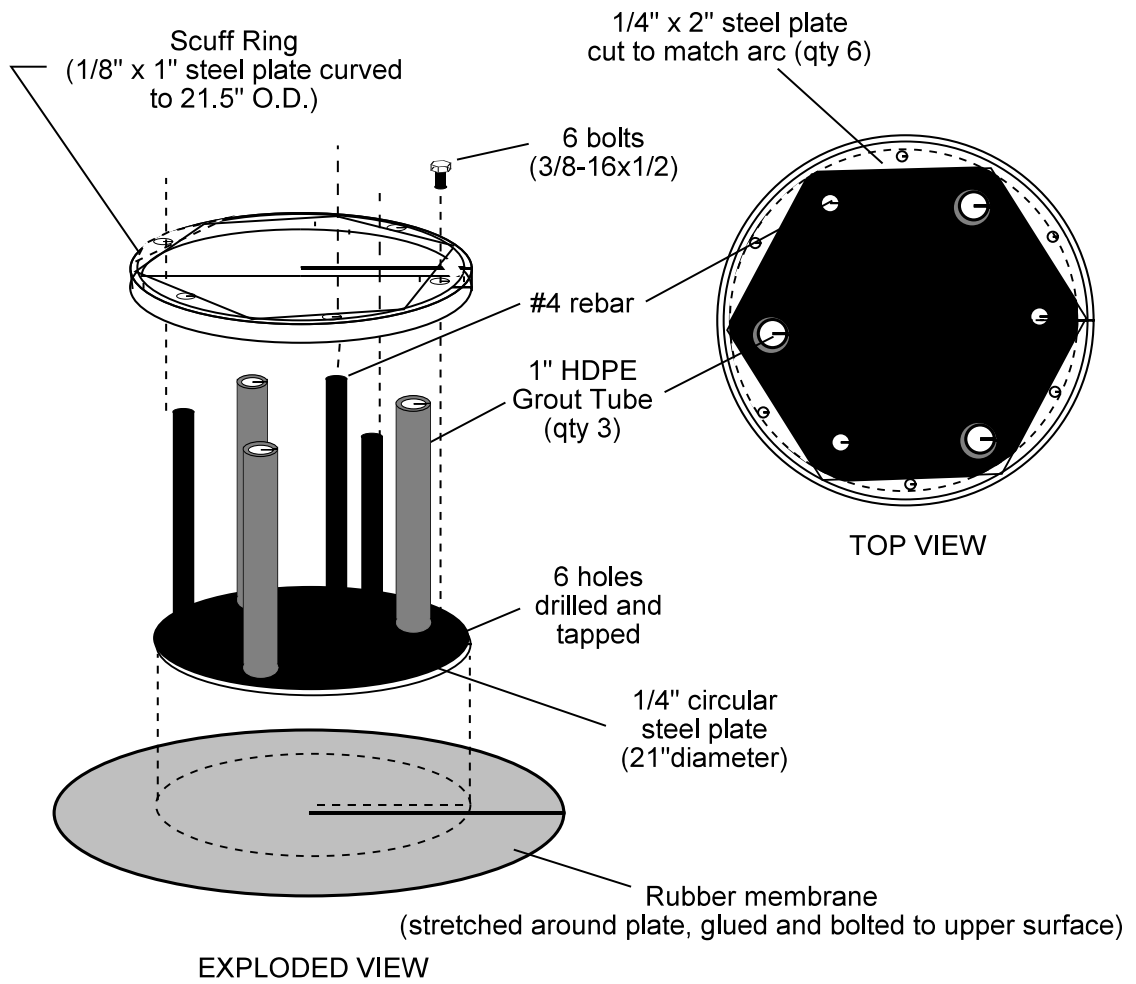


Figure 4-14. Site I and Site II flat-jack style grouting apparatus.

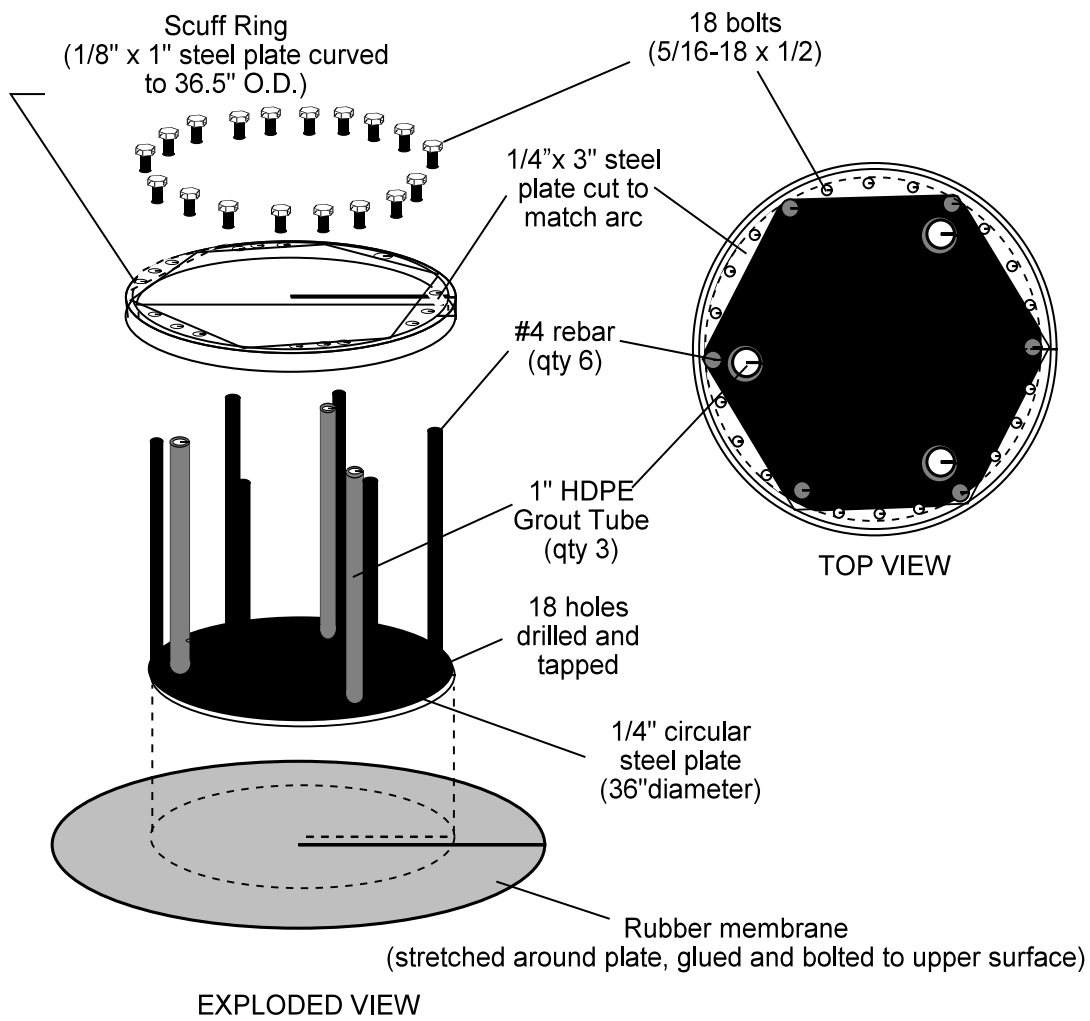


Figure 4-15. Site III flat-jack grouting apparatus.



Figure 4-16. Large flat-jack during fabrication (used at Site III).



Figure 4-17. Small flat-jack during fabrication (used at Site I and Site II).



Figure 4-18. Small flat-jack completed (used in Sites I and II).

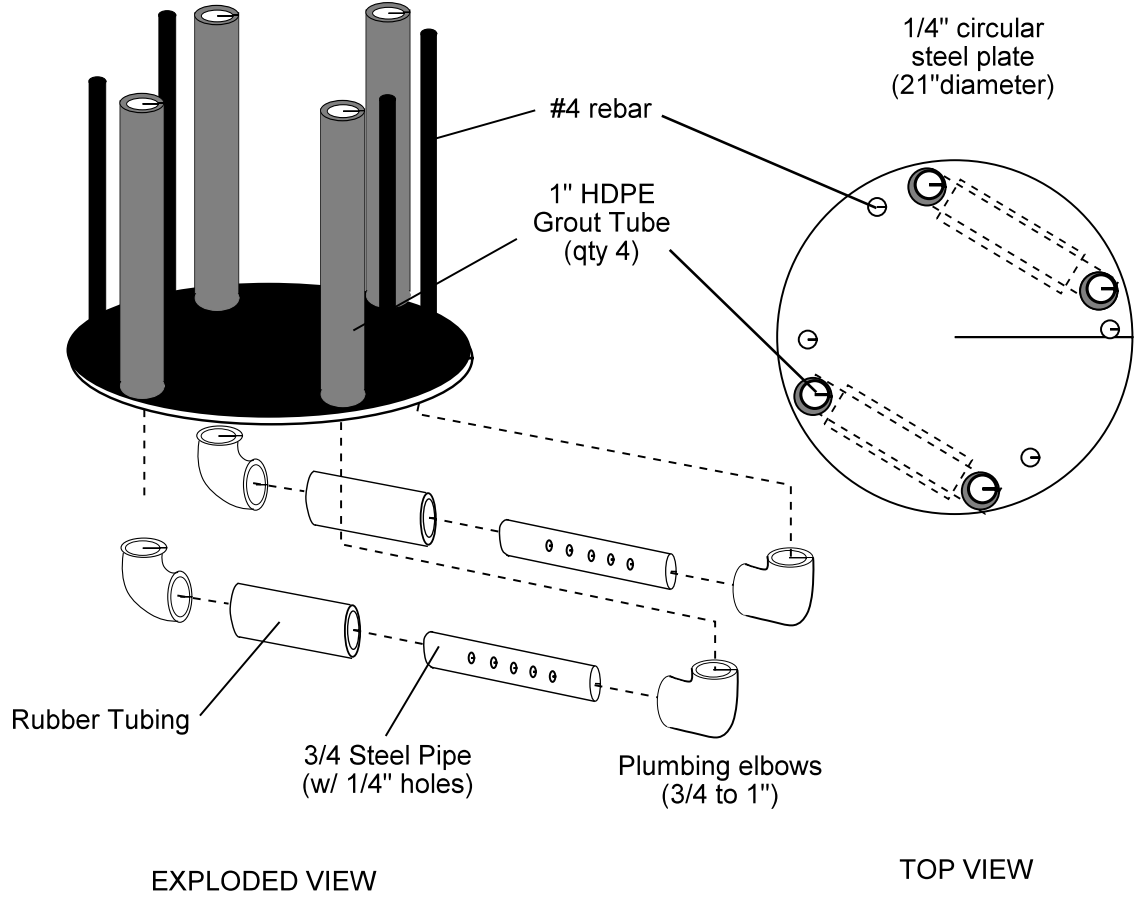


Figure 4-19. Sleeve-port grouting apparatus.



Figure 4-20. Drilling grout holes in sleeve-port apparatus.



Figure 4-21. Grout delivery pipes for sleeve-port apparatus.



Figure 4-22. Site I sleeve-port apparatus tied into reinforcing cages.



Figure 4-23. Sleeve-port device with optional top steel plate.

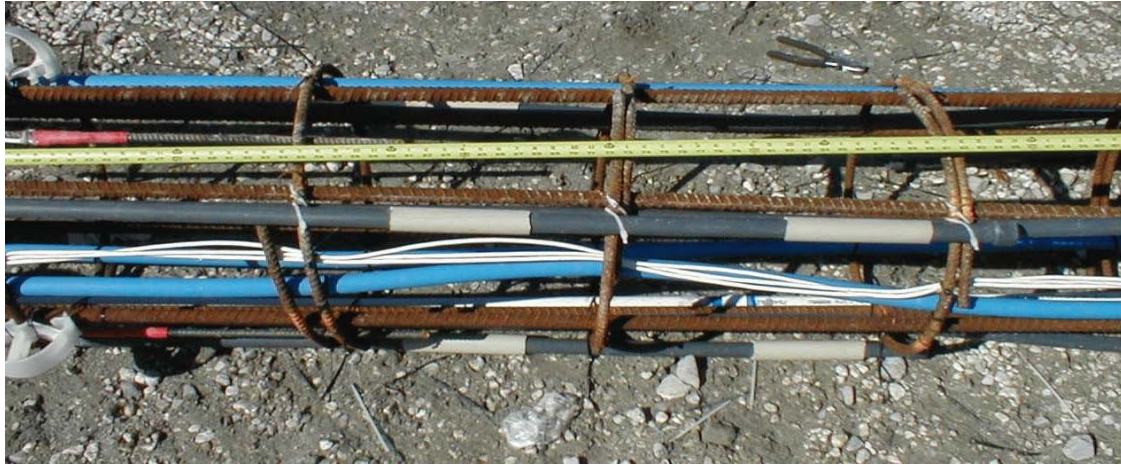


Figure 4-26. Skin grouting sleeve-port. (Site II)



Figure 4-25. Skin grouting Sleeve-ports Tied into Cage (Site II).



Figure 4-26. Site III tension telltale fabrication.



Figure 4-27. Site III tension telltale installed.



Figure 4-28. Sites I and II reinforcing cage fabrication.



Figure 4-29. Sites I and II completed reinforcing cages with grouting apparatuses.



Figure 4-30. Site I excavation with a Texoma 700 drill rig.



Figure 4-31. Site II excavation with a Bauer BG-7 drill rig.



Figure 4-32. Auger used to excavate Sites I and II.



Figure 4-33. Site II reinforcing cage set into excavation with Hitachi crane.



Figure 4-34. Site II concreting operation.



Figure 4-35. Site II exhumed flat-jack (left), sleeve-port (right) tips.



Figure 4-36. Site II exhumed Control Shaft.



Figure 4-37. Site III LT-2 cage with flat-jack grouting apparatus.



Figure 4-38. Site III LT-2 completed cage tip.



Figure 4-39. Slurry plume as Delmag drill rig excavates Site III LT-2.



Figure 4-40. Kobelco crane lifting cage for Site III LT-3.



Figure 4-41. Kobelco crane lifting Site III LT-2 Cage.



Figure 4-42. Scuff ring protecting flat-jack edge of Site III LT-2



Figure 4-43. Concrete placement for Site III LT-2.



Figure 4-44. Helical-style grout pump used for Sites I and II.



Figure 4-45. 500 ton Statnamic device being moved at Site I.



Figure 4-47. Statnamic load test in progress at Site II.



Figure 4-46. Dual-piston (ram-style) grout pump used on Site III.



Figure 4-48. Grout lines flushed on Site III LT-2.

## 5. GROUTING AND LOAD TESTING DATA REGRESSIONS

The sign convention for load and displacement utilized was as follows: a downward force exerted upon the shaft was designated as a negative (-) load, and a downward deflection of the shaft was designated as a negative (-) displacement. When combined into a load deflection curve the load was plotted as the abscissa, and the deflection was plotted as the ordinate. However, as is consistent with full-scale load testing tradition, the abscissa axis (load) was “flipped” such that the negative direction of this axis was directed to the right.

The initial loading of the shaft experiences a negative (-) load and displacement, and the subsequent unloading of the shaft experiences limited positive (+) displacements as the elastic rebound portion of deflection was recovered, while the load became less negative. To be consistent with this convention, an upward force exerted upon the shaft by the grout pressure during tip grouting was designated as a positive (+) load, and the upward deflection experience by the shaft was a positive (+) displacement.

The choice of the displacement as the ordinate is consistent with basic engineering stress strain relationships, and is logical in this application as the displacement of the shaft can be visualized as occurring “up” or “down” along this vertical axis. The “flipping” of the abscissa results in a negative “downward” load occurring in the fourth quadrant of the Cartesian coordinate system.

All data reduction and analysis was carried out in English units. Thus all figures have their primary axis in English units with SI units placed on secondary axis for convenience.

### 5.1 Grouting

The data regression of the tip grouting operations was very straight forward as the shaft deflections were directly measured with LVDT, and the bottom of shaft deflections were measured directly using tension telltales. Note that with relatively short shaft lengths for Sites I and II, 15 ft (14.6 m), very little shaft compression was experienced and these top and bottom of shaft deflections measured are nearly identical. Upward load on the shaft bottom was calculated using strain gage data with a composite modulus determined from the concrete modulus, the steel-to-concrete area ratio, and modulus of the steel reinforcing.

Grout pressure was measured directly utilizing a pressure transducer in-line with the grout supply line from the grout pump to the grout delivery system exposed at the top of shaft. Note that grout pressure was the pressure delivered to the soil directly beneath the shaft tip, where the cavity expansion was occurring. The measured deflections are those of the shaft tip being forced upward by this grout pressure, not the downward movement of the soil to grout interface zone below the grout bulb. This interface may be displaced many times more than that of the shaft movement.

The parameters that are used to specify a tip grouting project are the limiting values of grout take (volume), grout pressure, and shaft uplift. The grout pressure that must be accounted for is the maximum sustained pressure, transient spikes in pressure transducer readings are discounted. The displacements reported are those occurring at the bottom of the shaft, and were directly measured in every case with tension type telltales. For the relatively short shafts of Sites I and II the difference between top and bottom displacements were insignificant. However, with relatively long shafts, as those at Site III, the elastic shortening can be significant. Therefore care must be taken when specifying the maximum allowable uplift, as will be measured at the top of shaft during regular production, such that elastic shortening has been taken into account. These parameters obtained during this research investigation are summarized below in Table 5-1.

Table 5-1. Grout Data Summary

Site	Grout Apparatus	Shaft Designation	Grout Take ft <sup>3</sup> /(m <sup>3</sup> )	Grout Press. psi/(kPa)	Shaft Uplift in/(mm)
I	Flat-Jack	SI-FJ1 (release press.)	1.75 (0.050)	85 (587)	0.149 (3.78)
		SI-FJ2 (lock press.)	3.79 (0.107)	67 (462)	0.190 (4.83)
	Sleeve-Port	S2-SP1 (with plate)	5.82 (0.165)	165 (1139)	0.108 (2.74)
		S2-SP2 (no plate)	3.05 (0.086)	177 (1221)	0.056 (1.42)
II	Flat-Jack	S2-FJ (hold press.)	7.65 (0.217)	99 (683)	0.150 (3.81)
	Sleeve-port	S2-TM (with plate)	6.34 (0.180)	125 (863)	0.040 (1.02)
III	Flat-Jack*	SIII LT-3 (cycle 2)	21.51 (0.609)	500 (3450)	0.276 (7.01)
	Flat-Jack	SIII LT-2 (cycle 2)	4.132 (0.117)	450 (3105)	0.191 (4.85)

\* behaved as a sleeve-port apparatus due to damage of flat-jack rubber membrane.

### 5.1.1 Site I (Shelly Sand)

The data obtained during the tip grouting was the grout pressure, grout volume, shaft displacement (top and bottom), and the shaft strains (top and bottom). A force was determined at the shaft tip using the strain gage data and an estimated composite modulus from the concrete modulus, the steel to concrete area ratio, and modulus of the vertical steel reinforcing. The force at the shaft tip was also calculated using the measured grout pressure assumed to act upon the full cross-sectional area of the 2.0 ft (0.61 m) diameter shaft. This is a fictitious construct allowing for comparison to the more accurately calculated load by means of the strain gage data. For each shaft at this site, a complete set of time trace data can be found in Appendix E which includes the following:

- The time trace of grout pressure.
- The time trace of shaft tip displacement.
- The time trace of shaft tip load where the tip load has been calculated directly from the measured strain gage and pressure gage as described previously.

Figures 5-1 through 5-7 present the bottom-up load displacement response during grouting shafts at Site I. Figures 5-1 and 5-2 show the load displacement during grouting for Flat-Jack's 1 and 2, respectively. Both show a strong correlation between the strain gage measured load and that predicted using the grout pressure and the shaft tip area. The sleeve-port grout cycles are presented on separate graphs (3 cycles for sleeve-port 1, and 2 cycles for sleeve-port 2). A full grout cycle delineates the time grouting was conducted through a particular "U" tube system. Figures 5-3 through 5-5 indicate the load displacement response for sleeve-port 1 while Figures 5-6 and 5-7 are from sleeve-port 2. Each graph, for both Sites I and II, is presented using the same scale for easy comparison.

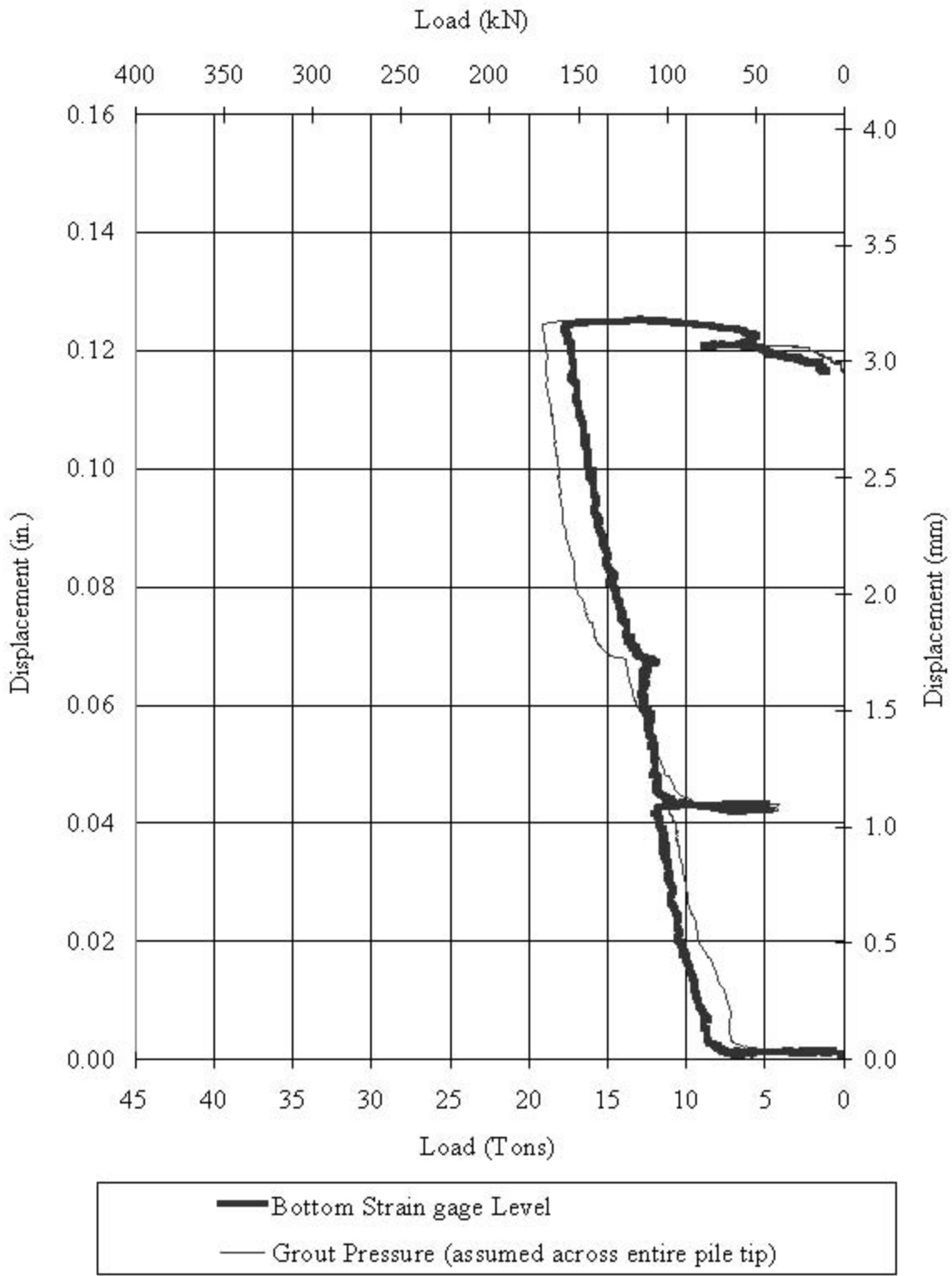


Figure 5-1. Site I Flat-Jack 1 tip grouting load vs. displacement.

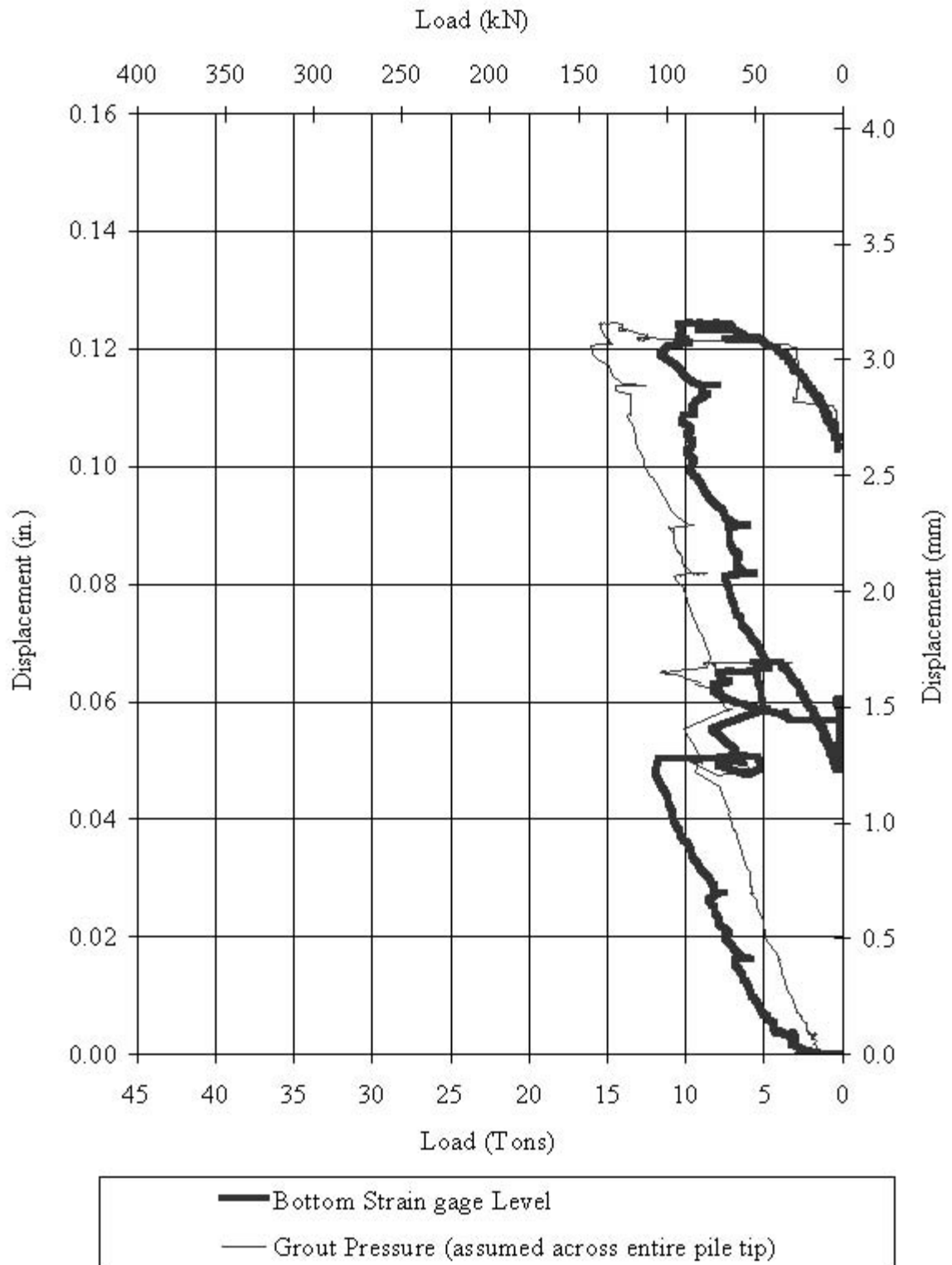


Figure 5-2. Site I Flat-Jack 2 tip grouting load vs. displacement.

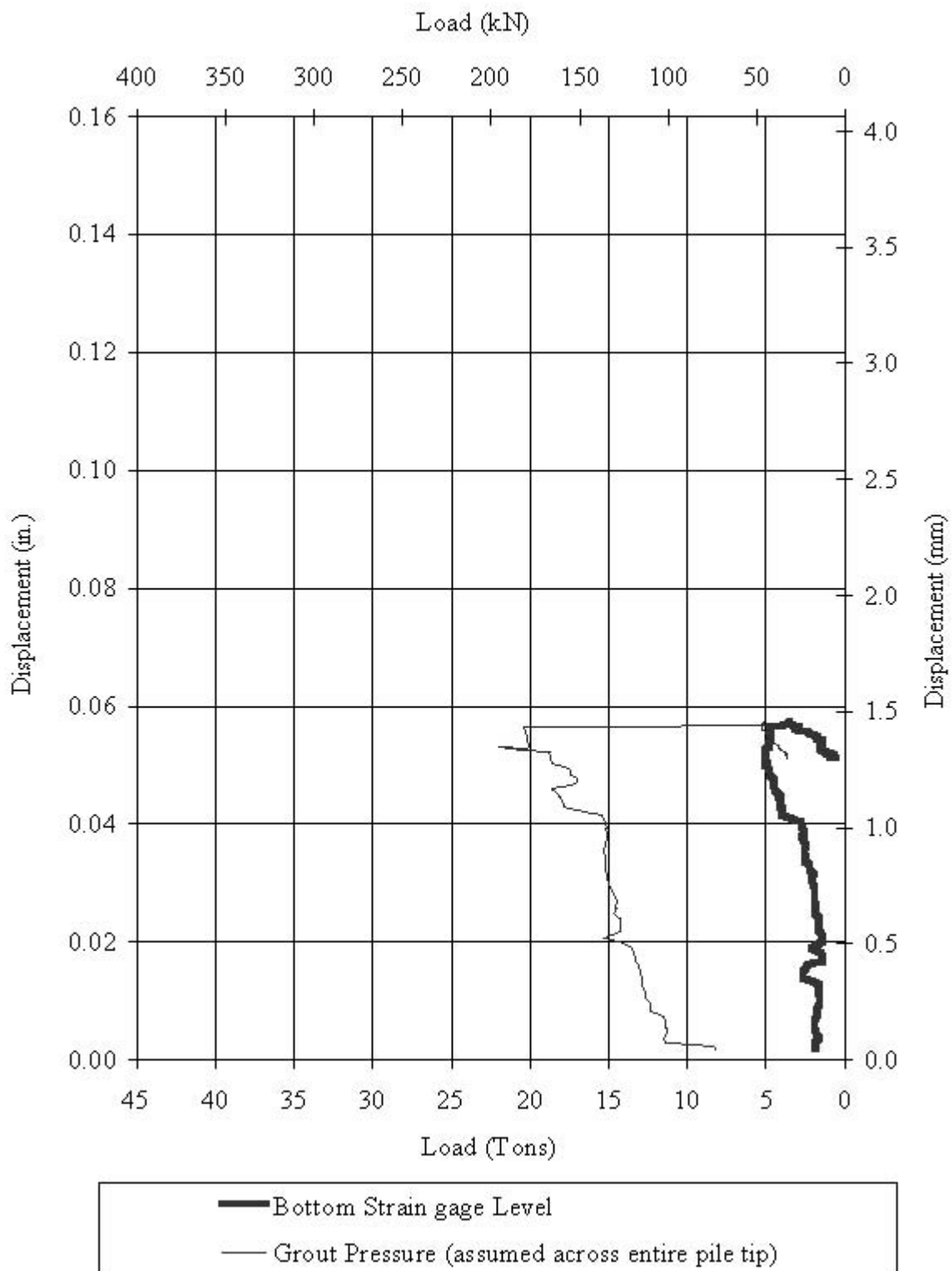


Figure 5-3. Site I Sleeve-Port 1 tip grouting load vs. displacement, cycle 1.

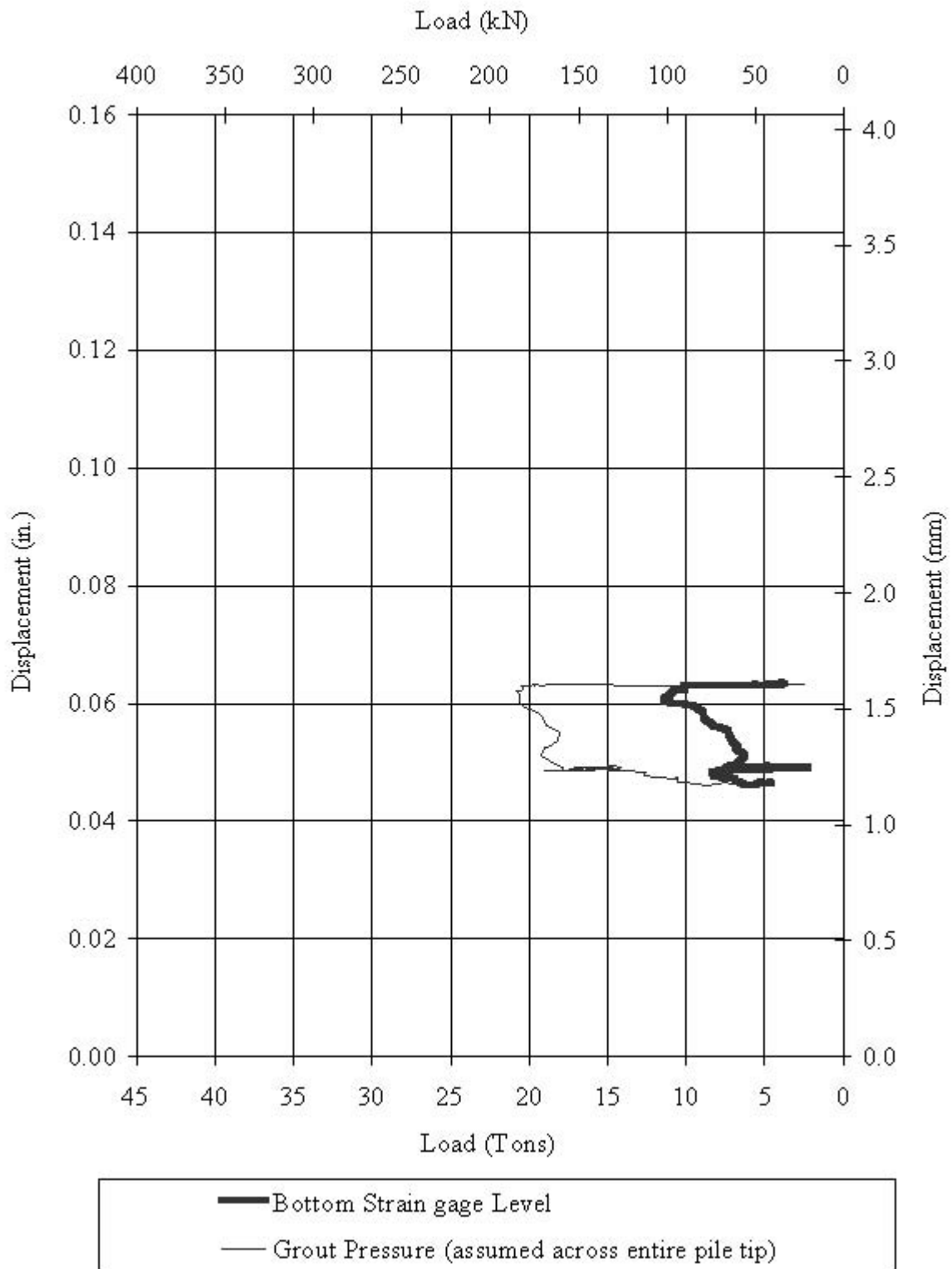


Figure 5-4. Site I Sleeve-Port 1 tip grouting load vs. displacement, cycle 2.

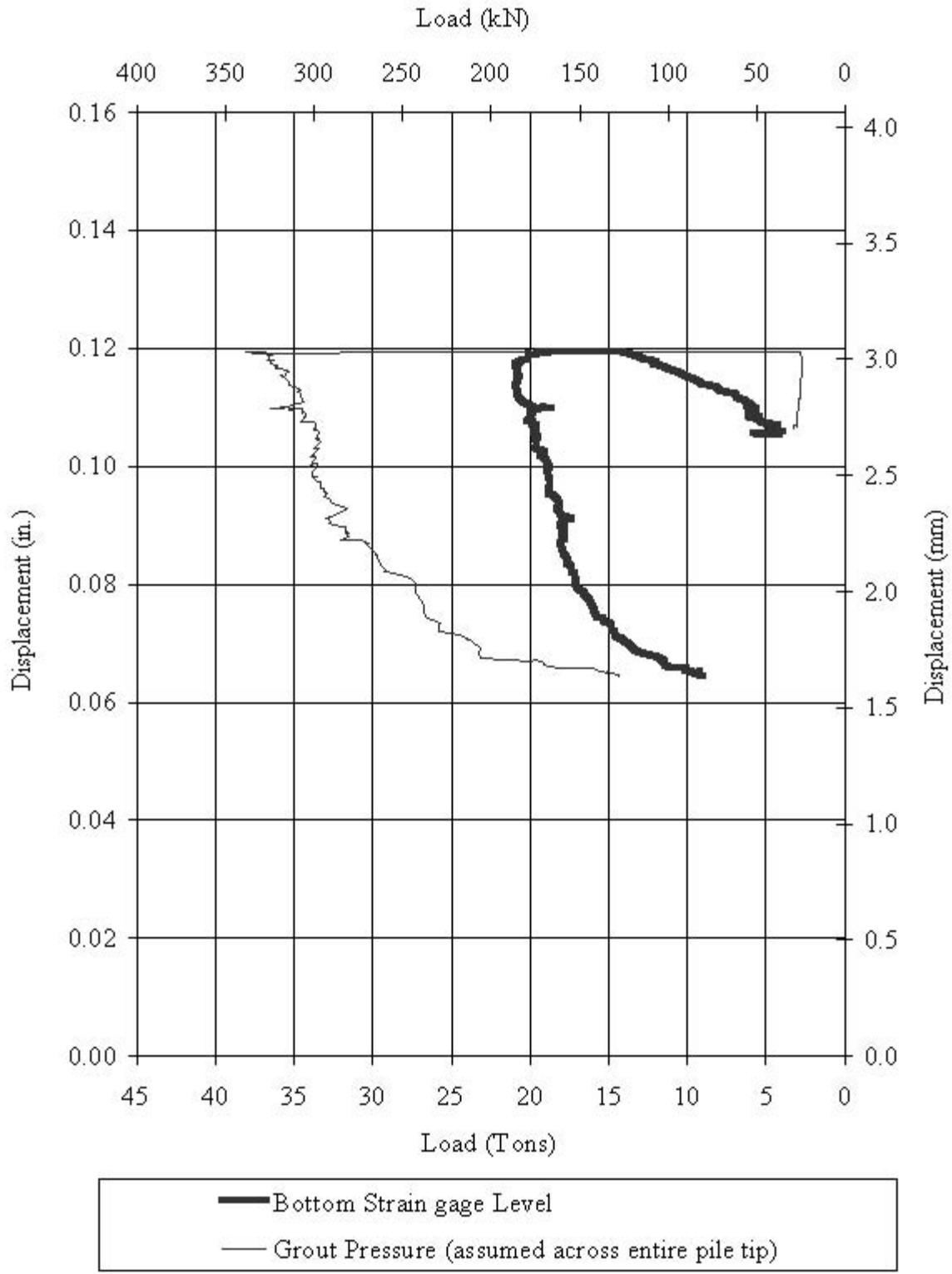


Figure 5-5. Site I Sleeve-Port 1 tip grouting load vs. displacement, cycle 3.

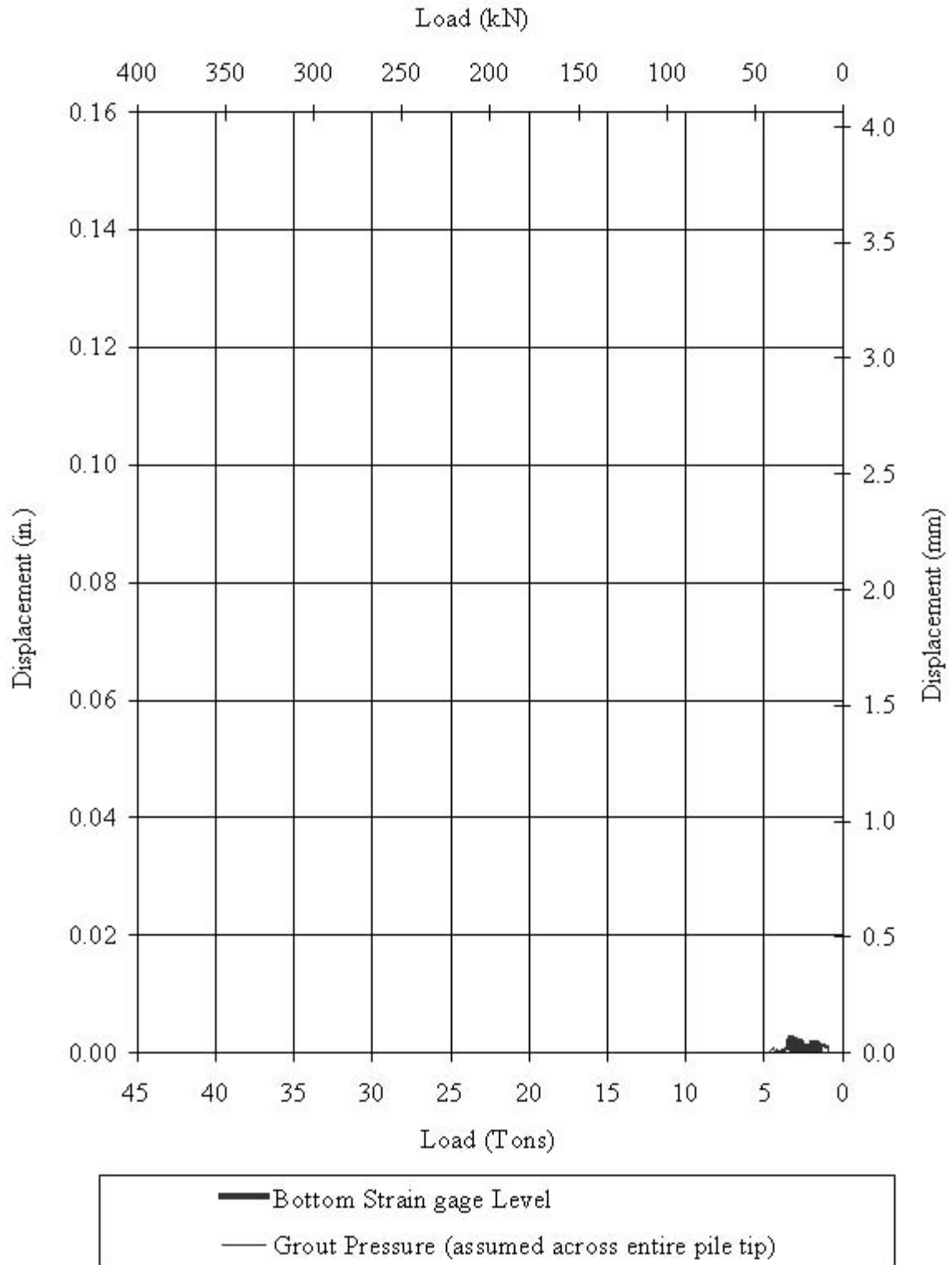


Figure 5-6. Site I Sleeve-Port 2 tip grouting load vs. displacement, cycle 1.

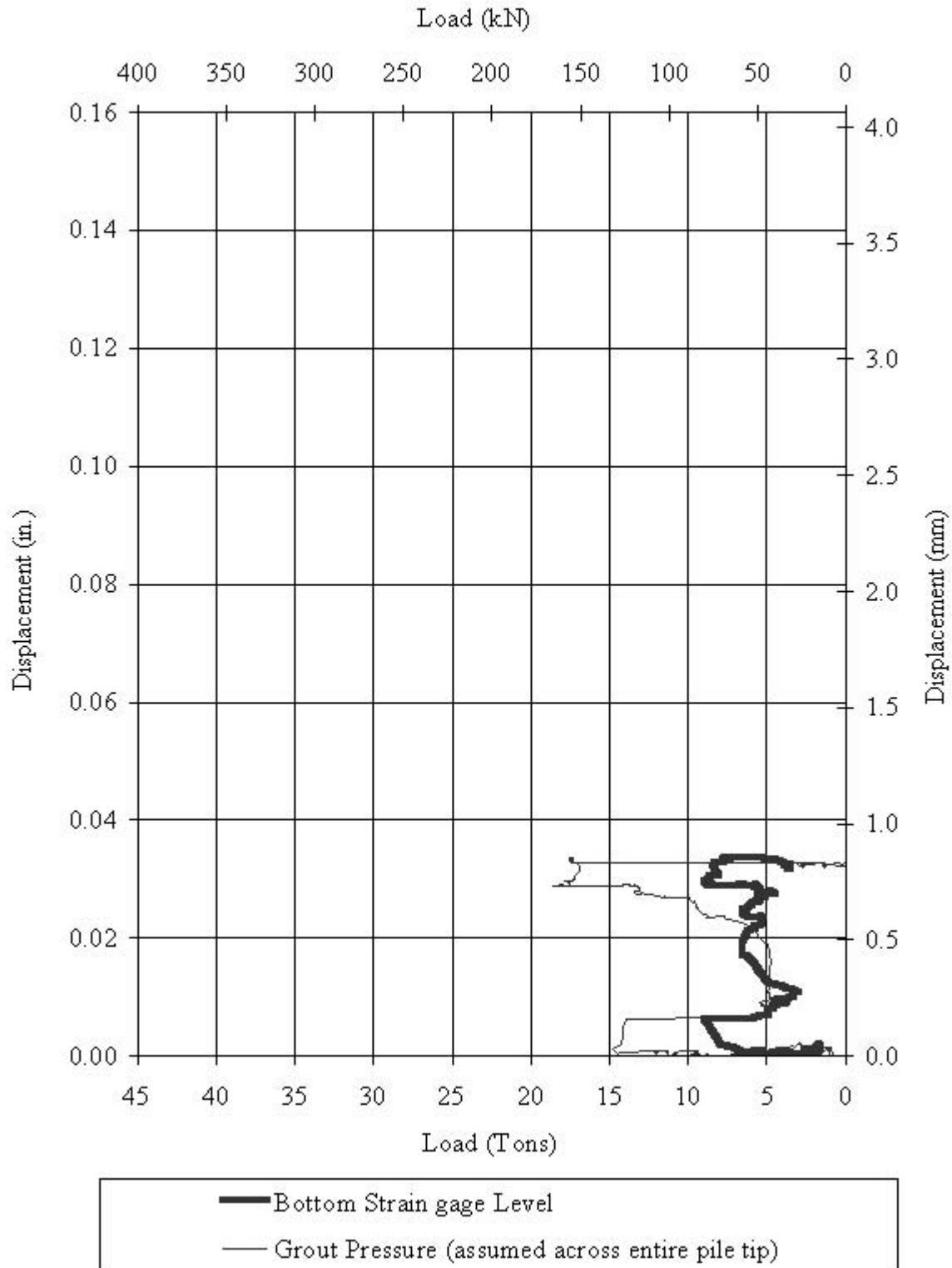


Figure 5-7. Site I Sleeve-Port 2 tip grouting load vs. displacement, cycle 2.

### 5.1.2 Site II (Silty Silica Sand)

The data obtained during the tip grouting was again the grout pressure, grout volume, shaft displacement (both top and bottom), and the strains in the shaft at the top and bottom strain gage elevations. As in site I the force was determined at the shaft tip using the strain gage data and a composite shaft modulus. Assuming the full cross sectional area of a 2.0 ft (0.61 m) diameter shaft, the force due to the grout pressure was determined as the product of this area and the measured pressure. For each shaft at this site, a complete set of time trace data can be found in Appendix E which includes the following:

1. The time trace of grout pressure,
2. The time trace of shaft tip displacement,
3. The time trace of shaft tip load where the tip load has been calculated directly from the measured strain gage and pressure gage as described previously.

Figures 5-8 through 5-11 present the bottom-up load displacement response during grouting shafts at Site II. Figure 5-8 shows the load displacement during grouting for the flat-jack. As with Site I flat-jacks, there was a strong correlation between the strain gage measured load and that predicted using the grout pressure and the shaft tip area. The sleeve-port grout cycles are presented on separate graphs (3 cycles total), as Figures 5-9 through 5-11. A full grout cycle delineates the time grouting was conducted through a particular "U" tube system. Each graph, for both Sites I and II, is presented using the same scale for easy comparison.

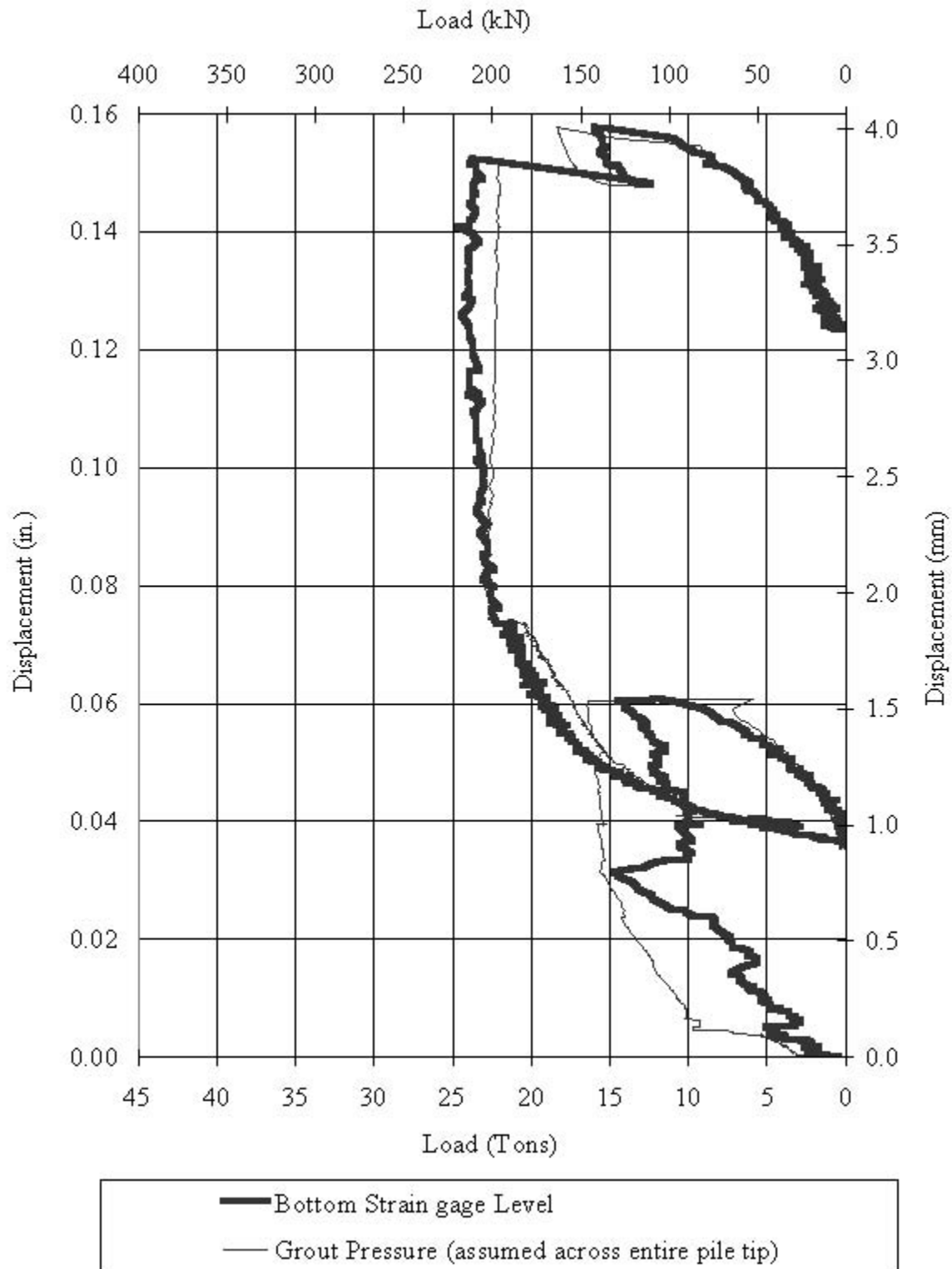


Figure 5-8. Site II Flat-Jack tip grouting load vs. displacement.

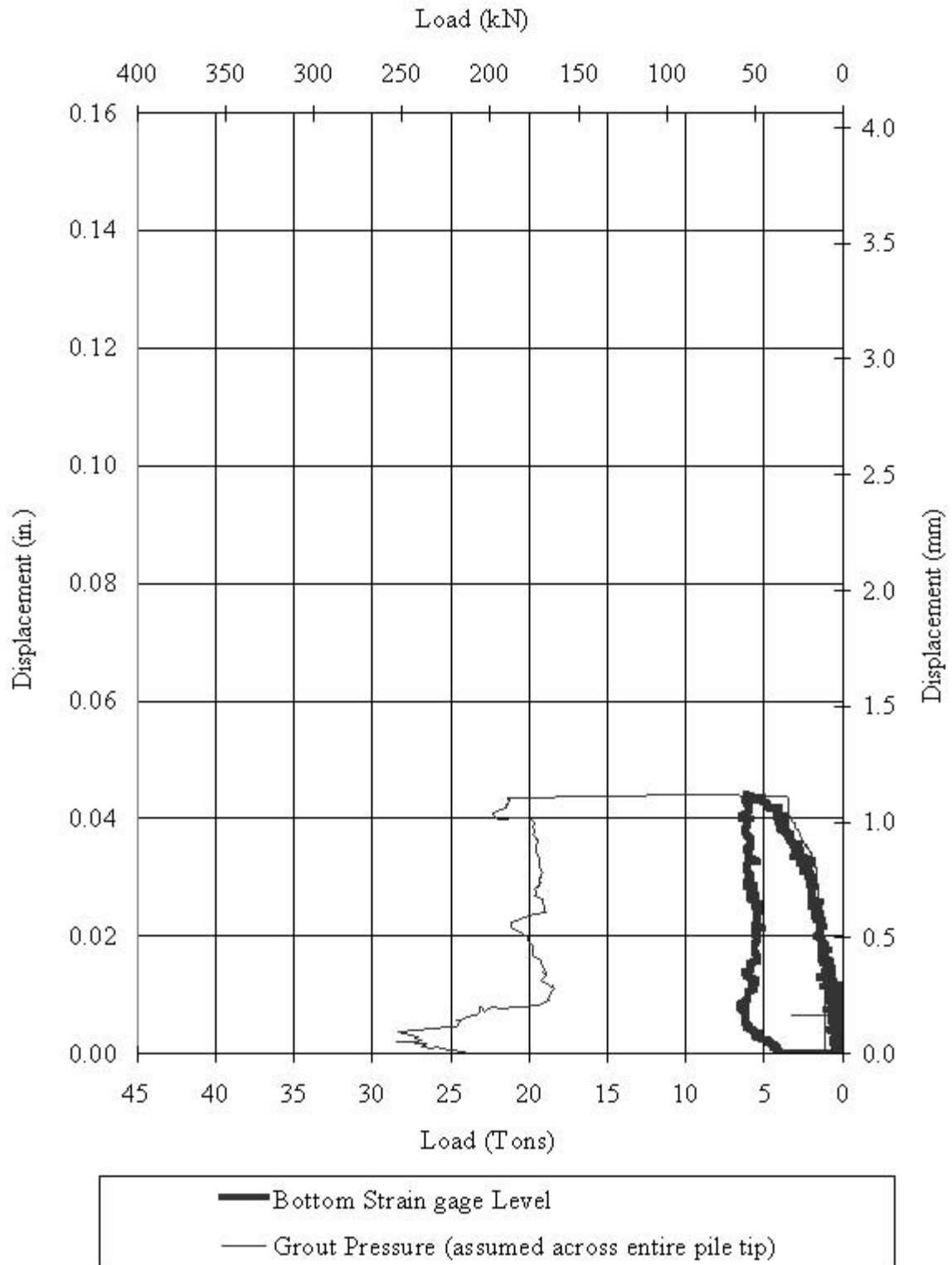


Figure 5-9. Site II Sleeve-Port tip grouting load vs. displacement, cycle 1.

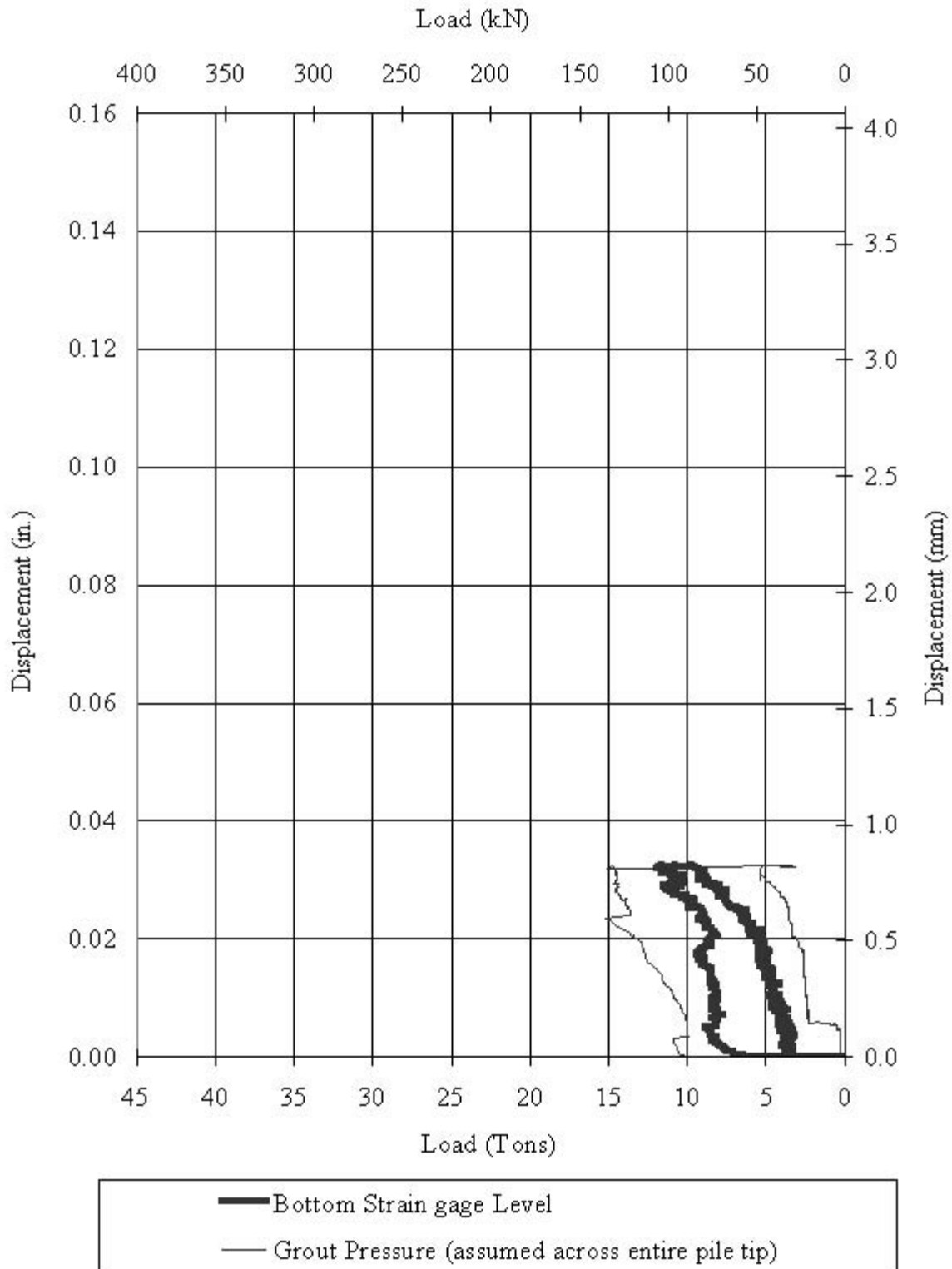


Figure 5-10. Site II Sleeve-Port tip grouting load vs. displacement, cycle 2.

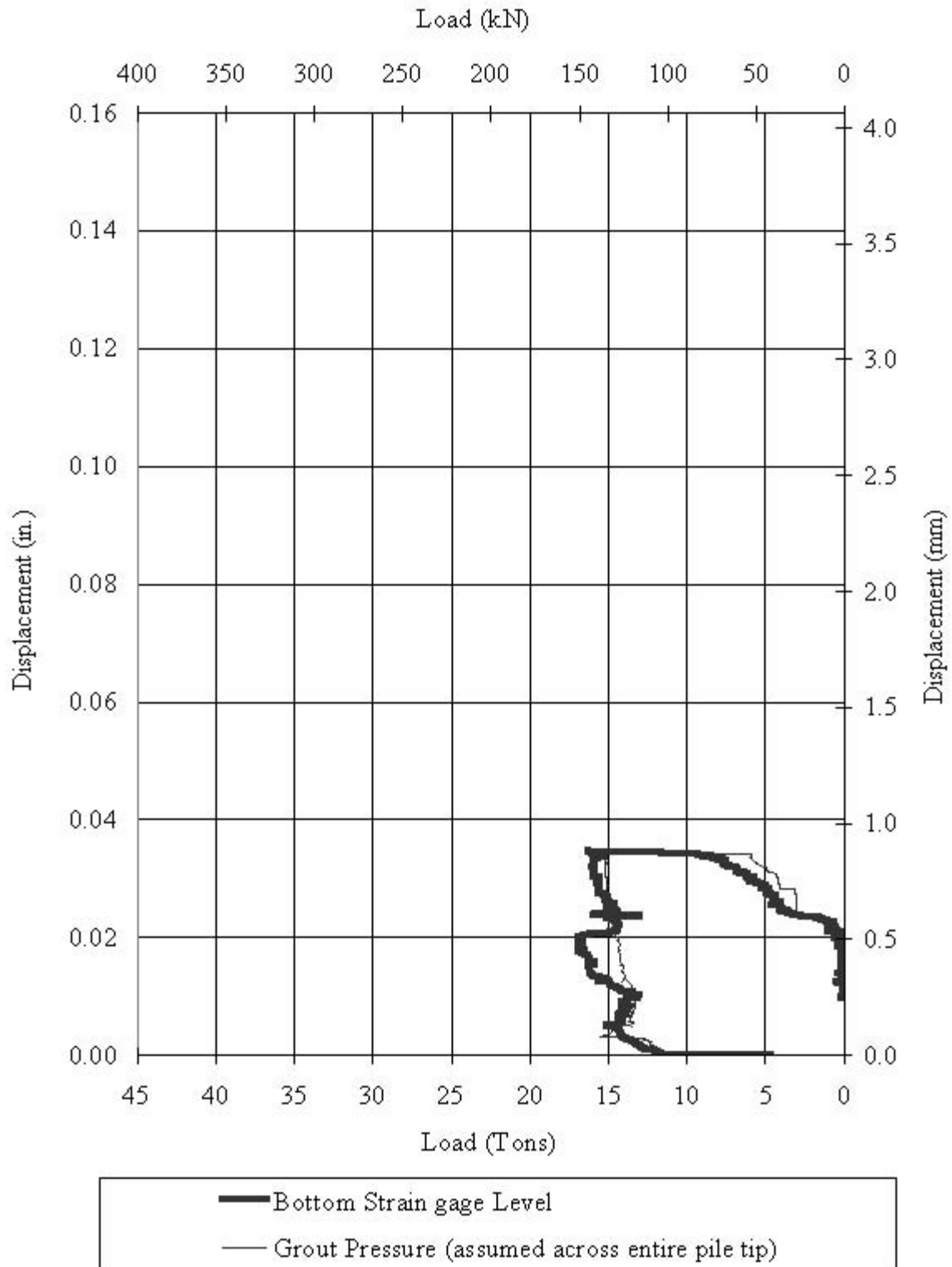


Figure 5-11. Site II Sleeve-Port tip grouting load vs. displacement, cycle 3.

### 5.1.3 Site III (Cemented Coquina)

The data obtained during the tip grouting at site III consisted of grout pressure, grout volume, shaft displacement (both top and bottom), and the shaft strains at the top and bottom levels. Intermediate gage levels were also monitored from various levels, although they are not pertinent to this study. The force developed at each strain gage level was calculated using the shaft cross-sectional area, the measured, and the composite modulus of elasticity. As with Sites I and II, the force exerted upward on the toe of the shaft was also determined from the measured grout pressure assuming it acted upon the full cross-sectional area of the 4.0 ft (1.22 m) diameter shaft. For each shaft at this site, a complete set of time trace data can be found in Appendix E which includes the following:

1. The time trace of grout pressure,
2. The time trace of shaft tip displacement,
3. The time trace of shaft tip load where the tip load has been calculated directly from the measured strain gage and pressure gage as described previously.

There was no cross-communication of grout pressure between the three grout pipes connected to the flat-jack of LT-3. Each of these three grout pipes were pressurized individually as grout stems, resulting in three grout cycles that resembles the response of a sleeve-port style apparatus. Review of the LT-3 data shows the shaft tip being flexed back and forth during the grout cycles. No movement occurred at the top of shaft; however, approximately 0.25 inches total elastic compression occurred. This estimate was based upon averaged strain gage data near the tip of the shaft. LT-2 data was quite remarkable, Figure 5-12, showing classic bottom-up load displacement characteristics as grout pressure was dispersed across the entire flat-jack apparatus with this test shaft. The grout volume vs. time for LT-3 and LT-2 is shown in Figures 5-13 and 5-14, respectively.

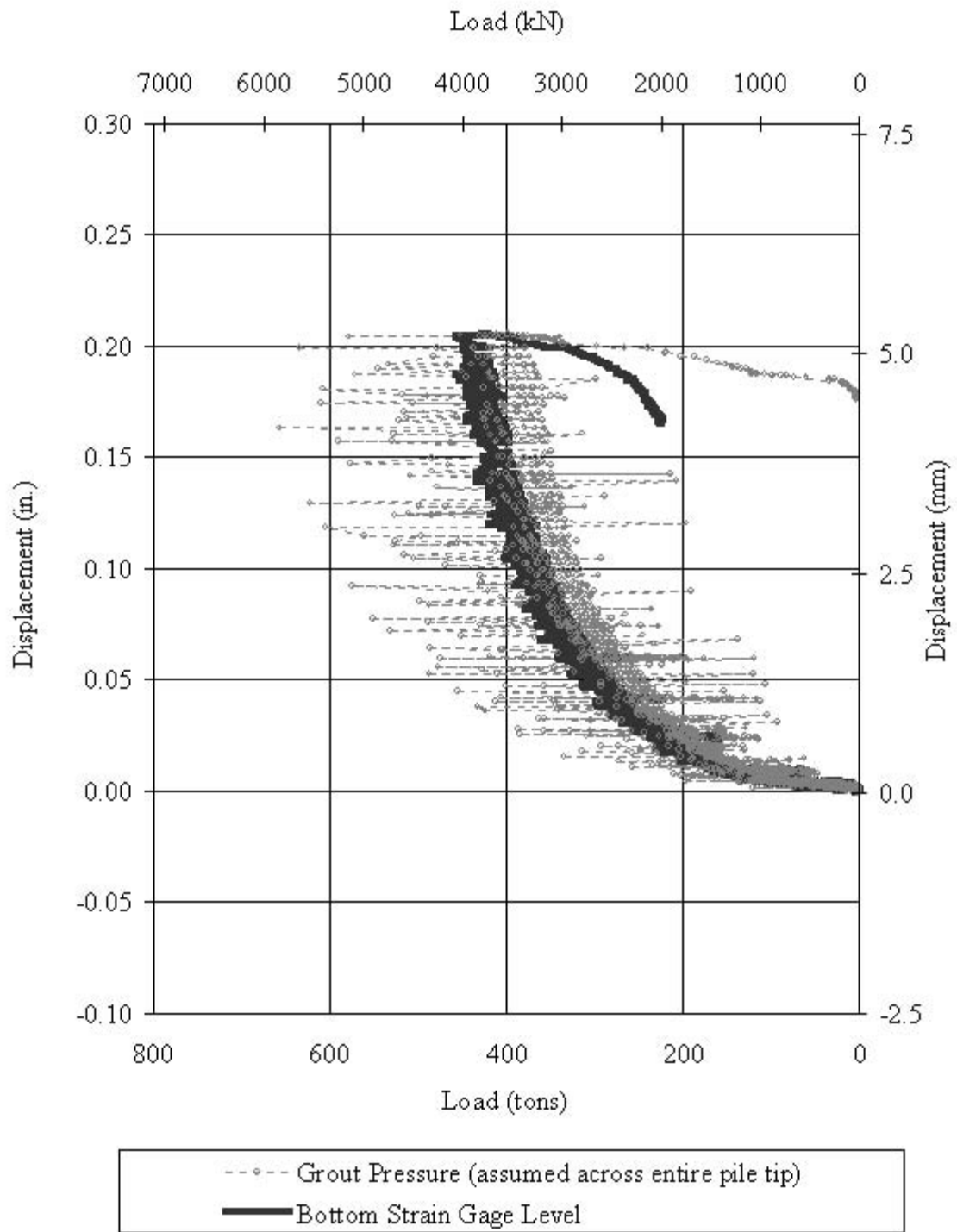


Figure 5-12. Site III LT-2 tip grouting load vs. displacement.

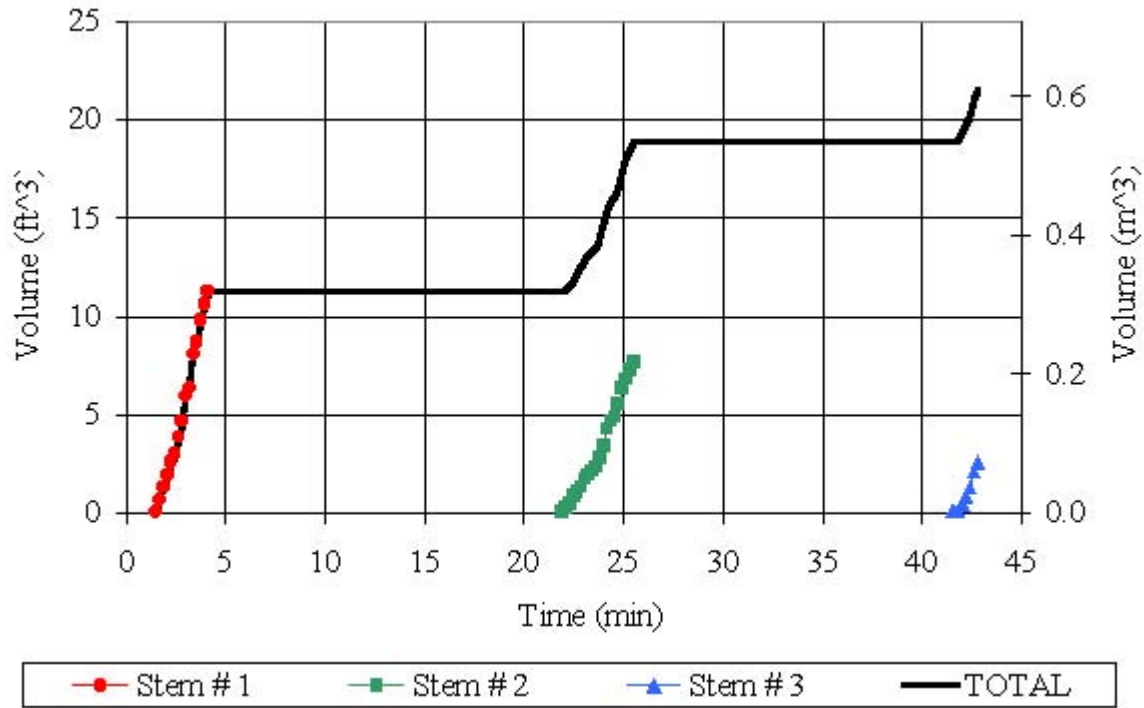


Figure 5-13. Site III LT-3 grout volume vs. time.

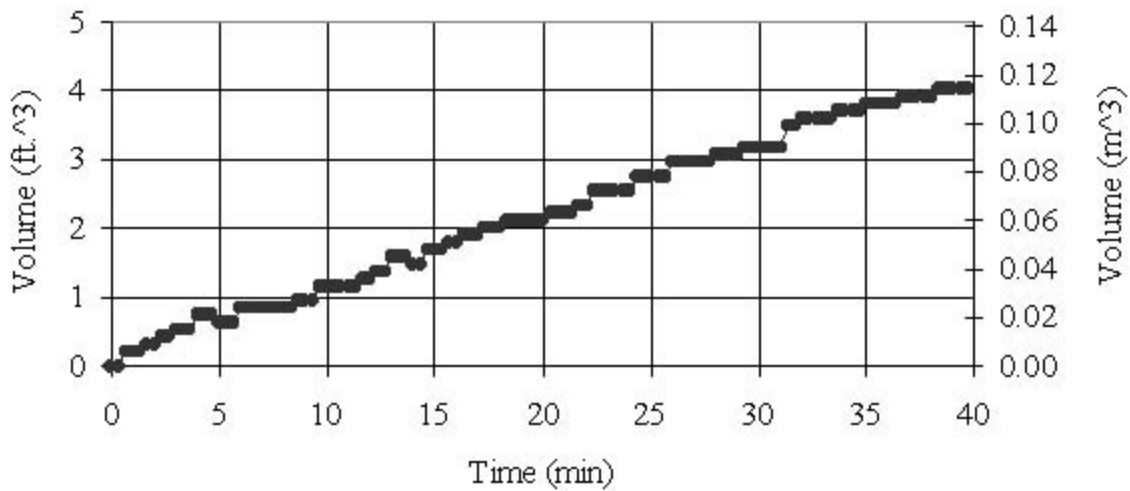


Figure 5-14. Site III LT-2 grout volume vs. time.

## 5.2 Load Testing

All load testing was accomplished utilizing the Statnamic load testing method. The University of South Florida's 500 ton device with hydraulic catch mechanism was used for Sites I and II, while a 3,500 ton device with a gravel catch system was used for Site III. Since this is a rapid load test method delivering an impulse load with an approximate duration of 100 milliseconds, it was necessary to account for the inertial and viscous forces that were generated, in order to determine static soil response.

Rearranging the fundamental equation of motion such that the inertial and viscous forces are subtracted from the total force (in this case the measured Statnamic load at the top of the shaft), the desired static response can be expressed as shown below:

$$\mathbf{k} \cdot \vec{\mathbf{X}} = \vec{\mathbf{F}}_{\text{total}} - \mathbf{m} \cdot \vec{\mathbf{A}} - \mathbf{c} \cdot \vec{\mathbf{V}}$$

where:  $\mathbf{k} \cdot \vec{\mathbf{X}}$  = the desired static response

$\vec{\mathbf{F}}_{\text{total}}$  = the measured Statnamic (total) force

$\mathbf{m} \cdot \vec{\mathbf{A}}$  = the inertial force

$\mathbf{c} \cdot \vec{\mathbf{V}}$  = the viscous force

The acceleration was directly measured with an accelerometer placed at the top of the shaft for the shorter shafts (Sites I and II), and at both the top and toe for the considerably longer shafts (Site III). The velocity was then obtained by numerically integrating the acceleration data, and the displacements were obtained by double integrating the acceleration data. Top of shaft displacements were also measured directly using a laser displacement transducer. The Statnamic force was measured directly at the top of shaft in all cases with a load cell. The mass was calculated utilizing construction dimensions, and the viscous (damping) coefficients were estimated utilizing the Modified Unloading Point (MUP) method employed within the Statnamic Analysis Workbook (SAW), (Garbin, 1999).

Strain gage data within the shaft provided loads at their respective shaft elevations using an estimated modulus of elasticity based on concrete strength. Given that the loads and displacements were either measured or calculated at both the top of shaft and toe, all load testing data was analyzed using the Segmental Unloading Point method (SUP), as is described in Lewis (1999).

Although the Statnamic method of testing was utilized for all test shafts, the load testing method was not the focus of this research. The focus of this research was the improvement of shaft tip capacity by means of pressure grouting. As such, all the load testing results presented will be static load curves. The static load curves were obtained from the Statnamic curves (or total load curves) utilizing the methods described above.

### **5.2.1 Site I (Shelly Sand)**

Site I consisted of 5 shafts load tested with multiple Statnamic load cycles performed on each shaft. The first load test cycle performed on the control shaft was the first of all those in Sites I and II, and was considerably small, reaching a peak force of only 50 tons. The Statnamic fuel and reaction weight for all remaining load cycles were optimized such that the shafts were loaded to full capacity with each load cycle, and exhibited plunging type failure. Thus, Site I control shaft had a total of 4 load cycles, while all others at Sites I and II had a total of three load cycles. The multiple load cycles ensured that the combined load displacement curves were fully defined through ultimate failure, and reload curves were defined.

An analysis was performed, as described in Section 5.2, to reduce each Statnamic load displacement curve to its equivalent static load curve. Each of the load cycles for a particular shaft were then placed tail-to-head with subsequent load cycles to form the load displacement history. Appendix E contains these static load displacement curves for each individual shaft for Site I. Note that all load displacement curves for Sites I and II in Appendix E are to the same scale for easy comparison, with the exception of Site II Control being re-plotted with large scale displacements to show the entire set of its load displacement curves.

Figures 5-15 to 5-18 combine an individual Site I grouted shaft load displacement curves with the load displacement curves of Site I control shaft. The analysis of the grouted shafts load capacity improvement, to follow in Chapter 6, will make use of these figures. In each of these figures the tip and total capacity curves of both the grouted shaft and control shaft is identified.

Figure 5-15 shows comparison of flat-jack 1 to the Site I control shaft, and Figure 5-16 shows comparison of flat-jack 2 to the Site I control shaft. Figure 5-17 shows comparison of sleeve-port 1 to the Site I control shaft, and Figure 5-18 shows comparison of sleeve-port 2 to the Site I control shaft.

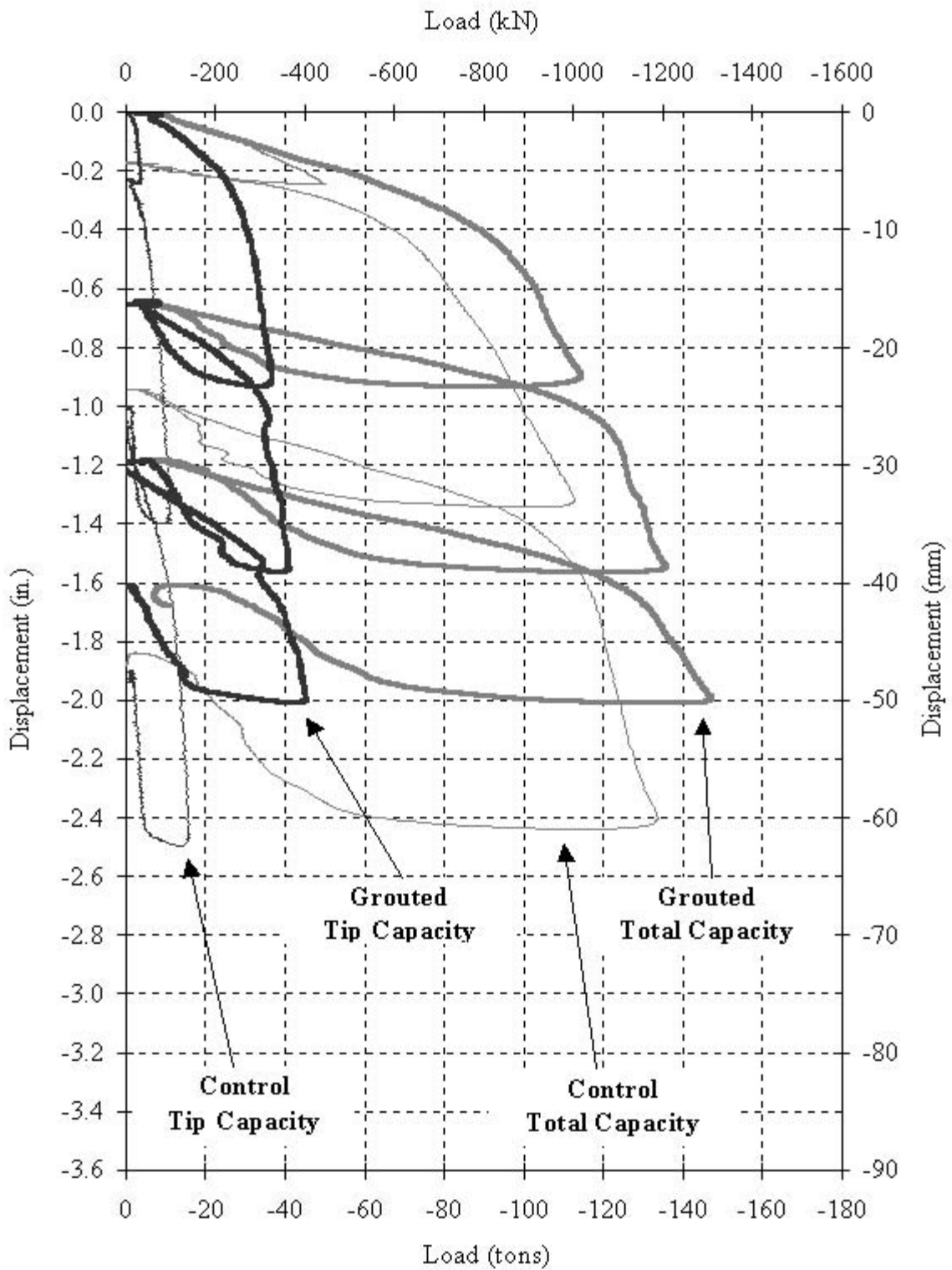


Figure 5-15. Site I Flat-Jack 1 load vs. displacement compared to Control.

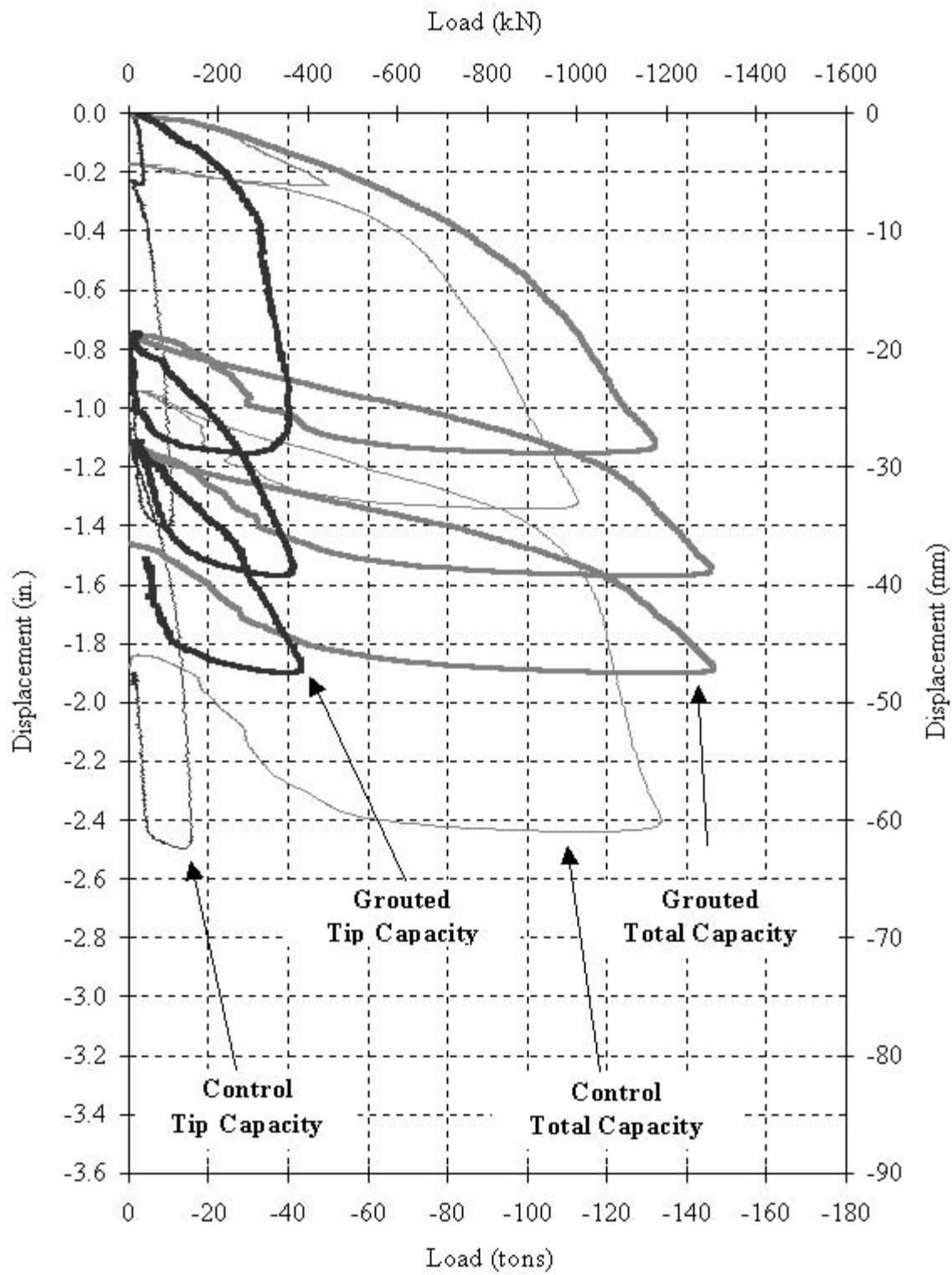


Figure 5-16. Site I Flat-Jack 2 load vs. displacement compared to Control.

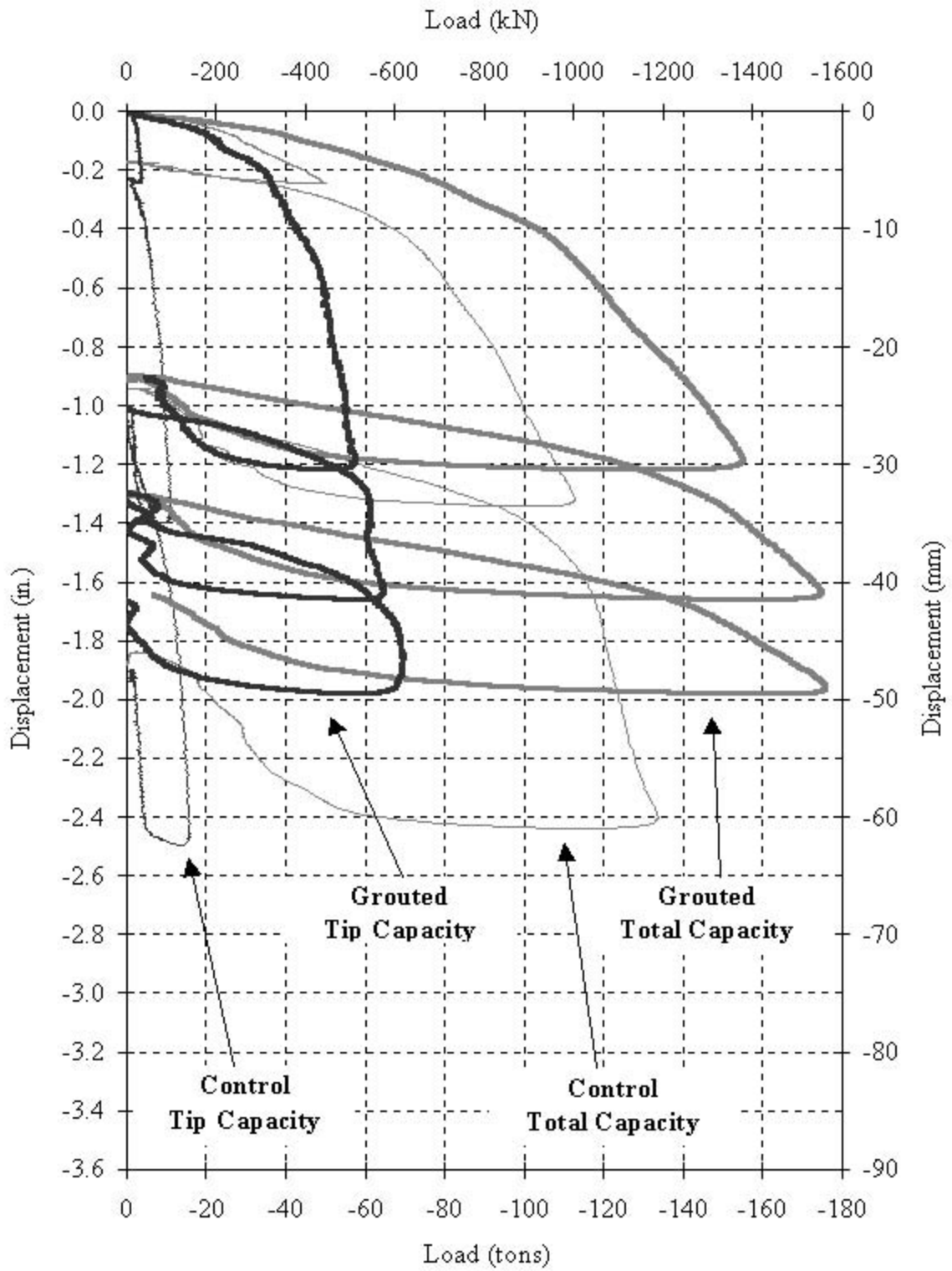


Figure 5-17. Site I Sleeve-Port 1 load vs. displacement compared to Control.

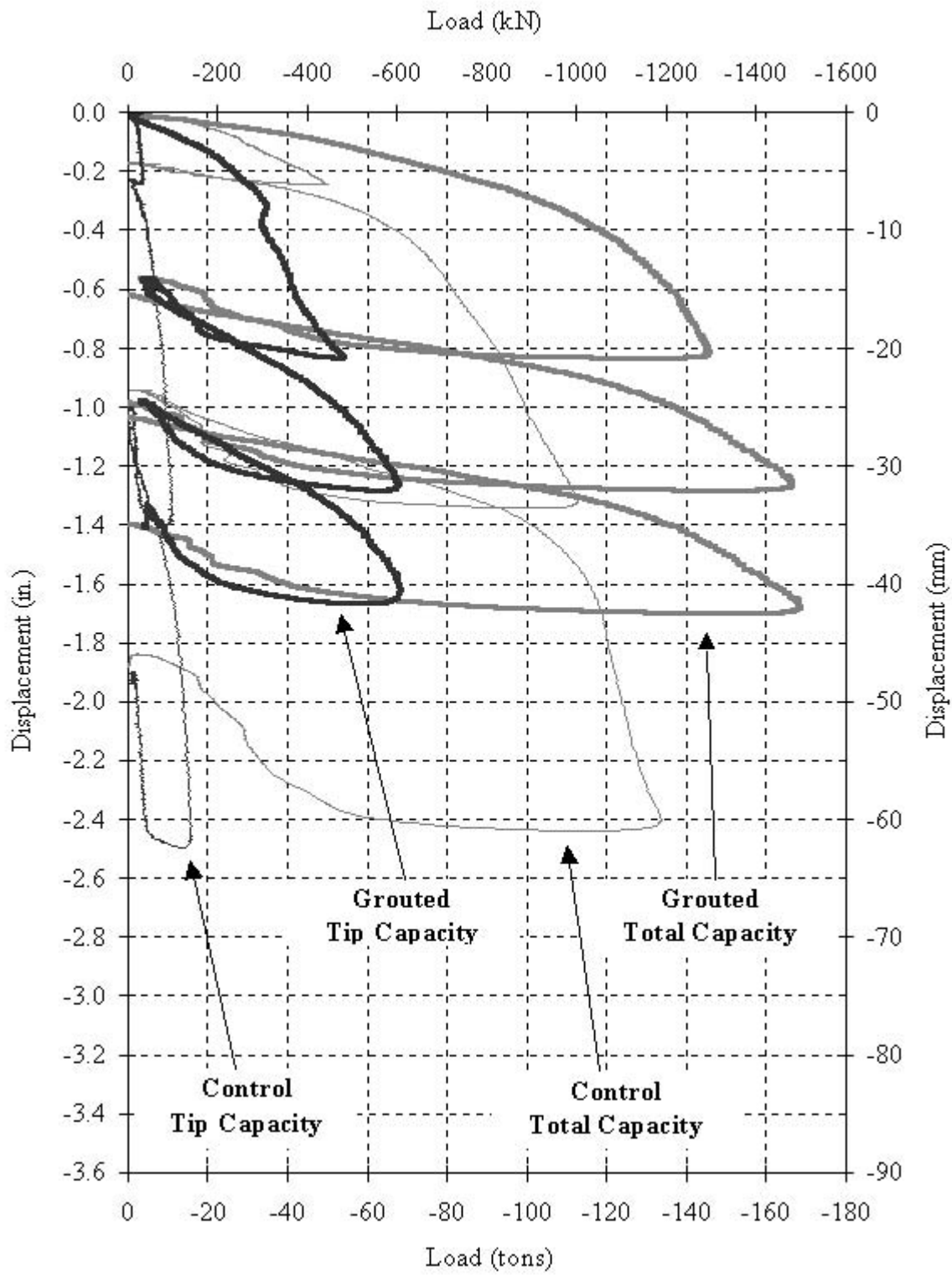


Figure 5-18. Site I Sleeve-Port 2 load vs. displacement compared to Control.

### 5.2.2 Site II (Silty Silica Sand)

Site II consisted of 3 shafts load tested with multiple Statnamic load cycles performed on each shaft. The first load test cycle performed on the control shaft exhibited massive movements. Subsequent cycles were performed for confirmation but were mostly unnecessary. All shafts, both control and grouted, at Site II had a total of three load cycles. The multiple load cycles ensured that the combined load displacement curves were fully defined through ultimate failure, and reload curves were defined.

An analysis was performed, as described in Section 5.2, to reduce each Statnamic load displacement curve to its equivalent static load curve. Each of the load cycles for a particular shaft were then placed tail-to-head with subsequent load cycles to form the load displacement history. Appendix E contains these static load displacement curves for each individual shaft for Site II. Note that all load displacement curves for Sites I and II in Appendix E are to the same scale for easy comparison, with the exception of Site II control shaft being replotted with large scale displacements to show the entire set of its load displacement curves. All analysis was carried out and plotted in English units, with secondary axis placed with SI units.

Figure 5-19 combines the Site II flat-jack load displacement curves with the load displacement curves of Site II control shaft. Figures 5-20 combines the Site II flat-jack load displacement curves with the load displacement curves of Site II control shaft. The analysis of the grouted shafts load capacity improvement, to follow in Chapter 6, will make use of these figures. In each of these figures the tip and total capacity curves of both the grouted shaft and control shaft is identified.

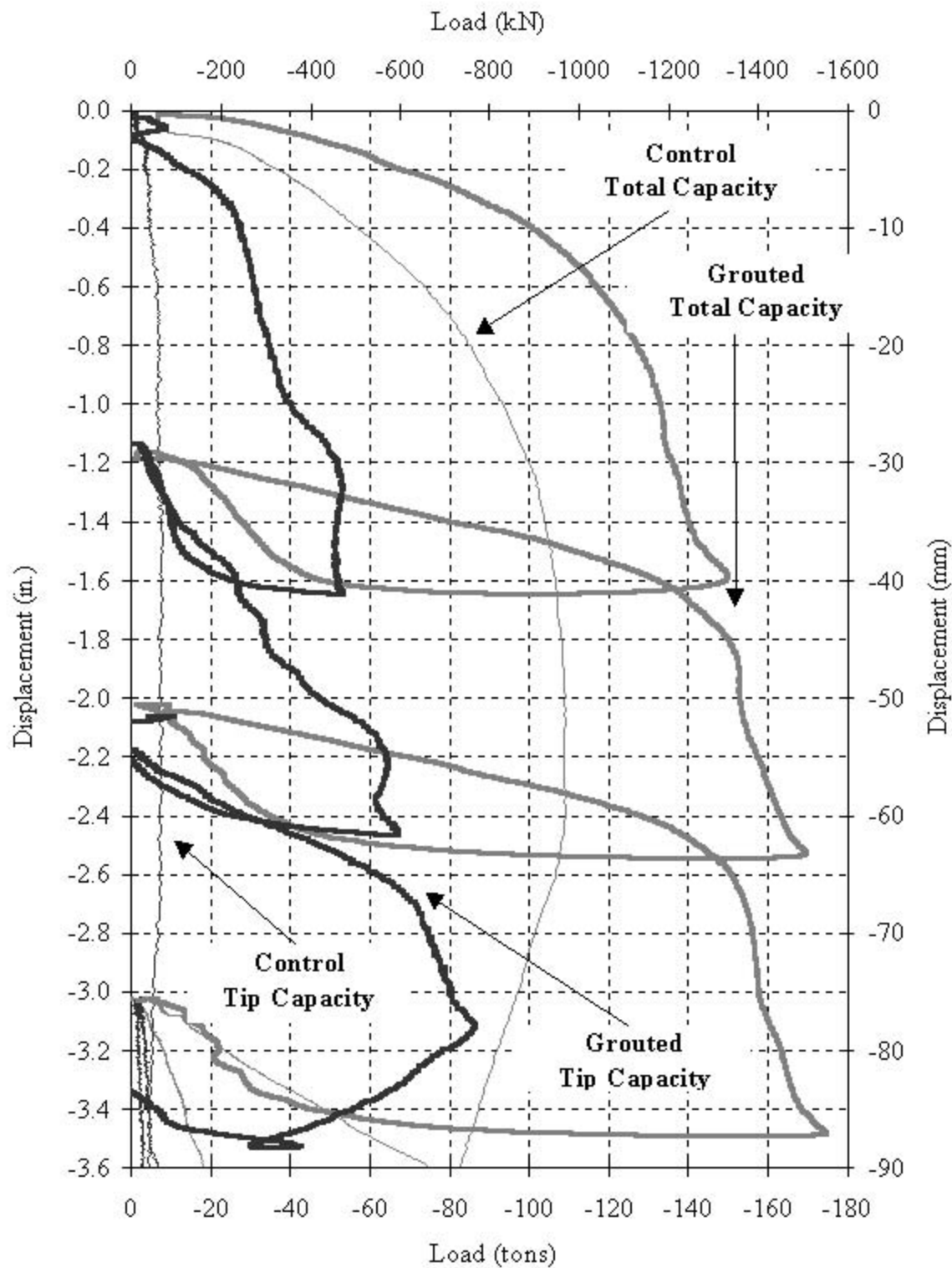


Figure 5-19. Site II Flat-Jack load vs. displacement compared to Control.

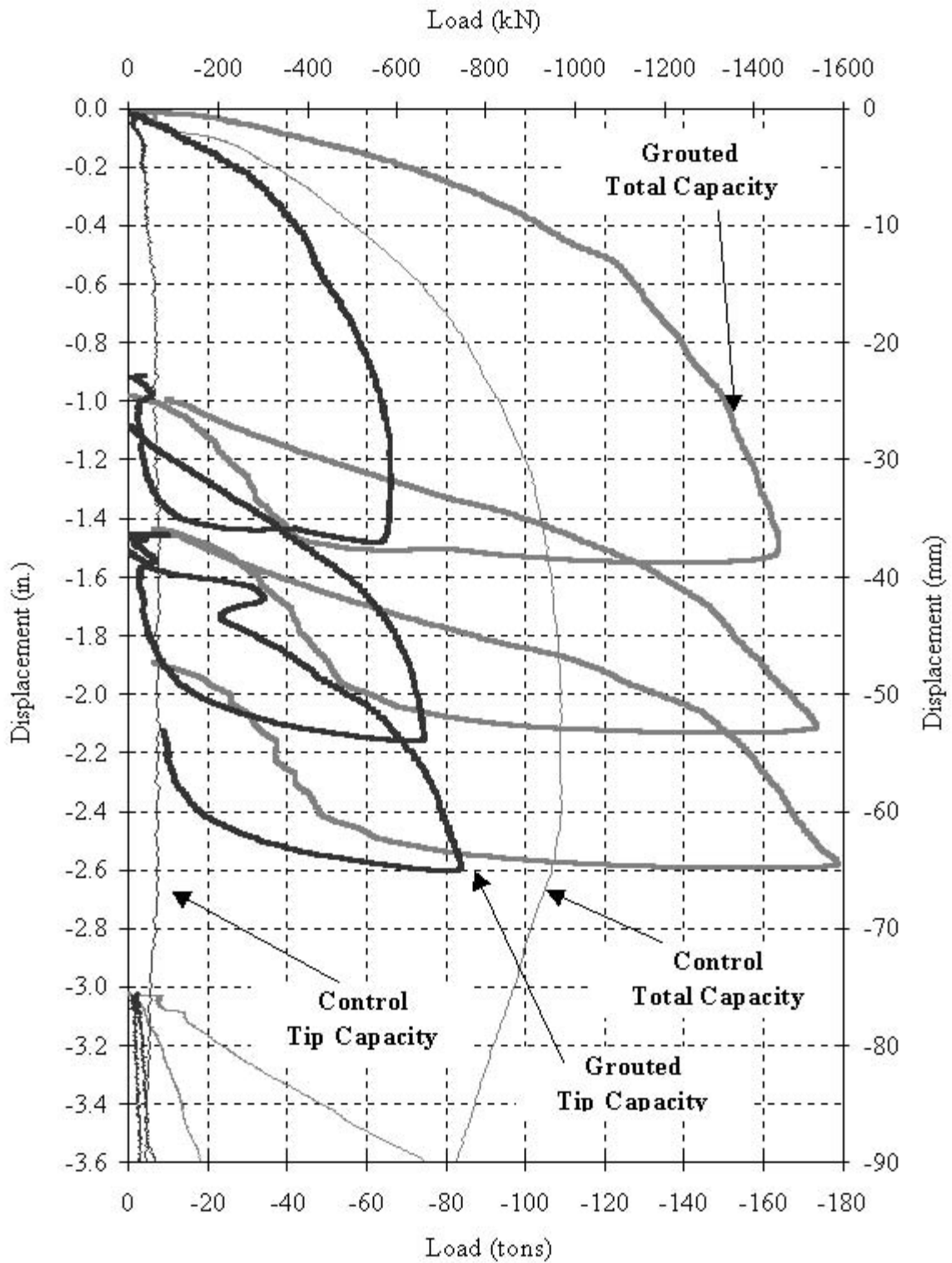


Figure 5-20. Site II Sleeve-Port load vs. displacement compared to Control.

### 5.2.3 Site III (Cemented Coquina)

In that the shafts at this site were so much larger than sites I and II, testing at site III was conducted with a 3500 ton-capacity Statnamic device. Two shafts were tested to evaluate post-grouting effects; LT-3 and LT-2 (listed chronologically in order of testing). Both shafts were tested with two load cycles: 1 cycle prior to grouting to provide the control (un-grouted) capacity, and a second after grouting to assess the capacity improvement. While this scenario was cost effective and negates any potential for soil property spacial variation, it also carries the negative effect of pre-loading the soil toe area prior to grouting. This pre-loading may cause the measured improvement due to grouting appear less than it would otherwise achieve. In these cases, use of strain gage load measurements in the toe of the shaft proved to accurately monitor the progression of the full program (i.e. from load test to grouting to load test).

Figure 5-21 shows the end bearing and total shaft capacity for both load cycles (before and after grouting) for LT-3. Large values of elastic compression, 0.25 in. (6.35 mm) are shown from the independent displacement measurements obtained from top and toe accelerometers. LT-3 could not be fully mobilized by the second load cycle. This shaft was obviously stiffened by the tip grouting, but the extent of improvement was inconclusive.

Similarly, Figures 5-22 shows the end bearing and total shaft capacity for LT-2 for both load cycles. This shaft was approximately 30 feet shorter than LT-3 and was fully mobilized during both load cycles. Load cycle 2 showed a loss of side shear, but showed an improvement in end bearing of approximately 400 tons. This graph does not reflect the stress locked into the shaft by grouting (i.e., the tip load was re-zeroed), as would be similar to a normal construction and loading sequence. This is evident as the reloading released the locked in stress resulting in the tip load to become positive as the cycle terminated.

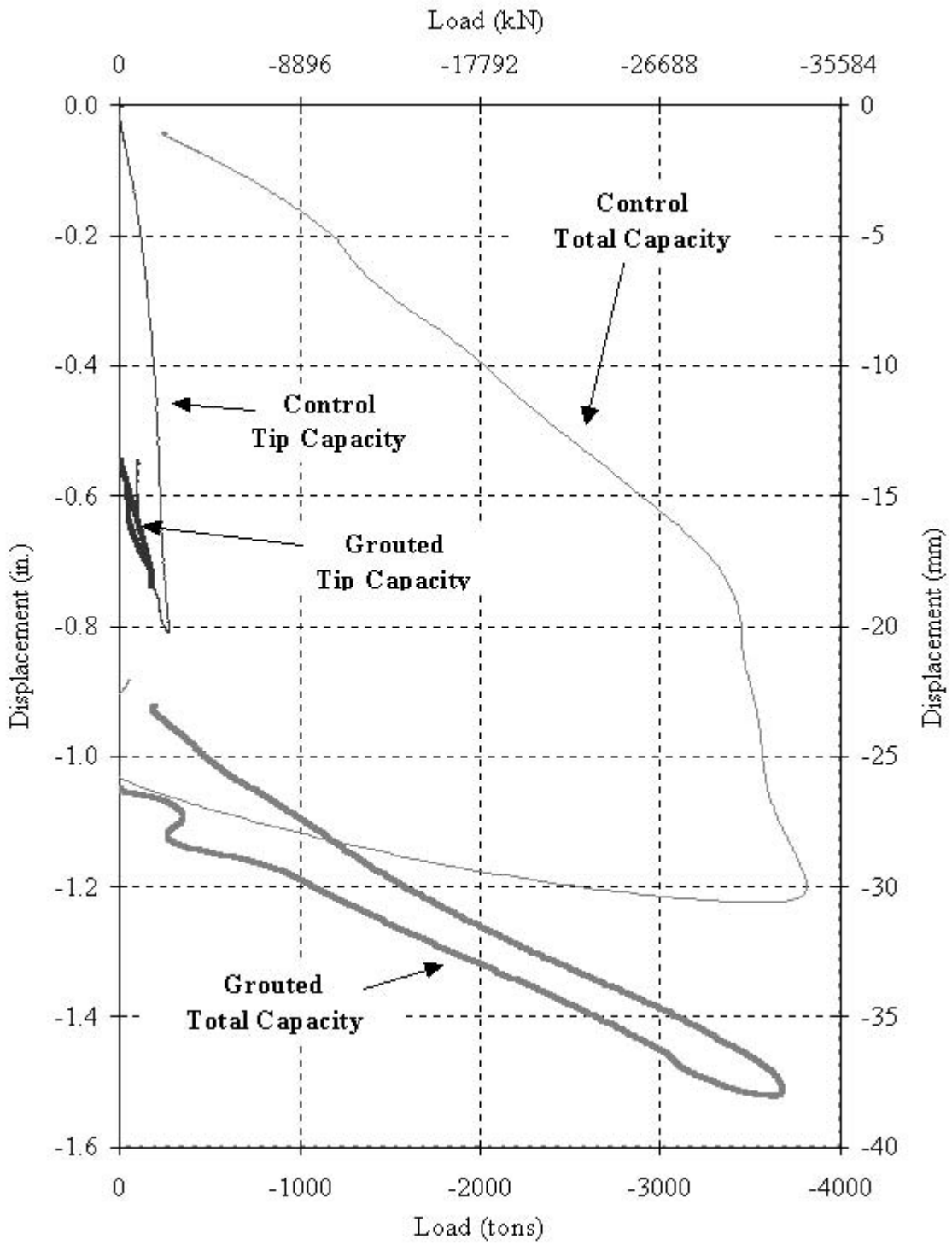


Figure 5-21. Site III LT-3 cycle 2 (grouted) load vs. displacement compared to LT-3 cycle 1 (control).

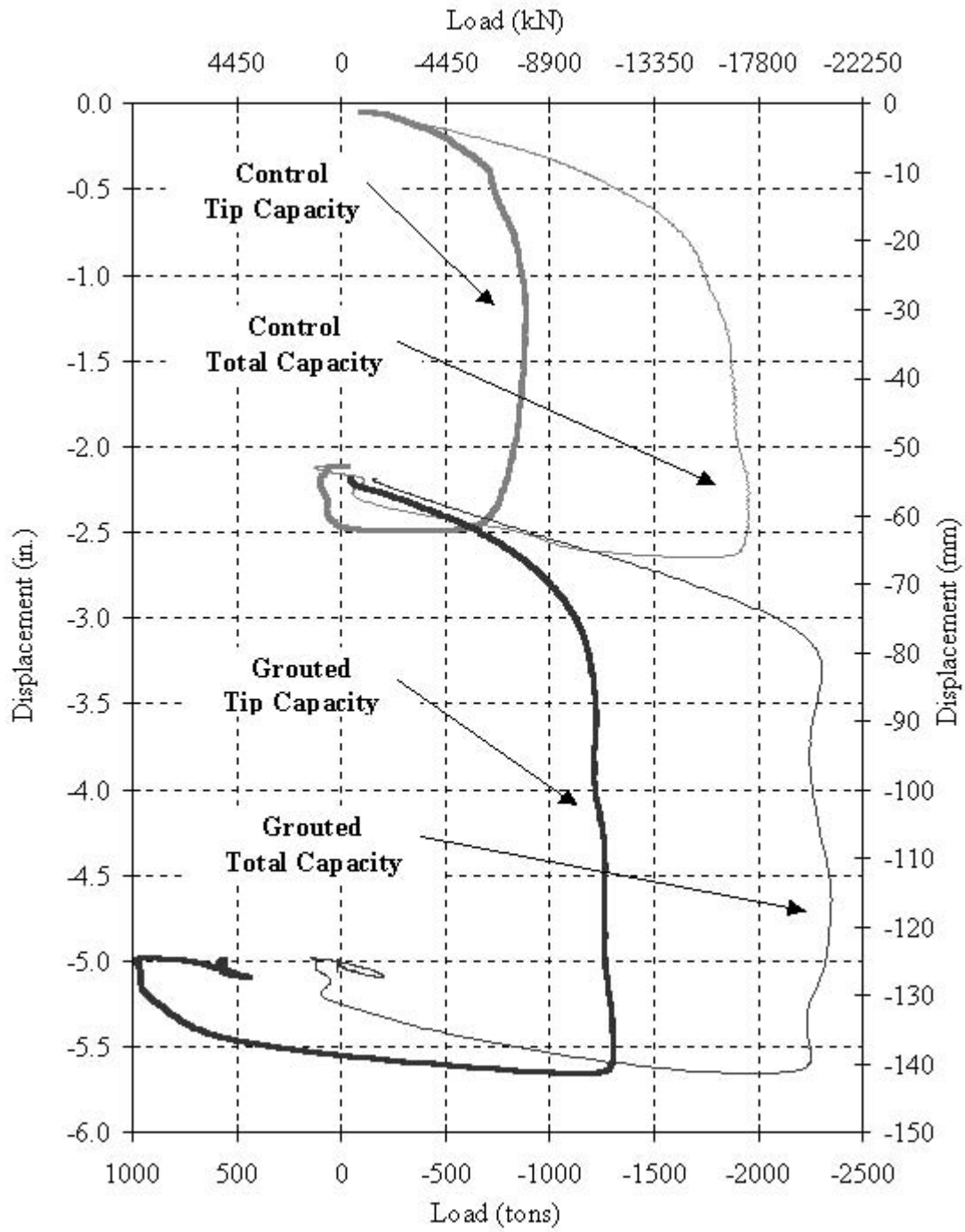


Figure 5-22. Site III LT-2 cycle 2 (grouted) load vs. displacement compared to L-2 cycle 1 (control).

## 6. ANALYSIS

Section 6.1 presents specifics in grouting performance evaluation, while section 6.2 presents load testing evaluations where the end bearing and total capacity for every shaft are compared to its respective control shaft. Section 6.3 contains the conclusions regarding the shaft capacity improvements due to the tip grouting process.

### 6.1 Grouting

The time traces of the force that the grout pressure, as measured by the pressure gage at the inlet line to the shaft, would exert on a shaft tip with an assumed full cross-sectional diameter of 2 ft was presented in section 5.1. This, of course, was a fictitious construction as the grout pressure was most likely acting upon only a portion of the shaft tip at any given time. In order to approximate the actual area that the grout pressure was acting on, the force experienced by the shaft tip (as determined from the strain gage readings), is divided by the grout pressure to yield an effective area, and in turn used to define the area ratio:

$$A_{\text{effective}} = \frac{\text{Force}_{\text{StrainGage}}}{\text{Pressure}_{\text{Grout}}}$$

$$\text{AreaRatio} = \frac{A_{\text{effective}}}{A_{\text{piletip}}}$$

As a result of this definition, an area ratio = 1 would convey that the grout pressure is acting upon the full cross-sectional area of the shaft tip, and any area ratio < 1 would convey that the grout pressure is acting upon that same fraction of the shaft tip area. Note that this area ratio theoretically should never be greater than one, as the grout pressure can only act upon the full cross sectional area of the shaft. Further, the area assumed for the actual shaft tip diameter is the same used for both the area ratio as well as the force calculation from the strain gage readings. As this same assumed area appears in both the numerator and denominator of the equations, any error in assumed shaft tip area would cancel. However, this calculation is extremely sensitive to the grout pressures which can vary widely and quickly due to transient response in the lines. Further, the grout pressures measured are at the pump discharge, and may be artificially high compared to that actually experienced by the shaft tip due to line losses. This is a reason that data is only compared during active grouting periods, and for a particular grout sequence after the pressures and shaft loads have had a chance to stabilize.

Figures 6-1 and 6-2 present area ratios for flat-jack and sleeve-port style grouting apparatus, respectively. As expected, the flat-jacks trend about an area ratio of one, as pressure can very quickly and effectively distribute itself across the shaft tip. The sleeve-ports tend to have a low area ratio, then build towards a value of one during consecutive

grouting sequences. This also is as expected. As the individual U-tubes are grouted, the shaft flexes back and forth under the eccentric grout tip load until at last the pressure may become distributed across the entire shaft tip. Note that LT-3, of Site III, behaved as a sleeve-port system even though it had a flat-jack apparatus due to its membrane being punctured, as was detailed in Section 4.6.2, and acted as three individual grouting orifices. Of particular interest was how the Site I sleeve-port 2 (no plate) never increased in area ratio (about 0.2) as compared to all the others that did have plates. Apparently, the plate did assist in the pressure distribution across the shaft tip, as was expected.

## **6.2 Load Testing Comparisons**

Determination of tip improvement was calculated based upon comparison of the grouted shaft capacity to its respective control shaft capacity, rather than comparing the grouted capacity to any predicted values of un-grouted capacity. In the case of Site III, the second load test cycle (post-grouted) was compared to the first load test cycle (before grouting) for both LT-2 and LT-3. All comparisons made in this chapter use the static load, as derived from the Statnamic load test data presented in chapter 5.

The design procedure, to be presented, will allow utilization of any capacity prediction equation, or actual load test data obtained from un-grouted shafts at the site in question. Thus the inability for any given equation (empirical or otherwise) to exactly predict the un-grouted capacity will not be carried into the following design synthesis. For example, The values predicted for the tip capacity of the 24 in. diameter un-grouted control shafts, based upon SPT blow counts, using the design equations by Reese and O'Neill (1988) and Reese and Wright (1977) are 15.0 tons and 17.0 tons respectively for Site I, and 5.0 tons and 5.6 tons respectively for Site II. These design equations predict the tip loads at a displacement of 5% of shaft diameter, 1.2 in. (30.5 mm). These predicted values were reasonably close to those measured with an over-prediction of the capacity by 36 % and 55 % respectively for Site I, and under-prediction of 29 % and 20 %, respectively for Site II. The test shafts at Site III were unable to be displaced to 5% of their 48 in. diameter, 2.4 in. (61.0 mm), due to limitations of the testing apparatus, and thus can not be directly compared to predicted values at this displacement. However, it does appear that both design equations listed greatly under-predicted the tip capacity if the shafts were to be displaced this much. Tip capacity vs. displacement for each Site will be specifically presented in the sub-sections to follow.

Comparisons of grouted capacity to an un-grouted control shaft will be of great benefit, as there is no "one" best equation for prediction of capacity, and a practicing engineer may rely on whichever has providing the best results in the particular formation in question (soil type) in the past. Further, if load test data is available for the particular site, then this may be utilized in lieu of a prediction equation. Actual load test data for a site, given the same construction methodology, is considered more reliable than prediction equations.

In comparing a grouted shaft performance to its respective control shaft at any given displacement, Improvement is defined as follows:

$$\% \text{ Improvement} = \frac{(\text{Capacity}_{\text{grouted pile}} - \text{Capacity}_{\text{control}})}{\text{Capacity}_{\text{control}}} * 100\%$$

The end bearing and total capacity for every shaft are compared to its respective control shaft, as was shown for every grouted shaft in Section 5.2. Figure 6-3 is an example showing the tip and total load scenarios for both the grouted and control shaft that are utilized in the above stated definition for determining improvement. Note that this example shows the values at a displacement of 5% the shaft diameter. Similar comparisons are made of shaft improvement at displacements of 0.25 in. (6.4 mm), 0.5 in. (12.7 mm), 1.0 in. (25.4 mm), and at ultimate. Tables 6-1 through 6-3 present the total and tip load, the percent tip contribution, percent tip improvement, and the total shaft improvement for each of the shafts tested at displacements of 0.5 in. (12.7 mm), 1.0 in. (25.4 mm), and 5% the shaft diameter, respectively. Table 6-4 presents similar data at the ultimate load, while additionally listing the displacement at the ultimate load for each shaft. These tabulated values form the database by which shaft improvement vs. top of shaft displacement, both tip and total, are plotted and compared in Section 6.3, to follow.

The shaft tip displacements are significantly less than the top of shaft for the relatively long shafts of Site III due to elastic compression of the shaft. However, they are compared using the top of shaft displacements as this is the critical design displacement to consider.

The large difference in tip improvement between Sites I and II can be attributed to the skin grouting at Site II providing more grouting reaction compounded by the low ungrouted tip capacity.

Table 6-1. Load Performance at 0.5 inch Displacement

Site	Grout Delivery Mech.	Shaft Designation	Total Load tons (kN)	Tip Load tons (kN)	Tip Contrib. (%)	Tip Improve (%)	Total Improve (%)
Site I (Shelly Sand)	Control	G1-CON (no grout)	75 (667)	5 (44)	7	N/A	N/A
	Flat-Jack	G1-FJ1 (release press.)	98 (872)	31 (276)	32	520	31
		G1-FJ2 (hold press.)	96 (854)	36 (320)	38	620	28
	Sleeve-Port	G1-SP1 (with plate)	114 (1014)	46 (409)	40	820	52
		G1-SP2 (no plate)	129 (1148)	42 (374)	33	740	72
Site II (Silty Sand)	Control	G2-CON (no grout)	65 (578)	5.5 (49)	8	N/A	N/A
	Flat-Jack	G2-FJ (release press.)	120 (1068)	32 (285)	29	482	69
	Sleeve-Port	G2-SP (with plate)	100 (890)	44 (391)	37	700	85
Site III (Cem. Coquina)	LT-3	Cycle 1 (no grout)	2440 (21706)	98 (872)	4	N/A	N/A
		Cycle 2 (grouted)	2970 (26421)	190 (1690)	6	94	22
	LT-2	Cycle 1 (no grout)	1405 (12499)	572 (5089)	41	N/A	N/A
		Cycle 2 (grouted)	1662 (14785)	1125 (10008)	68	97	18

Table 6-2. Load Performance at 1.0 inch Displacement

Site	Grout Delivery Mech.	Shaft Designation	Total Load tons (kN)	Tip Load tons (kN)	Tip Contrib. (%)	Tip Improve (%)	Total Improve (%)
Site I (Shelly Sand)	Control	G1-CON (no grout)	100 (890)	10 (89)	10	N/A	N/A
	Flat-Jack	G1-FJ1 (release press.)	118 (1050)	37 (329)	31	270	18
		G1-FJ2 (hold press.)	126 (1121)	40 (356)	32	300	26
	Sleeve-Port	G2-SP1 (with plate)	145 (1290)	55 (489)	38	450	45
		G2-SP2 (no plate)	158 (1406)	60 (534)	38	500	48
Site II (Silty Sand)	Control	G2-CON (no grout)	94 (836)	6.6 (59)	7	N/A	N/A
	Flat-Jack	G2-FJ (hold press.)	138 (1228)	50 (445)	36	658	47
	Sleeve-Port	G2-SP	150 (1334)	62 (552)	41	839	60
Site III (Cem. Coquina)	LT-3	Cycle 1 (no grout)	3568 (31741)	287 (2553)	8	N/A	N/A
		Cycle 2 (grouted)	Unmob.	Unmob	Unmob	Unmob	Unmob
	LT-2	Cycle 1 (no grout)	1758 (15639)	784 (6974)	45	N/A	N/A
		Cycle 2 (grouted)	2465 (21929)	1375 (12232)	56	75	40

Table 6-3. Load Performance at a Displacement of 5% of Shaft Diameter

Site	Grout Delivery Mech.	Shaft Designation	Total Load tons (kN)	Tip Load tons (kN)	Tip Contrib. (%)	Tip Improve (%)	Total Improve (%)
Site I (Shelly Sand)	Control	G1-CON (no grout)	108 (961)	11 (98)	10	N/A	N/A
	Flat-Jack	G1-FJ1 (release press.)	123 (1094)	39 (347)	32	225	14
		G1-FJ2 (hold press.)	136 (1210)	41 (365)	30	273	26
	Sleeve-Port	G2-SP1 (with plate)	155 (1379)	57 (507)	37	418	44
		G2-SP2 (no plate)	163 (1450)	64 (569)	39	482	51
Site II (Silty Sand)	Control	G2-CON (no grout)	100 (890)	7 (62)	7	N/A	N/A
	Flat-jack	G2-FJ (hold press.)	145 (1290)	52 (463)	36	643	45
	Sleeve-Port	G2-SP (with plate)	157 (1397)	66 (587)	42	843	57
Site III (Cem. Coquina)	LT-3	Cycle 1 (no grout)	Unmob.	Unmob.	Unmob.	N/A	N/A
		Cycle 2 (grouted)	Unmob.	Unmob.	Unmob.	Unmob.	Unmob.
	LT-2	Cycle 1 (no grout)	1946 (17312)	796 (7081)	41	N/A	N/A
		Cycle 2 (grouted)	2521 (22427)	1455 (12944)	58	83	30

Table 6-4. Load Performance at Ultimate Load

Site	Grout Delivery Mech.	Shaft Designation	Disp. at Ult. inch (mm)	Total Load tons (kN)	Tip Load tons (kN)	Tip Cont. (%)	Tip Improve (%)	Total Improve (%)
Site I (Shelly Sand)	Control	G1-CON (no grout)	2.40 (61.0)	120 (1068)	16 (142)	13	N/A	N/A
	Flat-Jack	G1-FJ1 (release press.)	1.49 (37.8)	130 (1156)	39 (347)	30	144	8
		G1-FJ2 (hold press.)	1.50 (38.1)	145 (1290)	42 (374)	29	163	21
	Sleeve-Port	G1-SP1 (with plate)	1.57 (39.9)	170 (1512)	63 (560)	37	294	42
		G1-SP2 (no plate)	1.70 (43.2)	167 (1486)	66 (587)	40	313	39
Site II (Silty Sand)	Control	G2-CON (no grout)	1.80 (45.7)	107 (952)	7.2 (64)	7	N/A	N/A
	Flat-Jack	G2-FJ (release press.)	1.50 (38.1)	145 (1290)	53 (471)	37	636	36
	Sleeve-Port	G2-SP (with plate)	1.50 (38.1)	164 (1459)	65 (578)	40	803	53
Site III (Cem. Coquina)	LT-3	Cycle 1 (no grout)	Unmob	Unmob	Unmob	Unmob	N/A	N/A
		Cycle 2 (grouted)	Unmob	Unmob	Unmob	Unmob	Unmob	Unmob
	LT-2	Cycle 1 (no grout)	2.4 (61.0)	1946 (17312)	796 (7081)	41	N/A	N/A
		Cycle 2 (grouted)	1.1 (27.9)	2480 (22062)	1392 (12383)	56	75	27

### 6.2.1 Site I (Shelly Sand)

Figures 6-4 and 6-5 present comparisons of the grouted shaft tip load with the control shaft tip load for Site I flat-jack and sleeve-port shafts, respectively. Figure 6-4 shows a 170% average ultimate improvement in flat jack cells at Site I over the control shaft. Figure 6-5 show a greater average ultimate improvement of over 300% for the sleeve-port shafts at Site I.

The tip capacity values of the 24 in. diameter un-grouted control shaft was made based upon an averaged SPT blow count profile measured at this Site. The tip capacity was calculated to be 15.0 tons and 17.0 tons using the design equations by Reese and O'Neill (1988) and Reese and Wright (1977), respectively. These design equations predict the tip loads at a displacement of 5% of shaft diameter, 1.2 in. (30.5 mm). These predicted values were reasonably close to those measured with an over-prediction of the capacity by 36 % and 55 % for Reese and O'Neill (1988) and Reese and Wright (1977), respectively.

Figure 6-6 shows the tip load capacity vs. top of shaft displacement for every shaft at site I, both grouted and control. The predictions, at 5% shaft diameter displacement, made by using the equations previously discussed, is also shown in this Figure.

Flat-Jack 1 (release grout pressure) had a slightly lower tip capacity than Flat-Jack 2 (lock in pressure), and then appeared to approach the same ultimate value. This was expected, as the locked in pressure in Flat-Jack 2 would more readily transfer the load to the tip due to the greater amount of locked in negative side shear, while Flat-Jack 1 would essentially be starting with no locked in stresses but would also be operating on the stiffened reload curve. As displacements become very large, they both approach the same ultimate value which is limited by essentially the same amount of soil strengths and improvements through the compaction grouting process.

Sleeve-Port 1 (with steel plate) started with a higher tip load than Sleeve-Port 2 (no plate), but was quickly surpassed by Sleeve-Port 2 as displacements became greater. The greater initial stiffness of Sleeve-Port 1 can be explained by the steel plate allowing a more even grout pressure distribution across the shaft tip. Thus, the soil across the entire shaft tip was locked into a pre-compressed condition, whereas only portions of the soil under Sleeve-Port 2 may have been compressed and able to contribute initially to the tip load capacity. However, Sleeve-Port 2 had the entire side shear available to react against as it mobilized only a portion of the soil during the first grout cycle, and more soil during the second grout cycle. Thus, as displacement progressed, the shaft tip may have felt the effects of a soil that had greater amounts of improvements in the sections around the individual sleeve-ports. Indeed, the effective grouting area ratio for this shaft, presented in Section 6.1.1, strongly suggests that the grout pressure never did distribute across the entire shaft tip.

### **6.2.2 Site II (Silty Silica Sand)**

Figure 6-7 presents comparisons of the grouted shaft tip load with the control shaft tip load for Site II. Figure 6-7 shows considerably more ultimate improvement at Site II over Site I. The flat-jack and sleeve-port grouted shafts at Site II have maximum improvements of 780% and 1000%, respectively. This is 4.6 and 3.3 times greater than the improvement at Site I for the flat-jack and sleeve-port style grouting apparatus, respectively. The reason for the greater improvement at Site II was not a function of the soil type alone. Rather, the un-grouted tip resistance values in this soil was much less, as will be shown. Further, these shafts had at least as much side shear to react against during grouting, as evidenced by the grout pressure, for the purpose of soil improvement. Skin grouting was performed on the grouted shafts at Site II which ensured these high side shear values. This has the effect of creating a higher Grout Pressure Index (GPI), to be defined in section 6.3, at Site II.

Tip capacity estimates of the 24 in. diameter un-grouted control shaft were made based upon an averaged SPT blow count profile measured at this Site. The tip capacity was calculated to be 5.0 tons and 5.6 tons using the design equations by Reese and O'Neill (1988) and Reese and Wright (1977), respectively. These design equations predict the tip loads at a displacement of 5% of shaft diameter, 1.2 in. (30.5 mm). These predicted values were reasonably close to those measured with an under-prediction of the capacity by 29% and 20% for Reese and O'Neill (1988) and Reese and Wright (1977), respectively.

Figure 6-8, shows a plot of the tip load capacity vs. top of shaft displacement for every shaft at Site II, both grouted and control. The predictions, at 5% shaft diameter displacement, made using the equations previously discussed, is also shown in this Figure.

### **6.2.3 Site III (Cemented Coquina)**

The end bearing and total capacity for every shaft are compared to the respective control shaft for Sites I and II. However, due to project cost constraints, there were no dedicated control (un-grouted) shafts for Site III. Instead, the second load test cycle performed on the shaft (after post-grouting) will be compared to the first load test cycle (before shaft was grouted) for both LT-2 and LT-3. As a result, the calculations of tip improvement may be conservative. This is due to the first load cycle compressing the soil at the tip that may have otherwise been improved with the grout pressure, and possibly allowed some greater amount of lateral expansion of the grout bulb. Further, the first load cycle mobilized the side shear values passed their peak strengths, and into their lower residual values. This soil type (cemented coquina) is very susceptible to loss of strength. Thus, the grouting process will have less side shear available to react against, and thus may be limited, as was the case with LT-2. Also, the side shear will be at the lower residual value during the second load test cycle, making the total capacity less.

Plots of shaft tip load vs. displacement curves for both LT-3 and LT-2 can be found in Section 5.2.3. With separate control cycles, test shafts LT-3 and LT-2 can not be plotted together as a typical load test curve in any way that would add to an understanding better than that obtained with these previous Figures.

Tip capacity estimates of the 48 in. diameter un-grouted control shaft (load cycle 1) were made for both LT-3 and LT-2 based upon a SPT blow count profile measured at each of these shaft locations. The tip capacity for LT-3 was calculated to be 187 tons and 208 tons using the design equations by Reese and O'Neill (1988) and Reese and Wright (1977), respectively. The tip capacity for LT-2 was calculated to be 539 tons and 503 tons using the design equations by Reese and O'Neill (1988) and Reese and Wright (1977), respectively. These design equations predict the tip loads at a displacement of 5% of shaft diameter, 2.4 in. (61.0 mm).

Figure 6-9, shows a plot of the tip load capacity vs. top of shaft displacement for both LT-3 and LT-2 at Site III, both grouted (load cycle 2) and control (load cycle 1). The predictions, at 5% shaft diameter displacement, made using the equations previously discussed for load cycle 1, are also shown in this Figure.

The load capacity of LT-2 cycle 1 (un-grouted control) reached and ultimate tip load of 796 tons at a 5% shaft diameter displacement. This value was under-predicted by 32% and 37% for the design equations of Reese and O'Neill (1988) and Reese and Wright (1977), respectively. The load capacity of LT-3 cycle 1 (un-grouted control) reached a tip load of 287 tons at a displacement of 1 in. (25.4 mm). This is not an ultimate value, as the tip was not mobilized passed this amount of displacement, knowing that a significant amount of side shear would be lost if this were to happen. However, it does appear that this may be very close to its ultimate value. If this value at 1 in. (mm) is taken as ultimate, it was under-predicted by 35% and 28% for the design equations of Reese and O'Neill (1988) and Reese and Wright (1977), respectively for a displacement of 2.4 in.

Tip capacity improvements were much less for Site III than for either Sites I or II. This was expected due to the soil type. Cemented sands are much more difficult to improve through compaction grouting than uncemented sands as detailed in Section 2.1.

### **6.3 Conclusions**

Shaft Improvement, for both total and tip capacity, was defined in Section 6.2 and was tabulated therein for various amounts of displacements. The improvements for shaft tip and total capacity vs. top of shaft displacement, to each shafts measured ultimate capacity, are shown as Figures 6-10 and 6-11, respectively. For the relatively long shafts of Site III, the shaft tip displacements are significantly less than the top of shaft. However, the top of shaft displacements are utilized in this comparison, as these are the displacements that a structure would experience during normal top-down loading of the drilled shaft.

The greatest amount of total improvement occurred in Site I at a displacement of only 2% of the shaft diameter (0.48 in. or 12.2 mm), in Site II at a displacement of 1% of the shaft diameter (0.24 in. or 6.1 mm), and in Site III LT-2 at a displacement of 2% of the shaft diameter (1.00 in. or 25.4 mm). Site III LT-3 cycle 2 could not be fully mobilized due to load limitations of the testing equipment, but was obviously improved to some unknown degree.

These improvements were due to the grouting locking in some amount of negative side shear, and thus more readily transferring the subsequent load to the shaft tip which was prestressed in compression, and operating on a stiffer reload curve. This was most fortunate from a performance point of view, as most service limit displacements are set to small displacements occurring well before ultimate shaft capacity was reached.

Historically, the shaft capacity improvement due to tip grouting has been shown many times to correlate directly with the grout take (volume of grout). This of course assumes that the volume measured remains within the grout bulb formed below the shaft tip, and does not hydro-fracture the soil and migrate away from the improvement zone below the shaft tip. In order to compare the grout takes of shafts differing in diameter (for example; 24 inch for Sites I and II, and 48 inch for Site III), a dimensionless parameter was established for the grout volume. Therefore, this parameter ( $\eta$ ) is the height of grout (expressed as a fraction of the shaft diameter) required to fill a cylinder whose diameter is that of the shaft. This is consistent with design procedures that are based on a capacity developed at a displacement expressed as a percent of the shaft diameter.

$$\eta = \frac{H_{cylinder}}{D_{shaft}}$$

where:  $H_{cylinder}$  = equivalent height of cylindrical grout volume.  
 $D_{shaft}$  = the shaft diameter.

Although this study corroborates these conclusions in that a general trend of increased improvement was observed with greater grout takes, the correlation does not appear to be strong. The maximum tip and total capacity improvements are plotted vs. their dimensionless grout takes in Figures 6-12 and 6-13, respectively. Many factors may influence the grout take (shaft toe disturbance, voids beneath grouting apparatus, escape of grout through weak or layered soil strata) that would have little or no effect on shaft tip improvement.

An increase in effective stress thus must be applied to the soil at the toe zone for shaft tip improvement. This is achieved with compaction grouting in free draining sands as the cavity expansion process, grout bulb formation, densifies the immediately surrounding soil. Further, this cavity expansion also allows for the grout pressure to react upward upon the

shaft tip, thus locking the soil at the toe zone in compression and the soil above the shaft tip in contact with the shaft in negative side shear. The amount of negative side shear locked in will be greatest at the bottom level of the shaft, and diminish up the shaft due to the compressibility of the shaft. This is termed load shedding, and is generated from a bottom-up loading condition during tip grouting. From a free body perspective of the shaft, this scenario looks like down drag on a shaft.

A rational design procedure based upon grout take would be extremely difficult to implement due to the inability to accurately estimate the percentage of the grout volume contributing to shaft tip improvement. It is interesting to note on Figure 6-12 that the Sleeve-ports consistently showed a greater tip capacity improvement over their respective flat-jack counterparts for a given grout take. Also, the maximum sustained pressure for the sleeve-ports was consistently higher than that for their flat-jack counterparts for a given grout take, as is shown in Figure 6-14.

This leads to the rationale that the sustained grout pressures may be a better indicator of the tip improvement. This would be of great advantage from a design point of view as estimates of grout pressure are easily estimated based upon the side shear available upon which the grout pressure can react. Figure 6-15 shows the maximum tip capacity improvement vs. the maximum sustained pressure.

The data presented to this point has expressed the tip improvements in terms of their maximum values. For an effective design procedure, the tip improvements must be expressed over the full range of shaft displacements experienced during load testing. Figures presenting the tip capacity vs. top of shaft displacement are presented for individual Sites in the subsections to follow.

In order to compare these different soil types (Sites) in terms of improvements over the control shaft at various shaft displacements, a dimensionless parameter was established. This dimensionless parameter is introduced as the quotient of the maximum sustained grout pressure and the observed control unit tip resistance at a displacement specified as a percentage of the shaft diameter. This parameter is herein termed as the Grout Pressure Index (GPI).

$$GPI = \frac{P_{\max}}{q_{(\text{ungrou ted})j}}$$

where:

GPI	=	grout pressure index
$P_{\max}$	=	maximum sustained grout pressure
$q_{(\text{ungrou ted})j}$	=	unit ungrouted tip resistance at displacement j
j	=	displacement of ungrouted tip expressed in % diameter

A second dimensionless parameter is introduced as the ratio of the grouted shaft tip capacity to the tip capacity of the control shaft at corresponding displacements specified as a percentage of the shaft diameter (%D). This parameter is herein termed as the Tip Capacity Multiplier (TCM).

$$TCM_{i,j} = \frac{q_{(grouted)i}}{q_{(ungrouted)j}}$$

where:  $TCM_{i,j}$  = tip capacity multiplier at displacement i  
 $q_{(grouted)i}$  = unit grouted tip resistance at displacement i.  
*i* = displacement of grouted tip expressed in % shaft diameter  
 $q_{(ungrouted)j}$  = unit ungrouted tip resistance at displacement j

Note that the Tip Capacity Multiplier (TCM) can be related to the % Tip Capacity Improvement, as defined in Section 6.2, by the following equation:

$$TCM = \left( \frac{\% \text{ Improvement}}{100} \right) + 1$$

Figure 6-16 shows a very strong correlation between the Tip Capacity Multiplier and the Grout Pressure Index for tip capacities calculated at displacements of 5 % shaft diameter. Linear fits of the three design curves at 1 %, 2 %, and 5 % diameter displacements were made using Microsoft Excel. The linear fits were performed with a weighting factor of 20 placed upon the control shafts TCM intercept point. This has the effect of calculating the best fit line through the grouted shafts data points, while forcing the TCM intercept to be that of the control shaft. The selection of 5% was somewhat arbitrary; however, a displacement of 5% the shaft diameter is common to many design prediction equations and is usually considered an upper limit on displacement at which tip resistance approaches its ultimate value.

At a Grout Pressure Index of zero (an un-grouted, control shaft) the 5 % displacement criteria line crosses the Ordinate (Tip Capacity Multiplier) at exactly 1. Further, the 1% and 2% displacement criteria lines cross the Ordinate (Tip Capacity Multiplier) at 0.49 and 0.63, respectively. This has been common practice that if a shaft is to be limited to some displacement less than that utilized by the design equation (in this case 5% shaft diameter), the unit tip resistance value must be limited to some fraction of that experienced at 5% shaft diameter displacement. Similarly, if the grouted shafts displacements are to be limited to a smaller value such as 1% or 2% of the shaft diameter, the 1% or 2% displacement criteria lines, respectively, should be used in conjunction with the Grout Pressure Index in order to determine what the allowable tip capacity multiplier should be limited to.

The selection of 1%, 2%, and 5% diameter displacement values was somewhat arbitrary, but provided a good distribution of design values with 5% being a common upper limit. For values other than these, interpolation between design charts (or between curves on a given design chart) may yield acceptably accurate results.

Similar to development of the previous design chart based upon a 5% shaft diameter displacement, design charts based upon 2% and 1% shaft diameter displacements are also developed and presented as Figures 6-17 and 6-18, respectively. Again, a summary of the linear fit is also shown in each of these figures. Note that this time, the 2% and 1% design displacement curves cross the ordinand (TCM) at exactly 1.0 in Figures 6-17 and 6-18, respectively. If a larger displacement can be tolerated than that specified by whatever design prediction equation utilized (or un-grouted load test data), the higher displacement design curve(s) will correctly intercept the ordinand (TCM) at a value higher than 1.0.

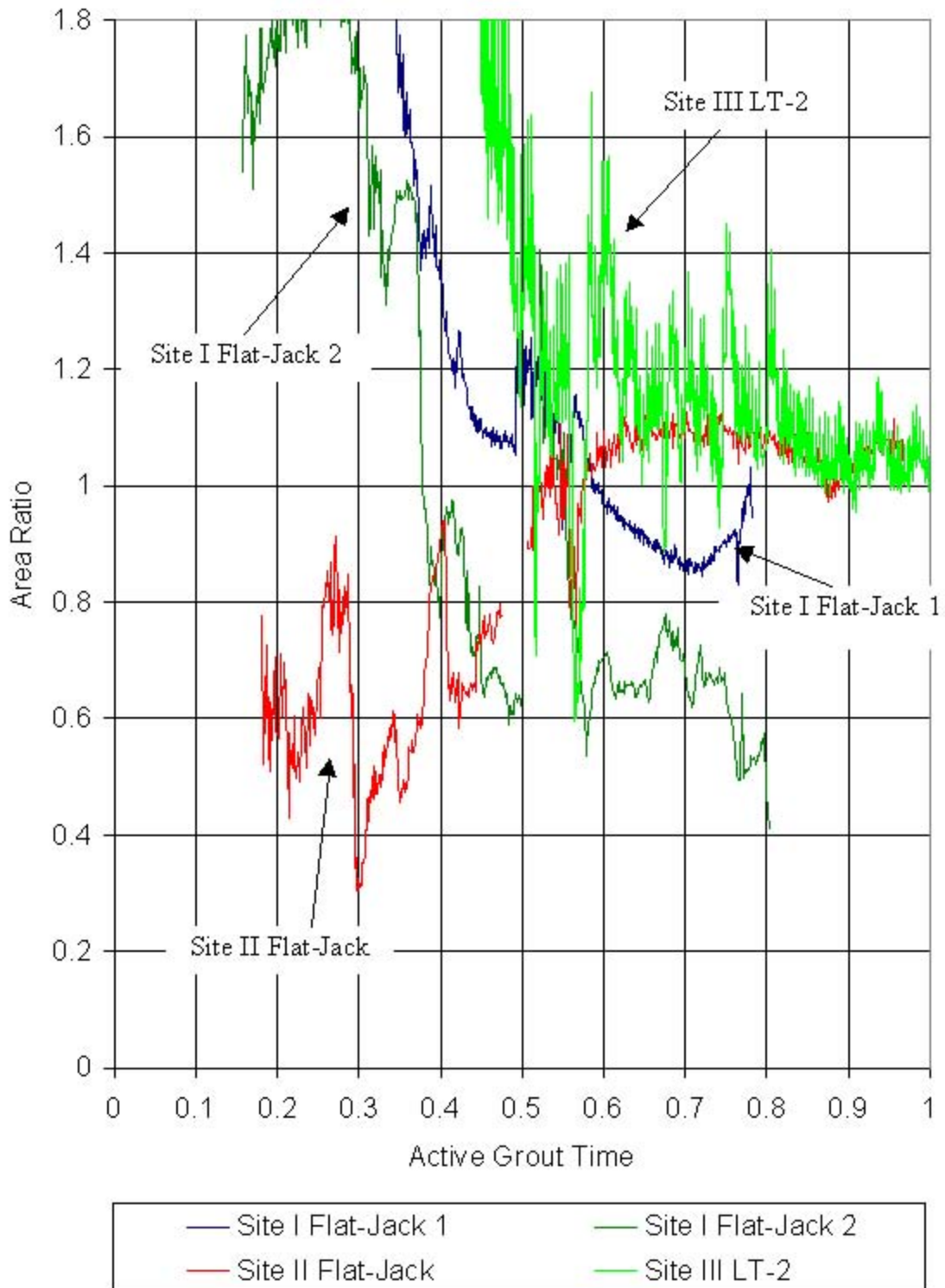


Figure 6-1. Area ratio vs. active grout time for flat-jack grouting apparatus.

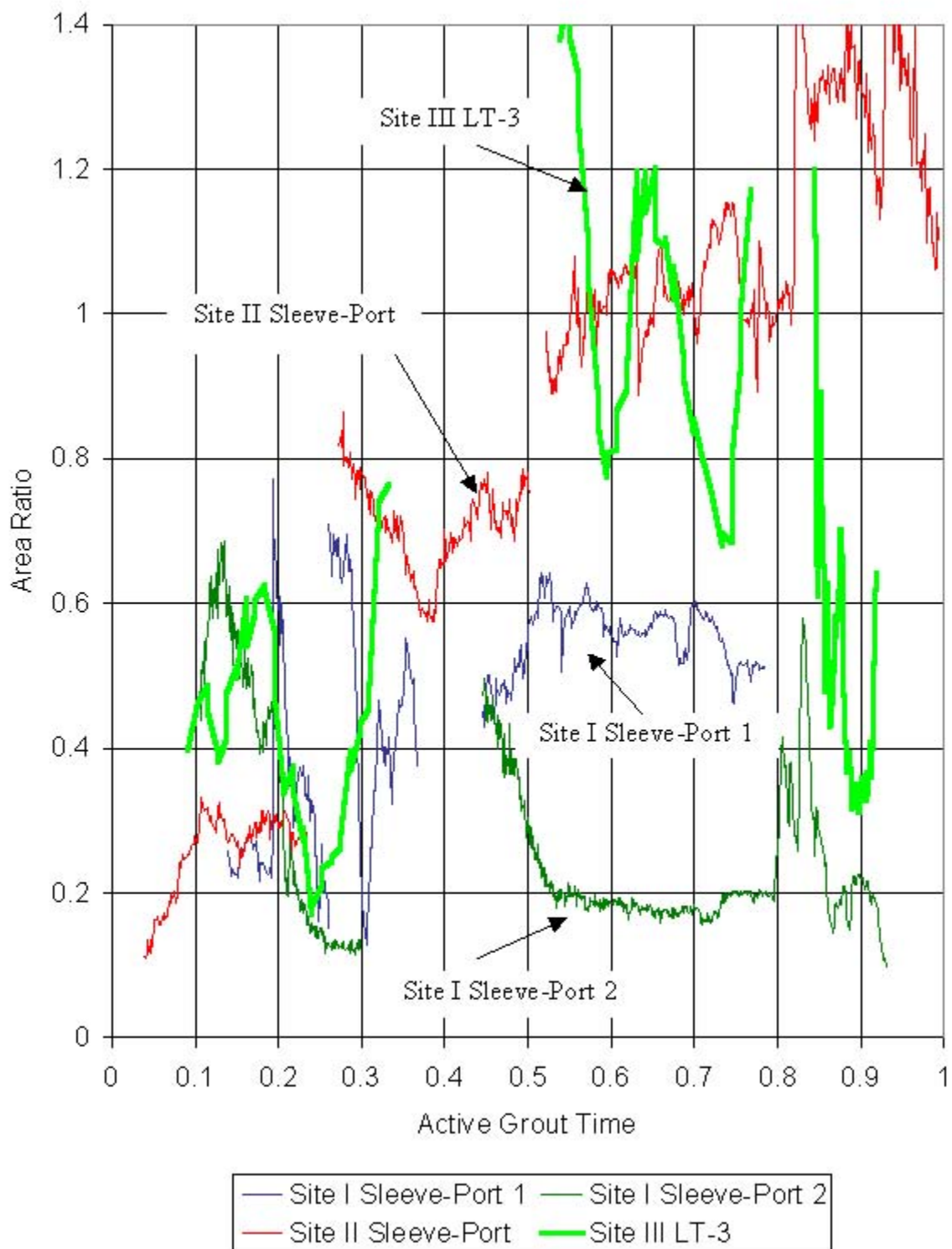


Figure 6-2. Area ratio vs. active grout time for sleeve-port grouting apparatus.

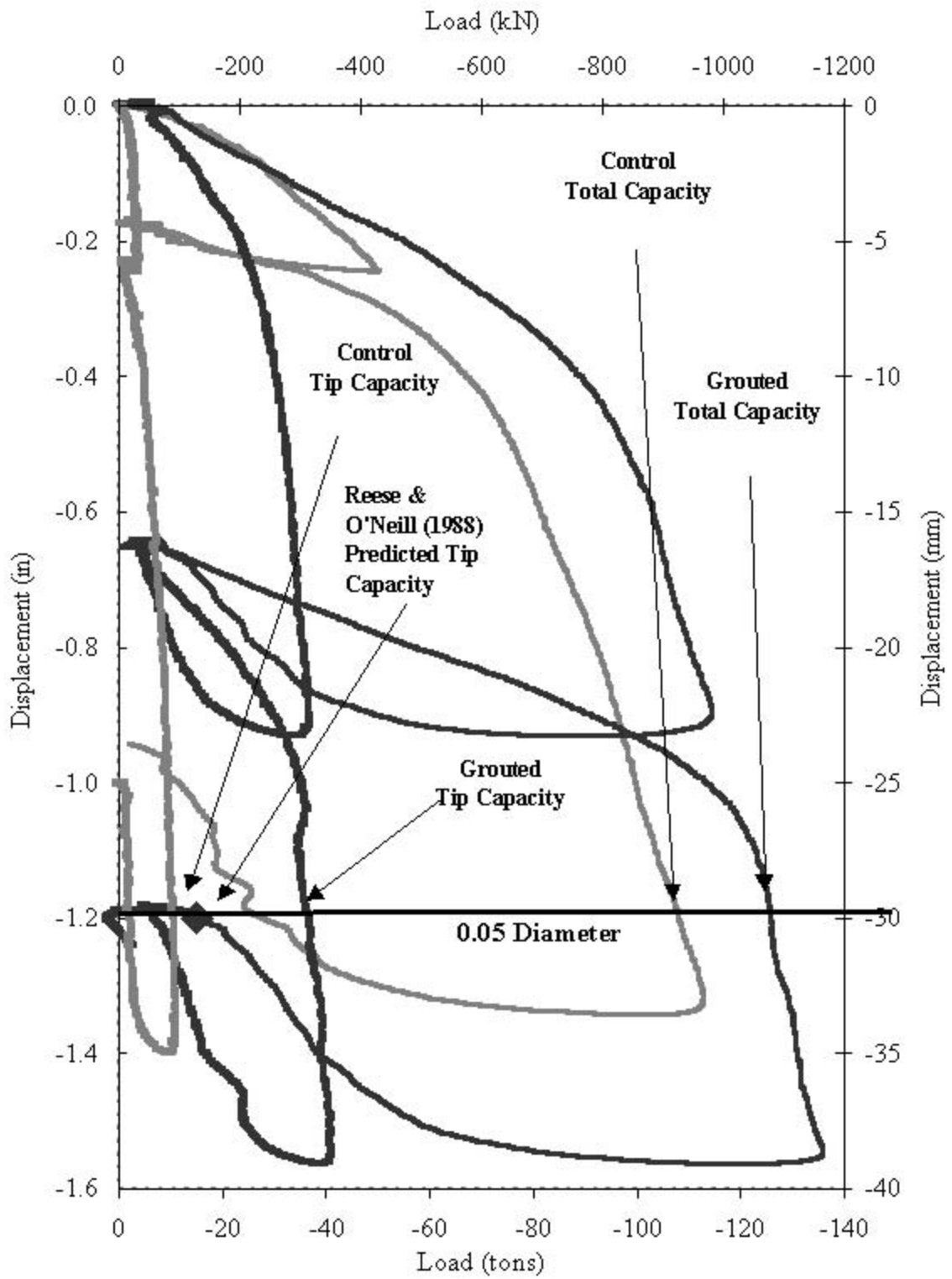


Figure 6-3. Shaft improvement example.

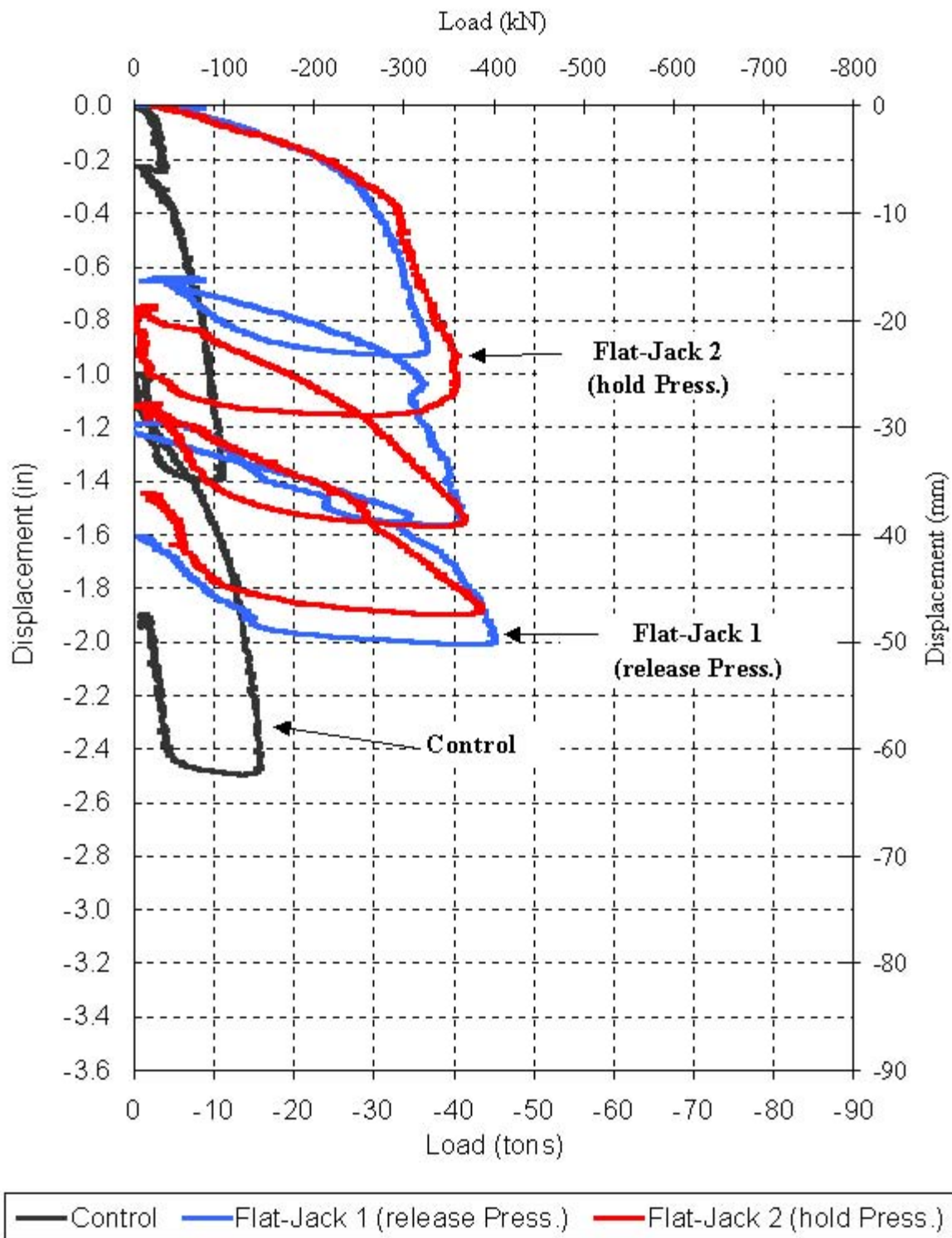


Figure 6-4. Site I Flat-Jack shaft tip load vs. top of shaft displacement.

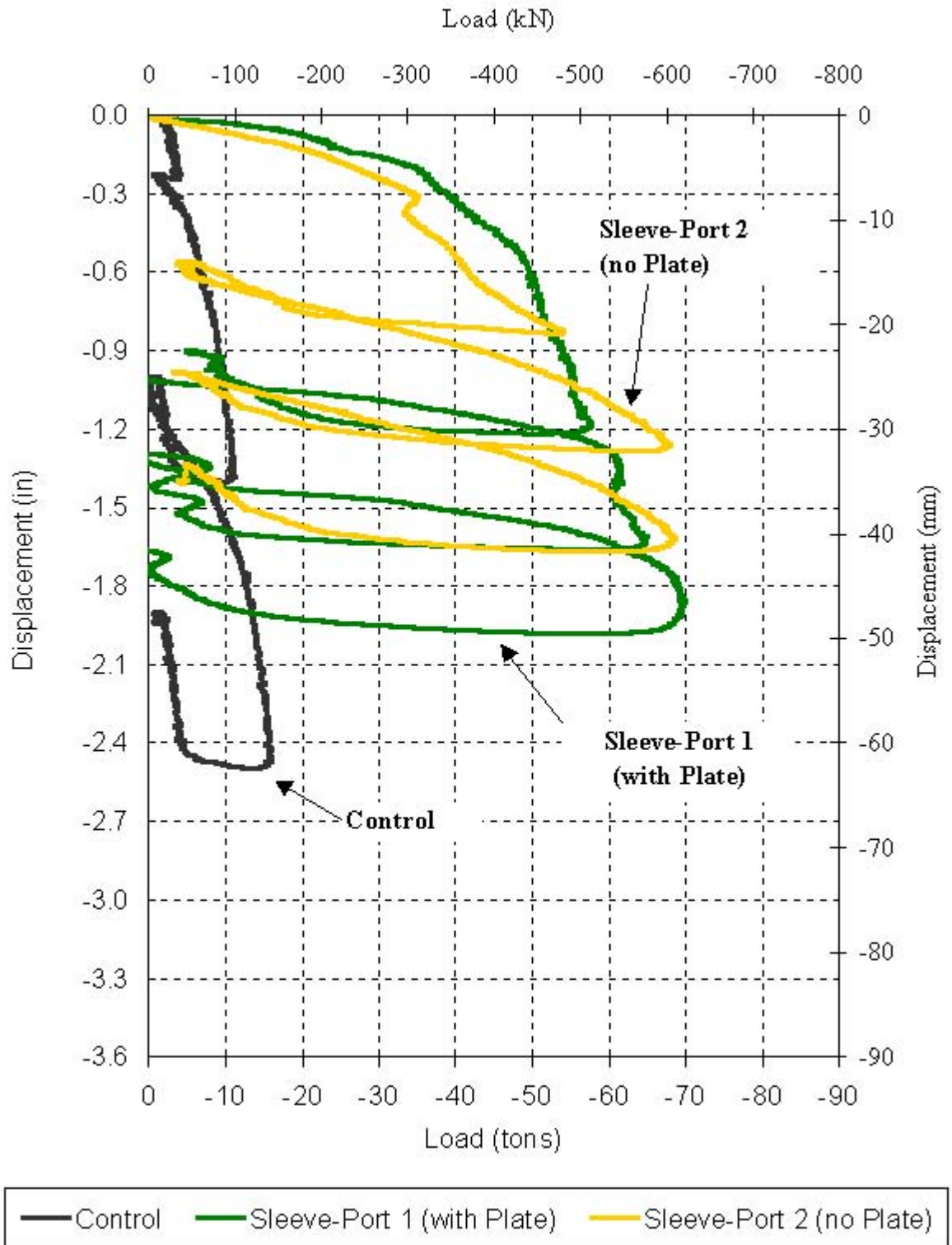


Figure 6-5. Site I Sleeve-Port shaft tip load vs. top of shaft displacement.

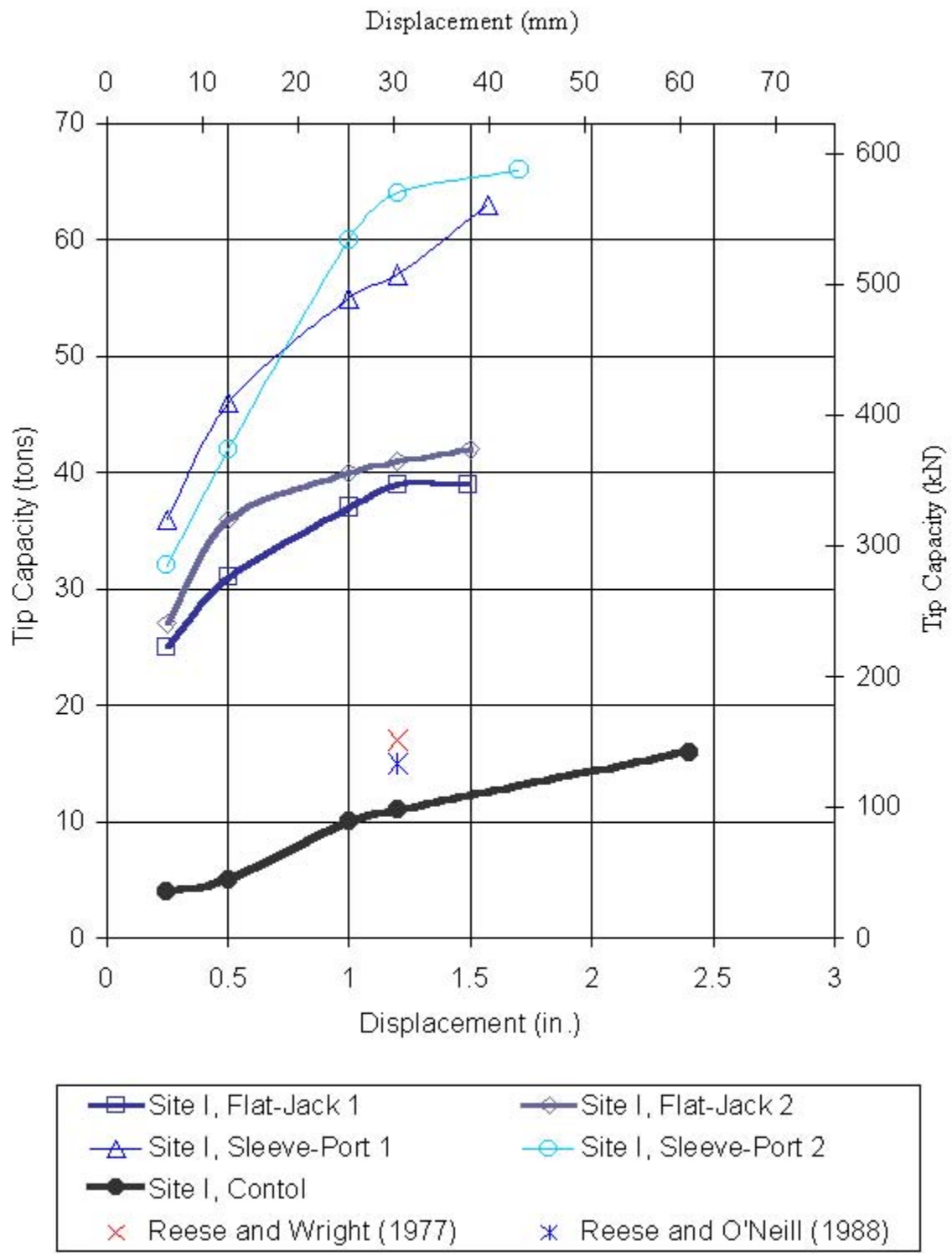


Figure 6-6. Site I tip load vs. top of shaft displacement comparisons.

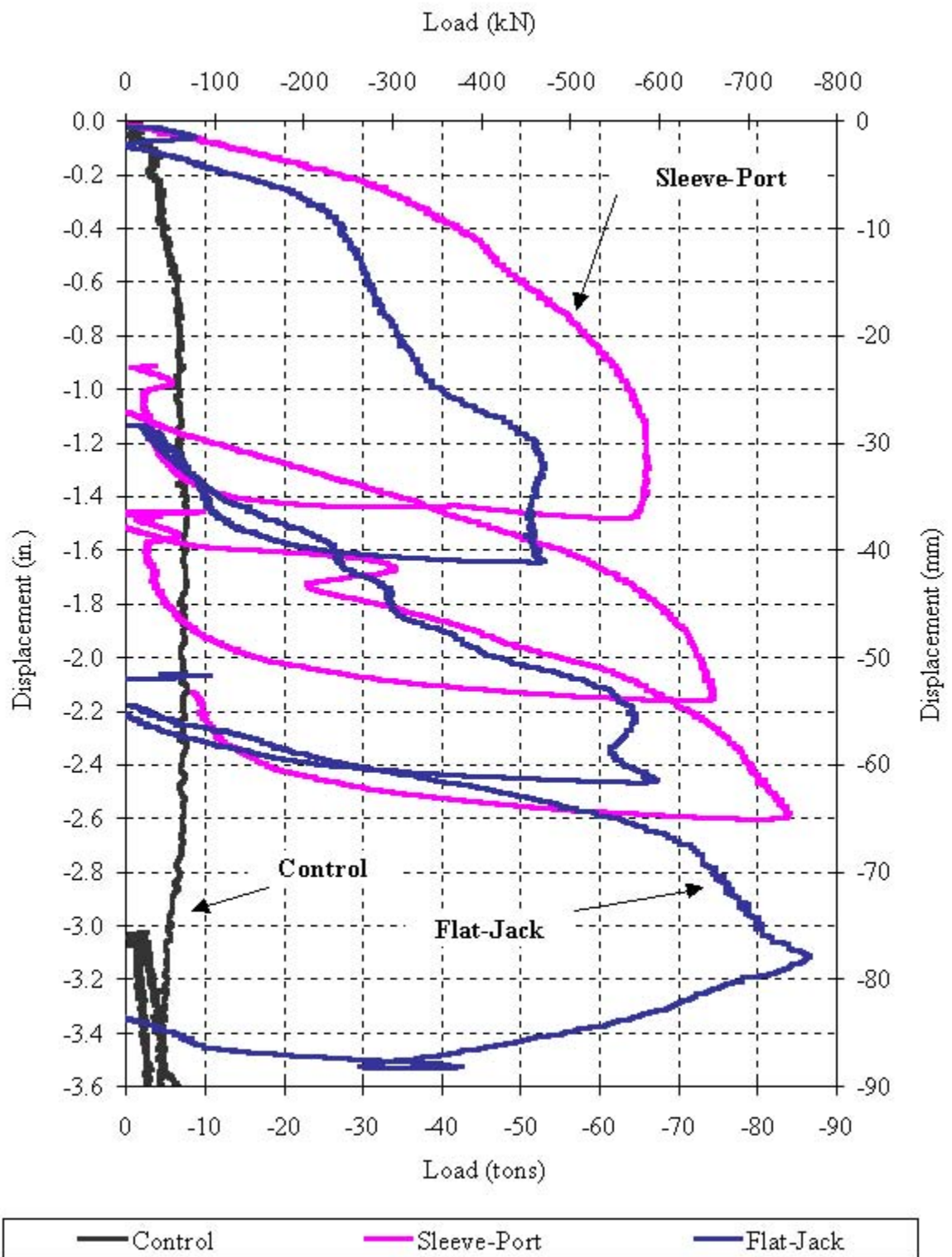


Figure 6-7. Site II shaft tip load vs. top of shaft displacement.

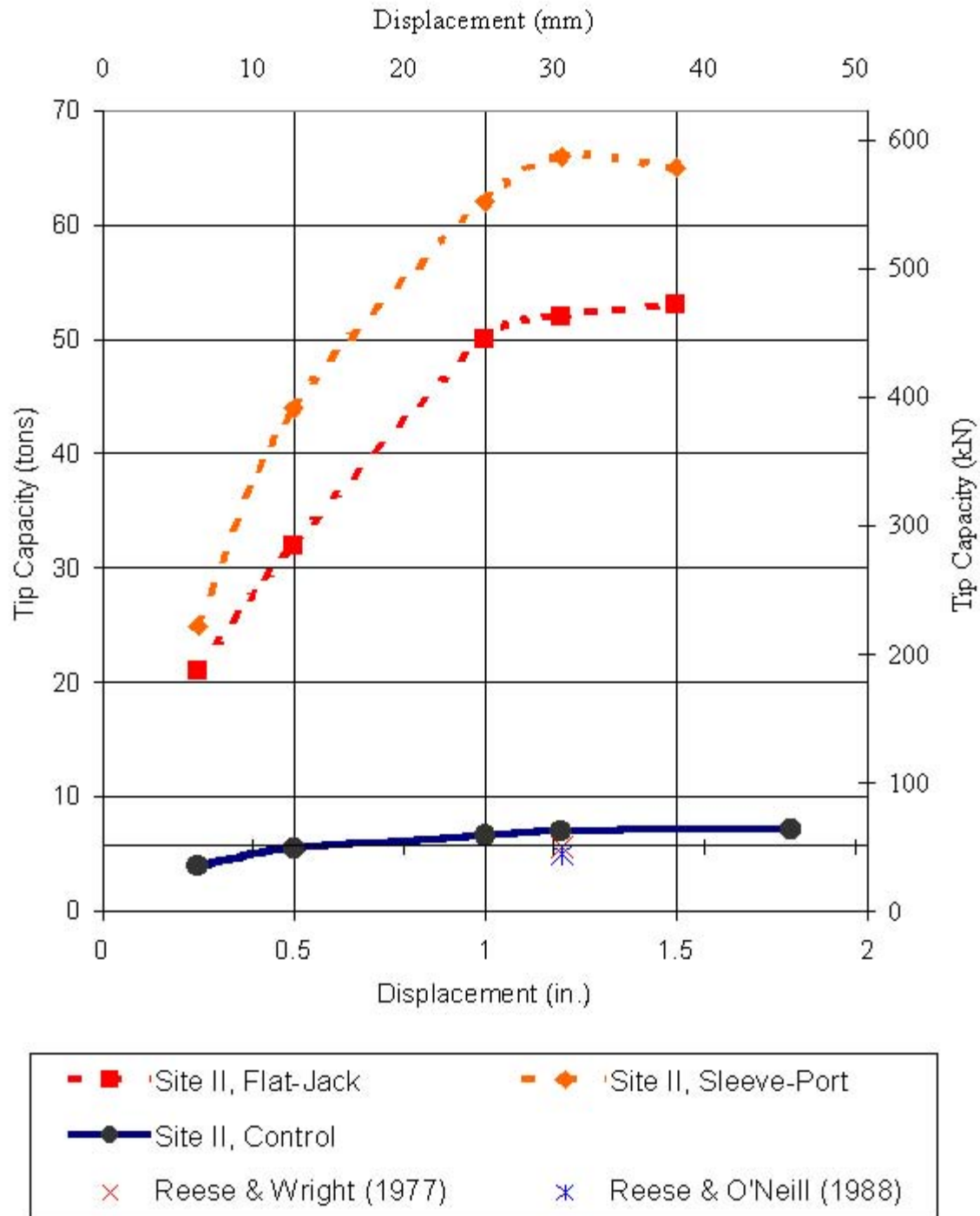


Figure 6-8. Site II tip load vs. top of shaft displacement comparisons.

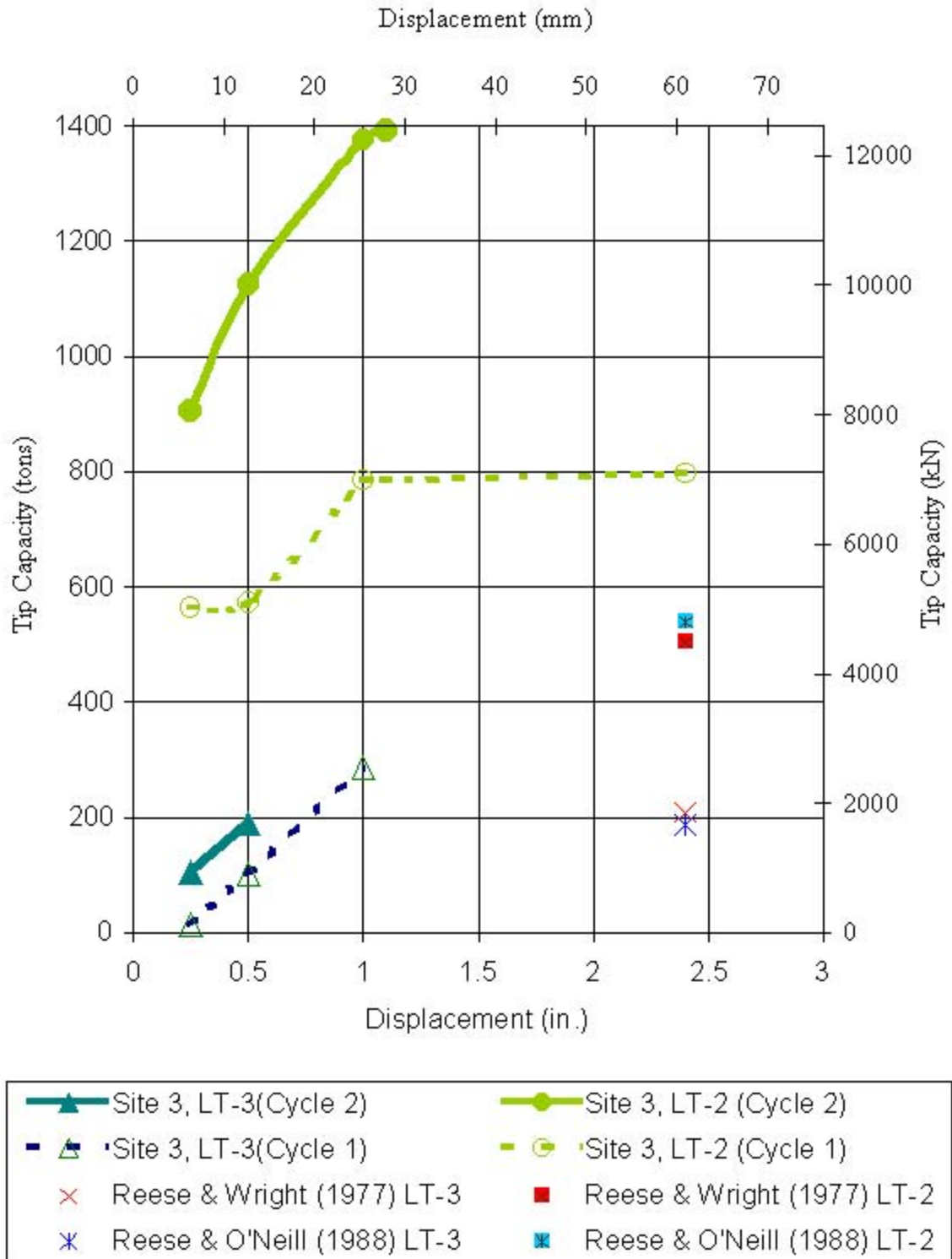


Figure 6-9. Site III tip load vs. top of shaft displacement comparisons.

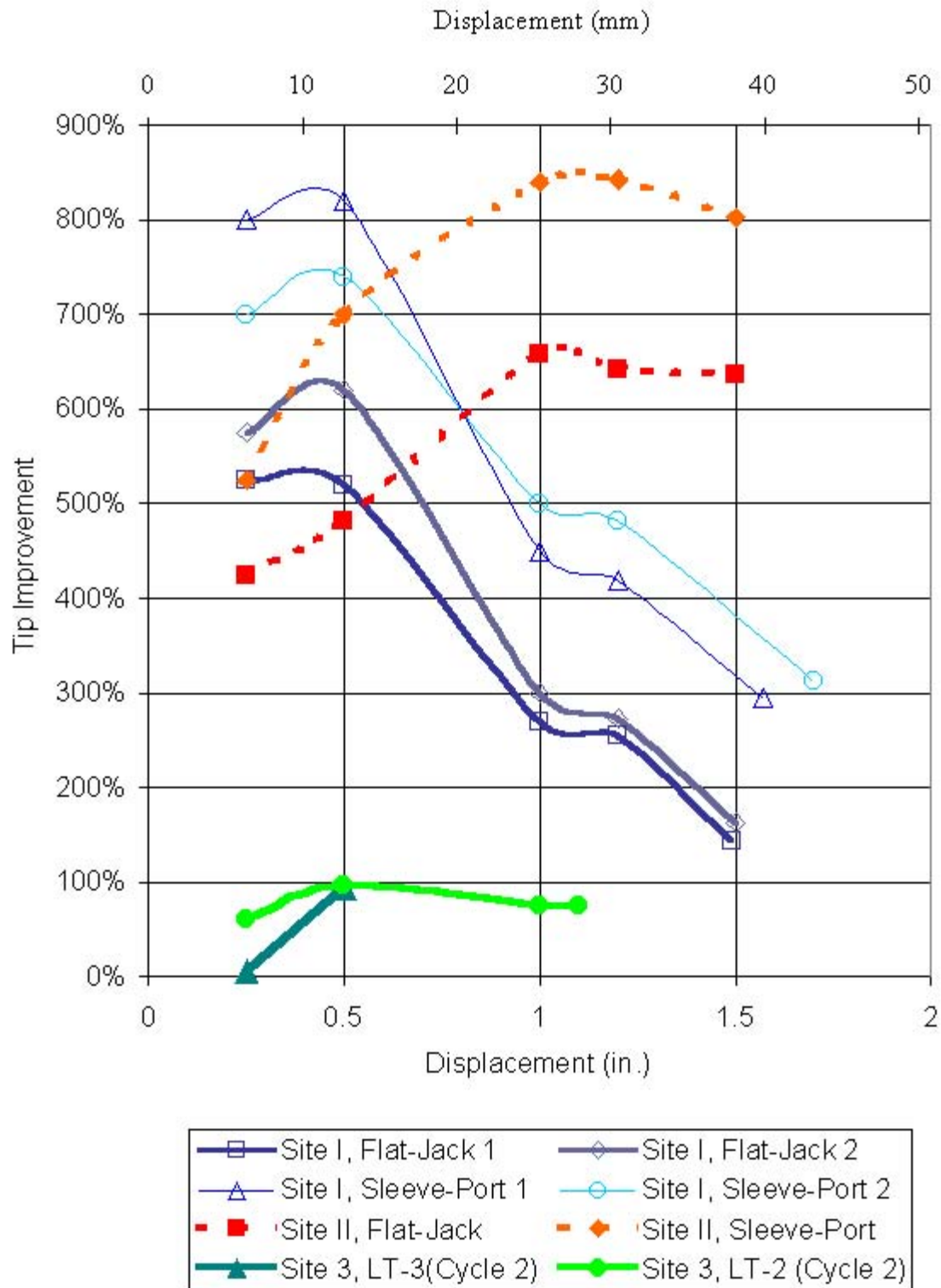


Figure 6-10. Tip capacity improvement vs. top of shaft displacement.

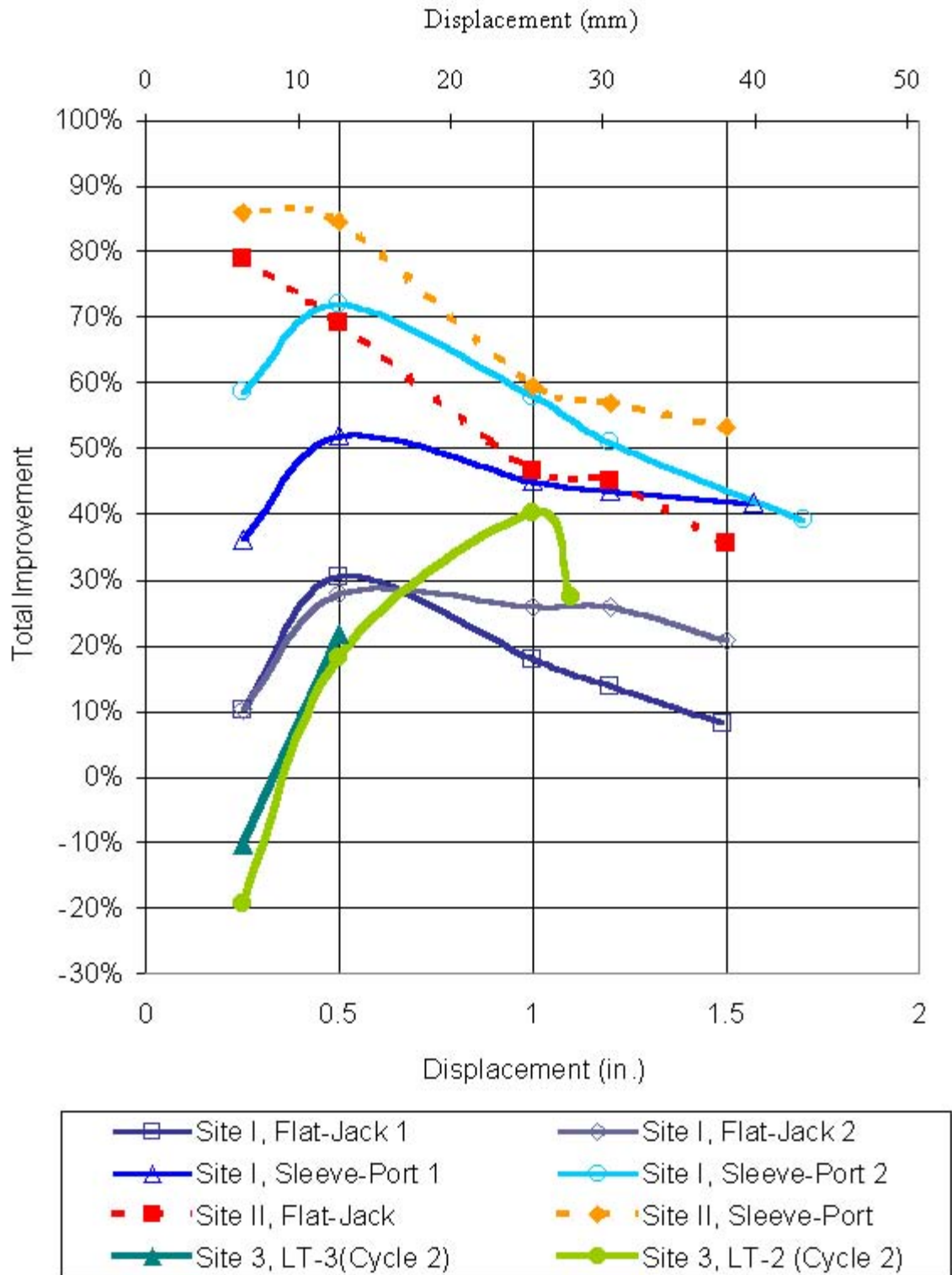


Figure 6-11. Total capacity improvement vs. top of shaft displacement.

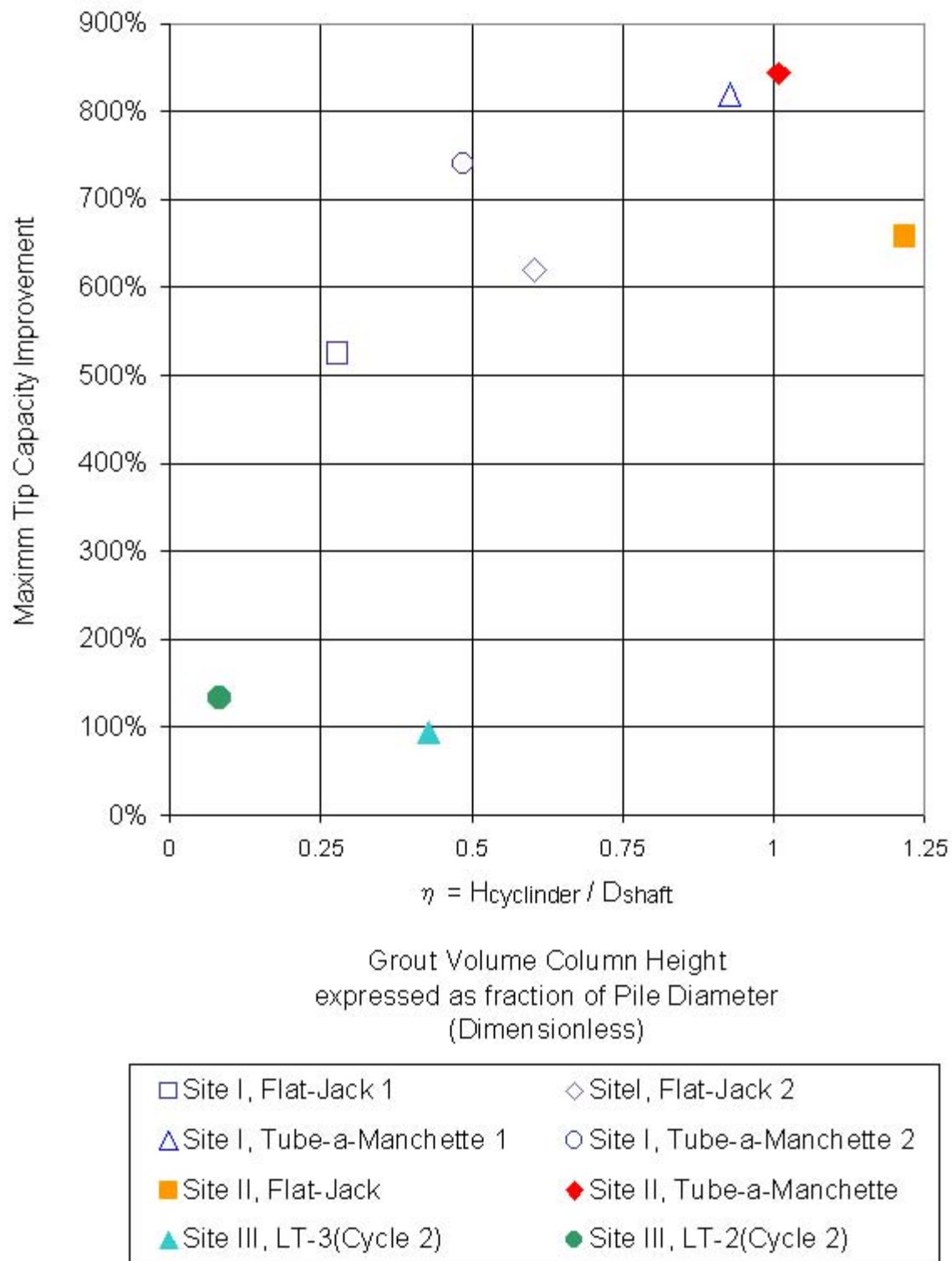


Figure 6-12. Maximum tip capacity improvement vs. dimensionless grout volume.

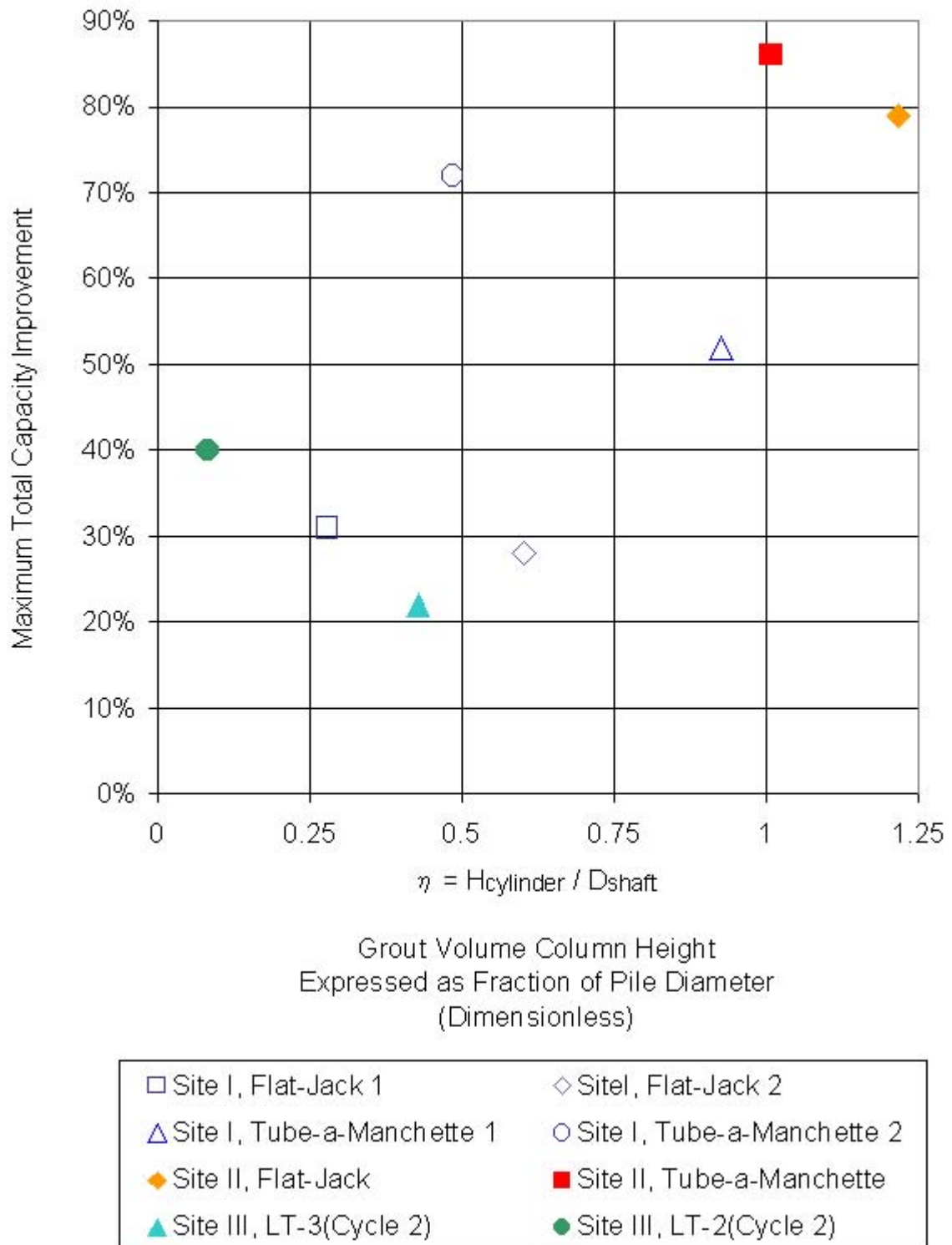


Figure 6-13. Maximum total capacity improvement vs. dimensionless grout volume.

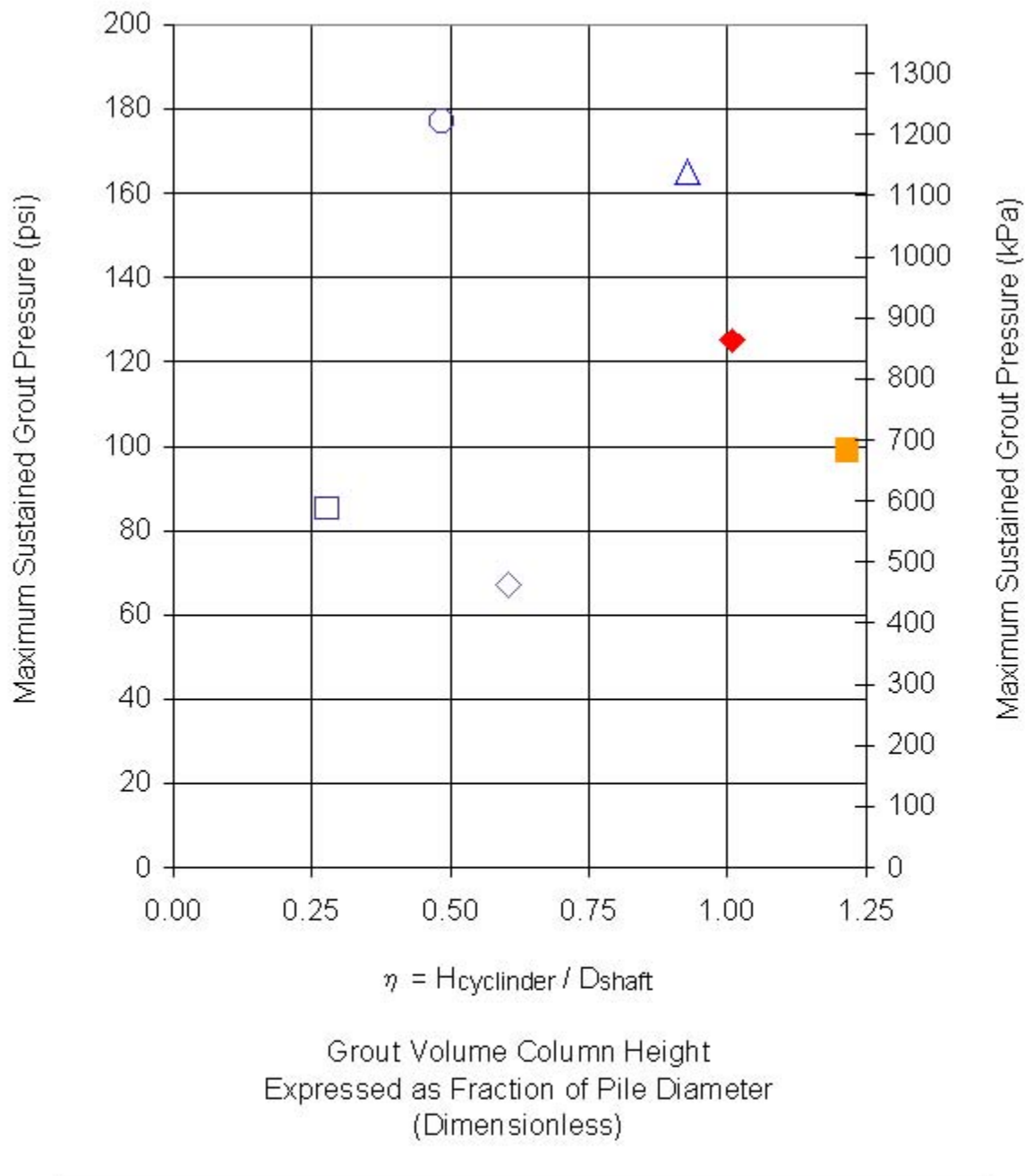


Figure 6-14. Maximum sustained grout pressure vs. dimensionless grout volume.

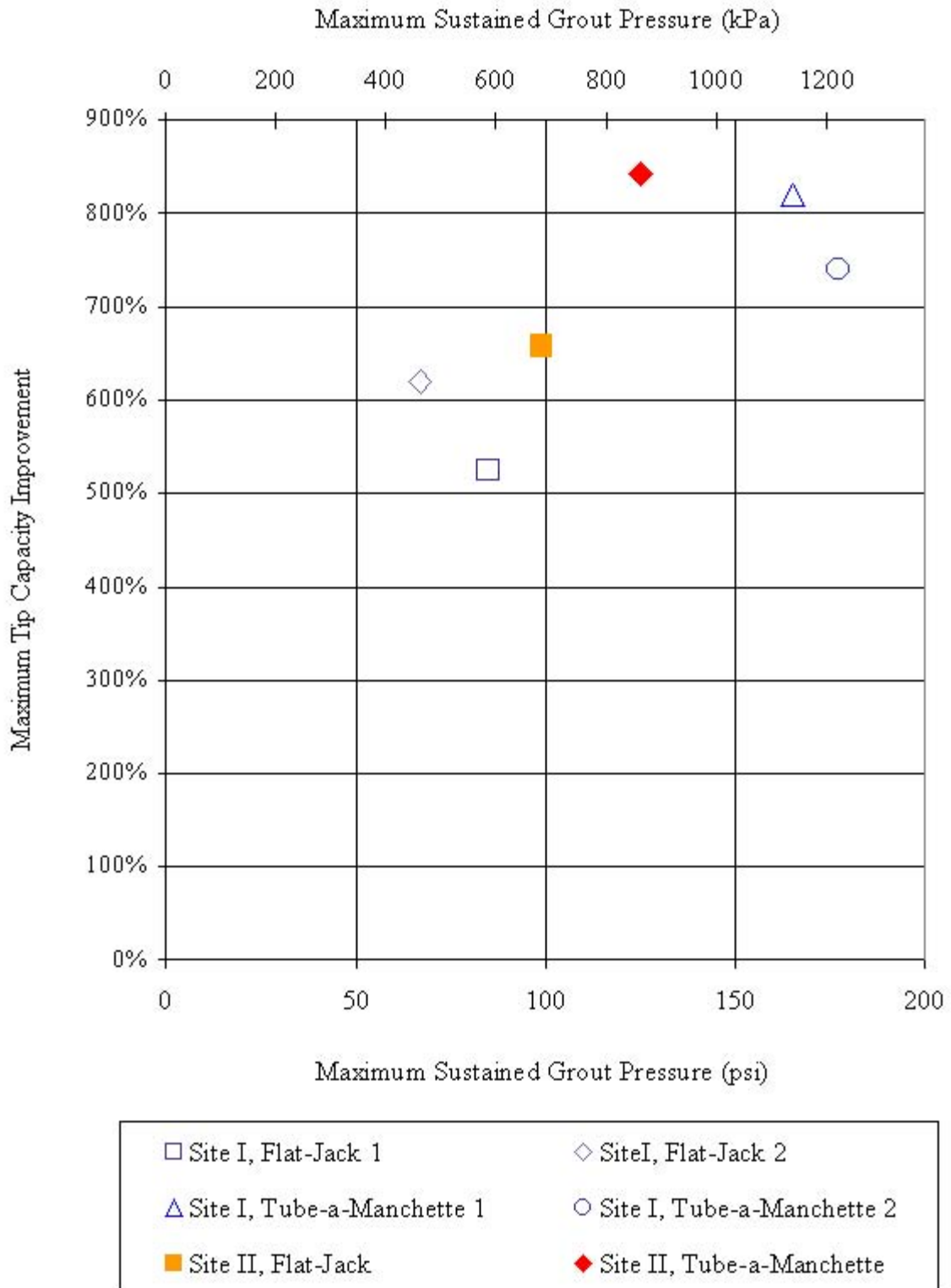


Figure 6-15. Maximum tip capacity improvement vs. maximum sustained grout pressure.

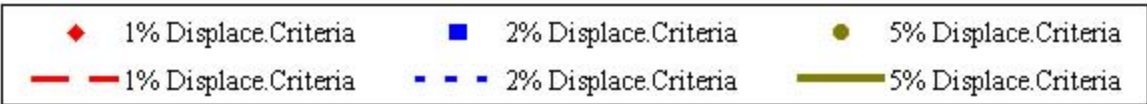
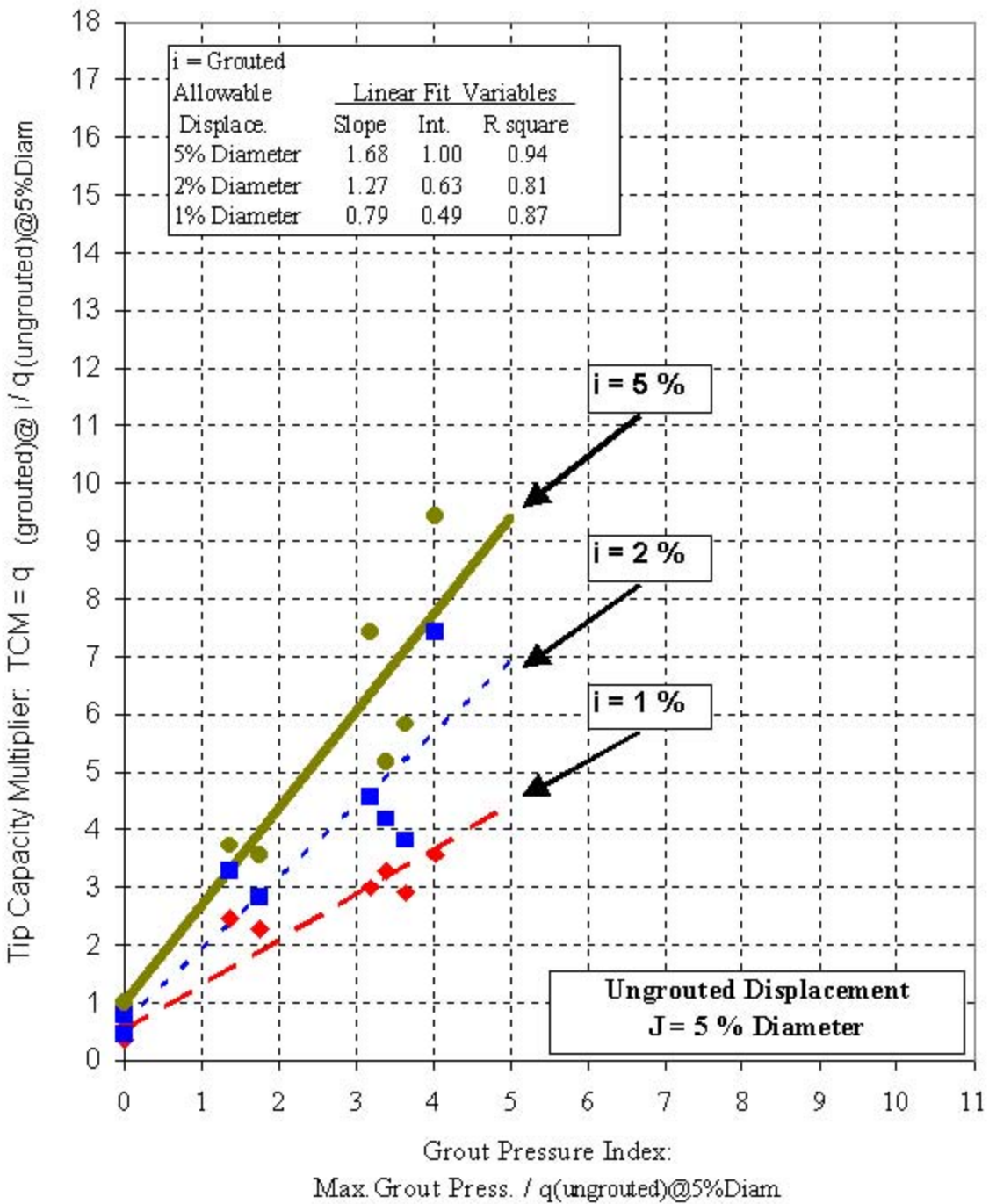


Figure 6-16. Grouted Tip Capacity Multipliers vs. Grout Pressure Index applied to ungrouted tip capacities at 5% diameter displacement.

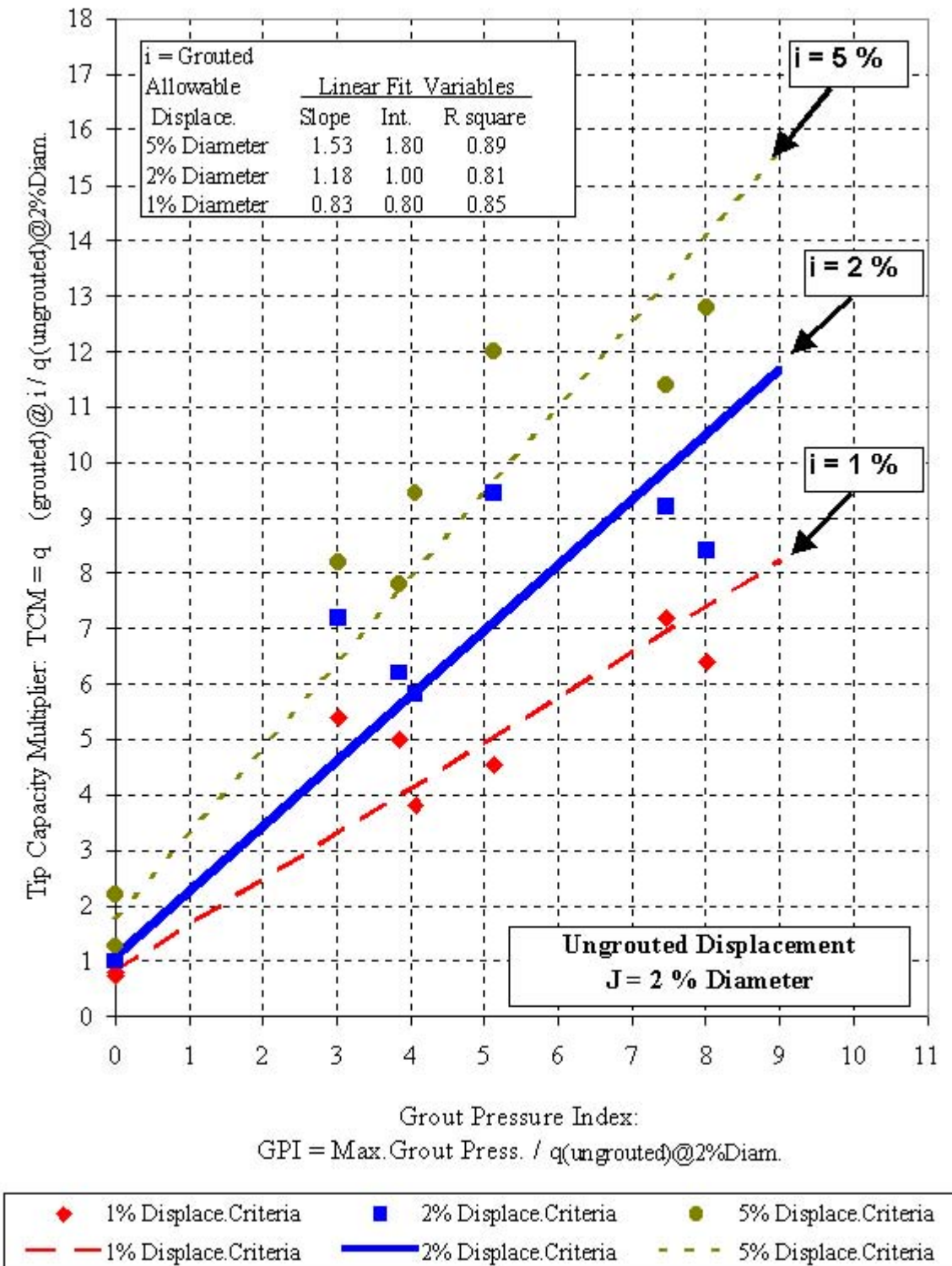


Figure 6-17. Grouted Tip Capacity Multipliers vs. Grout Pressure Index applied to ungrouted tip capacities at 2 % diameter displacement.

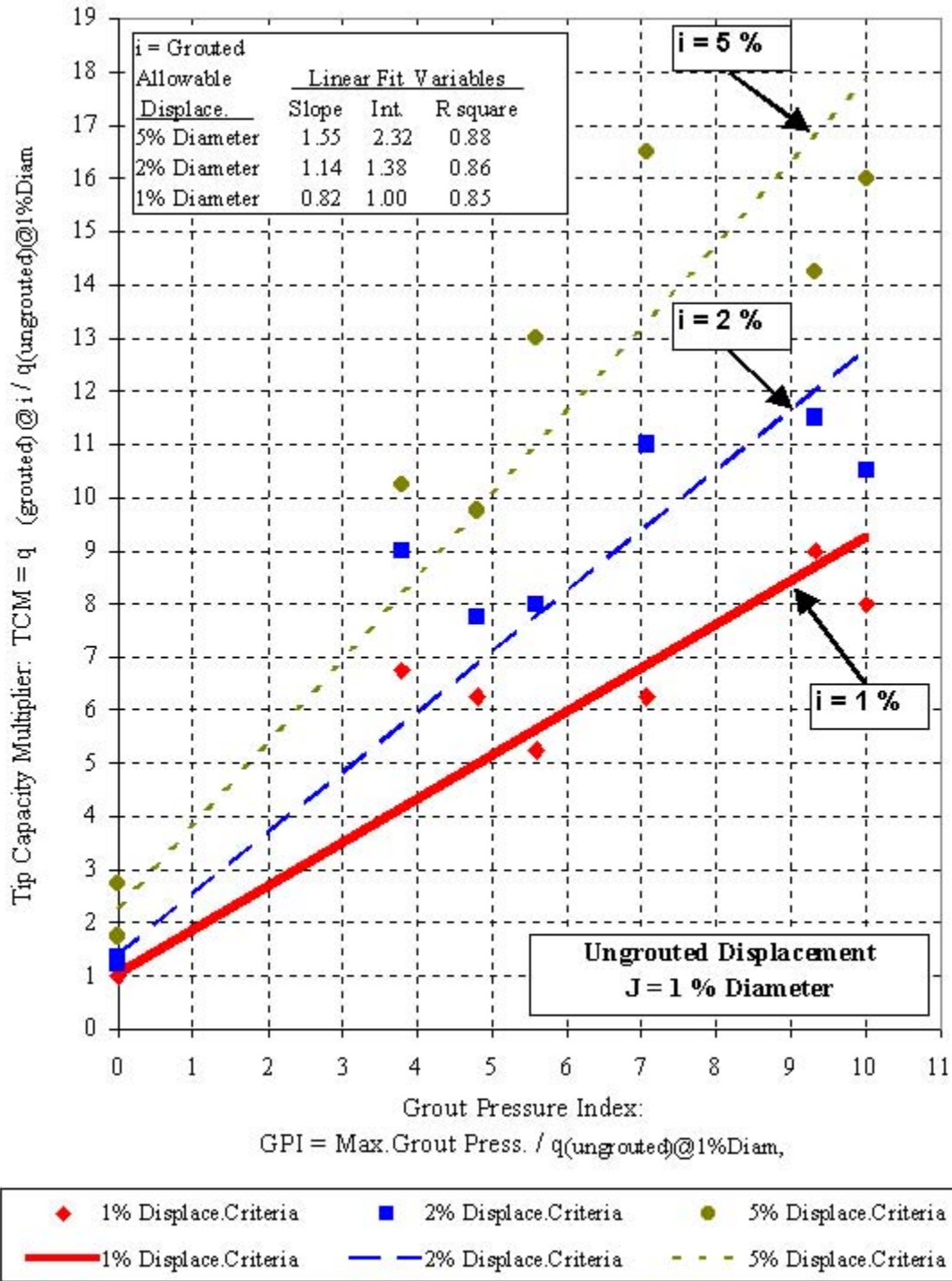


Figure 6-18. Grouted Tip Capacity Multipliers vs. Grout Pressure Index applied to ungrouted tip capacities at 1 % diameter displacement.

## 7. DESIGN AND CONSTRUCTION GUIDELINES

Using the correlations developed in Chapter 6 between the Tip Capacity Multiplier (TCM) and the Grout Pressure Index (GPI), a rational design procedure is presented herein for the use of post-grouted drilled shafts in sandy soils.

### 7.1 Design of Post-Grouted Tip Capacity

Many design methodologies exist for the calculation of drilled shaft tip capacities in sandy soils. For example, AASHTO (1999) presents four methods from which this determination can be made. These methods vary in the required parameters but use either SPT N values, the relative density state, and/or the depth of embedment expressed as a multiple of the diameter to calculate the end bearing capacity. An important aspect of this capacity is the displacement at which this capacity will be developed. Some methods clearly state this criterion as a percentage of the shaft diameter or as some service limit displacement (e.g. 5% of D, or 1"), while other methods do not.

Three design curves have been prepared based on present methods of calculating tip resistance of shafts in sand. These curves are compatible with methods that specify a displacement at which that tip resistance is mobilized (e.g. Reese and O'Neill, 1988; or Reese and Wright, 1977 specify a 5%D displacement). Figures 6-7, 6-8, and 6-9, shown previously, provide Tip Capacity Multipliers that can be applied to the original ungrouted tip resistance for designated displacements in terms of the shaft diameter of 1%D, 2%D, and 5%D, respectively. These linear fits are expressed by the following equation:

$$TCM = m(GPI) + b$$

where:

- TCM = tip capacity multiplier
- GPI = grout pressure index
- m = slope of the linear fit
- b = TCM intercept of linear fit (at GPI = 0)

Table 7-1, shown below, summarizes these linear fit variables shown in the previously mentioned figures, and defined by the above equation. Note that the R square value of each linear fit is also listed, indicating the precision of the fit.

Table 7-1. Linear Fit Variables of Tip Grouting Design Equations

Design Displacement	Allowable Displacement	Linear Fit Variables		
		m (slope)	b (intercept)	R square (error)
5 % Diameter (Figure 6-7)	5 % Diameter	1.68	1.00	0.94
	2 % Diameter	1.27	0.63	0.81
	1 % Diameter	0.79	0.49	0.87
2 % Diameter (Figure 6-8)	5 % Diameter	1.53	1.80	0.89
	2 % Diameter	1.18	1.00	0.81
	1 % Diameter	0.83	0.80	0.85
1 % Diameter (Figure 6-9)	5 % Diameter	1.55	2.32	0.88
	2 % Diameter	1.14	1.38	0.86
	1 % Diameter	0.82	1.00	0.85

The tip grouting process relies upon the negative (or upward) side shear capacity to react against the grout pressure applied at the shaft tip. Therefore, the aspect ratio (embedment length / diameter) of the drilled shafts should be carefully considered in order to provide the most cost efficient design. Note that potentially stringent lateral loading conditions may govern the foundation design, and may further define the shaft geometry that best supplies the capacities required (both axial and lateral).

For a given shaft diameter and embedment length, the method for estimating the unit tip resistance of grouted shafts involves the following steps:

1. Calculate the *ungROUTED* unit tip resistance of the shaft,  $q_{(\% \text{ Diam.})}$  (e.g. AASHTO, 10.8.3.4.3) and (1b) be sure to note at what displacement this value is valid (i.e. 5 % Diam.).
2. For the given shaft diameter, calculate the ultimate side shear resistance,  $S_{ult}$ , for the total length of embedded shaft (e.g. AASHTO 10.8.3.4.2).
3. Establish the maximum permissible service displacement as a ratio of the shaft diameter (e.g. 1 in. Disp. / 48 in. Diam. \* 100 % = 2 % Diam.).

4. Divide the ultimate shear resistance by the cross-sectional area of the shaft to determine the maximum available pressure that can be resisted by the grouting.

$$P_{\max} = S_{\text{ult}} / A_{\text{x-sec}}$$

5. Calculate the Grout Pressure Index as the ratio of the maximum available grout pressure (step 4) to the *ungrouded* unit tip resistance (step 1).

$$\text{GPI} = P_{\max} / q_{(\% \text{Diam.})}$$

6. Determine the Tip Capacity Multiplier given the Grout Pressure Index (step 5) using the equation below with appropriate linear fit values (m and b) from Table 7-1, or use the design curves generated from these equations as shown in Figures 6 - 7 through 6 - 9. Designated displacements are those from step 1(b), and allowable displacements are those from step (3).

$$\text{TCM} = m(\text{GPI}) + b$$

7. Estimate the grouted unit tip resistance as the product of the Tip Capacity Multiplier (step 6) and the ungrouted unit tip resistance (step1).

$$q_{\text{grouted}} = \text{TCM} [q_{(\% \text{ Diam.})}]$$

## 7.2 Design Example

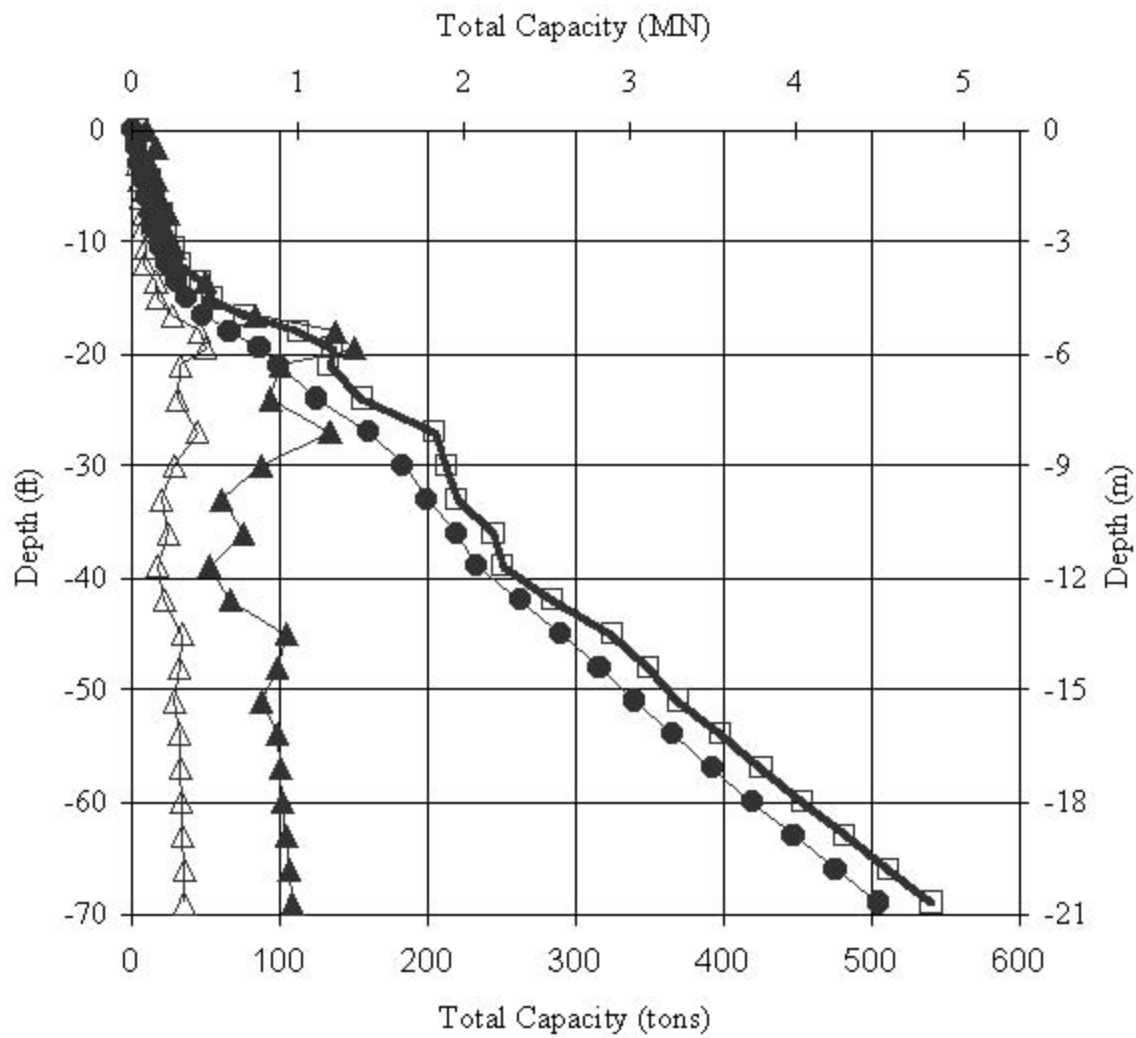
The design of the total tip capacity for grouted shafts is simply the sum of the ultimate side shear capacity and the grouted tip capacity at some specified allowable shaft displacement. Note that the side shear is assumed to develop with very little displacement, thus allowing for the use of this ultimate value. Care should be taken when specifying maximum allowable shaft uplift during grouting such that this side shear (contributing to the total capacity) is not displaced beyond a possible peak strength and into a lower residual value.

The ungrouted capacities (both side shear and end bearing) must first be determined before assessment of the tip grouting improvement can be made. Any method of predicting these capacities can be utilized in conjunction with the tip grouting improvement relationships presented herein. If actual load test data is available, or can be conducted, this data may be used in lieu of any prediction equations with more accuracy.

Given a capacity requirement, and tolerable shaft displacement at this specified load, the length of a tip grouted shaft (tipped in sand) capable of meeting these load displacement requirement can be determined. As the grouted capacity improvements are based upon the best linear fit of a limited number of shafts tested in this study, caution and engineering judgement is warranted in using the full values of the grouted tip capacity obtained from the procedure presented herein. For the example to follow, the design equation of Reese and Wright (1977) will be utilized to predict both the side shear and ungrouted end bearing capacities (step 1b. of Section 7.1) of a 2.0 ft (0.61 m) diameter shaft. Note that this design equation predicts the bearing capacity at a displacement of 1.2 inch (30.5 mm), which is 5% of the shaft diameter (step 1b. of Section 7.1). These capacities will be based upon the standard penetration testing (SPT) “N” values shown in Table 7-2. Also shown in Table 7-2 is the numerical values of these calculations as the depth of embedment is increased, note that the useable capacity is defined as the side shear added to one third (1/3) of the ultimate end bearing for a given depth of embedment. These capacities are plotted vs. depth of embedment in Figure 7-1.

Table 7-2. Example Capacity Predictions for an UngROUTed Shaft

Shaft Diameter (ft.) = 2.0					qc & qp found for SP using Rees e and Wright (1977)							
Boring Information				Side Shear Capacity			End Bearing Capacity			Total Capacity		
Depth		N	Soil Type (USCS)	Section Length (ft.)	qc (unit shear) (TSF)	Section (tons)	Cumulative (tons)	qp (unit bearing) (TSF)	Ultimate (tons)	(1/3) Ultimate (tons)	Ultimate (tons)	Useable (tons)
(ft)	(m)											
0.00	0.00	5	SM	1.5	0.147	1	1	3.333	10	3	12	5
-1.50	-0.46	8	SP-SM	1.5	0.235	2	4	5.333	17	6	20	9
-3.00	-0.91	6	SP-SM	1.5	0.176	2	5	4.000	13	4	18	9
-4.50	-1.37	8	SP-SM	1.5	0.235	2	7	5.333	17	6	24	13
-6.00	-1.83	9	SP-SM	1.5	0.265	2	10	6.000	19	6	29	16
-7.50	-2.29	12	SP-SM	1.5	0.353	3	13	8.000	25	8	38	22
-9.00	-2.74	11	SP-SM	1.5	0.324	3	16	7.333	23	8	39	24
-10.50	-3.20	14	SP-SM	1.5	0.412	4	20	9.333	29	10	50	30
-12.00	-3.66	13	SP-SM	1.5	0.382	4	24	8.667	27	9	51	33
-13.50	-4.11	24	SP-SM	1.5	0.706	7	30	16.000	50	17	81	47
-15.00	-4.57	25	SP-SM	1.5	0.735	7	37	16.667	52	17	90	55
-16.50	-5.03	40	SP-SM	1.5	1.176	11	49	26.667	84	28	132	76
-18.00	-5.49	66	SP-SM	1.5	1.941	18	67	44.000	138	46	205	113
-19.50	-5.94	72	SP-SM	1.5	2.118	20	87	48.000	151	50	238	137
-21.00	-6.40	48	SP-SM	1.5	1.412	13	100	32.000	101	34	201	134
-24.00	-7.32	45	SP-SM	3	1.324	25	125	30.000	94	31	219	156
-27.00	-8.23	64	SP-SM	3	1.882	35	160	42.667	134	45	295	205
-30.00	-9.14	42	SP-SM	3	1.235	23	184	28.000	88	29	272	213
-33.00	-10.06	29	SP-SM	3	0.853	16	200	19.333	61	20	261	220
-36.00	-10.97	36	SP-SM	3	1.059	20	220	24.000	75	25	295	245
-39.00	-11.89	25	SP-SM	3	0.735	14	234	16.667	52	17	286	251
-42.00	-12.80	32	SP-SM	3	1.553	29	263	21.333	67	22	330	285
-45.00	-13.72	50	SP-SM	3	1.471	28	291	33.333	105	35	395	326
-48.00	-14.63	47	SP-SM	3	1.382	26	317	31.333	98	33	415	350
-51.00	-15.54	42	SP-SM	3	1.235	23	340	28.000	88	29	428	369
-54.00	-16.46	47	SP-SM	3	1.382	26	366	31.333	98	33	465	399
-57.00	-17.37	48	SP-SM	3	1.412	27	393	32.000	101	34	493	426
-60.00	-18.29	49	SP-SM	3	1.441	27	420	32.667	103	34	522	454
-63.00	-19.20	50	SP-SM	3	1.471	28	448	33.333	105	35	552	482
-66.00	-20.12	51	SP-SM	3	1.500	28	476	34.000	107	36	583	511
-69.00	-21.03	52	SP-SM	3	1.529	29	505	34.667	109	36	614	541



Generated from Boring SPT Values,  
 Ungrouned Tip Capacity Calculated at 1.2 inches Displacement  
 (5% of 2 ft. Shaft Diameter)

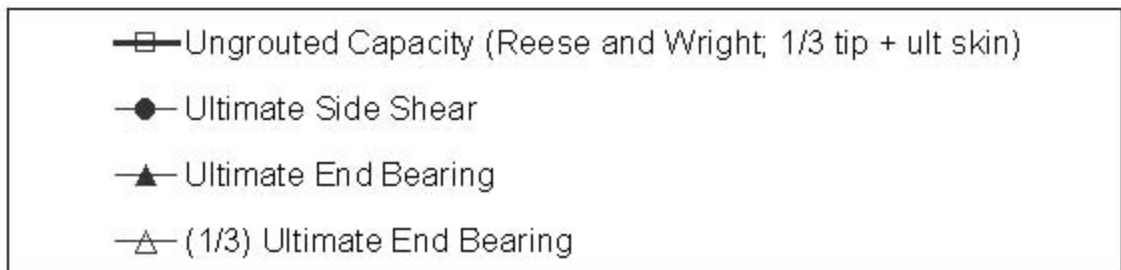


Figure 7-1. Example capacity predictions for an ungrouted shaft.

The grouted shaft capacity can now be determined based upon the information obtained from the analysis of the ungrouted shaft utilizing the tip grouting capacity improvement relationships presented. The maximum grout pressure that can be expected for a given depth of embedment is simply the side shear divided by the shaft tip area (step 4. of Section 7.1). Note that as the side shear increases with the depth of embedment, so does the grout pressure that can be reacted against by this side shear. Figure 7-2 shows the relationship of max grout pressure possible for the example calculation increasing with depth. Three scenarios are investigated for our example calculations:

1. No grout pressure limit (based on ult skin reaction), 2232 psi (15.4 MPa)
2. Grout pressure limited to 1000 psi (6.90 MPa)
3. Grout pressure limited to 300 psi (2.07 MPa)

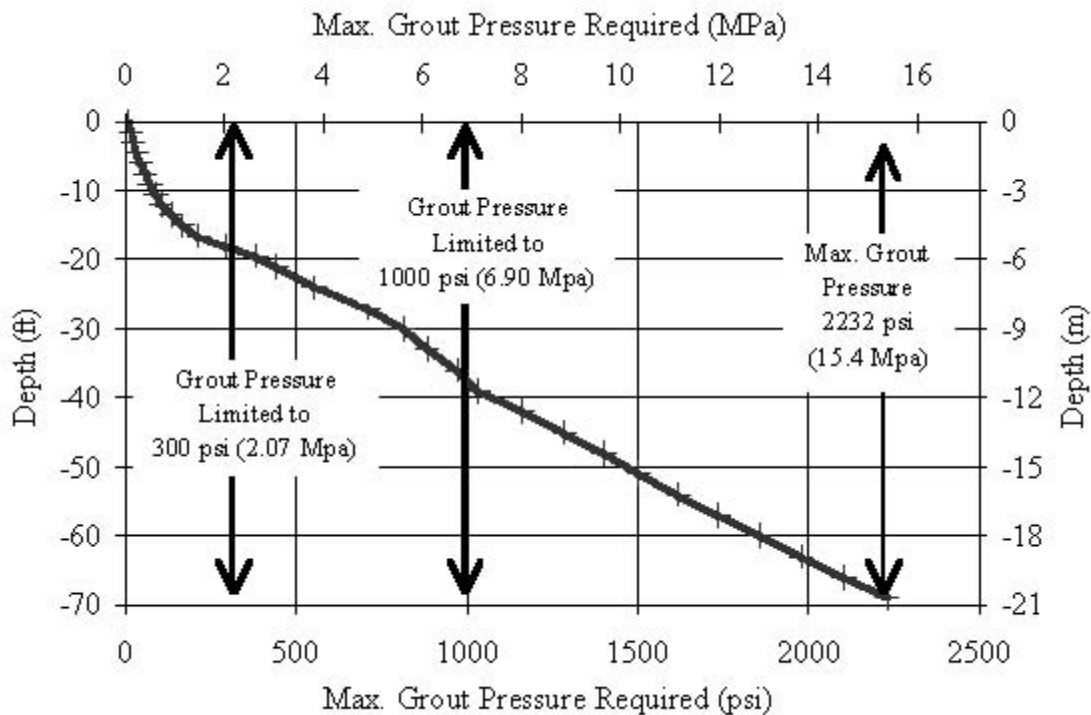


Figure 7-2. Example calculation of maximum grout pressure vs. depth of embedment.

Most helical style grout pumps should be able to achieve 200-300 psi max. The standard post grouting pumps are positive displacement (piston-type) which should have no problem achieving 1000 to 2000 psi.

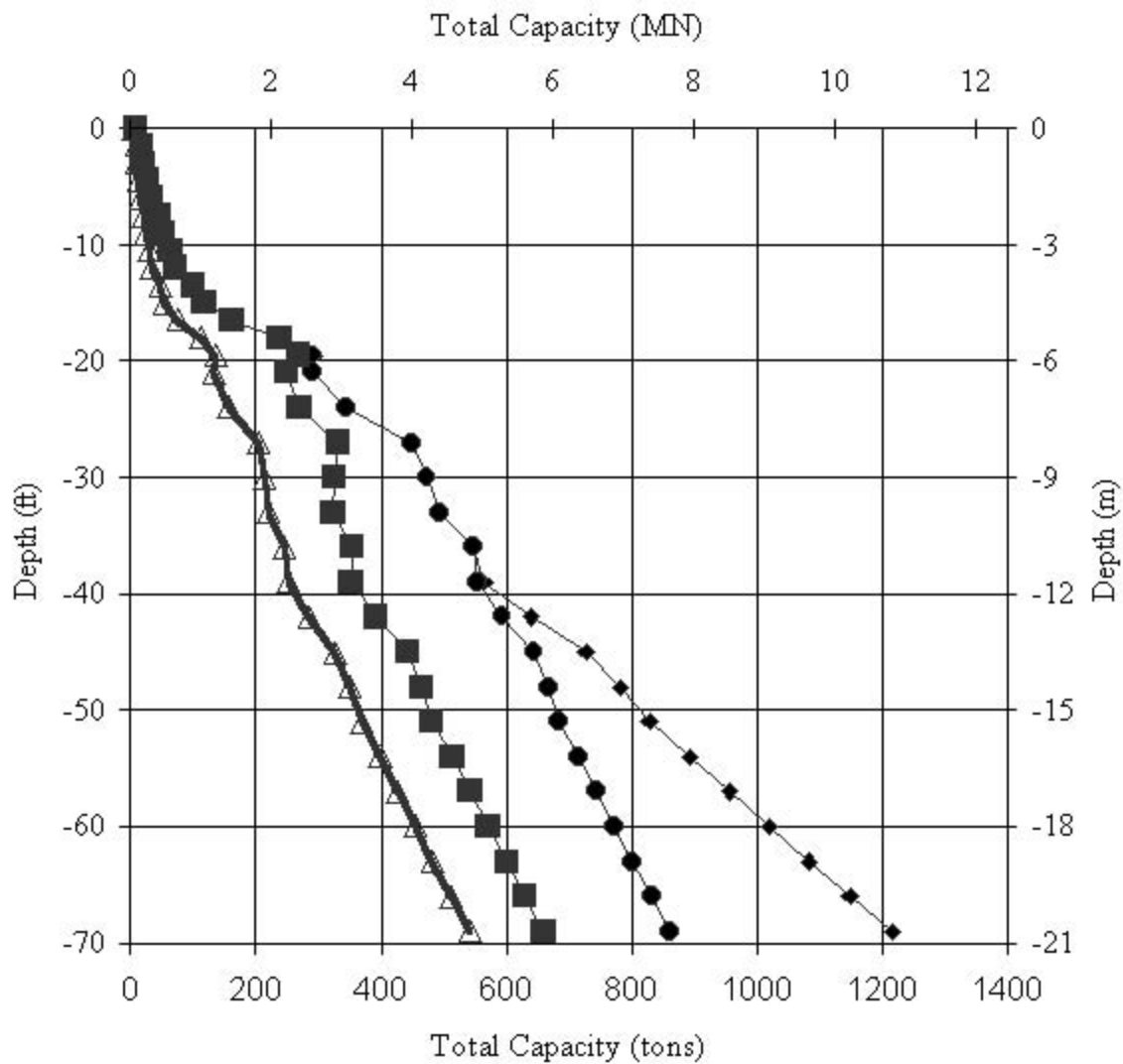
Numerical values of the example calculations, discussion to follow, are shown in Table 7-3, and plotted vs. depth of embedment in Figure 7-3. Note that an allowable shaft displacement of 0.5 inches (12.7 mm), which is 2 % of the shaft diameter, is specified (step 3. of Section 7.1).

The Grout Pressure Index (GPI) is calculated as the ratio of the grout pressure to the unit end bearing calculated for the ungrouted shaft (step 5. of Section 7.1). Note that our example calculation utilized the method of Reese and Write (1977) which made these predictions for a shaft displacement of 5 % of the shaft diameter. Therefore, the Tip Capacity Multiplier (TCM) will be determined for the GPI calculated (step 6. of Section 7.1) based upon the 5 % design relationships presented herein as Figure 6-16. The Tip Capacity Multiplier (TCM) utilized within this Figure will be that for the 2 % diameter allowable displacement of the tip grouted shaft. These values for the linear fits of these relationships were tabulated in Table 6-1, and are the following for our example calculation:  $m$  (slope) = 1.27, and  $b$  (intercept) = 0.63

The grouted tip resistance can then be determined as the Tip Capacity Multiplier times the ungrouted tip capacity (step 7 of Section 7.1). Note that for this example the ungrouted tip capacity utilized in the above step is that which was calculated by the method of Reese and Write (1977) for a 5 % diameter displacement, while the resulting grouted tip capacity is that developed at a 2 % diameter displacements. The total grouted shaft capacity then is this grouted tip capacity added to the respective side shear capacity at that depth.

Table 7-3. Example Calculation of Grouted Shaft Capacity

Max. Grout Pressure 2232 psi					Grout Pressure Limit 1000 psi					Grout Pressure Limit 300 psi				
Grout Pressure (psi)	GPI = Press./qp(5%)	TCM (2%D.Allow.Disp.)	Grouted Tip Cap. (2% D.) (tons)	Total Capacity (2% D.) (tons)	Grout Pressure (psi)	GPI = Press./qp(5%)	TCM (2%D.Allow.Disp.)	Grouted Tip Cap. (2% D.) (tons)	Total Capacity (2% D.) (tons)	Grout Pressure (psi)	GPI = Press./qp(5%)	TCM (2%D.Allow.Disp.)	Grouted Tip Cap. (2% D.) (tons)	Total Capacity (2% D.) (tons)
16	0.22	0.90	15	19	16	0.22	0.90	15	19	16	0.22	0.90	15	19
23	0.42	1.16	15	20	23	0.42	1.16	15	20	23	0.42	1.16	15	20
33	0.45	1.20	20	28	33	0.45	1.20	20	28	33	0.45	1.20	20	28
44	0.53	1.30	25	35	44	0.53	1.30	25	35	44	0.53	1.30	25	35
59	0.53	1.30	33	46	59	0.53	1.30	33	46	59	0.53	1.30	33	46
72	0.71	1.53	35	52	72	0.71	1.53	35	52	72	0.71	1.53	35	52
90	0.69	1.51	44	64	90	0.69	1.51	44	64	90	0.69	1.51	44	64
105	0.88	1.74	47	71	105	0.88	1.74	47	71	105	0.88	1.74	47	71
135	0.61	1.40	70	101	135	0.61	1.40	70	101	135	0.61	1.40	70	101
166	0.72	1.54	81	118	166	0.72	1.54	81	118	166	0.72	1.54	81	118
215	0.58	1.37	114	163	215	0.58	1.37	114	163	215	0.58	1.37	114	163
295	0.48	1.24	172	239	295	0.48	1.24	172	239	295	0.48	1.24	172	239
384	0.58	1.36	205	292	384	0.58	1.36	205	292	300	0.45	1.20	181	268
443	1.00	1.89	190	291	443	1.00	1.89	190	291	300	0.68	1.49	150	250
553	1.33	2.32	218	343	553	1.33	2.32	218	343	300	0.72	1.54	146	271
710	1.20	2.15	288	449	710	1.20	2.15	288	449	300	0.51	1.27	171	331
813	2.09	3.28	289	473	813	2.09	3.28	289	473	300	0.77	1.61	142	325
884	3.29	4.81	292	492	884	3.29	4.81	292	492	300	1.12	2.05	124	324
972	2.92	4.33	327	547	972	2.92	4.33	327	547	300	0.90	1.77	134	353
1034	4.47	6.30	330	564	1000	4.32	6.12	320	554	300	1.30	2.28	119	353
1163	3.93	5.62	376	639	1000	3.38	4.92	329	592	300	1.01	1.92	128	391
1286	2.78	4.16	435	726	1000	2.16	3.37	353	644	300	0.65	1.45	152	443
1401	3.22	4.72	464	781	1000	2.30	3.55	349	666	300	0.69	1.51	148	465
1504	3.87	5.54	487	827	1000	2.57	3.90	343	683	300	0.77	1.61	142	482
1619	3.72	5.36	527	893	1000	2.30	3.55	349	715	300	0.69	1.51	148	514
1737	3.91	5.59	562	955	1000	2.25	3.49	351	743	300	0.68	1.49	150	542
1857	4.09	5.83	598	1018	1000	2.20	3.43	352	772	300	0.66	1.47	151	571
1980	4.28	6.06	635	1082	1000	2.16	3.37	353	801	300	0.65	1.45	152	600
2105	4.46	6.29	672	1148	1000	2.12	3.32	355	830	300	0.64	1.44	153	629
2232	4.64	6.52	710	1215	1000	2.08	3.27	356	861	300	0.62	1.42	155	659



Grouted Capacity Limited to 0.5 in. Displacement  
(2% of 2 ft. Shaft Diameter)

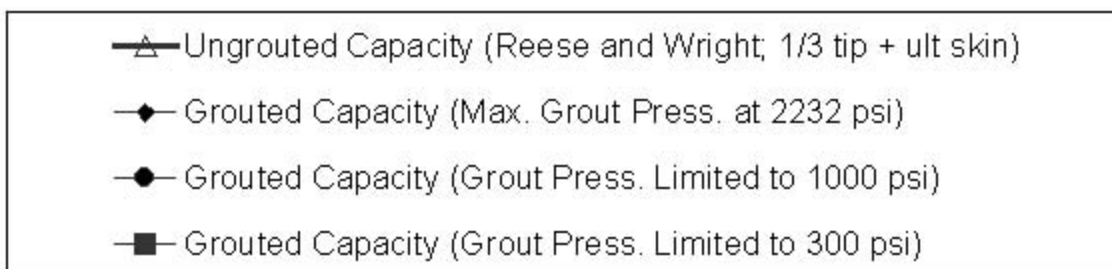


Figure 7-3. Example capacity predictions for a grouted shaft.

### 7.3 Construction of Tip-Grouted Shafts

Construction of a tip grouted shaft requires minimal additional preparation time and effort than that of an ordinary ungrouted shaft. The extra effort required is similar to installing *PVC* access tubes for cross-hole sonic logging. The same care should be applied when lifting the reinforcing cage as that of any cast-in-place foundation. Regardless of the apparatus used, all grout lines should be gently flushed with water until it emerges from the corresponding return line(s) within 24 hours of the initial concrete set. Once the lines of a sleeve-port apparatus are flushed, the individual sleeve-ports must be burst open. An ordinary pressure washer is ideally suited to this task due to its combination of high pressure and low flow characteristics.

#### 7.3.1 Grout Cell Considerations

Various types of grout cells can be used and obtain reasonable grouting benefit. Of these, two primary systems are most common: the sleeve port and the flat jack. The sleeve port (sleeve-port) system requires the least amount of prefabrication. This system must simply supply “U” shaped plumbing at the base of the cage such that grout can be pumped to base and have the ability to verify grout return up the other side as well as provide a flush mechanism once grouting has terminated. Within the “U” shaped base section, multiple sets of holes should be drilled (1/4" diameter) to allow the grout to escape. Each set of holes should be “sleeved” within a rubber hose to keep the access tubes clear during shaft concrete placement. The rubber hoses also serve as a one-way valve allowing the system to be flushed without contaminating any grout previously placed. This method precludes the selection of locking in the grouting pressure and is the preferred apparatus for staged grouting. This grouting method is the most widely used world-wide and can derive the most benefit from the grouting pressure. In contrast to the flat jack system, sleeve ports react upon only a portion of the shaft toe area while utilizing the full side shear available. Disadvantages to this type of grouting system are: (1) the pressure may not uniformly improve the underlying soil, and grout distribution cannot be predicted without post coring below the shaft through larger, secondary access tube, and (2) if the cage is not placed at the planned orientation with respect to the bottom elevation, the water pressure required to crack the concrete prior to grouting may be unattainable. Therein, when excavation depths are not precise, a floating distribution will need to be used.

The flat jack system has the advantage of being less effected by excavation inaccuracies in that it can develop enormous tensile cracking forces around the cell. These systems consist of a circular steel plate no larger than the reinforcing cage covered with a rubber membrane to maintain a large distribution area (the cross section of the cage). Thereby, the cell distributes the grout reliably to the entire tip of the shaft. This allows for good estimates of shaft tip loads during grouting and can be considered a reliable bottom-up proof test. Disadvantages of these cells are: (1) the large pressure surface develops larger forces that can potentially displace the shaft upward before the desired tip improvement is

developed, and (2) the flat surface attached to the base of the cage can slow the cage descent during cage placement and/or complicate clean-out procedures in the event of extended open excavation times.

Both systems perform similarly with respect to the design procedure listed above. However, maximum grout pressures for sleeve port systems (Step 4) will most likely be conservative. If the side shear available within the uplift displacement criterion is insufficient for the desired tip grouting pressure, then an initial skin grouting program may be of benefit (Section 4.3.3).

### 7.3.2 Grouting Guidelines

During the grouting of drilled shaft tips, several parameters should be monitored: (1) at minimum, the upward displacement should be recorded with a surveyor's level, and (2) the grout pressure and rate of pressure increase with respect to grout take. Reductions in the ratio of pressure increase to the grout volume indicate possible hydro-fracturing. This concern is only applicable to sleeve-port or unconfined systems. Considerations for the grout mix design, mixer and pump requirements, and access lines are summarized below:

1. Most post-grouted shaft projects will use access lines less than 2" in diameter and will require the use of a neat cement mix (Table 2-2).
2. The grout will be in direct contact with the tip of the shaft and therefore must be able to withstand the compressive stresses developed by the end bearing load,  $q_{grouted}$ , as calculated in Step 7. of Section 7.1
3. The mixer type needs to be capable of developing a rotational velocity greater than 700 rpm so that the slurry is semi-colloidal and remains stable during pumping.
4. Unless unusual circumstances exist, post-grouting shaft tips require small volumes of grout and therefore any pump that can produce sufficient grout pressure is acceptable (Step 4 from the design method above). Some mechanism must exist that can track the grout take and pumping rate.
5. The water cement ratio should provide sufficient strength and pumpability parameters. Therefore, the w/c ratio should fall between 0.3 and 0.6 depending on the strength requirement (Section 2.4). If at the lower range of the w/c ratios (below 0.4) the authors suggest some form of a water reducing agent and to conduct pumping trials with the exact equipment planned for the project.
6. Pumping rates can affect the ability of the soil to resist hydro-fracturing. The ultimate goal is to achieve the desired grout pressure without pumping excessive amounts of grout. Therefore pumping rates should be monitored with respect to rate

of pressure increase. As the rate of pressure increase lessens, pumping rates should be reduced.

7. When over water or in lightning-prone areas, consideration should be given to develop a procedure for saving the grout mix and/or pump in the event of unforeseen weather.
8. Flexible tubing, used to flush the grout access lines, must be readily available on-site of appropriate length and diameter such that it can be inserted through the grout access lines to the grouting apparatus level. It may be necessary to flush the access lines clear of sediment prior to grouting, as described in Section 4.6.2. It is also used to flush the access lines of grout in a flat-jack style apparatus immediately after a failed grouting attempt. Note that the U-tube design of a sleeve-port grouting apparatus may simply be flushed by gently circulating water through the U-tube, as was detailed in Section 2.2.3.

This page is intentionally blank.

## REFERENCES

AASHTO, LRFD Bridge Design Specifications, SI (1<sup>st</sup> Edition), American Association of State Highway and Transportation Officials, Washington, D.C., 1994, *w/1996 and 1997 interim revisions*.

Baker, A.C. and Broadrick, R.L., (1997), "Compaction Grouting, a twenty year update and a vision for the 21<sup>st</sup> century," Proceedings *Florida/South Florida Section Annual Meeting*, Clearwater, FL, September.

Bauer in Brooklyn Queen's Expressway, NY (1988) Bauer inner office Tech Note.

AASHTO, LRFD Bridge Design Specifications, Customary U.S. Units (2<sup>nd</sup> Edition), American Association of State Highway and Transportation Officials, Washington, D.C., 1998, *w/1999 interim revisions*.

American Society For Testing And Materials, (1998), "Standard Test Method For Piles Under Static Axial Compressive Load," D-1143-98, *Annual Book of ASTM Standards*, Part 20, Philadelphia, PA.

Armour, T., Groneck, P., Keeley, J., and Sharma, S. (2000), "Micropile Design and Construction Guidelines Implementation Manual Priority Technologies Program (PTP) Project," Report No. FHWA-SA-97-070, U. S. Department of Transportation Federal Highway Administration, McLean, Virginia.

Azizi, Fethi, (2000), "Applied Analyses In Geotechnics," E & FN Spoon, New York, NY.

Baker, W. H., (Ed) (1982), "Proceeding of the Conference on Grouting in Geotechnical Engineering," American Society of Engineers, Denver, Colorado.

Baker, A. C., and Broadrick, R. L. (1997), "Ground Improvement, Reinforcement, and Treatment: A Twenty Year Update and a Vision for the 21<sup>st</sup> Century," Earth Tech, Clear Water, Florida.

Bolognesi, A. J. L. and Moretto, O. (1973) "Stage Grouting Preloading of Large Piles on Sand" Proceedings of 8<sup>th</sup> ICSMFE, Moscow.

Bruce, D.A. (1986), "Enhancing the performance of large diameter piles by grouting," Parts 1 and 2, *Ground Engineering*, May and July, respectively.

Bruce, D. A., Nufer, P. J., and Triplett, R. E. (1995) "Enhancement of Caisson Capacity by Micro-Fine Cement Grouting - a Recent Case History" ASCE Special Publication 57, Verification of Geotechnical Grouting.

Dapp, S.D. (1998) "Interviews with engineers during load testing on the My Thuan Bridge" Mekong Delta, Vietnam."

Day, K. (1995), Concrete Mix Design, Quality Control and Specification," Second Edition, E&FN SPON, New York.

Dhir, V. K., (1984) "Grouting to save money," *Gulf Construction*, July.

Domone, P. L. J., and Jefferis, S. A. (1994), "Structural Grouts," Chapman and Hall, New York, New York.

Dunnicliff, J. (1988), "Geotechnical Instrumentation for Monitoring Field Performance," Wiley-Interscience, New York.

Flemming, W. G. K. (1993) "The Improvement of Pile Performance by Base Grouting" Proceedings of the Institution of Civil Engineers, London.

Gouvenot, D. and Gabiax, F. D. (1975), "A new foundation technique using piles sealed by concrete under high pressure," Proceedings, *Seventh Annual Offshore Technical Conference*.

Holtz, R. D., and Kovacs, W. D. (1981), "An Introduction to Geotechnical Engineering," Prentice Hall, New Jersey.

Horvath, Robert G. and Stolle, Dieter, (1996), "Frustum For Testing Model Piles," *Canadian Geotechnical Journal*, Vol. 33, No. 3, June, pp. 499-504.

Houlsby, A.C. (1990), "Construction and Design of Cement Grouting, A Guide to Grouting in Rock Foundations," Wiley-Interscience Publication, New Jersey.

Kahn, Y. (1984), "Innovative Cement Grouting," ACI Publication SP-83, American Concrete Institute, Detroit, Michigan.

Littlejohn, G. S., Ingle, J., Dadasbilge, K. (1983) "Improvement in Base Resistance of Large Diameter Piles Founded in Silty Sand" Proceedings, *Eighth European Conference on Soil Mechanics and Foundation Engineering*, Helsinki, May.

Lizzi, F., Viggiani, C., Vinale, F. (1983) "Some Experience with Pre-Loading Cells at the Base of Large Diameter Bored Piles" Proceedings of the 7<sup>th</sup> Asian Regional Conference on Soil Mechanics and Foundation Engineering, Haifa, Israel

Logie, C. V. (1984) "Drilled Pier Foundation Rehabilitation Using Cement Grouting" ACI Publication SP-83, Innovative Cement Grouting.

Mojabe, M.S., and Duffin, M. J. (1991) "Large Diameter, Rock Socket, Base Grouted Piles in Bristol" Proceedings of the 4<sup>th</sup> International Conference on Piling and Deep Foundations, Stresa, Italy, April

Mullins, A. G. (1999) "Interviews with engineers during load testing on the Taipei Financial Center " Taipei, Taiwan.

Mullins, G., Dapp, S., and Lai, P. (2000), "New Technological and Design Developments in Deep Foundations, Pressure-Grouting Drilled Shaft Tips in Sand," American Society of Civil Engineers, Denver, Colorado.

Piccione, M., Carletti, G., and Diamanti, L. (1984) "the Piled Foundations of the Al Gazira Hotel in Cairo" Proceedings of the International Conference on Advances in Piling and Ground Treatment for Foundations, Institution of Civil Engineers, London, UK.

Ramachandran, V. S. (1995), "Concrete Admixtures Handbook, Properties, Science, and Technology," Second Edition, Noyes Publication, Park Ridge, New Jersey.

Rixom, R., and Mailvaganam, N. (1999), "Chemical Admixtures for Concrete," Third Edition, Routledge, New York, New York.

Santosuossa, M., Rizzi, G., Diamanti, L. (1991) "Construction of Pile Foundation of the Postal Citadel in the Direction Center of Naples" Proceedings of the 4<sup>th</sup> International Conference on Piling and Deep Foundations, Stresa, Italy, April

Sedran, G. (1999) "Experimental and Analytical Study of a Frustum Confining Vessel," Doctoral Dissertation, McMaster University, Hamilton, ON, September.

Sedran, Gabriel, (1999), "Experimental and Analytical Study of A Frustum Confining Vessel," Doctoral Dissertation, McMaster University, Hamilton, ON.

Sliwinski, Z. J., and Flemming, W. G. K. (1984) "the Integrity and Performance of Bored Piles" Proceedings of the International Conference on Advances in Piling and Ground Treatment for Foundations, Institution of Civil Engineers, London, UK.

Sliwinski, Z. J., and Philpot, T. A. (1980) "Conditions for Effective End Bearing of bored Cast in Situ Piles" Proceedings of Recent Developments in the Design and Construction of Piles, Institute of Civil Engineers, London, UK

Stocker, M.F. (1983), "The influence of post grouting on the load bearing capacity of bored piles," Proceedings, *Eighth European Conference on Soil Mechanics and Foundation Engineering*, Helsinki, May.

Troughton, V. M. and Platis, A.(1989) “The Effects of Changes in Effective Stress on a Base Grouted Pile in Sand” Proceedings of the International Conference on Piling and Deep Foundations, London, UK, May.

Wagner, R. V. (2000a), “Personal interview with Ron Terrelonge, Materials Engineer Southdown Industries, on pump sizes and correlation to aggregate sizes,” Tampa, Florida.

Wagner, R. V. (2000c), “Personal interview with Jim Hussing, Hayward Baker, general compaction grouting discussion,” Tampa, Florida.

Wagner, R. V. (2000b), “Personal interview with a pumping consultant from Pioneer, a concrete pumping company, general concrete pumping guidelines,” Tampa, Florida.